



Univerza v Ljubljani
Zdravstvena fakulteta

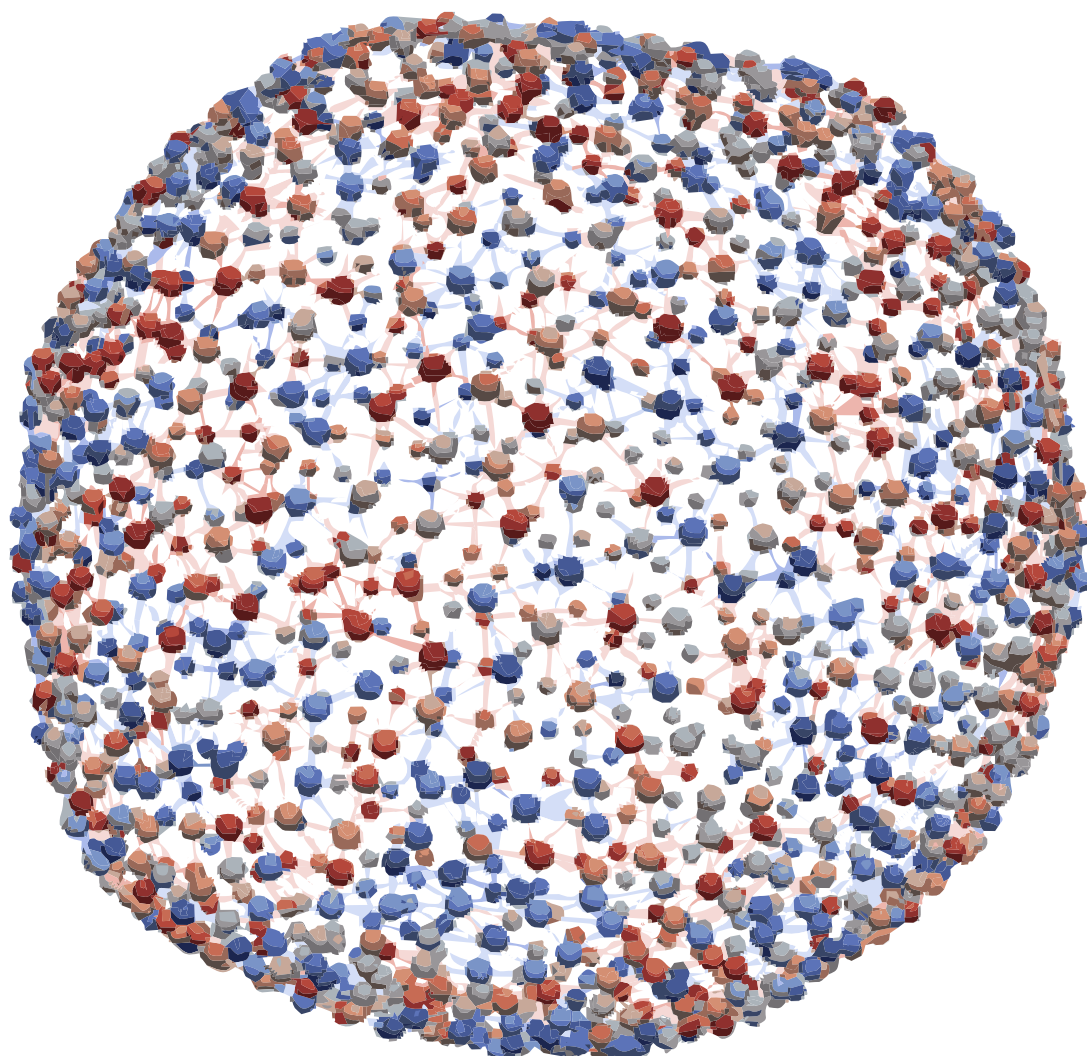
SOKRATSKA PREDAVANJA SOCRATIC LECTURES

4. MEDNARODNI MINISIMPOZIJ, LJUBLJANA, 11.-12. DECEMBER 2020
4TH INTERNATIONAL MINISYMPOSIUM, LJUBLJANA, 11.-12. DECEMBER 2020

ZBORNIK RECENZIRANIH PRISPEVKOV
PEER REVIEWED PROCEEDINGS

UREDILA: VERONIKA KRALJ-IGLIČ
EDITED BY: VERONIKA KRALJ-IGLIČ

ZDRAVSTVENA FAKULTETA, UNIVERZA V LJUBLJANI
FACULTY OF HEALTH SCIENCES, UNIVERSITY OF LJUBLJANA



Sokratska predavanja

4. Mednarodni minisimpozij, Ljubljana, 11.-12. december, 2020

Zbornik recenziranih prispevkov

Zbornik uredila: prof.dr. Veronika Kralj-Iglič, univ.dipl.fiz.

Recenzenta: prof.dr.Rok Vengust, dr. med. in Karin Schara, dr. med.

Izdala in založila: Univerza v Ljubljani, Zdravstvena fakulteta

Oblikovanje in fotografije: Anna Romolo

Slika na naslovnici: Samo Penič

Ilustracije: Stran 78: Niko Kralj, stran 123: ulična slikarka iz Firenc,
ostale: Marguerite de Saint Champs

Socratic lectures

4th International Minisymposium, Ljubljana, December 11.-12., 2020

Peer Reviewed Proceedings

Edited by Prof. Veronika Kralj-Iglič, Ph.D.

Reviewers: Prof. Rok Vengust, M.D., Ph.D. and Karin Schara, M.D.

Published by: University of Ljubljana, Faculty of Health Sciences

Design and photos: Anna Romolo

Image on the front page: Samo Penič

Illustrations: Page 78: Niko Kralj, Page 123: Street artist from Florence,
others: Marguerite de Saint Champs

Publikacija je dostopna v PDF formatu na spletni strani:

https://www.zf.uni-lj.si/images/stories/datoteke/Zalozba/Sokratska_2021.pdf

Publication is available online in PDF format at:

https://www.zf.uni-lj.si/images/stories/datoteke/Zalozba/Sokratska_2021.pdf

Ljubljana, 2021

To delo je dosegljivo pod licenco Creative Commons Priznanje avtorstva 4.0
Mednarodna

This work is available under a Creative Commons Attribution 4.0 International



Kataložni zapis o publikaciji (CIP) pripravili v Narodni in univerzitetni knjižnici v Ljubljani

COBISS.SI-ID=51797507

ISBN 978-961-7112-02-3 (pdf)



The members of the Organizing Committee of Socratic Lectures:
Antonella Bongiovanni, Tjaša Griessler Bulc, Aleš Iglič, Veronika Kralj Iglič,
Laura Sesma, Polonca Trebše

Program

Socratic Symposium December 11, 2020, 09:00 – 12:00 (Ljubljana time) Parallel Sections

Section 1: Emergent Environmental Pollution Problems

organized and moderated by prof. Tjaša Griessler-Bulc and prof. Polonca Trebše

9.00 - 9.20 Franja Prosenc, Faculty of Health Sciences, University of Ljubljana, Slovenia:

Microplastics in soil, problematics and quantification

9.20 – 9.40 Petra Procházková, Brno University of Technology, The Czech Republic: Effects of microplastics to aquatic environment

9.40 – 10.00 Urška Šunta, Faculty of Health Sciences, University of Ljubljana, Slovenia Insights into microplastics: from physical and chemical characterisation to its potential as a vector

10.00 – 10.20 Nevena Antić, Institute of Chemistry, Technology and Metallurgy, Department of Chemistry, University of Belgrade, Serbia: Extreme climate condition and acid rain impact on land degradation

10.20 – 11.40 Irina Vasileva, M.V. Lomonosov Moscow State University, Organic Chemistry Department, Moscow, Russia: Peculiarities of the *de novo* mass spectrometry sequencing of bioactive peptides secreted by Slovenian *Rana temporaria*

10.40 – 11.00 Valentina Polanc Rutar, Faculty of Civil and Geodetic Engineering, University of Ljubljana, Slovenia, Green wall systems for greywater treatment

Section 2: Membrane Biophysics

organized and moderated by prof. Aleš Iglič

9:00-9:30 Mitja Drab, Žiga Pandur, Samo Penič, Aleš Iglič, Veronika Kralj-Iglič, David Stopar.

Monte Carlo studies of detergent solubilization of lipid bilayers

9:30-10:00 Luka Mesarec, Wojciech Gózdź, Iglič Aleš, Kralj-Iglič Veronika, Epifanio Virga, Samo Kralj: Stability of normal red blood cells explained by membrane's in-plane ordering

10:00-10:30 Jeel Raval, Aleš Iglič, Wojciech Gózdź: Study of shapes and shape transformations of vesicles induced by their adhesion to a rigid surface

10:30-11:00 Break

11:00-11:30 Raj Kumar Sadhu, Nir Gov, Aleš Iglič, Samo Penič. Modelling cellular spreading in the presence of curved membrane proteins and active cytoskeleton forces

11:30-12:00 Metka Benčina, Ita Junkar, Eva Levičnik, Veronika Kralj-Iglič, Miran Mozetič, Aleš Iglič: Improved hemocompatibility of Ti-based nanostructures

Section 3: Cellular Nanovesicles

organized by partners of the VES4US project (a project funded by the FET Open Call of the Horizon2020) and moderated by prof. Veronika Kralj-Iglič

9:00-9:20 Ramila Mammadova, Gabriella Pocsfalvi - Nanovesicles from tomatoes: focus on the molecular cargo

9:20 – 9:40 Paulina Ramos Juarez, Gabriella Pocsfalvi - The human EV membranome: more ligand and adhesion proteins than receptors, what are the implications?

9:40-10:00 Marija Holcar, Jana Ferdin, Simona Sitar, Magda Tušek-Žnidarič, Vita Dolžan, Ana Plemenitaš, Ema Žagar, Metka Lenassi: Method for reliable enrichment of plasma extracellular vesicles for biomarker discovery

10:00-10:30 Break

10:30-10:50 Zala Jan, Mitja Drab, Damjana Drobne, Apolonija Bedina Zavec, Mojca Benčina, Barbara Drašler, Matej Hočevnar, Judita Lea Krek, Ljubiša Pađen, Manca Pajnič, Neža Repar, Boštjan Šimunič, Roman Štukelj, Veronika Kralj-Iglič: Impact of physical effort on cellular nanovesicles concentration in blood isolates

10:50-11.10 Domen Vozel, Nejc Steiner, Darja Božič, Zala Jan, Marko Jeran, Manca Pajnič, Ljubiša Pađen, Aleš Iglič, Veronika Kralj-Iglič, Saba Battelino: Preparation of platelet- and extracellular vesicle-rich gel and its role in management of cerebrospinal fluid leak in skull-base surgery

11.10-11:30 Ryan Garry, Dave Weitz: Harnessing nature communication system: Engineering exosomes

12:00 – 12:15 Cultural program

Slovenian folk song, I have made up something, trombone: **Emil Somun**, piano: **Elena Startseva Somun**

Elvis Presley, Love me tender: trombone: **Emil Somun**, piano: **Elena Startseva Somun**

Johann Sebastian Bach, Sarabande from Partita for Flute Solo in A minor BWV 1013, flute: **Anita Prelovšek**

Carlos Gardel: Poe una cabeza, violin: **Vittorio Sbordone**

Christina Perry: A thousand years, piano: **Elena Startseva Somun**

12:15 – 14:00 Joint Section Cross-Domain Communication for all participants of the Symposium and Lectures, with discussion of posters

Socratic Lectures, December 12, 2020, 16:00 – 18:00 (Ljubljana time)

<https://uni-lj-si.zoom.us/j/97287958341> Meeting ID: 972 8795 8341

Find your local number: <https://uni-lj-si.zoom.us/j/97287958341>

16:00-16:30 Leonid Margolis, National Institute of Health, Bethesda, U.S.A.: Viruses and extracellular vesicles – similarities and differences

16:30-17:00 Gabriella Pocsfalvi, National Research Council of Italy, Naples, Italy: Use of extracellular vesicles in COVID-19

17:00-17:30 Vesna Spasovski, Institute of Molecular Biology, Belgrade, Serbia: Stem cell extracellular vesicles

17:30-18:00 Duško Spasovski, Institute for Orthopaedic Surgery, Clinics Banjica, Belgrade, Serbia: Mechanisms of cartilage degeneration

18.00-18.30 Bojana Beović, University Medical Centre Ljubljana, Slovenia: Management of COVID-19 in Slovenia

18.30-19.00 Cultural program

Pjotr Iljič Čajkovski, Seasons, June, piano: **Elena Startseva Somun**

Johann Sebastian Bach, Badinerie from Suite in B major, BWV 1067, flute: **Anita Prelovšek**

Nicola Piovani, La vita e bella, violin: **Vittorio Sbordone**

EDITORIAL

Year 2020 was especially fruitful for Socratic lectures. Traditionally, held each year in April, in 2020, the lectures took place twice – on April 17 and on December 11 and 12. This happened because the elective course entitled Biomechanics of Joints at the Faculty of Medicine, University of Ljubljana leading to Socratic lectures, was moved to the first academic semester.

It was a pleasure and an honour to attend excellent lectures of Prof. Leonid Margolis, National Institute of Health, Bethesda, U.S.A., Dr. Gabriella Pocsfalvi, National Research Council of Italy, Naples, Italy, Prof. Duško Spasovski, Institute of Orthopaedy, Clinics Banjica, Belgrade, Serbia, Dr. Vesna Spasovski, Institute of Molecular Biology, Belgrade, Serbia and Prof. Bojana Beović, University Medical Centre Ljubljana, Ljubljana, Slovenia. This year's hot themes were COVID-19, viruses, extracellular vesicles and degenerative joint diseases.

Each year, Socratic lectures presented also the results of postgraduate students of the Doctoral school of the University of Ljubljana, Biosciences and Biomedicine, of young researchers and fellows. This time, due to increased interest, the lectures held on December 12 were appended by a Symposium a day before featuring the results of young scientists. Three sections were organized: Emergent environmental pollution problems, Biophysics of membranes and Cellular nanovesicles. The last section was organized by the members of the EU Commission – funded project Ves4us (Extracellular vesicles from a natural source for tailor-made nanomaterials) from Palermo and Naples, Italy and Ljubljana, Slovenia. Poster section to accompany lectures and symposium was organized at the homepage of the Laboratory of Clinical Biophysics, Faculty of Health Sciences, University of Ljubljana, www.lkbf.si. For the events, the homepage of the laboratory was re-designed by EnBit.d.o.o.

It was inspiring to acknowledge the results of emerging new science. We are especially grateful for the gifts of musicians Elena Startseva-Somun, Vittorio Sbordone, Anita Prelovšek and Emil Somun, who supported the scientific part with the cultural program on both days. Music attracted to the computer also the family members of the participants, including pets. The array with pictures of everyone who celebrated a moment of science and art, that appeared at the monitor was memorable. In that moment, our thoughts included those who have lost and suffered for COVID-19 directly or indirectly – remembering that no man is an island.

We are thankful to everyone who contributed to the events and the proceedings and hope to meet at the next Socratic lectures.

Veronika Kralj-Iglič and Anna Romolo

CONTENTS

INVITED LECTURES

1. Procházková P, Zlámalová Gargošová H : Effects of microplastics to aquatic environment.....2
2. Vasileva Irina D. : Peculiarities of the mass spectrometry de novosequencing of bioactive peptides secreted by Slovenian *Rana temporaria*8
3. Drab M, Pandur Ž, Penič S, Igljč A, Kralj-Igljč V, Stopar D: Monte Carlo studies of detergent solubilization of lipid bilayers14
4. Mesarec L, Gózdź W, Igljč A, Kralj-Igljč V, Virga EG and Kralj S : Stability of normal red blood cells explained by membrane's in-plane ordering21
5. Penič S, Drab M, Kralj-Igljč V, Igljč A: Towards implementation of numerical model for anisotropic inclusions into the phospholipid bilayer for Monte Carlo simulations29
6. Jan Z, Bedina Zavec A, Benčina M, Drab M, Drašler B, Drobne D, Hočevar M, Krek JL, Pađen L, Pajnič M, Repar N, Šimunič B, Štukelj R, Kralj-Igljč V: Impact of Physical Effort on Cellular Nanovesicle Concentration38
7. Vozel D, Battelino S: Preparation of platelet- and extracellular vesicle-rich gel and its role in the management of cerebrospinal fluid leak in anterior and lateral skull-base surgery47

SCIENTIFIC CONTRIBUTIONS

8. Rugelj D, Vidovič M: Evaluation the effect of frequency modulated transcutaneous electrical nerve stimulation on postural sway in healthy young adults. A pilot study60
9. Svete AN, Erjavec V: Routine coagulation parameters in brachycephalic dogs with brachycephalic obstructive airway syndrome70
10. Jeran M, Barrios-Francisco R, Sedušak Kljakič A, Remškar H, Novak U: Non-destructive characterisation of natural materials: quantitative determination of borneol and limonene in european spruce needles (*picea abies*) by ftir spectroscopy79
11. Paunovic O, Sabolc P, Prosen H, Krasevec I, Trebse P, Turk Sekulic M : Removal process optimisation for emerging pollutants onto two biochars synthesised with classic and microwave induced pyrolysis88
12. Radovic S, Sabolc Pap, Prodanovic J, Bremner B, Turk Sekulic M: Challenges in removal of emerging contaminants from the wastewater through hybrid treatment system: An eco-friendly approach98
13. Tomšič R, Heath D, Heath E, Markelj J and Prosen H: Development of an analytical method to determine contamination of propolis with neonicotinoid pesticides108
14. Tršek A, Smerkolj N, Jeran M: Pharmaceutical and financial aspect of research and development in nine pharmaceutical industry giants114

REVIEWS

15. Šuligoj A: Mental health during COVID-19124
16. Smajila M, Celin D, Kovačič D: Testing for SARS-CoV-2: a review of current methods134
17. Pevec V, Černe ŽP, Dobrin E, Beović B: Experience with glucocorticoids and other treatments on COVID-19 so far142
18. Zore LA, Stražar K: Problem of hip dysplasia in adults158
19. Steiner N, Battelino S : Extracellular vesicles and their use in inner ear167
20. Schara K, Kralj Igljč V: Charcot neuroarthropathy: What lies beneath?174

REFLECTIONS

21. Romolo A.: Post- COVID-19 Experiences182
22. Amon M, Kresal F: COVID-19 Health consequences management: proposed health rehabilitation of long-term care for older adults187
23. Mustar E: Regulation of gender verification in sport and future sustainable development196
24. Kralj-Igljč V: Exams at Socratic lectures in the time of COVID-19203
25. Prelovšek A: Fyodor Mikhailovich Dostoevsky and his relationship with music210

POSTERS

26. Antenen N, Mežek K, Junge R: A green wall system for laundry greywater treatmentP1
27. Kranjc Požar A, Istenič D, Žagar D: Pathways of microplastics from inland polluters in the Gulf of Trieste: determining the beaches for depositionP2
28. Tomšič R, Heath D, Heath E, Markelj J, Prosen H: Development of an analytical method to determine contamination of propolis with neonicotinoid pesticidesP3
29. Resnik N, Griessler Bulc T, Žgajnar Gotvajn A: Does microplastics in waste biological sludge impact biogas production?P4
30. Czarny K, Krawczyk B, Szczukocki D: Inhibition of growth of cyanobacteria *Anabaena variabilis* and *Microcystis aeruginosa* by single and mixed bisphenol analoguesP5
31. Leban P, Prosenc F, Bavcon Kralj M, Griessler Bulc T: Extraction of pet microplastics from soil and different soil and compost mixturesP6
32. Paunovic O, Pap S, Prosen H, Krasevec I, Polonca T, Turk Sekulic M: Removal process optimisation for emerging pollutants onto two biochars synthesised with classic and microwave induced pyrolysisP7
33. Radovic S, Pap S, Prodanovic J, Bremner B, Maja Turk Sekulic M: challenges in removal of emerging contaminants from the wastewater through hybrid treatment system: an eco-friendly approachP8
34. Goršak T, Drab M, Križaj D, Jeran M, Genova J, Kralj S, Lisjak D, Kralj-Igljč V, Igljč A, Makovec D: Disruption of phospholipid membranes with magneto-mechanical actuation using barium-hexaferrite nanoplateletsP9

35. Rawat N, Benčina M, Junkar I, Igljč A: Anodised Microflowers On The Surface of Titanium	P10
36. Schara P, Schara K: A novel approach to predicting hip dislocation in children with cerebral palsy a case report	P11
37. Steiner N, Battelino S : Extracellular vesicles and their use in inner ear	P12
38. Mitić J, Daniel M, Ponorac S, Gošnjak Dahmane R, Kralj-Igljč V: Determination of resultant hip force and contact hip stress from magnetic resonance images	P13
39. Kisslinger A, Božič D, Adamo G, Gai M, Picciotto S, Marko Jeran M, Stanly C, Pamela Santonicola P, Raccosta S, Paganini C, Capasso U, Cusimano A, Romancino D, Carrotta R, Martorana V, Noto R, Touzet N, Arosio P, Di Schiavi E, Manno M, Pocsfalvi G, Morsbach S, Landfester K, Igljč A, Kralj-Igljč V, Bongiovanni A, Liguori GL: Quality management tools and research activities: an innovative cross-contamination	P14
40. Žunko H, Vauhnik R: Ankle dorisflexion range of motion measurement tools	P15
41. Nemeč AS, Erjavec V: coagulation profile of brachycephalic dogs with brachycephalic obstructive airway syndrome	P16
42. Moubarak M, Chiaiese P, Pocsfalvi G: Towards the Development of a novel continuous Extracellular Vesicle production system in plants	P17
43. Paterna A, Rao E, Raccosta S, Adamo G, Picciotto S : Extracellular vesicles production from microalgae: a renewable bioprocess	P18
44. Picciotto S, Adamo A, Romancino D, Rao E, Paterna A, Raccosta S, Noto R, Carrotta R, Touzet N, Manno M, Antonella Bongiovanni A: Nanoaligosomes: analyses of the cellular uptake.....	P19
45. Božič D, Hočevār M, Pajnič M, Jeran M, Igljč A, Kralj Igljč V: The importance of considering sample specificities in optimization of centrifugation based vesicle harvesting	P20

SOCRATIC LECTURES 2021 SYMPOSIUM



Univerza v Ljubljani
Zdravstvena fakulteta



Effects of microplastics to aquatic environment

Procházková P^{1,*}, Zlámalová Gargošová H¹

¹Brno University of Technology, Faculty of Chemistry, Institute of Chemistry and Technology of Environmental Protection, Brno, Czech republic

[*Petra.Prochazkova1@vut.cz](mailto:Petra.Prochazkova1@vut.cz)

Abstract

Plastics with their pervasive distribution are gradually becoming a global threat to the environment. Plastic items undergo slow degradation and fragmentation to smaller particles called microplastics. Microplastics can be defined as solid synthetic particles or polymer matrices with regular or irregular shape and with a size in the range of 1 μm to 5 mm. These particles are insoluble in water. The contamination of microplastic particles occurs across all ecosystems at different trophic levels. Microplastics may have direct ecotoxicological effects as well as vector effects through the adsorption of co-contaminants. These days, we deal with influence of PHB microparticles to aquatic organism *Daphnia magna* via acute and reproductive ecotoxicity tests.

1. Introduction

As plastic particles are an increasing environmental problem, new more easily degradable polymers are being developed. These biodegradable plastics can be decomposed in the environment by microorganisms and fungi, which convert plastic materials into natural substances like water, carbon dioxide, methane and biomass. These substances do not represent a danger to the environment. The biodegradation process depends on the ambient conditions (temperature, pH, humidity) and can be both anaerobic (without oxygen) and aerobic (in the presence of oxygen) [1,2].

Two types of biodegradable materials are known – plastics made from renewable raw material and plastics from petrochemical with additives that increase their biodegradability. In this work, we focused on polyhydroxybutyrate (PHB). PHB was discovered by Lemoigne in 1925 as a product of biosynthesis *Bacillus megaterium*. It is a fully biodegradable polyester with optical activity, piezoelectricity, and very good barrier properties. PHB is a thermoplastic and belongs to the group of polyhydroxyalkanoate PHAs. It has physical and mechanical properties comparable to those of isotactic polypropylene [3,4,5].

Ecotoxicological studies of microplastics are focused on two types of compounds – to polymers and their additives and then to chemical compounds adsorbed on plastic particles from the environment (e.g. metals, PCBs). These compounds may be toxic, mutagenic or have effect as endocrine disruptors. Some of these compounds may be released again either in the environment or in living organisms. In our work, we use crustacean *D. magna* to study effects of PHB on representative of invertebrates in aquatic environment [6].

2. Methods

Culturing of D. magna The *D. magna* came from our laboratory breeding and has been cultured continuously at $21 \pm 2^\circ\text{C}$ and 16:8 h (light/dark) photoperiod. Animals were cultured in M4 medium (OECD – Test No. 211: Daphnia Magna Reproduction Test); medium was renewed, and organisms were fed with cultured green algae *Desmodesmus subcapitatus* three times a week.

Preparation of samples Samples of PHB were at first wet sieved using Milli-Q water on 63 and 125 μm sieves. Subsequently, they were dried in a hood at room temperature. After drying, PHB suspensions were prepared. A medium suitable for *D. magna* was used to prepare the suspensions, ultrasound was used to separate the aggregated particles. All the test concentrations were prepared immediately before the beginning of each experiment.

Acute experiments Two acute experiments were conducted: the first with particles of PHB smaller than 63 μm and the second with particles smaller than 125 μm .

In both experiments, newborn neonates of *D. magna* < 24 h old were exposed to 6 different concentrations of PHB microparticles (0, 6.25, 12.5, 25, 50 and 100 $\text{mg}\cdot\text{L}^{-1}$).

These suspensions were prepared by sonication of corresponding amount of PHB in medium immediately before the beginning of the experiments. The test took place in glass beakers. The immobilization of the individual *D. magna* was monitored visually after 24 and 48 h. According to the OECD 202 guideline, the animals were not fed, and the medium was not changed. No new PHB particles were added during the experiment [7].

Chronic experiments As well as the acute test, the chronic test was performed twice – with particles of PHB smaller than 63 μm and with particles smaller than 125 μm . We examined the effects of chronic exposure via total offspring number of test organism *D. magna* after exposure to different concentrations of PHB particles. The experiments design was based on the standard OECD 21 days Daphnia reproduction test (OECD 211). Animals were exposed as neonates, < 24 h old. Five nominal concentrations of PHB particles were used: 6.25, 12.5, 25, 50 and 100 $\text{mg}\cdot\text{L}^{-1}$, plus the control group (without particles). Neonates were incubated individually in 100 ml of PHB suspension at a temperature of 22°C under a 16:8 light/dark cycle. We had one neonate per test beaker and n=10 replicate for each concentration. Test suspensions were renewed 3 times a week, organisms were fed with 1 ml of the alga *D. subcapitatus* at the same time. The experiment lasted 21 days. The number of neonates was checked every day [8].

3. Results

Acute experiments First acute test with PHB particles smaller than 63 μm has shown that the presence of these particles in the test suspension has a negligible effect on the test organism *D. magna* (mortality only 5% of organisms at the highest concentration). The results are shown in Figure 1, which express the dependence of mortality of test organisms on concentration of PHB particles in suspension.

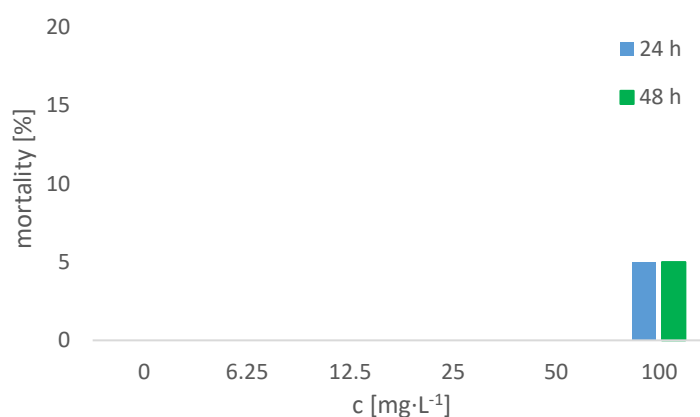


Figure 1. Results of acute test, PHB particles < 63 μm

The results of acute test with PHB particles smaller than 125 μm are shown in Figure 2 (dependence of mortality to concentration of PHB in suspension). After 24 h, the highest mortality (10%) could be observed at the highest tested concentration. After 48 h, mortality of a 15% was observed for concentrations from 12.5 to 100 $\text{mg}\cdot\text{L}^{-1}$.

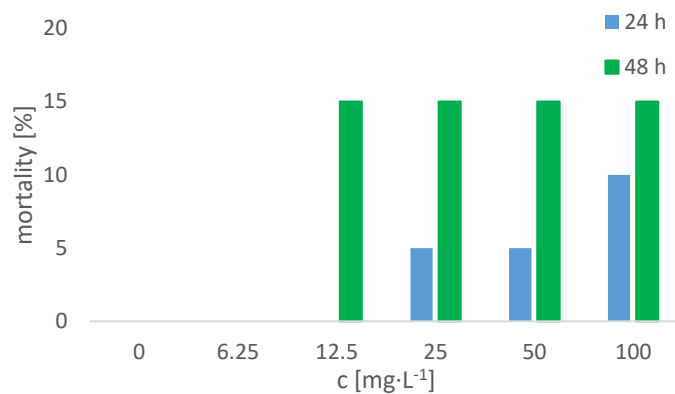


Figure 2. Results of acute test, PHB particles <125 μm

Chronic experiments

The results of both chronic test are shown in Figure 3, which is dependence of mean number of juvenils for mother organism on concentration of PHB particles in test suspension. With increasing concentration of PHB particles in the suspension, the birth rate of organism *D. magna* gradually decreased. At the end of the test, the birth rate of the organisms at the highest concentration was almost half of that the lowest concentration (6.25 mg·l⁻¹). This effect was observed for both size fractions of PHB. In addition, significantly lower birth rates were observed for particles smaller than 125 μm than for particles smaller than 63 μm.

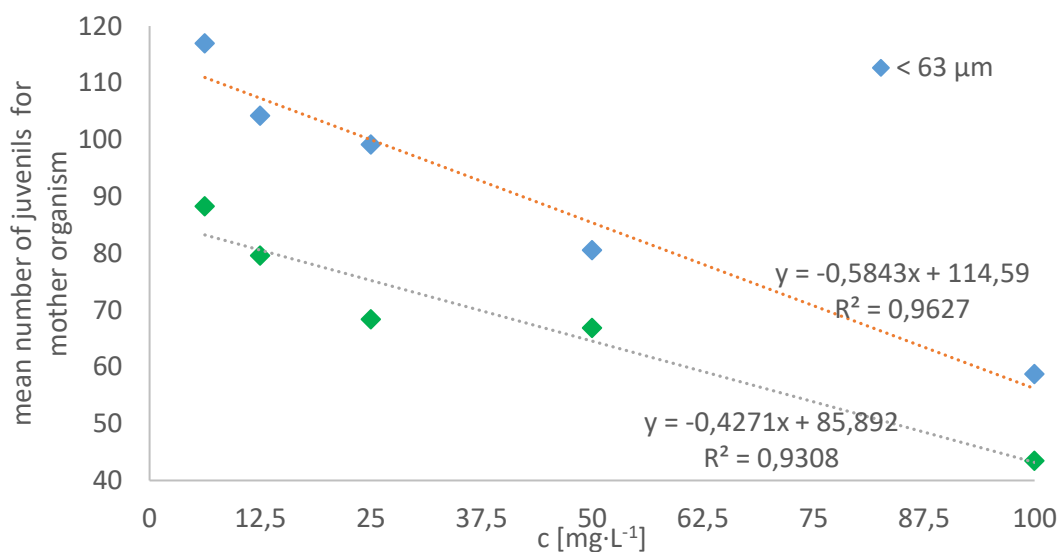


Figure 3. Results of reproduction tests.

4. Discussion

Given the first results we received from acute toxicity tests, it can be concluded that PHB has very small acute toxic effect on the organism *D. magna*. The highest observed mortality was 15%. This value is not statistically significant because the OECD guideline allows 10% mortality in the control. More interesting are the results of reproduction tests, when the average number of juveniles dropped almost on half from the lowest to the highest concentration. These results are preliminary, all performed tests must be repeated to confirm the obtained data.

Acknowledgements

This work was supported by the institution research number FCH-S-20-6446 from the Ministry of Education and by Youth and Sports of the Czech Republic.

References

1. Zhu J, Wang C, Biodegradable plastics: Green hope or greenwashing?. *Marine Pollution Bulletin* 2020, 161, Part B: 111774. doi: [10.1016/j.marpolbul.2020.111774](https://doi.org/10.1016/j.marpolbul.2020.111774)
2. Kroisová D, Biodegradovatelné polymery – úvod do problematiky. Technická univerzita v Liberci, Liberec, 2009. ISBN: 978-80-7372-468-9
3. Huang JC, Shetty AS, Wang MS, Biodegradable plastics: A review. *Advances in Polymer Technology* 1990, 10: 23-30. doi: [10.1002/adv.1990.060100103](https://doi.org/10.1002/adv.1990.060100103)
4. Hankermeyer CR, Tjeerdema RS, Polyhydroxybutyrate: Plastic Made and Degraded by Microorganisms. *Rev of Environ Contam Toxicol* 1999, 159:1-24. doi: [10.1007/978-1-4612-1496-0_1](https://doi.org/10.1007/978-1-4612-1496-0_1)
5. Kim YB, Lenz RW, Polyesters from Microorganisms. Babel W., Steinbüchel A. (eds) *Biopolyesters. Advances in Biochemical Engineering/Biotechnology*, 2001. 71: 51-79. doi: [10.1007/3-540-40021-4_2](https://doi.org/10.1007/3-540-40021-4_2)
6. Anbumani S, Kakkar P, Ecotoxicological effects of microplastics on biota: a review. *Environ Sci and Pollut Res* 2018, 25:14373-14396. doi: [10.1007/s11356-018-1999-x](https://doi.org/10.1007/s11356-018-1999-x)
7. OECD (2004), Test No. 202: *Daphnia sp. Acute Immobilisation Test*, OECD Guidelines for the Testing of Chemicals, Section 2, OECD Publishing, Paris, doi: [10.1787/9789264069947-en](https://doi.org/10.1787/9789264069947-en)
8. OECD (2012), Test No. 211: *Daphnia magna Reproduction Test*, OECD Guidelines for the Testing of Chemicals, Section 2, OECD Publishing, Paris, doi: [10.1787/9789264185203-en](https://doi.org/10.1787/9789264185203-en)



Peculiarities of the mass spectrometry *de novo* sequencing of bioactive peptides secreted by Slovenian *Rana temporaria*

Irina D. Vasileva¹

¹Lomonosov Moscow State University, Organic Chemistry Department, Leninskie Gory 1/3, Moscow, 119991, Russia

idvasilieva@gmail.com

Abstract

Temporins represent a family of short peptides (10-17 aa), possessing wide spectrum of biological activities. They belong to the most perspective group of peptides-antibiotics for the development on their basis pharmaceuticals of new generation. The search of new representatives of that class is an important scientific task. Skin secretion of *Rana temporaria* from Slovenian population was investigated, manual interpretation of CID and HCD tandem mass spectra allowed estimating the sequences of 13 temporins including 4 novel ones, peculiar for Slovenian population.

1. Introduction

Nowadays mass spectrometric peptide sequencing became the most efficient tool to establish the primary sequence of peptides demonstrating much better results than alternative Edman degradation. However, in some cases even MS sequencing can be difficult. For temporins, which structural features involve the presence of proline in the third position of the sequence, the presence of at least one basic amino acid (Lys or Arg) and amidated C-terminus, MS sequencing is complicated by secondary fragmentation, lack of cleavages Gly-Arg sites and possible cyclization of short fragment ions – scrambling. This work deals with peptide determination in sample of skin secretion of *Rana temporaria* from Slovenian population. We demonstrated efficiency of new approach, using HCD with normalized collision energy (NCE) 28 for manual *de novo* sequencing of short peptides. Its combination with mass chromatographic approach showed high usefulness for targeted peptide searching followed by their identification.

5. Methods

Secretion obtaining:

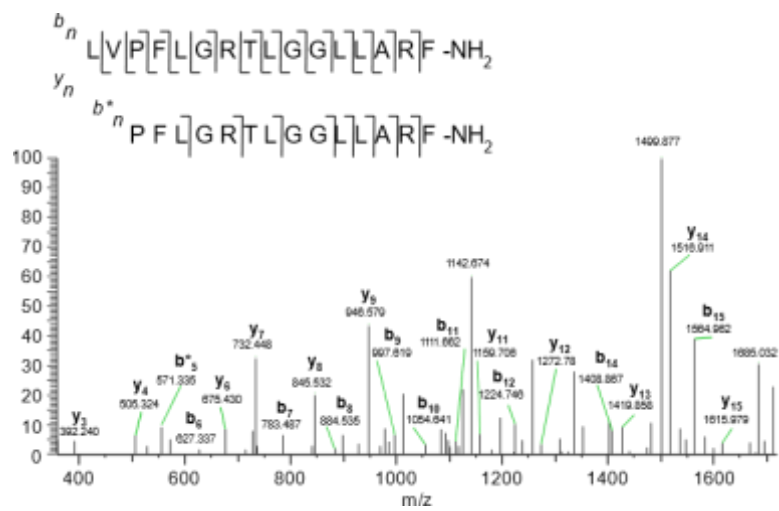
The procedure is described in detail in [1]. The moisturized frog back was stimulated with pulsed currents for 40 s using laboratory electrostimulator. The stimulation parameters were as follows: voltage, 10 V; pulse duration, 5 ms; pulse frequency, 50 Hz. The secretion was washed with 25 mL of MilliQ water into container with equal volume of methanol to deactivate proteases.

Mass spectrometric *de novo* sequencing:

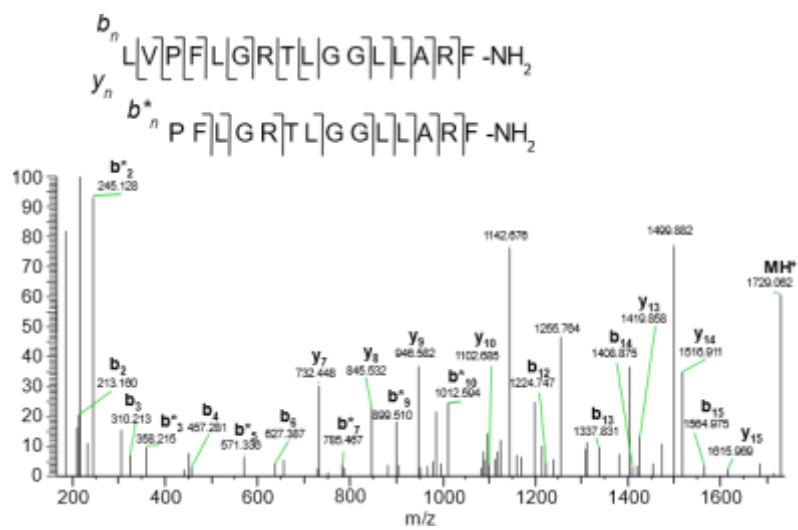
LC-MS/MS experiments were carried out using nano column with Easy nano-LC 1000 (Thermo Scientific, USA) chromatograph combined to Orbitrap Elite ETD (Thermo Scientific, Germany) mass spectrometer. Solution A - 0.1% formic acid in MilliQ water, B – 80% of acetonitrile and 20% 0.1% formic acid in MilliQ water. The separation was achieved with the gradient of B from 5% to 60 % in 120 min with eluent current 150 nL/min. The details of experiments were as follows: inlet capillar voltage – 1.6 kV, inlet capillar temperature – 200 °C, normalized cell energy (NCE) in CID mode was 35 and in HCD mode 28 and 40.

6. Results

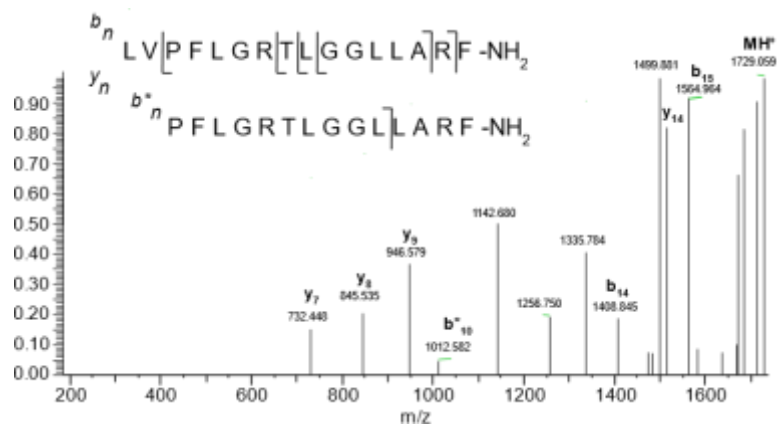
The sequences of 13 temporins identified in the skin secretion of Slovenian common frog *Rana temporaria* are presented in **Table 1**. Sequences of temporins 10-13 are reported for the first time. Sequences of all thirteen temporins, include four novel, were determined by manual interpretation of sum of spectra [HCD_{NCE 28} + HCD_{NCE 40} + CID_{NCE 35}] (**Figure 1**).



(a)



(b)



(c)

Figure 1. Tandem mass spectra of novel temporin 3, (a) – CID_{NCE35}, (b) – HCD_{NCE40}, (c) – HCD_{NCE28}. LVPFLGRTLGGLLARF-NH₂ = Σ [HCD_{NCE 28} + HCD_{NCE 40} + CID_{NCE 35}]. Fragment ions of y₁₄ ion marked as b*.



Table 1. Temporins identified in the skin secretion of Slovenian *R. temporaria*

	Peptide name or family	Sequence	MM, Da
1	Temporin A	FLPLIGRVLSGIL-NH ₂	1395.897
2	Temporin B	LLPIVGNLLKSL-NH ₂	1390.928
3	Temporin C	LLPILGNLLNGLL-NH ₂	1360.881
4	Temporin D	LLPIVGNLLNSLL-NH ₂	1376.876
5	Temporin E	VLPIIGNLLNSLL-NH ₂	1376.876
6	Temporin F	FLPLIGKVLSGLL-NH ₂	1367.890
7	Temporin G	FFPVIGRILNGIL-NH ₂	1456.892
8	Temporin L	FVQWFSKFLGRIL-NH ₂	1638.940
9	Temporin N	FLGALGNALSRVL-NH ₂	1328.793
10	Temporin 1 (new)	LVPFLGKTLGGLLARF-NH ₂	1700.050
11	Temporin 2 (new)	LVPFLGRTLGGLLARL-NH ₂	1694.072
12	Temporin 3 (new)	LVPFLGRTLGGLLARF-NH ₂	1728.056
13	Temporin 4 (new)	(LV)PLLGNLLSGLL-NH ₂	1319.854

7. Discussion

Mass chromatographic approach allowed us performing targeted searching of temporins using neutral loss of 130.111 Da from the protonated molecule equal to sum of the masses of ammonia and leucine. HCD and CID fragment spectra are complicated by secondary fragmentation of γ_{n-2} ions of Pro-containing temporins. For novel sixteen-membered temporins with N-terminus motif LARX (X = F or L) HCD_{NCE 40} spectra are more informative than HCD_{NCE 28} because in their case fragmentation occurs in a proton deficit conditions due to two basic amino acids in sequences. On the contrary, in case of the presence of one basic amino acid in the sequence, such as in short thirteen-membered temporins, HCD_{NCE 28} become more informative than HCD_{NCE 40}.

Acknowledgements

Author acknowledge prof. Polonca Trebše (Faculty of Health Sciences, University of Ljubljana, Slovenia) and prof. Gregor Torkar (Faculty of Education, University of Ljubljana, Slovenia) for providing skin secretion and Dr Alexey K. Surin (Pushchino Branch, Shemyakin–Ovchinnikov Institute of Bioorganic Chemistry, Russia), Prof. Albert Lebedev and Dr. Tatiana Samgina (Chemistry Department of the Moscow State University, Russia) for the help in spectral interpretation, and Dr Roman A. Zubarev (Department of Medical Biochemistry and Biophysics, Karolinska Institutet, Stockholm, Sweden) for instruments provided for this research.

References

1. Tyler MJ, Stone DJ, Bowie JH. A Novel Method for the Release and Collection of dermal, glandular secretions from the skin of frogs. *J PharmacolToxicol Methods*. 1992;28(4):199-200. Doi: 10.1016/1056-8719(92)90004-k.
2. Simmaco M, Mignogna G, Canofeni S, Miele R, Mangoni ML, Barra D. Temporins, antimicrobial peptides from the European red frog *Rana temporaria*. *Eur J Biochem*, 1996, 242(3):788-92. Doi: 10.1111/j.1432-1033.1996.0788r.x
3. Pukala TL, Bowie JH, Maselli, VM, Musgrave IF, Tyler MJ. Host-defence peptides from the glandular secretions of amphibians: structure and activity. *Nat Prod Rep*, 2006, 23 (3):368–393. Doi: 10.1039/b512118n
4. Romero SM, Cardillo AB, Martínez Ceron MC, Camperi SA, Giudicessi SL. Temporins: An Approach of Potential Pharmaceutic Candidates. *Surg Infect (Larchmt)*. 2020, 21(4):309-322. <https://doi.org/10.1089/sur.2019.266>



Monte Carlo studies of detergent solubilization of lipid bilayers

M. Drab^{1,*}, Ž. Pandur², S. Penič³, A. Iglič^{1,4}, V. Kralj-Iglič⁵, D. Stopar²

¹ University of Ljubljana, Faculty of Electrical Engineering, Laboratory of Physics, Ljubljana, Slovenia;

² University of Ljubljana, Biotechnical Faculty, Department of Food Science and Technology, Ljubljana, Slovenia;

³ University of Ljubljana, Faculty of Electrical Engineering, Laboratory of Bioelectromagnetics, Ljubljana, Slovenia;

⁴ University of Ljubljana, Faculty of Medicine, Laboratory of Clinical Biophysics, Ljubljana, Slovenia;

⁵ University of Ljubljana, Faculty of Health Sciences, Laboratory of Clinical Biophysics, Ljubljana, Slovenia.

[*mitja.drab@fe.uni-lj.si](mailto:mitja.drab@fe.uni-lj.si)

Abstract

Giant unilamellar vesicles (GUVs) undergo dynamic morphological changes when exposed to a detergent such as Triton X-100 (TR). The beginning stages of membrane solubilization have been studied in the past empirically, with the underlying mechanisms of the first stage, where the two amphiphiles coexist, remaining largely unknown. In this work we present results of fluorescence microscopy of a binary mixture of DOPC GUVs and TR and construct a simple numerical simulation aimed at explaining the possible underlying mechanisms. A three-dimensional Monte Carlo scheme emulating the non-equilibrium conditions of the beginning stages of solubilization shows to be a good predictor of vibrant morphological changes of lipid dynamics when exposed to a detergent.

1. Introduction

Lipid vesicles are soft spherical structures. Under shear flow conditions a fascinating vesicle dynamic behavior has been observed such as: (i) tumbling, where a vesicle undergoes a periodic flipping motion, (ii) trembling, where vesicle shape fluctuates and the orientation oscillates in time, and (iii) tank-treading, where an ellipsoid vesicle's major axis maintains a fixed orientation with respect to the flow direction while the membrane rotates about the vorticity axis [1].

In this work we will show that extensive lipid vesicle reshaping can be induced in the absence of shear flow with the addition of detergent molecules. The detergent reshaping of lipid vesicle can lead to vesiculation and solubilization. Lipid vesicle is composed of two flexible layers of phospholipids where in an aqueous solution polar headgroups are oriented outward facing the solution, while hydrophobic tails of the two layers are facing each other. Two factors primarily govern whether a lipid will form a stable bilayer: solubility and molecular shape. For a self-assembled structures such as a bilayers the lipid should have low solubility in water, which can be described as a low critical micelle concentration [2, 3].

2. Experimental results

Giant DOPC unilamellar lipid vesicles were prepared as described by Moscho et al. [4]. Giant DOPC lipid vesicles were exposed to TR detergent under the microscope and monitored online to capture the early lipid vesicle dynamics. In the experiments, the concentration of GUV were between 10^6 and 10^7 vesicles/mL. All experiments were made under ambient conditions (room temperature, ambient air pressure). The binary solutions were prepared with 9 μ L of vesicle solution pipetted onto #1,5 microscope cover glass to form hemispheric drop, after positioning and focusing the solution on the microscope, approximately 1 μ L of appropriate TR solution final concentrations of TR were approx. 0,2 mM. Image acquisition started right after the start of addition of detergent. Dynamics of lipid solubilization with detergent was visualized with laser microscope fluorescence microscope Zeiss Axio Observer Z1 equipped with confocal unit LSM 800 (**Figure 1**).

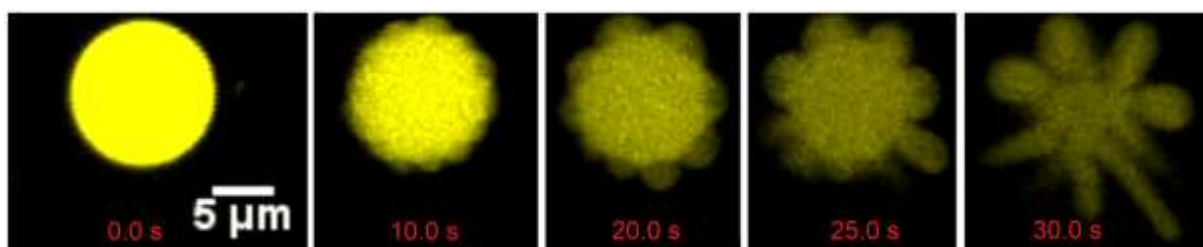


Figure 1. Time evolution snapshots of binary mixtures of DOPC GUVs and TR. Slight undulations are caused by the intrinsic curvature of TR rafts that group together and bend the membrane locally and with time cause elongated protrusions from the vesicle before completely solubilizing into many smaller micelles.

3. Theoretical background

Amphiphiles such as phospholipids self-assemble in a way that prevents exposure of their hydrophobic moieties to water. In absence of detergent, DOPC amphiphiles are likely to form self-assembled flat bilayers because such packing entails a minimal exposure of hydrophobic chains to water. The molecular structure of TR, like most detergents, can be idealized as a cone. The volume of such a conical molecule is less than the product of the polar surface cross-area and the length of the extended chain, therefore its packing parameter is less than 1. When phospholipid bilayers are mixed with a detergent, the two components are forced by entropy to reside in mixed aggregates. Prior to being solubilized, the bilayers retain their lamellar structure, but as the detergent: lipid ratio in the bilayers increases, detergent molecules agglomerate leading to local membrane undulations.

4. Monte Carlo simulation results

The membrane is represented by a set of N vertices that are linked by tethers of variable length l to form a closed, dynamically triangulated, self-avoiding two-dimensional network (as described in [5-7]). The microstates of the membrane are sampled according to the Metropolis algorithm. The probability of accepting the change of the microstate due to vertex move or bond flip is $\min[1, \exp(-\Delta E/kT)]$, where ΔE is the energy change, k is the Boltzmann constant and T is absolute temperature. The energy for a given microstate is specified by the standard Helfrich equation [8]:

$$W_b = \frac{\kappa}{2} \int_A (c_1 + c_2 - c_0)^2 dA, \quad (1)$$

where the integral runs over the whole area of the membrane with bending stiffness κ , c_1 and c_2 are principal curvatures and c_0 the spontaneous curvature of the detergent inclusions. The detergent inclusions on the membrane are therefore modeled as patches of the membrane with given spontaneous curvature c_0 . The patches occupied by the detergents we set $c_0 > 0$ and elsewhere we assume a symmetric membrane $c_0 = 0$. Additionally, to account for associative nature of membrane inclusions, a step potential between neighboring curved inclusions is taken into account by an additional energy term:

$$W_d = -w \sum_{i < j} \mathcal{H}(r_0 - r_{ij}), \quad (2)$$

where w is a direct interaction constant, the sum runs over all detergent-detergent pairs, r_{ij} are their mutual in-plane distances, $\mathcal{H}(r)$ is the Heaviside step function and r_0 is the range of the direct interaction. We consider here attractive interactions $w > 0$ that induce phase-separation of the lipid bilayer.

In this work we set N_d of the total $N = 1447$ vertices to represent detergent domains (curved inclusions), which have spontaneous curvature c_0 that can be described well by the discrete mesh. All other vertices represent symmetric membrane and have zero spontaneous curvature. The positive sign of c_0 for curved inclusions indicates a tendency to curve the

membrane outwards. The density of curved inclusions on the membrane is given by a fraction:

$$\rho = \frac{N_d}{N}. \quad (3)$$

We presume that the detergent binds to the membrane in a gradual process, which is accounted for in the simulations by adding only a fraction of N_d into the mesh every 5 iterations and then succeeded by 2000 MC steps before the same fraction of curved inclusions are added. In each such step, the total energy $W = W_b + W_d$ is numerically minimized.

Simulation results shown in **Figure 2** reveal that detergents have a major effect on the lipid vesicle shape. At low interactions between detergent molecules (i.e. $w = 0.5$) the increasing detergent concentration decreased the flat membranes patches and the vesicle shape became irregular. The vertices of the irregular vesicle shape were composed mainly of the detergent molecules. At higher detergent concentrations ($\rho > 0.6$) the percolation threshold has been reached and the majority of the detergent molecules were interconnected.

When the association between the detergent molecules was high (i.e. $w = 2$) the shape of the lipid vesicle become distorted already at much lower detergent concentrations. The vesicle structure evolved quickly into lobed structure with increasing detergent concentration and vesicles had significantly increased surface-to-volume ratio. The detergent density was simulated from 0.28 to 0.8. Below $\rho = 0.28$ there was not enough curved detergent inclusions to have a significant effect on morphology and vesicles generally retain their quasi-spherical shape. On the other hand, we found that at $\rho > 0.8$ vesicle shapes become pronouncedly spiculated and branched, with high local curvature.

5. Discussion

Solubilization mechanisms are not completely understood and their use remains empirical even for systems of liposomes. The structural changes of liposomes induced by detergent solutions are known experimentally for some time and reveal that liposomes take various types of solubilization pathways depending on the types of lipids and detergents [9, 10]. In the present work, a possible mechanism of membrane structural changes seen in experiments with DOPC liposomes and TR detergent is presented within a simple Monte Carlo model of curved inclusions that can move over the membrane laterally and induce local curvature changes due to their molecular shape. This leads to a “rock-and-roll” dynamics seen in experiments before total solubilization and micellization of liposomes takes place. Morphology changes observed in experiments and simulations alike encompass symmetry breaking, resulting in protrusion growth and undulating geometries.

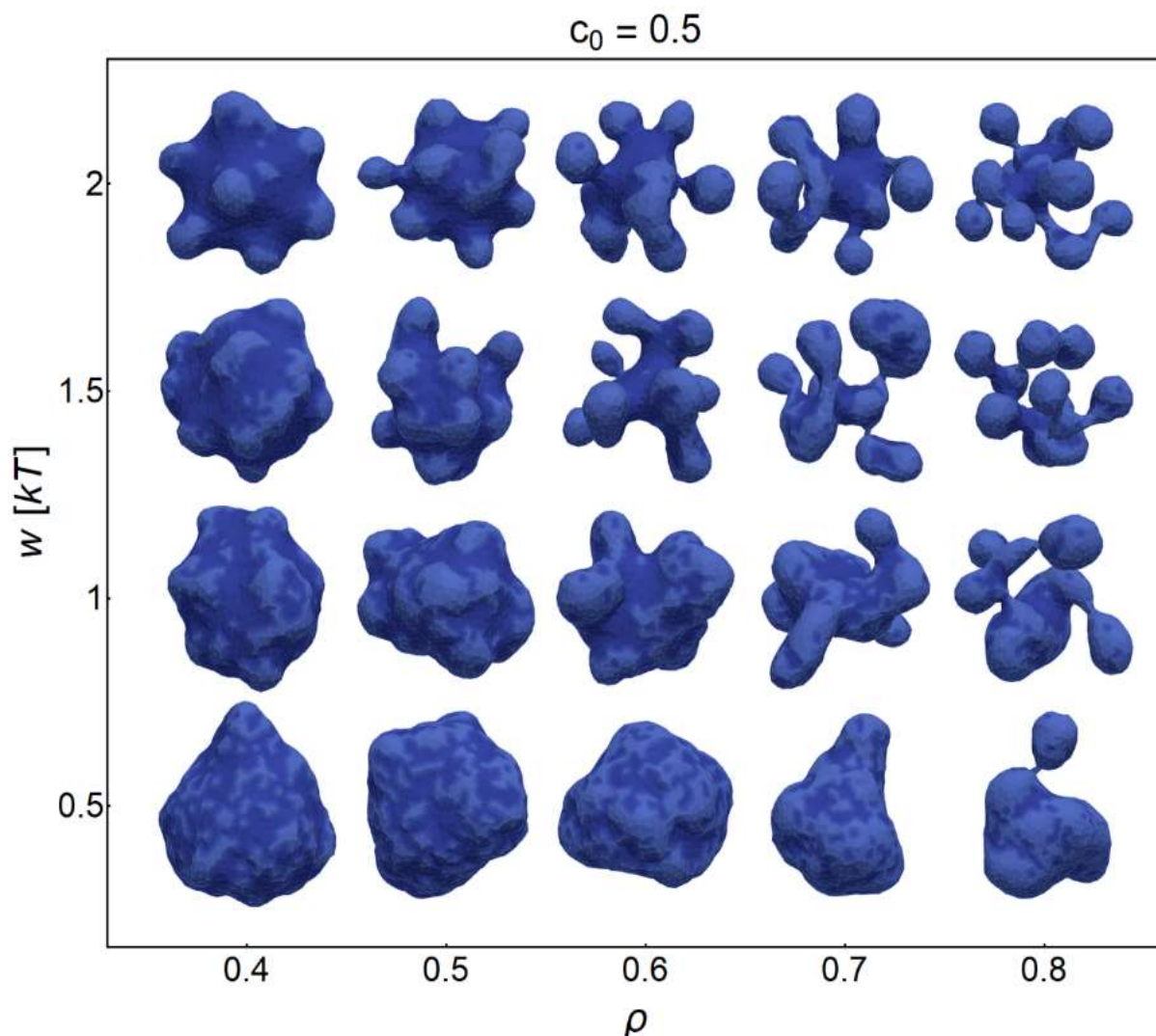


Figure 2. Final microstates of vesicles for gradual adding of curved inclusions (N_d) every 5 iterations for $c_0 = 0.5$. The patches of flat membrane with no spontaneous curvature are shown in dark blue, while the grey areas correspond to positive spontaneous curvature c_0 where curved inclusions are present.

6. Conclusions

In this work the interaction between DOPC GUVs and non-ionic detergent Triton X-100 was studied with an emphasis on the processes prior to solubilization. An intensive and dynamic changes of DOPC liposomes morphology were observed. A possible mechanism for such a dynamic process was proposed that is based on the geometrical and associative properties of the detergent molecules that are adsorbed and laterally diffuse across the lipid vesicle. A 3D Monte Carlo numerical simulations were used to study the phase space of metastable shapes and their dependence on detergent inclusion spontaneous curvature and the attraction between detergent molecules under non equilibrium detergent concentrations. It was found that the gradual addition of curved detergent inclusions predicts very well morphological shapes observed in experiment (spheroids, pears, undulations, lobes,

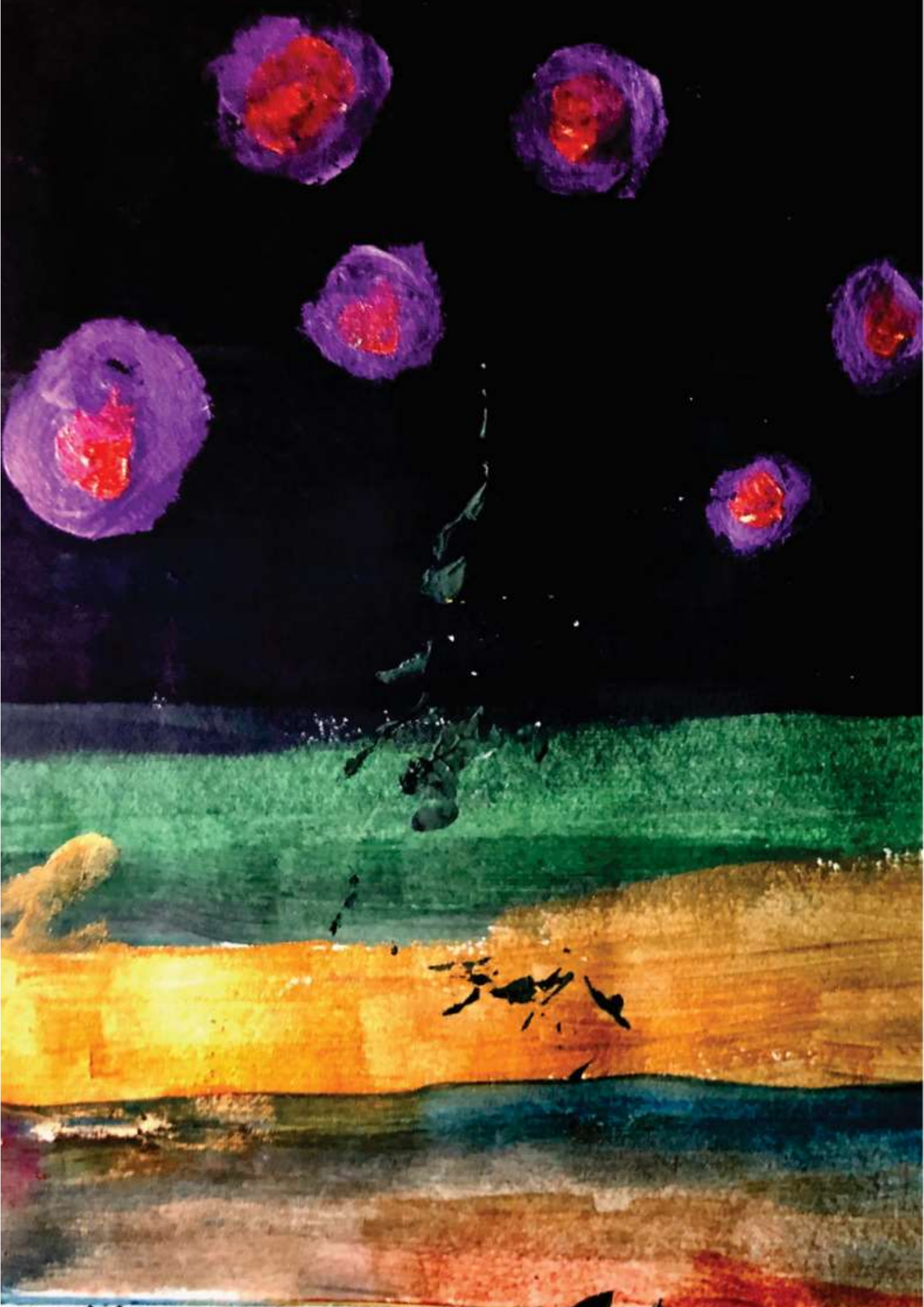
spicules, budding vesicles with thin necks connecting regions of quasi-spherical vesicles). The results are in line with the existing literature and shed a new light on the mechanical and dynamical aspects of the early stages of the solubilization process.

Acknowledgements

Authors acknowledge support of ARRS, grant J1-9162, P2-0232, P3-0388 and P4-0116.

References

1. Kumar, D., C.M. Richter, and C.M. Schroeder, *Conformational dynamics and phase behavior of lipid vesicles in a precisely controlled extensional flow*. *Soft Matter*, 2020. 16(2): p. 337-347.
2. Heerklotz, H. and R.M. Eppand, *The enthalpy of acyl chain packing and the apparent water-accessible apolar surface area of phospholipids*. *Biophysical journal*, 2001. 80(1): p. 271-279. Doi: 10.1016/S0006-3495(01)76012-2
3. Israelachvili, J., *Interactions of Biological Membranes and Structures*. Intermolecular Surface Forces, 3rd ed., Academic Press, San Diego, 2011.
4. Moscho, A., O. Orwar, D.T. Chiu, B.P. Modi, and R.N. Zare, *Rapid preparation of giant unilamellar vesicles*. *Proceedings of the National Academy of Sciences*, 1996. 93(21): p. 11443-11447. Doi: 10.1073/pnas.93.21.11443
5. Gompper, G. and D. Kroll, *Random surface discretizations and the renormalization of the bending rigidity*. *Journal de Physique I*, 1996. 6(10): p. 1305-1320. Doi: 10.1051/jp1:1996246
6. Gompper, G. and D. Kroll, *Triangulated-surface models of fluctuating membranes*, in *Statistical mechanics of membranes and surfaces*. 2004, World Scientific. p. 359-426. Doi: 10.1142/9789812565518_0012
7. Fošnarič, M., S. Penič, A. Iglič, V. Kralj-Iglič, M. Drab, and N.S. Gov, *Theoretical study of vesicle shapes driven by coupling curved proteins and active cytoskeletal forces*. *Soft Matter*, 2019. 15(26): p. 5319-5330. Doi: 10.1039/c8sm02356e
8. Helfrich, W., *Elastic properties of lipid bilayers: theory and possible experiments*. *Zeitschrift für Naturforschung C*, 1973. 28(11-12): p. 693-703. Doi: 10.1515/znc-1973-11-1209
9. Arnulphi, C., J. Sot, M. García-Pacios, J.-L.R. Arrondo, A. Alonso, and F.M. Goñi, *Triton X-100 partitioning into sphingomyelin bilayers at subsolubilizing detergent concentrations: effect of lipid phase and a comparison with dipalmitoylphosphatidylcholine*. *Biophysical journal*, 2007. 93(10): p. 3504-3514. <https://doi.org/10.1021/la011381c>
10. Tomita, T., T. Sugawara, and Y. Wakamoto, *Multitude of morphological dynamics of giant multilamellar vesicles in regulated nonequilibrium environments*. *Langmuir*, 2011. 27(16): p. 10106-10112. Doi: 10.1021/la2018456



Stability of normal red blood cells explained by membrane's in-plane ordering

¹Mesarec L*, ²Gózdź W, ^{1,3,4}Iglič A, ^{3,5}Kralj-Iglič V, ⁶Virga E G and ^{7,8}Kralj S

¹Laboratory of Biophysics, Faculty of Electrical Engineering, University of Ljubljana, 1000 Ljubljana, Slovenia

²Institute of Physical Chemistry, Polish Academy of Sciences, 01-224 Warsaw, Poland

³Laboratory of Mass Spectrometry and Proteomics, Institute of Biosciences and BioResources, National Research Council of Italy, Napoli 80132, Italy

⁴Laboratory of Clinical Biophysics, Faculty of Medicine, University of Ljubljana, 1000 Ljubljana, Slovenia

⁵Laboratory of Clinical Biophysics, Faculty of Health Sciences, University of Ljubljana, 1000 Ljubljana, Slovenia

⁶Department of Mathematics, University of Pavia, Via Ferrata 5, 27100 Pavia, Italy

⁷Department of Physics, Faculty of Natural Sciences and Mathematics, University of Maribor, 2000 Maribor, Slovenia

⁸Condensed Matter Physics Department, Jožef Stefan Institute, 1000 Ljubljana, Slovenia

*luka.mesarec@fe.uni-lj.si

Abstract

Red blood cells (RBCs) are present in almost all vertebrates. Their main function is the transport of oxygen to the body tissues. In almost all mammals, RBCs adopt discocyte (oblate) shape, which optimizes their flow properties in vessels and capillaries. As observed in experiments, stable discocytes range in a relatively broad window of relative volume values between $v \sim 0.58$ and $v \sim 0.8$. However, these observations are not supported by existing theoretical models, which predict stable discocyte RBC shapes only in a quite narrow interval between $v \sim 0.59$ and $v \sim 0.65$. We demonstrate that this interval is broadened if we take into account membrane's in-plane ordering. In our study, we model RBCs by using a hybrid Helfrich-Landau mesoscopic approach. We show that an extrinsic (deviatoric) curvature free energy term is crucial for explaining experimentally observed wide stability range of discocyte RBC shapes.

1. Introduction

Red blood cells (RBCs) play a vital role in all vertebrates. In mammals, their main role is to transport oxygen to all parts of a body's tissue. In normal conditions, RBCs have a biconcave (discocyte) shape, which can be transformed into other shapes, such as stomatocytes or spiculated echinocytes [1-8]. Optimal RBCs flow and their transport capabilities in "healthy" conditions depend on discocyte RBC shape [9], while in pathological conditions, a larger number of RBCs may have also stomatocyte or echinocyte shapes.

The key geometric parameter controlling the stability of closed membrane shapes such as cells and vesicles is the reduced volume $v = V/V_0$. Here V stands for the cell/vesicle volume and $V_0 = 4\pi R^3/3$ represents the volume of a sphere with the same surface area, where $R = \sqrt{A/4\pi}$ is the radius of the sphere and A the surface area of the cell/vesicle. In different mammals, the reduced volume values in healthy cells possess a relatively broad range [1,5,10,11]. In humans, the reduced volumes of discocyte RBCs range within the interval $v \in [0.58, 0.81]$ [1]. However, experimentally observed range of v values for which disk-like RBC shapes are stable cannot be reproduced using the existing theoretical approaches [4,7,12-15].

The Helfrich model predicts three qualitatively different RBC shapes upon varying of the reduced volume v , i.e. stomatocytes, oblate discocytes and prolate shapes [4,12]. Within that model, discocyte red blood cell shapes are stable only within a relatively narrow interval $v \in [0.59, 0.65]$. This window could be slightly widened by adding additional free energy contributions, for instance, by taking into account the bi-layer structure of the membrane [15-17]. However, the experimentally observed stability range of v for discocyte shapes has so far not been reproduced.

We will show that by taking into account in-plane ordering of membranes, it is possible to explain the experimentally observed broad stability window of v for discocyte shapes [18]. Biological membranes likely possess some degree of in-plane ordering, especially in highly and anisotropically curved membrane regions [19-21]. For example, nematic ordering might be present due to two flexible hydrocarbon chains of lipids [22-25] or to anisotropic Band 3 proteins embedded within membranes [19,20,26-28]. Nematic ordering in membranes may also occur due to membrane attached rod-like BAR domains [29]. Furthermore, the tails of lipid molecules in the bilayer may tilt relative to the surface normal and develop tilt and hexatic orientational ordering [30-32].

The effect of orientational ordering is primarily determined by intrinsic and extrinsic [33-35] curvature contributions to the elastic free energy. We show that the extrinsic term is crucial for explaining the broad stability window of discocyte RBC shapes [18]. In studies of biological cells, such terms were considered already previously and referred to as deviatoric terms [19-23,36-38].

2. Methods

We study axisymmetric closed surfaces, which exhibit nematic in-plane ordering. We refer to them as nematic vesicles. We use a 2D mesoscopic model in which the shape of the closed membrane is determined by the curvature tensor \underline{C} [4,12] and the orientational ordering is described by the 2D nematic tensor order parameter \underline{Q} [39,40]. These tensors are expressed as:

$$\underline{C} = C_1 \vec{e}_1 \otimes \vec{e}_1 + C_2 \vec{e}_2 \otimes \vec{e}_2, \quad (1)$$

$$\underline{Q} = \lambda (\vec{n} \otimes \vec{n} - \vec{n}_\perp \otimes \vec{n}_\perp). \quad (2)$$

The unit vectors $\{\vec{e}_1, \vec{e}_2\}$ determine a local principal curvature frame with principal curvatures $\{C_1, C_2\}$, $\lambda \in [0, 1/2]$ is the orientational order parameter, and \vec{n} is the nematic director field indicating the direction of a local in-plane ordering (states $\pm \vec{n}$ are physically equivalent). The total free energy density per surface area is expressed as [18]

$$f = f_H + f_c + f_e. \quad (3)$$

The first term $f_H = \frac{\kappa}{2} (Tr \underline{C})^2$ stands for the Helfrich curvature contribution [12], where κ represents a bending modulus. The second term $f_c = \alpha_0 (T - T^*) Tr \underline{Q}^2 + \frac{\beta}{4} (Tr \underline{Q}^2)^2$ is the nematic condensation contribution, which enforces nematic orientational order below a critical temperature T^* . The quantities α_0 and β are positive phenomenological constants. Below the critical temperature, the equilibrium degree of order is $\lambda_0 = \sqrt{\alpha_0 (T^* - T) / \beta}$. The elastic contribution f_e consists of the intrinsic, $f_{int} = \frac{1}{2} k_i |\nabla_s \underline{Q}|^2$, and extrinsic, $f_{ext} = k_e \underline{Q} \cdot \underline{C}^2$, contributions. Here, k_i and k_e represent intrinsic and extrinsic elastic constants, which we set to be positive, and ∇_s stands for the surface gradient operator [41]. The extrinsic (deviatoric) term has similar impact as an external ordering field, which is present in regions where $C_1 \neq C_2$. The essential characteristic material dependent length of the model is the nematic order parameter correlation length, which we express in the nematic phase as $\xi = \sqrt{k_i / (\alpha_0 (T^* - T))}$ [18].

3. Results

The stability range of oblate and prolate nematic vesicles within our model as a function of v is shown in Fig. 1. When the extrinsic (deviatoric) elasticity is neglected (dashed line), discocytes are stable within a relatively narrow window of v for all ratios k_i / κ . The stability window of discocyte and oblate shapes significantly widens when the extrinsic contribution is switched on (solid line in Fig. 1). For example, for $\frac{k_i}{\kappa} = 1.4$, discocyte shapes of red blood cells are stable up to the value $v \sim 0.83$, thus recovering the experimentally observed regime [18]. Broader stability range of discocytes in the presence of the extrinsic (deviatoric) term is a consequence of their unique shape.

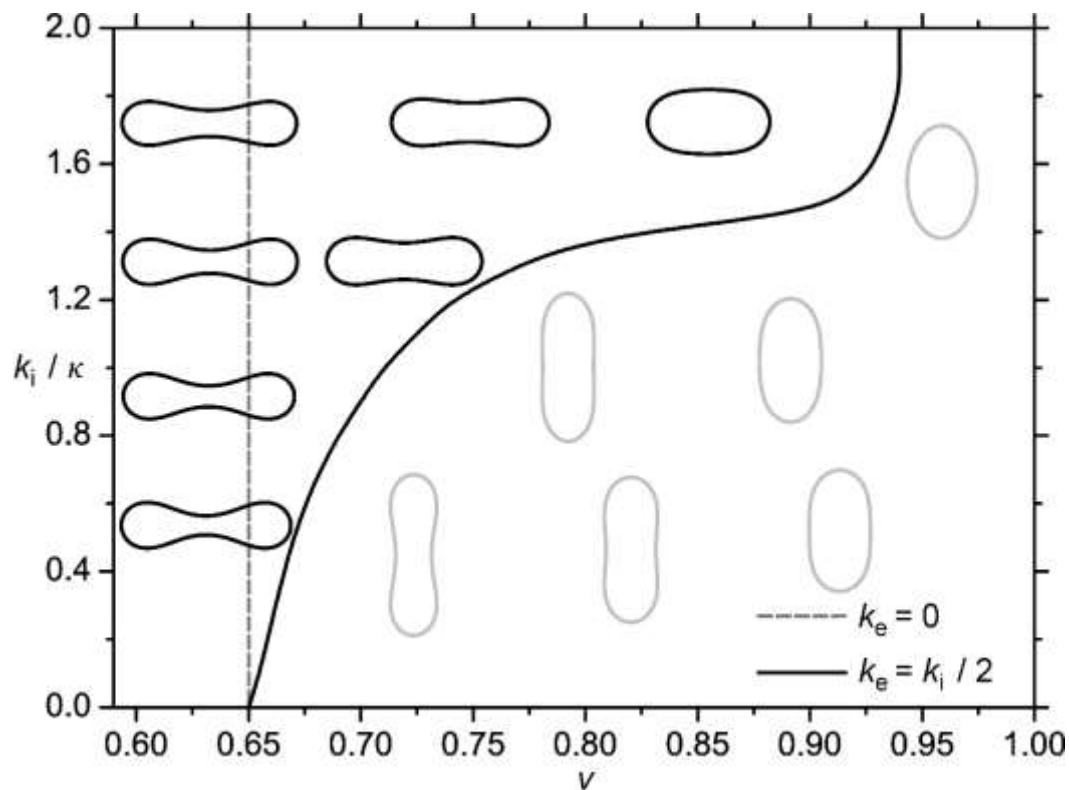


Figure 1. Phase diagram of nematic vesicles. The solid and dashed lines separate the stability regions of oblates and prolates for $k_e = k_i/2$ and $k_e = 0$, respectively. Stable shapes presented in the diagram are shown for different values of the reduced volume v and k_i/κ . $R/\xi = 7$. Adapted from [18].

In equatorial region of discocytes, there is a large difference between the principal curvatures C_1 and C_2 . Consequently, the extrinsic term enforces strong orientational order in that region, which contributes to the lower total free energy [18]. Such surface patches are therefore energetically favorable in the presence of the extrinsic (deviatoric) term. For this reason, discocyte shapes of red blood cells become energetically more favorable than prolate shapes in a wider window of v , which is clearly visible in Fig. 1 [18].

4. Discussion

We considered theoretically the stability of red blood cells focusing on the competition between prolates and oblates (discocytes). Existent theoretical models fail to explain a relatively broad range of relative volumes for which oblate discocyte shapes of red blood cells are experimentally observed. We demonstrate that taking into account the in-plane orientational ordering and extrinsic (deviatoric) curvature elasticity, the stability window of stable discocytes becomes comparable with experimentally observed values [18].

Acknowledgements

L.M., V.K.I., A.I. and S.K. acknowledge the financial support from the grants No. P2-0232, P3-0388, J5-7098, L7-7566, J2-8166 and P1-0099 from the Slovenian Research Agency (ARRS). V.K.I. and A.I. also acknowledge the funding from the European Union's Horizon 2020 research and innovation programme VES4US No. 801338. E.G.V. acknowledges the kind hospitality of the Oxford Centre for Nonlinear PDE, where part of this work was done while he was visiting the Mathematical Institute at the University of Oxford.

References

1. Canham, P. B. & Burton, A. C. Distribution of size and shape in populations of normal human red cells. *Circ. Res.* 22(3), 405-422 (1968). <https://doi.org/10.1161/01.RES.22.3.405>
2. Deuticke, B. Transformation and restoration of biconcave shape of human erythrocytes induced by amphiphilic agents and changes of ionic environment. *Biochim. Biophys. Acta* 163, 494-500 (1968). [https://doi.org/10.1016/0005-2736\(68\)90078-3](https://doi.org/10.1016/0005-2736(68)90078-3)
3. Brecher, G. & Bessis, M. Present status of spiculated red cells and their relationship to the discocyte-echinocyte transformation: critical review. *Blood* 40, 333-344 (1972). <https://doi.org/10.1182/blood.V40.3.333.333>
4. Deuling, H. J. & Helfrich, W. Red blood cell shapes as explained on the basis of curvature elasticity. *Biophys. J* 16(8), 861-868 (1976). Doi: 10.1016/S0006-3495(76)85736-0
5. Fung, Y. C., Tsang, W. C. & Patitucci, P. High-resolution data on the geometry of red blood cells. *Biorheology* 18(3-6), 369-385 (1981). Doi: 10.3233/BIR-1981-183-606
6. Igljč, A. A possible mechanism determining the stability of spiculated red blood cells. *J. Biomech.* 30(1), 35-40 (1997). [https://doi.org/10.1016/S0021-9290\(96\)00100-5](https://doi.org/10.1016/S0021-9290(96)00100-5)
7. Gerald Lim, H. W, Wortis, M. & Mukhopadhyay, R. Stomatocyte-discocyte-echinocyte sequence of the human red blood cell: Evidence for the bilayer-couple hypothesis from membrane mechanics. *PNAS* 99(26), 16766-16769 (2002). <https://doi.org/10.1073/pnas.202617299>
8. Kumar, G., Ramakrishnan, N. & Sain, A. Tubulation pattern of membrane vesicles coated with biofilaments. *Phys. Rev. E* 99(2), 022414 (2019). <https://doi.org/10.1103/PhysRevE.99.022414>
9. Bryngelson, S. H. & Freund, J. B. Global stability of flowing red blood cell trains. *Phys. Rev. Fluids* 3(7), 073101 (2018). <https://doi.org/10.1103/PhysRevFluids.3.073101>
10. Gruber, W. & Deuticke, B. Comparative aspects of phosphate transfer across mammalian erythrocyte membranes. *J. Membr. Biol.* 13(1), 19-36 (1973). <https://doi.org/10.1007/BF01868218>
11. Emmons, W. F. The interrelation of number, volume, diameter and area of mammalian erythrocytes. *J. Physiol.* 64(3), 215-228 (1927). Doi: 10.1113/jphysiol.1927.sp002431
12. Helfrich, W. Elastic properties of lipid bilayers: theory and possible experiments. *Z. Naturforsch. C* 28(11-12), 693-703 (1973). <https://doi.org/10.1515/znc-1973-11-1209>
13. Seifert, U., Berndl, K. & Lipowsky, R. Shape transformations of vesicles: Phase diagram for spontaneous-curvature and bilayer-coupling models. *Phys. Rev. A* 44(2), 1182 (1991). <https://doi.org/10.1103/PhysRevA.44.1182>
14. Canham, P. B. The minimum energy of bending as a possible explanation of the biconcave shape of the human red blood cell. *J. Theor. Biol.* 26(1), 61-81 (1970). [https://doi.org/10.1016/S0022-5193\(70\)80032-7](https://doi.org/10.1016/S0022-5193(70)80032-7)

15. Evans, E. A. Bending resistance and chemically induced moments in membrane bilayers. *Biophys. J.* 14(12), 923-931 (1974). [https://doi.org/10.1016/S0006-3495\(74\)85959-X](https://doi.org/10.1016/S0006-3495(74)85959-X)
16. Sheetz, M. P. & Singer, S. J. Biological membranes as bilayer couples. A molecular mechanism of drug-erythrocyte interactions. *PNAS* 71(11), 4457-4461 (1974). <https://doi.org/10.1073/pnas.71.11.4457>
17. Helfrich, W. Blocked lipid exchange in bilayers and its possible influence on the shape of vesicles. *Z. Naturforsch. C* 29(9-10), 510-515 (1974). <https://doi.org/10.1515/znc-1974-9-1010>
18. Mesarec, L., Gózdź, W., Iglíč, A., Kralj-Iglíč, V., Virga, E. G., & Kralj, S. Normal red blood cells' shape stabilized by membrane's in-plane ordering. *Sci. Rep.* 9(1), 1-11 (2019). <https://doi.org/10.1038/s41598-019-56128-0>
19. Kralj-Iglíč, V., Svetina, S. & Žeks, B. Shapes of bilayer vesicles with membrane embedded molecules. *Eur. Biophys. J.* 24, 311-321 (1996). <https://doi.org/10.1007/BF00180372>
20. Fournier, J. B. Nontopological saddle-splay and curvature instabilities from anisotropic membrane inclusions. *Phys. Rev. Lett.* 76(23), 4436 (1996). <https://doi.org/10.1103/PhysRevLett.76.4436>
21. Kralj-Iglíč V., Heinrich V., Svetina S. & Žeks B. Free energy of closed membrane with anisotropic inclusions. *Eur. Phys. J. B* 10, 5-8 (1999). <https://doi.org/10.1007/s100510050822>
22. Kralj-Iglíč, V., Babnik, B., Gauger, D. R., May, S. & Iglíč, A. Quadrupolar ordering of phospholipid molecules in narrow necks of phospholipid vesicles. *J. Stat. Phys.* 125, 727–752 (2006). <https://doi.org/10.1007/s10955-006-9051-9>
23. Mareš, T. *et al.* Role of phospholipid asymmetry in the stability of inverted hexagonal mesoscopic phases. *J. Phys. Chem. B* 112(51), 16575-16584 (2008). <https://doi.org/10.1021/jp805715r>
24. Perutková, Š. *et al.* Elastic deformations in hexagonal phases studied by small-angle X-ray diffraction and simulations. *Phys. Chem. Chem. Phys.* 13(8), 3100-3107 (2011). <https://doi.org/10.1039/C0CP01187H>
25. Alimohamadi, H., Vasan, R., Hassinger, J., Stachowiak, J. & Rangamani, P. The role of traction in membrane curvature generation. *Biophys. J.* 114(3), 600a (2018). <https://doi.org/10.1091/mbc.E18-02-0087>
26. Wang, D. N. Band 3 protein: structure, flexibility and function. *FEBS Lett.* 346(1), 26-31 (1994). [https://doi.org/10.1016/0014-5793\(94\)00468-4](https://doi.org/10.1016/0014-5793(94)00468-4)
27. Delaunay, J. The molecular basis of hereditary red cell membrane disorders. *Blood Rev.* 21(1), 1-20 (2007). <https://doi.org/10.1016/j.blre.2006.03.005>
28. Reithmeier, R. A. *et al.* Band 3, the human red cell chloride/bicarbonate anion exchanger (AE1, SLC4A1), in a structural context. *BBA Biomembranes* 1858(7), 1507-1532 (2016). <https://doi.org/10.1016/j.bbamem.2016.03.030>
29. Mesarec, L., Gózdź, W., Kralj-Iglíč, V., Kralj, S. & Iglíč, A. Closed membrane shapes with attached BAR domains subject to external force of actin filaments. *Colloids Surf., B* 141, 132-140 (2016). <https://doi.org/10.1016/j.colsurfb.2016.01.010>
30. Smith, G. S., Sirota, E. B., Safinya, C. R. & Clark, N. A. Structure of the L β phases in a hydrated phosphatidylcholine multimembrane. *Phys. Rev. Lett.* 60(9), 813 (1988). <https://doi.org/10.1103/PhysRevLett.60.813>
31. Helfrich, W. & Prost, J. Intrinsic bending force in anisotropic membranes made of chiral molecules. *Phys. Rev. A* 38(6), 3065 (1988). <https://doi.org/10.1103/PhysRevA.38.3065>
32. Lubensky, T. C. & Prost, J. Orientational order and vesicle shape. *J. Phys. II* 2(3), 371-382 (1992). <https://doi.org/10.1051/jp2:1992133>

33. Kamien, R. D. The geometry of soft materials: a primer. *Rev. Mod. Phys.* 74, 953 (2002). <https://doi.org/10.1103/RevModPhys.74.953>
34. Selinger, R. L. B., Konya, A., Travasset, A. & Selinger, J. V. Monte Carlo studies of the XY model on two-dimensional curved surfaces. *J. Phys. Chem. B* 115, 13989-13993 (2011). <https://doi.org/10.1021/jp205128g>
35. Napoli, G. & Vergori, L. Extrinsic curvature effects on nematic shells. *Phys. Rev. Lett.* 108, 207803 (2012). <https://doi.org/10.1103/PhysRevLett.108.207803>
36. Kralj-Iglič, V., Iglič, A., Hägerstrand, H. & Peterlin, P. Stable tubular microexovesicles of the erythrocyte membrane induced by dimeric amphiphiles. *Phys. Rev. E* 61, 4230 (2000). <https://doi.org/10.1103/PhysRevE.61.4230>
37. Kralj-Iglič, V., Remškar, M., Vidmar, G., Fošnarič, M. & Iglič, A. Deviatoric elasticity as a possible physical mechanism explaining collapse of inorganic micro and nanotubes. *Phys. Lett. A* 296, 151–155 (2002). [https://doi.org/10.1016/S0375-9601\(02\)00265-7](https://doi.org/10.1016/S0375-9601(02)00265-7)
38. Iglič, A., Babnik, B., Gimsa, U. & Kralj-Iglič, V. On the role of membrane anisotropy in the beading transition of undulated tubular membrane structures. *J. Phys. A: Math. Gen.* 38, 8527 (2005). <https://doi.org/10.1088/0305-4470/38/40/004>
39. Kralj, S., Rosso, R. & Virga, E. G. Curvature control of valence on nematic shells. *Soft Matter* 7, 670–683 (2011). <https://doi.org/10.1039/C0SM00378F>
40. Rosso, R., Virga, E. G. & Kralj, S. Parallel transport and defects on nematic shells. *Continuum Mech. Therm.* 24, 643–664 (2012). <https://doi.org/10.1007/s00161-012-0259-4>
41. Virga, E. G. Curvature potentials for defects on nematic shells. Lecture notes, Isaac Newton Institute for Mathematical Sciences, Cambridge. (2013).

BROWN DARK
KOHINOOR



Towards implementation of numerical model for anisotropic inclusions into the phospholipid bilayer for Monte Carlo simulations

Penič S^{1,*}, Drab M², Kralj-Iglič V³, Iglič A²

¹University of Ljubljana, Faculty of Electrical Engineering, Laboratory of Bioelectromagnetics, Ljubljana, Slovenia

²University of Ljubljana, Faculty of Electrical Engineering, Laboratory of Physics, Ljubljana, Slovenia

³University of Ljubljana, Faculty of Health Sciences, Laboratory of Clinical Biophysics, Ljubljana, Slovenia

[*samo.penic@fe.uni-lj.si](mailto:samo.penic@fe.uni-lj.si)

Abstract

Monte Carlo simulations software of triangulated network phospholipid bilayer membrane model, called Trisurf is used for investigation of biophysical phenomena in biological cells. One of the important features is capability of modelling rigid membrane inclusions (such as proteins) that have bent shape (curved proteins). They induce local change in curvature of the bilayer and can influence the properties and working of the membrane. There is a limitation however, that is the inclusion curvature must be isotropic, meaning that it has same values for both principal curvatures. To overcome the limitation a new model for energy calculation is proposed and discussed. With changed method of calculating local principal curvatures of the membrane, the simulations of the anisotropic curved inclusions will be possible with some performance degradation.

1. Introduction

The main building block of the biological membrane is the lipid bilayer with embedded inclusions like proteins, glycolipids and many other biologically active components [1, 2]. These inclusions induce local curvature changes of the membrane resulting in a global change of cell shape [3,4,5]. Membrane shape depends on the intrinsic shape of membrane constituents and their interaction with other constituents. Many proteins and other molecules that have anisotropic intrinsic curvature can be found in membranes [6,7]. Monte Carlo simulations based on triangulated surface model of the membrane is useful tool for investigation of phenomena of the membrane physics. Current model of simulation software Trisurf currently in use, allow modelling of inclusion that have only isotropic intrinsic curvature [8]. This limitation greatly lowers usability of the simulator. In this article, the advanced theoretical model for energy calculations for anisotropic inclusions is presented. With this addition to the energy terms calculation, the usability of the simulator will be extended, where many of the current features will not be changed or removed. Drawbacks of the proposed approach will be discussed.

2. Methods

Monte Carlo (MC) triangulated mesh was used to numerically model and investigate the vesicle shape and the lateral distribution of membrane inclusions by means of computer simulations [8]. Phospholipid bilayer membranes can be treated due to their small thickness in the first approximation as a two dimensional surface, allowing the continuum approach in the theoretical description of membrane surfaces [9]. In the model we discretize the membrane into patches consisting of many molecules (**Figure 1**). A single patch is represented by a vertex in a triangulated surface model. The main model parameter that defines mechanical bilayer properties is bending stiffness.

The vesicle is represented by a set of N vertices that are linked by bonds of flexible length d to form a closed, randomly triangulated, self-avoiding network [10, 11]. The lengths of the tethers can vary between a minimal (d_{min}) and a maximal (d_{max}) value. The self-avoidance of the network can be implemented by ensuring that no vertex can penetrate through the triangular network. The maximal possible random displacement of the vertex in a single step (s), should be small enough so that the fourth vertex cannot move through the plane of the other three to the minimal allowed distance, d_{min} , from the three vertices. In our scenario, we use $s=0.15 d_{min}$ and $d_{max}=1.7 d_{min}$. For details about the expressions to calculate self-avoidance constraint d_{max} , see [12].

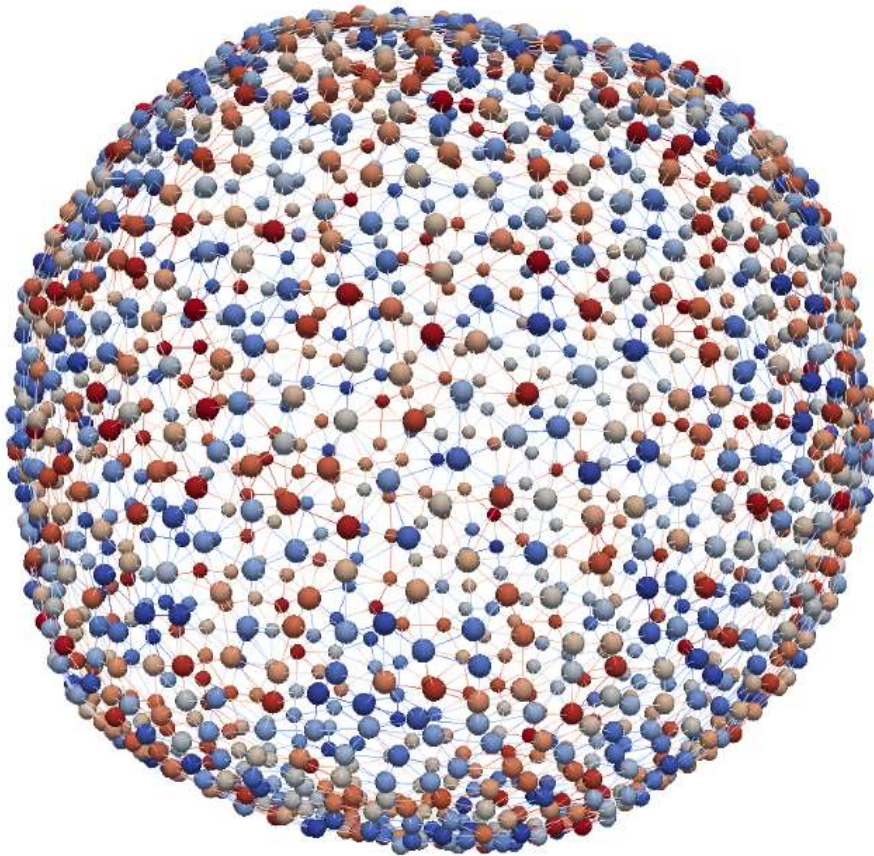


Figure 1: Triangulated network of vertices with their connection for thermalized semi-spherical vesicle. The color represents the vertex index. This allows visual following the mixing of the vertices.

The initial state of triangulated surface is a pentagonal bipyramid with all the edges divided into equilateral bonds so that the network is composed of $3(N-2)$ bonds forming $2(N-2)$ triangles. N_c randomly selected vertices are given non-zero isotropic intrinsic curvature of c_0 , thus they become the model of the membrane inclusion. The rest of the vertices have zero intrinsic curvature. Positive curvature means that the membrane will locally bulge towards the exterior, negative curvature will force the membrane to bulge towards the interior compartment of the vesicle.

The system is developed into the thermal equilibrium state. The evolution of the system is measured in Monte Carlo sweeps (mcs). One mcs consists of individual attempts to displace each of the N vertices by a random increment in the sphere with radius s – the action we will refer to as a vertex move. Membrane fluidity is maintained by flipping bonds within the triangulated network.

In each mcs, the vertex move attempts are followed by a $3N$ attempts to flip a randomly chosen bond. A single bond flip involves the four vertices of two neighboring triangles. The tether between the two vertices is cut and re-established between the other two, previously

unconnected vertices (a detailed description was published elsewhere [13]). Each individual Monte Carlo step (vertex move shown in **Figure 2** or bond flip shown in **Figure 3**) is accepted with probability according to Metropolis Hastings algorithm, based on free energy change due to the Monte Carlo step.

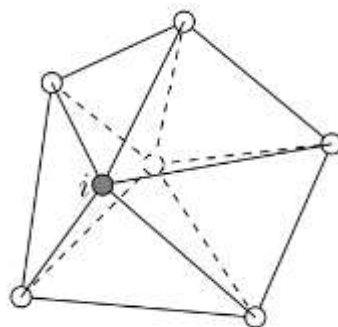


Figure 2. Part of the Monte Carlo step: moving a vertex. The i -th vertex is moved within the limits of size of the step s .

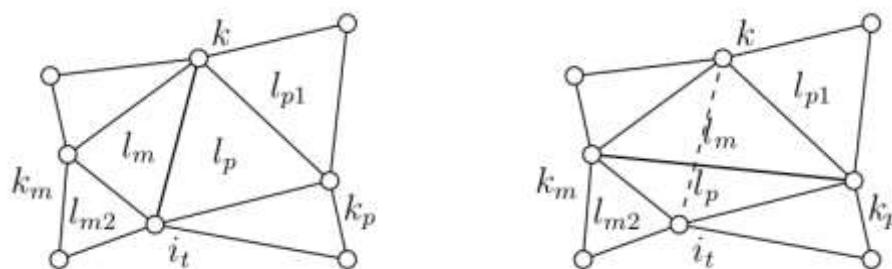


Figure 3. Part of the Monte Carlo step: flipping a bond. The chosen bond is flipped. The connection between i_t and k -th vertex is severed and a new connection between k_m and k_p is generated to keep the topology constant. Triangles that are annotated with l change their neighbor relationships.

For the bending energy W_b of the membrane, we use the standard Helfrich expression for a tensionless membrane with a term that represents intrinsic curvature of isotropic inclusions [14].

The membrane keeps fixed topology, thus the contribution of the Gaussian curvature to the change of bending energy is cancelled out.

$$W_b = \frac{\kappa}{2} \oint_A (c_1 + c_2 - c_0)^2 dA, \quad (1)$$

where κ is the bending stiffness of the membrane, c_1 , c_2 and c_0 are the two principal curvatures and the isotropic intrinsic curvature of the vesicle membrane at the point under consideration. The integration is performed over the membrane area A .

3. Results

Currently the simulator permits only calculations of the vesicle where the inclusions have isotropic intrinsic curvatures. There is a major deficiency in the algorithm that can acquire only the sum of principal curvatures ($c_1 + c_2$) and not individual values of c_1 and c_2 . This design choice was made in the past, because in this way the energy calculations can be done much faster than evaluating each principal curvature individually.

The proposed change in the algorithm will extend its capabilities to calculations of both principal curvatures local to the given vertex and will lead towards simulations. The Helfrich expression given in eq. 2 can now be rewritten:

$$W_b = \frac{\kappa}{2} \oint_A ((c_1 - c'_0)^2 + (c_2 - c''_0)^2) dA. \quad (3)$$

The intrinsic curvatures c'_0 and c''_0 in the equation above represents the two principal curvatures of the inclusion.

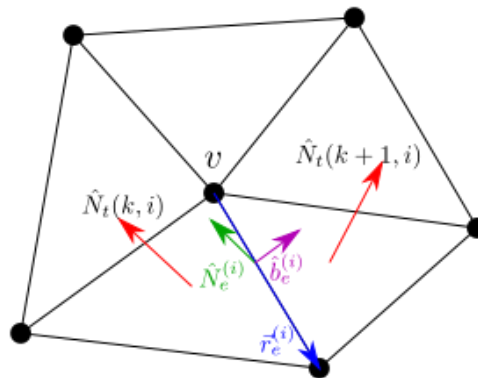


Figure 4: Patch of the membrane with triangles around vertex v . Red vectors represent normal to the triangle and green vector is normal at the vertex, whereas binormal is colored purple.

The proposed algorithm works in three parts. In first part, the chosen vertex v is taken into the consideration together with neighboring vertices and triangles that the vertex v belongs to (see **Figure 4**). The bond (or edge) vectors from vertex v to each of its neighbors i is defined with their local vectors as

$$\vec{r}_e^{(i)} = \vec{R}_v - \vec{R}^{(i)}. \quad (4)$$

The normal of the edge can furthermore be expressed as averaged and normalized normal of corresponding triangles \hat{N}_t that share this edge (triangles are denoted with indexes k and $k + 1$, as they are listed in the simulator internal data structure in this order)

$$\hat{N}_e^{(i)} = \frac{\hat{N}_t(k,i) + \hat{N}_t(k+1,i)}{\|\hat{N}_t(k,i) + \hat{N}_t(k+1,i)\|}. \quad (5)$$

Edge binormal (see figure 4) is expressed by using vector along the bond $\vec{r}_e^{(i)}$ and $\widehat{N}_e^{(i)}$

$$\widehat{b}_e^{(i)} = \widehat{N}_e^{(i)} \times \vec{r}_e^{(i)}. \quad (6)$$

Last expression of the first part is the normal defined at the vertex v

$$\widehat{N}_v = \frac{\sum_k A_t^{(k)} \widehat{N}_t^{(k)}}{\left\| \sum_k A_t^{(k)} \widehat{N}_t^{(k)} \right\|}, \quad (7)$$

where $A_t^{(k)}$ is the area of the k -th triangle that belong to the vertex v and $\widehat{N}_t^{(k)}$ triangle's normal.

With expressions above, the shape operators are defined in second step of the procedure. Firstly the tensor that is shape operator of the edge is expressed using the angle Φ as shown in **Figure 5**:

$$\underline{S}_e^{(i)} = 2 \left\| \vec{r}_e^{(i)} \right\| \cos(\Phi(e)^{(i)}/2) \cdot \left[\widehat{b}_e^{(i)} \otimes \widehat{b}_e^{(i)} \right]. \quad (8)$$

Additionally, the projection to tangent plane is expressed as inner product of vertex normal by itself

$$\underline{P}_v = \underline{1} - \left[\widehat{N}_v \otimes \widehat{N}_v \right], \quad (9)$$

and finally the vertex vector operator as

$$\underline{S}_v = \frac{1}{A_v} \sum_i \widehat{N}_v \cdot \widehat{N}_e^{(i)} \cdot \underline{P}_v^T \cdot \underline{S}_e^{(i)} \cdot \underline{P}_v, \quad (10)$$

Where A_v is the area belonging to the vertex v that is expressed as $\frac{1}{3}$ of a sum of all the triangles touching the vertex

$$A_v = \frac{1}{3} \sum_k A_t^{(k)}. \quad (11)$$

In the last step, the principal curvatures are acquired as eigenvalues of the vertex shape operator \underline{S}_v .

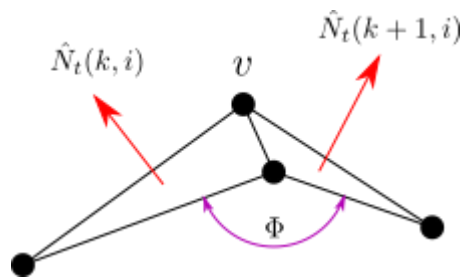


Figure 5: Two neighboring triangles that share same vertex v . The angle Φ used to calculate edge operator is the angle between two triangle normals.

4. Discussion

The described algorithm for acquiring individual local principal curvatures at each vertex in the triangulated network will extend the functionality and usability of the simulation software. The result will be used for bending energy calculations in Monte Carlo, allowing simulations of the inclusions (such as proteins) with anisotropic intrinsic curvatures. Its major drawback is in its complexity which will result in prolonged simulation times, therefore it is not recommended in situations where the inclusion have isotropic shapes or in situations the inclusions are not present. In these two cases the existing algorithm is proposed.

Acknowledgements

This project has received funding from the European Union's Horizon 2020 research and innovation programme under grant agreement No. 801338 (VES4US project). The authors also acknowledge the financial support from the grants No. P2-0232, P3-0388, J1-9162 and J2-8166 from the Slovenian Research Agency (ARRS).

References

1. Cevc G, Marsh D. Phospholipid bilayers: physical principles and models. Wiley, 1987.
2. Israelachvili JN. Intermolecular and surface forces. Academic press, 1997.
3. Szleifer I, Kramer D, Ben-Shaul A, Gelbart WB, Safran SA. Molecular theory of curvature elasticity in surfactant films. J Chem Phys 1990, 92: 6800–6817. <https://doi.org/10.1063/1.458267>
4. C. Nielsen C, Goulian M, Andersen OS. Energetics of inclusion-induced bilayer deformations. Biophys J 1998, 74: 1966–1983. DOI: 10.1016/S0006-3495(98)77904-4
5. Fošnarič M, Bohinc K, Gauger DR, Igljič A, Kralj-Igljič V, May S. The influence of anisotropic membrane inclusions on curvature elastic properties of lipid membranes. J Chem Inf Model 2005, 45: 1652–1661. <https://doi.org/10.1021/ci050171t>.
6. Singer SJ, Nicolson GL. The fluid mosaic model of the structure of cell membranes. Science 1972, 175: 720–731. DOI: 10.1126/science.175.4023.720
7. Gómez-Llobregat J, Elías-Wolff F, Lindén M. Anisotropic membrane curvature sensing by amphipathic peptides. Biophys J 2016, 110: 197–204. DOI: 10.1016/j.bpj.2015.11.3512
8. Fosnarič M, Penič S, Igljič A, Kralj-Igljič V, Drab M, Gov N. Theoretical study of vesicle shapes driven by coupling curved proteins and active cytoskeletal forces. Soft Matter 2019, 15: 5319-5330. DOI: 10.1039/C8SM02356E

9. Noguchi H. Membrane simulation models from nanometer to micrometer scale. *J. Phys. Soc. Japan* 2009, 78:041007-. <https://doi.org/10.1143/JPSJ.78.041007>
10. Gompper G, Kroll DM. Triangulated-surface models of fluctuating membranes. In: Nelson D, Piran T, Weinberg S editors. *Statistical mechanics of membranes and surfaces*. Singapore, World Scientific, 2004, pp. 359-426.
11. Gompper G, Kroll DM. Random surface discretizations and the renormalization of the bending rigidity. *J de Physique I* 1996, 6:1305-20. <https://hal.archives-ouvertes.fr/jpa-00247247>
12. Fošnarič M, Penič S, Iglič A, Bivas I. Thermal Fluctuations of Phospholipid Vesicles Studied by Monte Carlo Simulations. In: Iglič A, Genova J editors. *Advances in Planar Lipid Bilayers and Liposomes*. Academic Press, Elsevier, 2013, pp. 331-357.
13. Penič S, Iglič A, Bivas I, Fošnarič M. Bending elasticity of vesicle membranes studied by Monte Carlo simulations of vesicle thermal shape fluctuations. *Soft matter* 2015, 11:5004-9. DOI: 10.1039/C5SM00431D
14. Helfrich W. Elastic properties of lipid bilayers: theory and possible experiments. *Z Naturforsch C* 1973: 28:693-703. DOI: 10.1515/znc-1973-11-1209



Impact of Physical Effort on Cellular Nanovesicle Concentration

Jan Z^{1,*}, Bedina Zavec A², Benčina M³, Drab M⁴, Drašler Barbara⁵, Drobne D⁵, Hočevar M⁶, Krek JL¹, Pađen L¹, Pajnič M¹, Repar N⁵, Šimunič B⁷, Štukelj R¹, Kralj-Iglič V¹

¹University of Ljubljana Faculty of Health Sciences, Laboratory of Clinical Biophysics, Ljubljana, Slovenia

²National Institute of Chemistry, Department of Molecular Biology and Nanobiotechnology, Ljubljana, Slovenia

³National Institute of Chemistry, Department of Synthetic Biology and Immunology, Ljubljana, Slovenia

⁴University of Ljubljana, Faculty of Electrical Engineering. Laboratory of Physics, Ljubljana, Slovenia

⁵University of Ljubljana, Biotechnical Faculty, Nanobiology and Nanotoxicology group, Ljubljana, Slovenia

⁶Institute of Metals and Technology, Ljubljana, Slovenia

⁷Institute for Kinesiology Research, Science and Research Centre Koper, Koper, Slovenia

*zala.jan@gmail.com

Abstract

Cellular nanovesicles (CNVs), that are shed from cells, have been recognized as promising indicators of health status. In the study presented here we studied possible change of CNV concentration in isolates from peripheral blood samples and concomitant change of some physiological state-related blood parameters that reflect response to inflammation and stress (cholinesterase (ChE) and Glutathione S-transferase (GST) activity, interleukin 6 (IL-6) and tumor necrosis factor alpha(TNF-alpha) concentrations). We compared these quantities two days before and >15 hours after long distance running. We discuss the applicability of CNVs concentration and ChE activity as indicators of the response of human body to physiological stress and inflammation after physical effort. Understanding these mechanisms and using the knowledge in planning of physical activities will decrease risk for adverse effects of physical effort and improve physical performance in various fields, including recreational and competitive sport. Also, understanding the effects of physical activity on the assessment of CNVs in isolates will improve the repeatability and accuracy of CNV-based diagnostic and therapeutic methods by instructing the blood donors how to prepare for blood sampling.

1. Introduction

Regular physical effort, especially aerobic exercise, offers protection against all-cause morbidity and mortality, elevates the metabolic rate and increases oxygen consumption by the entire body, particularly by locomotive muscles [1]. Physical effort also results in adaptation of endocrine, cardiovascular and immune systems to oxidative stress [2] and inflammation [3,4] caused by physical effort. Due to stress and immune response mechanisms during the exercise, several tissues release molecules into the blood stream, with the aim to mediate stress-related effects throughout the whole body [5].

“Cellular Nanovesicles” is the term for sub-micron sized membrane-enclosed fragments that can be found in isolates from different body fluids, in our work [6] isolates from blood. A related term “Extracellular Vesicles (EVs)” is defined as a generic term for particles naturally released from the cell that are delimited by a lipid bilayer and cannot replicate [7]. EVs, discharged into the circulation could assist with disposal of cellular waste products generated under stress conditions and help the cells to preserve homeostasis [8]. EV formation by cells is considered a physiological process [9] that can be accelerated by oxidative stress [10] and by inflammation process [4]. EVs may have an important role in microvascular [11], skeletal muscle and systemic [9] adaptation to physical effort. Physical effort enhances also other physiological state-related parameters that reflect inflammation and stress response of human body [12], such as ChE [13] and GST [2] activity as well as the concentrations of cytokines [4,14] and C-reactive protein (CRP) [3] in the blood samples. Lipogram parameters and blood cell parameters are also of interest, in particular due to possible interference with concentration of EVs isolated from peripheral blood and possible risk for thromboembolism. It has been previously shown that the concentration of EVs in peripheral blood correlates with total blood cholesterol and the prandial state of the individuals [15].

2. Materials and methods

27 volunteers (15 females, 12 males), aged from 24 to 62, were included in the study. Blood was collected twice: First, two days before the marathon, when all of the participants were pre-prandial for at least 8 hours, and second >15 and <22 hours after the marathon, when the participants were pre-prandial for at least 10 hours. Cellular nanovesicles were isolated by repetitive centrifugation and washing of samples and assessed by flow cytometer with 405 nm, 488 nm, and 640 nm air-cooled lasers. Flow cytometer was calibrated using the MACSQuant Calibration Beads, 2 μm and 3 μm in size. The presence of CNVs and residual cells was determined within the forward scatter parameters and side scatter parameters (FFC and SSC axes on the scatterplot, respectively, **Figure 1**).

To adjust the channels and set the gate, 460 nm beads were used as a reference to the CNVs in the plasma sample. For all channel settings, the hyper log (hlog) settings were selected. The threshold or trigger on side scatter parameters (SSC) was set to 4 and secondary trigger was shut off. Events in buffer (PBS citrate) were measured and excluded as the background.

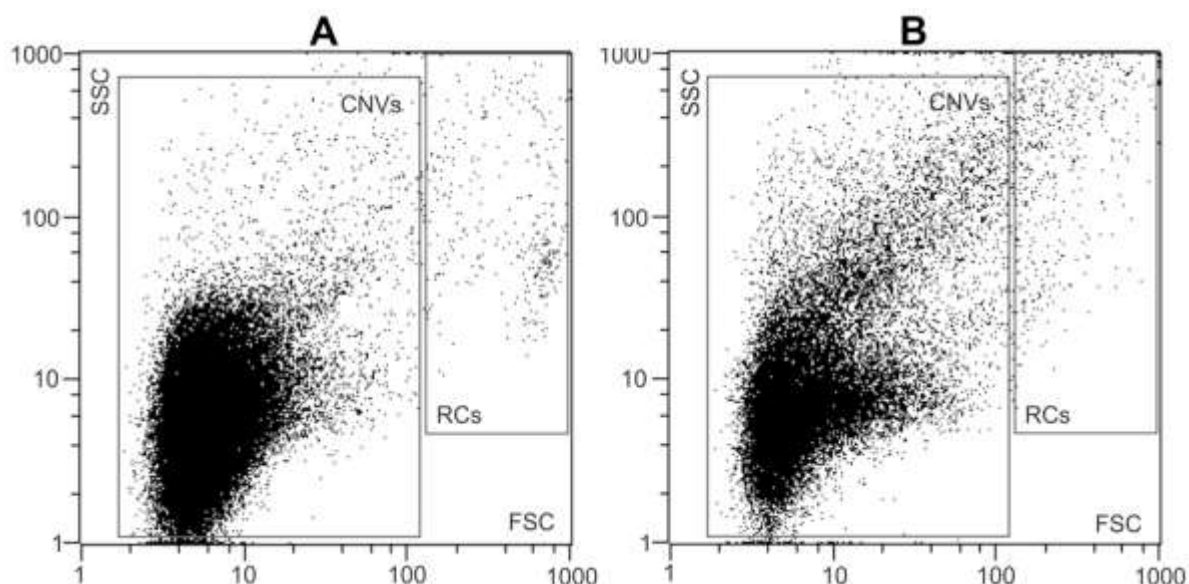


Figure 1 Gating strategy for the analysis of CNVs by FCM. 2D-plot of typical CNV isolates, prepared from blood plasma of a donor before (A) and after (B) the marathon. Gating of the CNVs and residual cells (RCs) was as indicated. The total number of events in the CNVs gate were taken [6]. Abbreviations: CNVs, cellular nano vesicles; RCs, residual cells; FCM, Flow Cytometry; FSC, forward scatter; SSC, side scatter. From [6].

Also, isolates from blood were fixed and previously validate using scanning electron microscopy (SEM). Interleukin-6 and (IL-6) Tumor necrosis factor- α (TNF- α) concentrations were measured using enzyme-linked immunosorbent assay (ELISA). Standard blood parameters were measured in the diagnostic laboratory.

3. Results

CNV isolates were visualized by SEM [16,17]. A typical image of the isolate is shown in **Figure 2**. The shapes of the particles have characteristics of membrane-enclosed vesicles [17]. Immunolabeling showed that the CNVs obtained by this method carry receptors that are found in membranes of endothelial cells, platelets, and erythrocytes [16].

More than 15 hours after physical effort a decrease was found in CNVs' concentration in isolates from blood (46%; $p < 0.05$), in ChE activity in whole blood (47%; $p < 0.001$), in plasma (34%; $p < 0.01$), and in erythrocyte suspension (54%; $p < 0.001$), as well as in GST activity in erythrocyte suspension (16%; $p < 0.01$) and in IL-6 concentration in plasma (63%; $p < 0.05$). We found no change in GST activity in plasma and in TNF- α concentration in plasma. Results can be seen in **Figure 3**. Correlations (> 0.8 ; $p < 0.001$) between CNVs' concentration and ChE activity, and GST activity, respectively, in erythrocyte suspension were found.

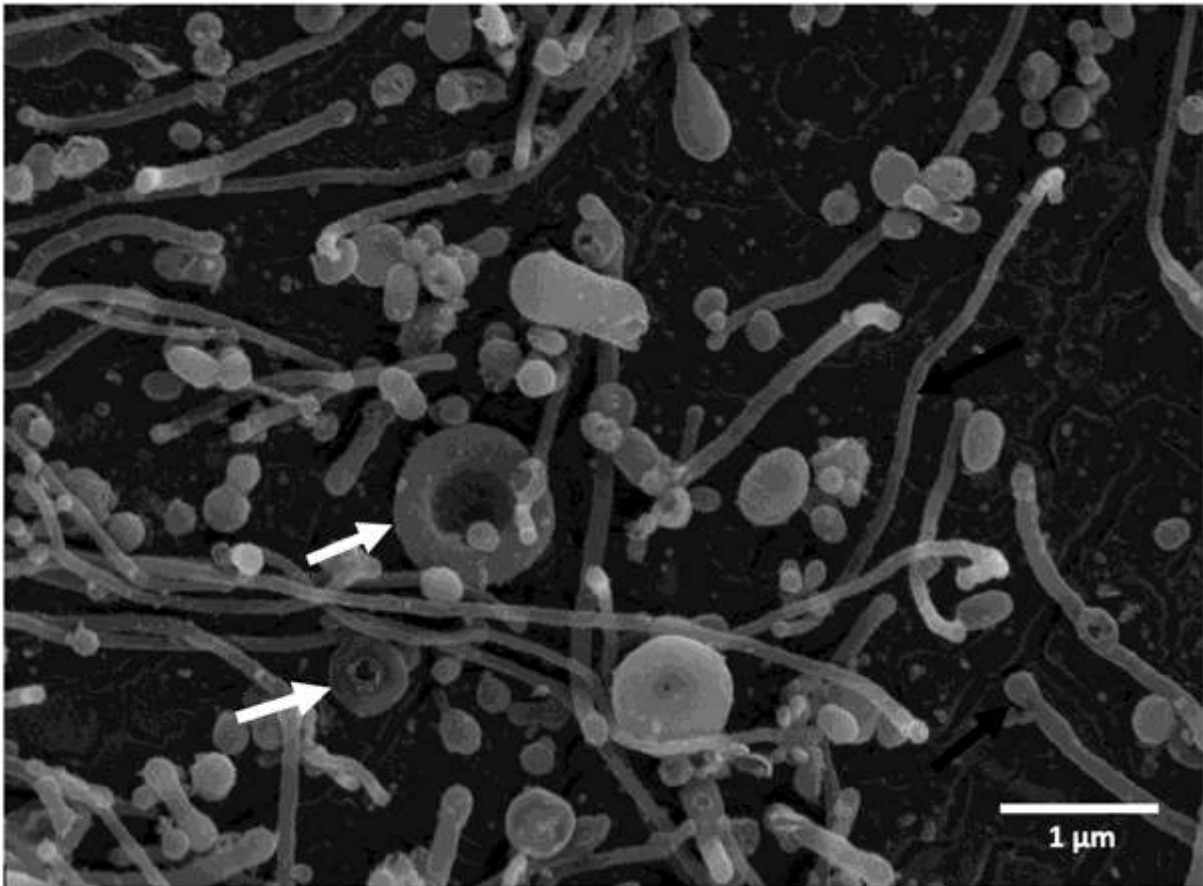


Figure 2. Scanning electron micrograph of a typical isolate of CNVs from the blood plasma sample with characteristic shapes of particles without internal structures including spheres, tubules (black arrows), and tori (white arrows). No residual cells are observed in the figure. From [6].

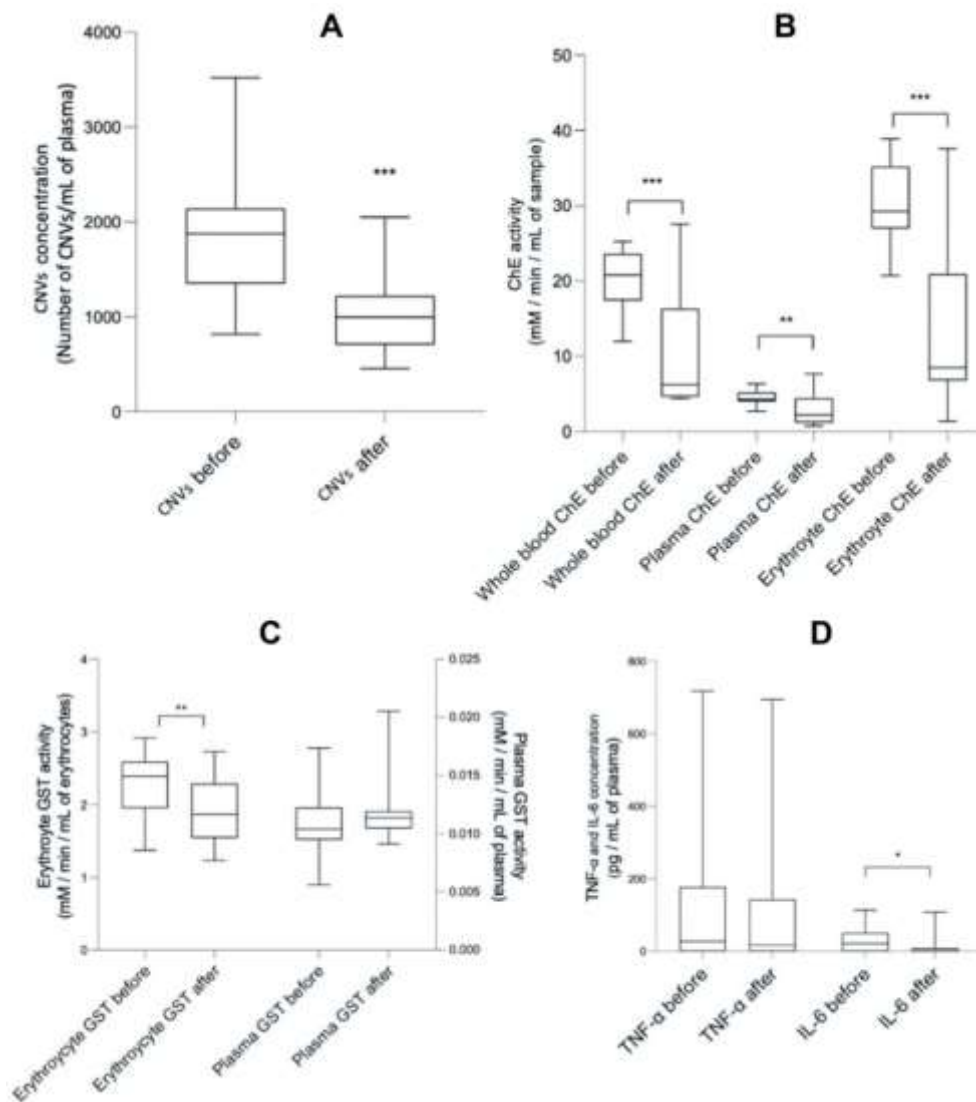


Figure 3. The effect of physical effort on concentration of microparticles and measured physiological state-related parameters in blood. (A) CNVs concentration in 1 mL plasma samples two days before and >15 hours after physical effort. (B) Activity of ChE (n=24) (in mM/min/mL of sample) two days before and >15 hours after physical effort in plasma, erythrocyte suspension and whole blood samples. (C) Activity of GST (n=24) (in mM/min/mL of sample) in plasma and erythrocyte suspension samples two days before and >15 hours after physical effort. Scale on the left represents values of plasma GST activity and scale on the right represents values of erythrocyte suspension GST activity. (D) Concentration of IL-6 and TNF- α (n=26) (in pg/mL of plasma) two days before and >15 hours after physical effort. Statistical differences before and after physical effort at: * $p < 0.05$, ** $p < 0.01$ and *** $p < 0.001$. From [6]. Abbreviations: CNVs, cellular nanovesicles; ChE, cholinesterase; GST, Glutathione S-transferase; TNF- α , tumor necrosis factor; IL-6 -interleukin 6.

4. Discussion

According to most of the previous reports, physical effort causes an increase in concentration of CNVs during or immediately after the effort [8, 18-20]. Yet, according to our results, the concentration of Cellular nanovesicles in isolates decreases after the rest and may reach values lower than initial. Evidence on GST in connection with physical effort is limited in previous studies. Connection between GST activity in erythrocyte suspension and concentration of CNVs in blood isolates, as shown in our study, can indicate a decrease in oxidative stress >15 hours after recovery period [21].

Connection between ChE activity in erythrocyte suspension and concentration of CNV was previously considered in other studies [22-25]. Our results suggest that ChE is a potential indicator of the response of human body to physiological stress and inflammation after physical effort, since ChE activity was lower after >15 hours of rest concomitantly with CNVs. We found decrease in IL-6 concentration in blood plasma samples after >15 hours of rest. Previous studies [3,4,26] report elevated plasma IL-6 concentration and connect the elevation with running intensity, duration and level of fitness. Plasma TNF- α concentration was not changed after >15 hours of rest and that is similar to previously reported results [27].

5. Conclusion

We obtained lower concentration of CNVs in isolates from peripheral blood >15 hours after physical effort with lower values of other measured physiological state-related parameters: whole blood, plasma and erythrocyte suspension ChE activity, erythrocyte suspension GST activity and IL-6 plasma concentrations. This suggests that CNVs concentration and ChE activity have the potential to indicate impact of physical effort on inflammation in the human body. Also, concentration of the measured parameters depends on the duration of recovery period. According to previous reports, physical effort causes an increase in concentration of CNVs, but according to our results, the concentration of CNVs in isolates decreases after rest and may reach values lower than initial ones. With this, our study provides novel insights into the beneficial effects of physical effort on the human body and guidance about physical effort for donors before blood collection in procedures focusing on CNV-containing diagnostic and therapeutic compounds.

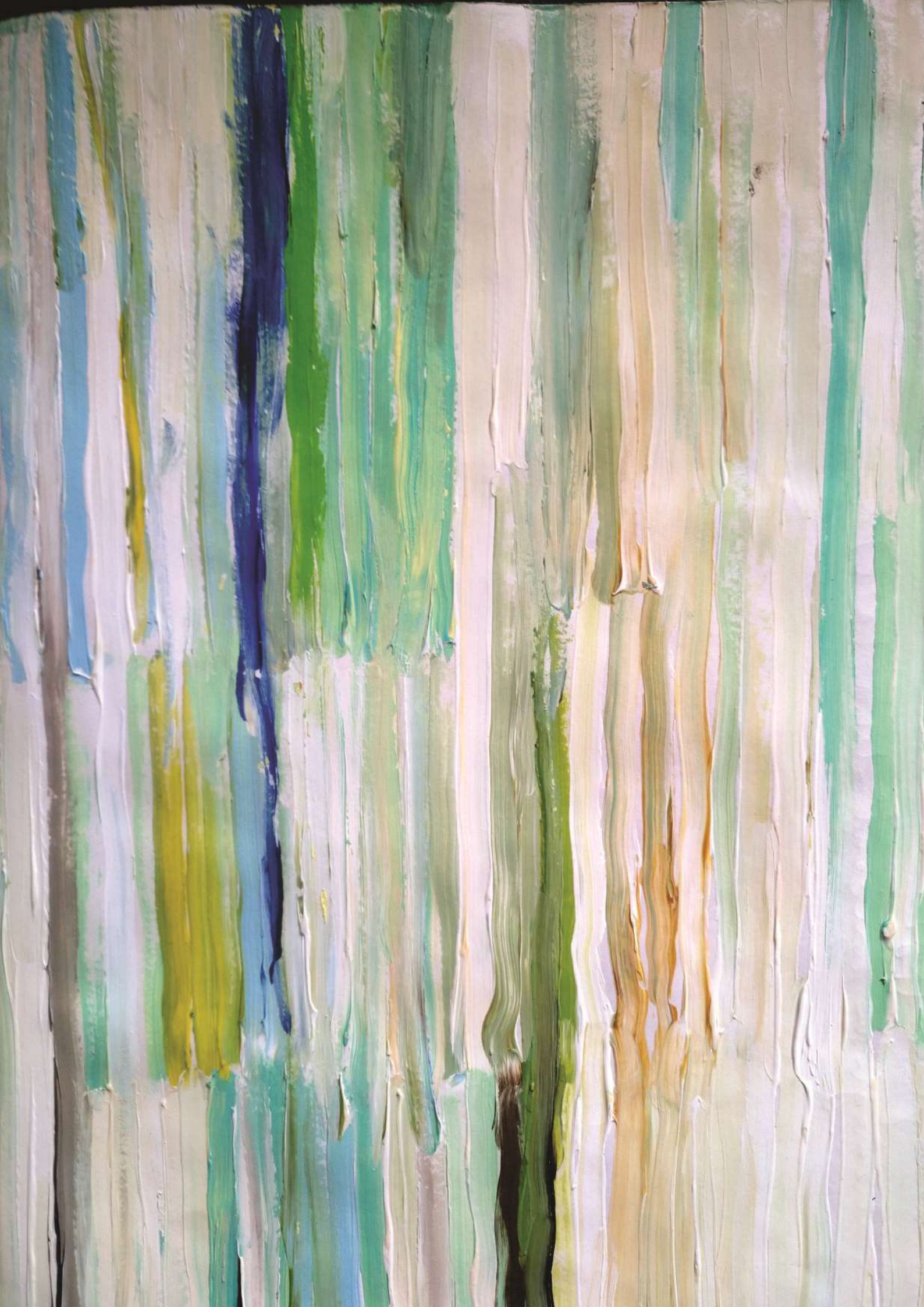
Acknowledgments

Authors acknowledge support from EU Commission (Ves4us) and Slovenian Research 770 Agency (P3-0388, P2-9232, P1-0132, J1-9162, L3-2621, J5-7098).

References

1. Whitham M, Parker BL, Friedrichsen M, et al. Extracellular Vesicles Provide a Means for Tissue Crosstalk during Exercise. *Cell Metab.* 01 2018;27(1):237-251.e4. doi:10.1016/j.cmet.2017.12.001
2. Evelo CT, Palmen NG, Artur Y, Janssen GM. Changes in blood glutathione concentrations, and in erythrocyte glutathione reductase and glutathione S-transferase activity after running training and after participation in contests. *Eur J Appl Physiol Occup Physiol.* 1992;64(4):354-8. doi:10.1007/bf00636224
3. Mendham AE, Donges CE, Liberts EA, Duffield R. Effects of mode and intensity on the acute exercise-induced IL-6 and CRP responses in a sedentary, overweight population. *Eur J Appl Physiol.* Jun 2011;111(6):1035-45. doi:10.1007/s00421-010-1724-z
4. Chaar V, Romana M, Tripette J, et al. Effect of strenuous physical exercise on circulating cell-derived microparticles. *Clin Hemorheol Microcirc.* 2011;47(1):15-25. doi:10.3233/CH-2010-1361
5. Brahmer A, Neuberger E, Esch-Heisser L, et al. Platelets, endothelial cells and leukocytes contribute to the exercise-triggered release of extracellular vesicles into the circulation. *J Extracell Vesicles.* 2019;8(1):1615820. doi:10.1080/20013078.2019.1615820
6. Jan Z, Drab M, Drobne D, et al. Decrease in Cellular Nanovesicles Concentration in Blood of Athletes More Than 15 Hours After Marathon. *Int J Nanomedicine.* 2021; 6:1-14. doi: 10.2147/IJN.S282200.
7. Witwer KW, Théry C. Extracellular vesicles or exosomes? On primacy, precision, and popularity influencing a choice of nomenclature. *J Extracell Vesicles.* 2019;8(1):1648167. doi:10.1080/20013078.2019.1648167
8. Frühbeis C, Helmig S, Tug S, Simon P, Krämer-Albers EM. Physical exercise induces rapid release of small extracellular vesicles into the circulation. *J Extracell Vesicles.* 2015;4:28239. doi:10.3402/jev.v4.28239
9. Morshed A, Karawdeniya BI, Bandara YMND, Kim MJ, Dutta P. Mechanical characterization of vesicles and cells: A review. *Electrophoresis.* Jan 2020;doi:10.1002/elps.201900362
10. Borrás C, Mas-Bargues C, Sanz-Ros J, et al. Extracellular vesicles and redox modulation in aging. *Free Radic Biol Med.* Mar 2020;149:44-50. doi:10.1016/j.freeradbiomed.2019.11.032
11. Rakobowchuk M, Ritter O, Wilhelm EN, et al. Divergent endothelial function but similar platelet microvesicle responses following eccentric and concentric cycling at a similar aerobic power output. *J Appl Physiol (1985).* Apr 2017;122(4):1031-1039. doi:10.1152/jappphysiol.00602.2016
12. Liem RI, Onyejekwe K, Olszewski M, et al. The acute phase inflammatory response to maximal exercise testing in children and young adults with sickle cell anaemia. *Br J Haematol.* Dec 2015;171(5):854-61. doi:10.1111/bjh.13782
13. Chamera T, Spieszny M, Klocek T, et al. Post-Effort Changes in Activity of Traditional Diagnostic Enzymatic Markers in Football Players' Blood. *J Med Biochem.* Apr 2015;34(2):179-190. doi:10.2478/jomb-2014-0035
14. Petersen AM, Pedersen BK. The anti-inflammatory effect of exercise. *J Appl Physiol (1985).* Apr 2005;98(4):1154-62. doi:10.1152/jappphysiol.00164.2004
15. Eichner NZM, Gilbertson NM, Musante L, et al. An Oral Glucose Load Decreases Postprandial Extracellular Vesicles in Obese Adults with and without Prediabetes. *Nutrients.* Mar 2019;11(3)doi:10.3390/nu11030580

16. Štukelj R, Schara K, Bedina-Zavec A, et al. Effect of shear stress in the flow through the sampling needle on concentration of nanovesicles isolated from blood. *Eur J Pharm Sci.* Feb 2017;98:17-29. doi:10.1016/j.ejps.2016.10.007
17. Suštar V, Bedina-Zavec A, Stukelj R, et al. Post-prandial rise of microvesicles in peripheral blood of healthy human donors. *Lipids Health Dis.* Mar 2011;10:47. doi:10.1186/1476-511X-10-47
18. Augustine D, Ayers LV, Lima E, et al. Dynamic release and clearance of circulating microparticles during cardiac stress. *Circ Res.* Jan 2014;114(1):109-13. doi:10.1161/CIRCRESAHA.114.301904
19. Wilhelm EN, González-Alonso J, Parris C, Rakobowchuk M. Exercise intensity modulates the appearance of circulating microvesicles with proangiogenic potential upon endothelial cells. *Am J Physiol Heart Circ Physiol.* 11 2016;311(5):H1297-H1310. doi:10.1152/ajpheart.00516.2016
20. Sossdorf M, Otto GP, Claus RA, Gabriel HH, Lösche W. Cell-derived microparticles promote coagulation after moderate exercise. *Med Sci Sports Exerc.* Jul 2011;43(7):1169-76. doi:10.1249/MSS.0b013e3182068645
21. Neefjes VM, Evelo CT, Baars LG, Blanco CE. Erythrocyte glutathione S transferase as a marker of oxidative stress at birth. *Arch Dis Child Fetal Neonatal Ed.* Sep 1999;81(2):F130-3. doi:10.1136/fn.81.2.f130
22. Yarana C, St Clair DK. Chemotherapy-Induced Tissue Injury: An Insight into the Role of Extracellular Vesicles-Mediated Oxidative Stress Responses. *Antioxidants (Basel).* Sep 2017;6(4)doi:10.3390/antiox6040075
23. Cantin R, Diou J, Bélanger D, Tremblay AM, Gilbert C. Discrimination between exosomes and HIV-1: purification of both vesicles from cell-free supernatants. *J Immunol Methods.* Sep 2008;338(1-2):21-30. doi:10.1016/j.jim.2008.07.007
24. Johnstone RM, Adam M, Hammond JR, Orr L, Turbide C. Vesicle formation during reticulocyte maturation. Association of plasma membrane activities with released vesicles (exosomes). *J Biol Chem.* Jul 1987;262(19):9412-20.
25. Park IW, He JJ. HIV-1 is budded from CD4+ T lymphocytes independently of exosomes. *Virology.* Sep 2010;7:234. doi:10.1186/1743-422X-7-234
26. Liao Z, Jaular LM, Soueidi E, et al. Acetylcholinesterase is not a generic marker of extracellular vesicles. *J Extracell Vesicles.* 2019;8(1):1628592. doi:10.1080/20013078.2019.1628592
27. Timmerman KL, Flynn MG, Coen PM, Markofski MM, Pence BD. Exercise training-induced lowering of inflammatory (CD14+CD16+) monocytes: a role in the anti-inflammatory influence of exercise? *J Leukoc Biol.* Nov 2008;84(5):1271-8. doi:10.1189/jlb.0408244



Preparation of platelet- and extracellular vesicle-rich gel and its role in the management of cerebrospinal fluid leak in anterior and lateral skull-base surgery

Vozel D^{1,2,*}, Battelino S^{1,2}

¹University Medical Centre Ljubljana, Department of Otorhinolaryngology and Cervicofacial Surgery, Ljubljana, Slovenia

²University of Ljubljana, Faculty of Medicine, Ljubljana, Slovenia

*domen.vozel@kclj.si

Abstract

Platelet- and extracellular vesicle-rich plasma (PVRP) is a blood-derived product with the concentrations of platelets and extracellular vesicles (EVs) above the blood levels. Moreover, EVs are believed to possess the PVRP's leading regenerative roles since they are essential mediators of inter- and intracellular communication. PVRP has been named inconsistently, e.g. as platelet-rich plasma (PRP), platelet-rich fibrin (PRF), platelet concentrate, platelet-rich growth factors, platelet-rich fibrin matrix and platelet-rich gel due to different methods of preparation, activation and analyses. Taken nomenclature aside, autologous PVRP has been applied in various medical specialities, including in otorhinolaryngology, head & neck surgery (ORL-HNS). Despite that, there is a lack of comparable randomised controlled clinical studies. This article presents autologous PVRP and platelet- and extracellular vesicle-rich gel (PVRG) preparation protocols and autologous PVRG's role in skull-base surgery, performed by ORL-HNS. Since the autologous PVRG can provide a watertight seal and induce osteogenesis, the mini-review presents PVRG's role in skull-base reconstruction via anterior and lateral approaches.

1. Platelet- and extracellular vesicle-rich plasma and gel

1.1 Definitions

Platelet- and extracellular vesicle-rich plasma (PVRP) is defined as a blood-derived product with platelet and EV concentrations higher than in blood. In a strict sense, PVRP is a liquid preparation that can be transformed into a PVRG (i.e. platelet- and extracellular vesicle-rich gel) via the coagulation cascade's activation with different substances [1].

Despite the strict definition, PVRP's terminology is inconsistent due to different preparation methods, activation and analyses. Accordingly, it has been named as platelet-rich plasma, platelet concentrate, platelet-rich fibrin, platelet-rich fibrin matrix, platelet-rich growth factors, platelet gel etc. [1]

The PVRP's main regenerative functions are believed to be exhibited by platelets and especially extracellular vesicles (EVs) [2]. These roles enable introducing PVRP and PVRG in the treatment of various diseases covered by otorhinolaryngology, head & neck surgery (ORL-HNS).

If the blood donor and PVRP acceptor is the same person, the PVRP is autologous. Otherwise, it is heterologous. Adverse reactions to PVRP-based treatment are infrequent. There is a minute risk of malignant or infectious disease transmission or causing a rejection reaction, especially by heterologous PVRP [3].

1.2 Preparation basics

PVRP preparation protocols can be classified according to the blood fraction from which the PVRP is prepared. Namely, the PVRP preparation protocol can be plasma-based or buffy coat-based. Plasma-based protocols yield higher PVRP volume, lower leukocyte and lower platelet concentrations compared to buffy coat-based protocols (Figure 1) [1].

Moreover, PVRP can be prepared by one-stepped or multiple-stepped centrifugation of blood fractions. The majority of commercially available kits utilise one-stepped plasma-based PVRP preparation protocols. These kits advantageously provide the closed system to prevent sample contamination. However, non-commercial multiple-stepped plasma-based centrifugation methods can yield higher platelet concentrations compared to commercial kits. To prevent contamination, strict measures need to be undertaken.

To prepare PVRP, anticoagulated tubes must be used to collect blood. If not, the blood clots, but the preparation cannot be defined as PVRG. ACD (acid citrate dextrose solution) or sodium citrate can be used as anticoagulants in PVRP preparation. The sodium citrate is recommended since it stimulates the proliferation of mesenchymal stromal cells without interfering with their phenotype and enables more concentrated PVRP [4]. It is not recommended to collect blood in EDTA tubes, because EDTA irreversibly inactivates thrombocytes [5]. After PVRP is prepared, it can be administered to the target tissue where it activates endogenously via interaction with type I collagen. The activation process results in the release of numerous growth factors from platelet and EVs granules [1].

On the other hand, PVRP can be activated before administration with different substances (i.e., activators) which activate coagulation cascade. This results in PVRG formation, which can be laid over or under the target tissue or defect. The activators are components of coagulation cascade: e.g. CaCl_2 , thrombin and other coagulation factors. CaCl_2 is used to calcify blood but can lower the pH if administered in too high concentration. Therefore, it is important to titrate the CaCl_2 . The activation can be achieved with the blood serum, which contains the components of the coagulation cascade. It is essential to keep in mind that the glass activates this cascade, also. Anticoagulant or antithrombotic drugs hamper PVRP gel production [1].

Instant freezing and storing of PVRP at $-80\text{ }^\circ\text{C}$ for up to 1 month do not decrease some growth factors after thawing according to the McClain and McCarrel (2019) [6]. On the other side, freezing at $-20\text{ }^\circ\text{C}$ for up to two weeks reduces some growth factor levels according to the Hosnuter et al. (2017) [7]. Roffi et al. (2014) concluded that one freeze/thaw cycle at $-30\text{ }^\circ\text{C}$ (for 2 hours) and $37\text{ }^\circ\text{C}$, respectively, sufficiently preserves PVRP quality and ability to promote regeneration via stimulation of chondrocytes and synoviocytes [8]. To sum up, PVRP cryopreservation remains controversial, so far, and clinical studies are required to determine the efficacy of PVRP and PVRG after different freeze/thaw cycles. Nevertheless, PVRP freezing enables administration of PVRP during surgical procedures with the expected gross blood volume loss, which restricts any additional blood collection.

Since the PVRG preparation protocol is an extension of the PVRP preparation protocol, the latter is described first.

1.3 Platelet- and extracellular vesicle-rich plasma preparation protocol

Our multiple-stepped plasma-based PVRP preparation protocol is as follows:

1. Blood is drawn into four 4.5 mL tubes with sodium citrate anticoagulant (9 NC sodium citrate 0.105 M, BD Vacutainer, Becton Dickinson, USA, stored at room temperature) (9 NC sodium citrate 0.105 M, BD Vacutainer, Becton Dickinson, USA, stored at room temperature) using a 21 G wing needle (Safety-Lok Blood Collection Set, BD Vacutainer, Becton Dickinson, USA). Tubes must be full.
2. Soft spin centrifugation (i.e., 5 minutes, $300\times g$, $18\text{ }^\circ\text{C}$) of blood tubes to distinguish two fractions: haematocrit (red layer in the bottom) and plasma with platelets (yellow upper layer). Occasionally a buffy coat (thin opaque whitish layer of leukocytes on top of haematocrit) could be observed.
3. Plasma directly above the buffy coat is transferred by a sterile pipette into a sterile polypropylene tube. Caution is required to prevent mixing layers, i.e., disruption of haematocrit and buffy coat and consequent leukocyte and erythrocyte harvesting.
 - 3.1. Haematocrit can be centrifuged with soft spin (i.e., additional soft spin) if higher PVRP volume is required.
 - 3.2. The harvested plasma yielded with soft spins is merged
4. Harvested plasma is equally distributed among two sterile polypropylene tubes (i.e., plasma from two blood tubes is distributed in one sterile polypropylene tubes)
5. Hard spin centrifugation (i.e., 17 minutes, $700\times g$, $18\text{ }^\circ\text{C}$) to sediment the platelets in plasma.

6. The upper half of the centrifuged plasma (i.e., platelet-poor plasma) is carefully removed and discarded without disruption of layers.
7. The remaining pellet is resuspended in the remaining volume of plasma (Fig. 3, Panel 5B) in the same tube to produce PVRP
8. The whole PVRP is pooled in a larger tube.

Then, PVRP is administered to the target tissue or activated to produce the PVRG.

1.4 Platelet- and extracellular vesicle-rich gel preparation protocol

Our PVRP preparation protocol is an extension of the PVRP preparation protocol (i.e., step 8) and follows these steps:

9. 1M CaCl₂ (14.7%, Pharmacy of University Medical Centre Ljubljana, stored at room temperature) in the ratio with PVRP 1: 100 (i.e., 1%; e.g., 17 µL to activate 1.7 mL of PVRP) is administered with the sterile pipette to the plastic petri dish
10. Autologous serum in the ratio with PVRP 1: 5 (i.e., 20 %; e.g., 0.34 mL to activate 1.7 mL of PVRP) is administered with the sterile pipette on the top of CaCl₂.
 - a. The autologous serum is prepared by centrifugation (i.e., 10 min, 1260×g, 18°C) of blood collected into one 4 mL plastic blood tube without anticoagulant (i.e., red cap, Z Serum, Vacutube, LT Burnik, d.o.o., Slovenia, stored at room temperature). The blood serum (i.e., supernatant above the red layer) is transferred by a sterile pipette into a sterile polypropylene tube. Caution is required to prevent the mixing of layers and consequential clot formation.
11. Autologous PVRP is administered with the sterile pipette on the top of CaCl₂ and autologous serum mixture.
12. Waiting for the PVRP to transform to the PVRG
13. PVRG trimming (if necessary) and application to the target tissue.
 - 13.1. Alternatively, the PVRP can be transformed into PVRG (with CaCl₂ and autologous serum) in the target tissue
 - 13.2. Alternatively, the PVRP can be mixed with CaCl₂ and autologous serum in the petri dish and then immediately (i.e., without step 12) administered to the target tissue, transforming into a gel.

PVRG preparation with different concentrations of CaCl₂ and autologous serum and the effect of the freeze-thawing cycle are depicted in **Table 1**.

Table 1: Preparation of PVRG from the PVRP of four healthy donors (A-D).

	Freeze/thaw	V _{PVRP} (mL)	CaCl ₂		Serum		Time (minutes)
			μL	% of V _{PVRP}	μL	% of V _{PVRP}	
A	None	1.5	15	1	300	20	4
	Yes	1	10		200		2
B	None	0.5	5	1	100	20	2
					250	50	2
		0.5	none		250	50	none
				100	20		
	Yes	0.5	5	1	100	20	2
C	None	0.5	5	1	none		20
		0.5	10	2	none		20
		0.5	5	1	250	50	2
		0.5	10	2			2
	Yes	0.5	5	1	none		8
		0.5	10	2	none		6
		0.5	5	1	250	50	1
		0.5	10	2			4
D	None	0.5	2.5	0.5	50	10	none
					25	5	
		0.5	5	1	50	10	5
				25	5	5	
	Yes	0.5	5	1	50	10	2
					25	5	2

Remarks: Different activation methods and freeze-thaw cycle were tested in PVRG preparation. Both PVRP and serum samples were instantly frozen at -80 °C and thaw at room temperature before the activation and gel formation; PVRP – platelet- and extracellular vesicle-rich plasma; PVRG – platelet- and extracellular vesicle-rich gel; V_{PVRP} – Volume of PVRP; Time – the time from mixing of PVRP with an activator(s) to gel formation.

2. Platelet- and extracellular vesicle-rich gel and skull-base surgery

The main hallmark of skull-base surgery is a meticulous dissection of skull-base, which is intimately related with vital neurovascular structures and special senses (i.e., vision, hearing, balance, smell and taste). The anterior skull-base surgery denotes anterior transnasal endoscopic and/or transfacial approach, and lateral skull-base surgery indicates lateral (i.e., otosurgical microscopic) approach to the skull-base. The anterior, middle and posterior cranial fossa can be dissected via these approaches.

Anterior and lateral skull-base surgery involves treatment of numerous acquired or congenital disorders involving the bones of the skull-base (i.e., frontal, ethmoid, sphenoid, temporal, occipital bone): e.g. resection of neoplasms (e.g. meningioma, esthesioneuroblastoma, middle ear cancer) or inflamed tissue (e.g., invasive fungal disease, cholesteatoma), decompression of cranial nerves (e.g., traumatic facial or optic nerve compression) and closure of cerebrospinal fluid (CSF) leak.

The CSF leak is caused when the communication between arachnoid space, which contains CSF, and an external environment (e.g., nasal cavity) is created due to the dural and arachnoid tear. The tear results from either accidental trauma or iatrogenically (deliberately during the resection of skull-base or inadvertently). If there is no identifiable cause, a spontaneous CSF leak is diagnosed, typically associated with idiopathic intracranial hypertension. The hallmark of CSF leak is a rhinoliquorrhea or otoliquorrhea. These patients suffer from headache, visual and hearing loss, disequilibrium, vertigo and are prone to develop meningitis [9].

2.1 Transnasal endoscopic repair of the cerebrospinal fluid leak using platelet- and extracellular vesicle-rich gel

According to the international consensus, it is essential to close the CSF leak as soon as possible without delay. The skull-base defect closure is necessary already at the primary surgery, later at the revision surgery or in the treatment of spontaneous CSF leaks. A multi-layered closure is required, but there is no consensus which material to be used [9]. The main goal of closure is to provide watertight closure which can be achieved with different autologous (e.g. lat. *fascia lata*, abdominal fat, mucosal flap, pericranial flap), or commercial heterologous materials.

According to the application of PVRP and PVRG in ORL-HNS so far, there is a lack of clinical studies in the field of skull-base surgery, including CSF leak closure (**Table 2**).

The role of PVRP or PVRG has been extensively studied in in-vitro and in animal studies. For instance, in the recent study of Vasilikos et al. (2020), the hermetic effect of PVRG has been elucidated.

In-vitro created dural tears reconstructed with PVRG and suture withheld higher water pressure than those reconstructed with suture only [49]. In addition to the PVRG's hermetic properties, an increased cranial bone formation has been reported to reconstruct rabbits' cranial defects with PVRG in a prospective randomised controlled study by Kim et al. (2014) [50].

Table 2: A review of clinical studies involving the application of PVRP or PVRG in otorhinolaryngology, head & neck surgery [1].

An anatomical area in otorhinolaryngology	Medical indication, disease or surgical procedure associated with PVRP/PVRG application
Skull-base, paranasal sinuses and nasal cavity	Reconstruction of sellar, parasellar, and suprasellar lesions defects (10–12)
	Anterior skull base cerebrospinal fluid leaks (12,13)
	Frontal sinus obliteration (14–16)
	Olfactory dysfunction (17)
Face and neck	Facial rejuvenation (18,19)
	Neck rejuvenation (19)
	Facial acne scars* (20)
	Facelift (21)
	A neck lift (21)
	Rhinoplasty (22,23)
Lips and oral cavity	Postsurgical nasal packing (24)
	Cleft lip (25)
	Oral mucosal lesions (26,27)
	Oral pemphigus vulgaris (28)
Pharynx and oesophagus	Osteoradionecrosis of the mandible (29)
	Pharyngoplasty for obstructive sleep apnoea (30)
Salivary glands	Traumatic oesophagocutaneous fistula (31)
	Suprafacial parotidectomy (32,33)
Ear	
External ear	Auricle amputation (34)
Middle ear	Acute eardrum perforation (35)
	Chronic eardrum perforation (36–45)
	Reconstruction of the posterior external ear canal wall (46)
	Mastoid reconstruction after CWD mastoidectomy (47,48)

Remarks: PVRP – platelet- and extracellular vesicle-rich plasma; PVRG – platelet- and extracellular vesicle-rich gel; CWD – canal wall down; * –systematic review or meta-analysis.

Since the in-vitro and animal studies report promising results, PVRG has been administered in the transnasal endoscopic reconstruction of skull-base defects. The largest sample size has been reported by Soldatova et al. (2017) to our best knowledge. The study reports L-PRF administration (i.e., leukocyte-platelet-rich fibrin) in 47 patients undergoing the resection of sellar, parasellar and suprasellar benign and malignant (i.e., metastatic and non-metastatic) disease, which required transsphenoidal, transplanum, transclival, transcribriform,

transthemoid or transpterygoid approach. L-PRF was prepared without an anticoagulant, which results in gel formation during the centrifugation. For that reason, this is not PVRP or PVRG in its strict sense, according to the [4]. L-PRF has been administered as inlay and overlay with mucoperiosteal graft or flap. Although the reported incidence of CSF's postoperative leak is low and crusting and scar formation was satisfactory, more studies need to be conducted. Namely, this study's main limitations are a retrospective type of analysis, no control group, and group heterogeneity [10].

L-PRF has been used by Khafagy et al. (2018) in the transnasal endoscopic treatment of spontaneous CSF leak in underlay and overlay fashion as an adjunct to autologous grafts and flaps. None statistically significant differences between CSF pressures and defect sizes and in CSF leak recurrence have been identified between the control and intervention group [13]. The study by Fredes et al. (2017) reported the neoosteogenesis visible on the CT in the region of skull-base, which was reconstructed with L-PRF membranes and autologous flaps or grafts [12].

Rasmussen et al. (2018) administered L-PRF, to reconstruct defects after transsphenoidal endoscopic approach to the sellar region. Although the L-PRF has been administered as overlay solely, there was no CSF leak and favourable crusting [11].

2.2 Repair of the cerebrospinal fluid leak using platelet- and extracellular vesicle-rich gel in otological surgical procedures

PVRP and PVRG have been effectively used in the treatment of skull-base defects and long-bone fractures. Moreover, its use has been described in treating calvarial defects, e.g. frontal sinus obliteration with PVRG and bone chips via bicoronal approach [14–16]. Since the otological surgical procedures routinely expose dura of middle cranial fossa (i.e., via lateral microscopically-based approaches), PVRP and PVRG could be used to prevent CSF leak or meningocele formation via mechanisms of neosteogenesis and remucosalisation. Moreover, PVRG's obliterative properties could place it as an adjunct to the fat inobliteration after subtotal petrosectomy. Since the EVs can readily cross the hemato-encephalic barrier [51] and have been proposed as vectors in the treatment of hearing loss [52], PVRP and PVRG could have the potential role in the treatment of inner ear disorders due to its high concentrations of EVs [53].

3. Conclusion

PVRG prepared by our protocol possesses good therapeutic properties due to the regenerative roles of platelets and extracellular vesicles. It has already been described as effective in treating the spectrum of diseases, including those covered by otorhinolaryngology, head & neck surgery. Despite its great potential, there is a lack of clinical evidence to establish this therapeutic modality adjuvant to the skull-base surgery. Nevertheless, there is some evidence of PVRG application in anterior transnasal endoscopic skull-base surgery, including cerebrospinal fluid leak closure, which provides the basis for

further research. Some parallels could also be drawn with skull-base reconstruction during otological surgery, where the PVRG's potential remains unexploited.

Acknowledgements

Authors acknowledge support of EU Commission (Ves4us) and Slovenian Research Agency (grants P3-0388, J1-9162, J2-8166, L3-2621 and J2-8169).

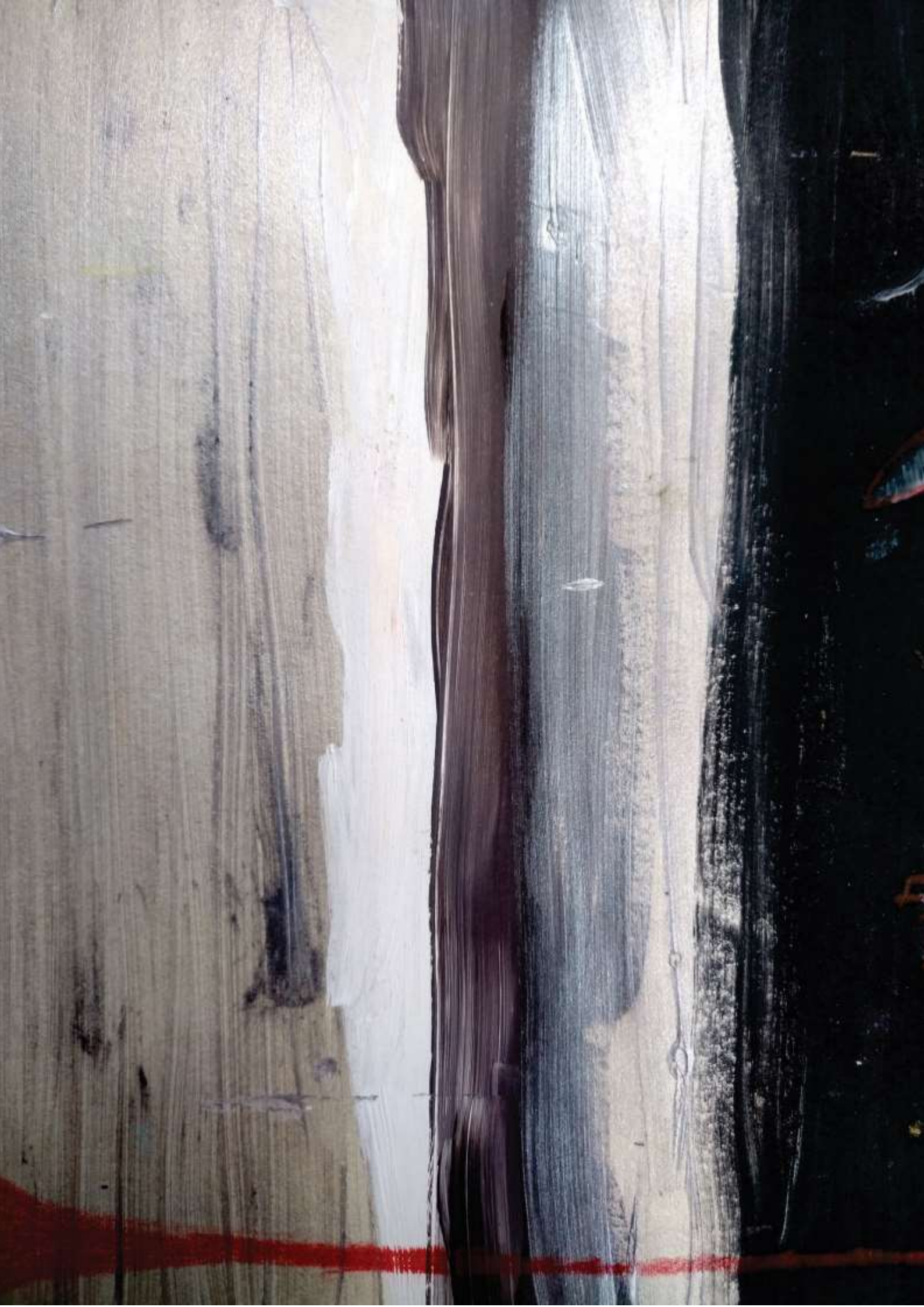
References

1. Vozel D, Božič D, Jeran M, et al. Treatment with platelet- and extracellular vesicle-rich plasma in otorhinolaryngology-a review and future perspectives. In: *Advances in Biomembranes and Lipid Self-Assembly* [Internet]. Academic Press; 2020. Available from: <http://www.sciencedirect.com/science/article/pii/S2451963420300224>
2. Guo S-C, Tao S-C, Yin W-J, Qi X, Yuan T, Zhang C-Q. Exosomes derived from platelet-rich plasma promote the re-epithelisation of chronic cutaneous wounds via activation of YAP in a diabetic rat model. *Theranostics*, 2017, 7(1):81–96.
3. Dhillon RS, Schwarz EM, Maloney MD. Platelet-rich plasma therapy - future or trend? *Arthritis Res Ther*, 2012, 14(4):219.
4. do Amaral RJFC, da Silva NP, Haddad NF, et al. Platelet-Rich Plasma Obtained with Different Anticoagulants and Their Effect on Platelet Numbers and Mesenchymal Stromal Cells Behavior In Vitro. Fan J, editor. *Stem Cells Int*, 2016, 2016:7414036.
5. White JG, Escolar G. EDTA-induced changes in platelet structure and function: adhesion and spreading. *Platelets*, 2000, 11(1):56–61.
6. McClain AK, McCarrel TM. The effect of four different freezing conditions and time in frozen storage on the concentration of commonly measured growth factors and enzymes in equine platelet-rich plasma over six months. *BMC Vet Res*, 2019, 15(1):292.
7. Hosnuter M, Aslan C, Isik D, Caliskan G, Arslan B, Durgun M. Functional assessment of autologous platelet-rich plasma (PRP) after long-term storage at -20°C without any preservation agent. *J Plast Surg Hand Surg*, 2017, 51(4):235–9.
8. Roffi A, Filardo G, Assirelli E, et al. Does Platelet-Rich Plasma Freeze-Thawing Influence Growth Factor Release and Their Effects on Chondrocytes and Synoviocytes? Sánchez M, editor. *BioMed Res Int*, 2014, 2014:692913.
9. Georgalas C, Oostra A, Ahmed S, et al. International Consensus Statement: Spontaneous Cerebrospinal Fluid Rhinorrhea. *Int Forum Allergy Rhinol* [Internet]. n/a(n/a). Available from: <https://onlinelibrary.wiley.com/doi/abs/10.1002/alr.22704>
10. Soldatova L, Campbell RG, Elkhatab AH, et al. Role of Leukocyte-Platelet-Rich Fibrin in Endoscopic Endonasal Skull Base Surgery Defect Reconstruction. *J Neurol Surg Part B Skull Base*, 2017, 78(1):59–62.
11. Rasmussen J, Ruggeri C, Ciraolo C, Baccanelli M, Yampolsky C, Ajler P. Application of Fibrin Rich in Leukocytes and Platelets in the Reconstruction of Endoscopic Approaches to the Skull Base. *World Neurosurg*, 2018, 118:32–41.
12. Fredes F, Pinto J, Pinto N, et al. Potential Effect of Leukocyte-Platelet-Rich Fibrin in Bone Healing of Skull Base: A Pilot Study. Nathan C-AO, editor. *Int J Otolaryngol*, 2017, 2017:1231870.
13. Khafagy YW, Abd Elfattah AM, Moneir W, Salem EH. Leukocyte- and platelet-rich fibrin: a new graft material in endoscopic repair of spontaneous CSF leaks. *Eur Arch Otorhinolaryngol*, 2018, 275(9):2245–52.

14. Mendonça-Caridad JJ, Juiz-Lopez P, Rubio-Rodriguez JP. Frontal sinus obliteration and craniofacial reconstruction with platelet rich plasma in a patient with fibrous dysplasia. *Int J Oral Maxillofac Surg*, 2006, 35(1):88–91.
15. Mendonça-Caridad JJ, Juiz-Lopez P, Fayos FV, Miery G. A novel approach to human cranial tissue regeneration and frontal sinus obliteration with an autogenous platelet-rich/fibrin-rich composite matrix: 10 patients with a 6-10 year follow-up. *J Tissue Eng Regen Med*, 2013, 7(6):491–500.
16. Taglialatela Scafati C, Taglialatela Scafati S, Aveta A, Cassese M, Vitale C. Chronic frontal sinus disease: combined use of platelet-rich plasma and calvarial bone grafts for sinus obliteration in aggressive and secondary cases. *Rev Stomatol Chir Maxillofac*, 2010, 111(4):216–20.
17. Yan CH, Mundy DC, Patel ZM. The use of platelet-rich plasma in treatment of olfactory dysfunction: A pilot study. *Laryngoscope Investig Otolaryngol*, 2020; 5(2):187–93.
18. Maisel-Campbell AL, Ismail A, Reynolds KA, et al. A systematic review of the safety and effectiveness of platelet-rich plasma (PRP) for skin aging. *Arch Dermatol Res* [Internet], 2019, [cited 2020 Jan 25]; Available from: <https://doi.org/10.1007/s00403-019-01999-6>
19. Gawdat HI, Tawdy AM, Hegazy RA, Zakaria MM, Allam RS. Autologous platelet-rich plasma versus readymade growth factors in skin rejuvenation: A split face study. *J Cosmet Dermatol*, 2017, 16(2):258–64.
20. Hsieh T-S, Chiu W-K, Yang T-F, Wang H-J, Chen C. A Meta-analysis of the Evidence for Assisted Therapy with Platelet-Rich Plasma for Atrophic Acne Scars. *Aesthetic Plast Surg*, 2019, 43(6):1615–23.
21. Man D, Plosker H, Winland-brown JE. The Use of Autologous Platelet-rich Plasma (platelet Gel) and Autologous Platelet-poor Plasma (fibrin Glue) in Cosmetic Surgery. *Plast Reconstr Surg*, 2001, 107(1):229–36.
22. Gode S, Ozturk A, Kismali E, Berber V, Turhal G. The Effect of Platelet-Rich Fibrin on Nasal Skin Thickness in Rhinoplasty. *Facial Plast Surg FPS*, 2019, 35(4):400–3.
23. Gode S, Ozturk A, Berber V, Kismali E. Effect of Injectable Platelet-Rich Fibrin on Diced Cartilage's Viability in Rhinoplasty. *Facial Plast Surg FPS*, 2019, 35(4):393–6.
24. Kuzucu I, Beriat GK, Ezerarslan H, Ozdemir S, Kocaturk S. Effects of the Autologous Platelet-Rich Plasma in Nasal Pack on Postoperative Quality of Life. *J Craniofac Surg*, 2017, 28(3):e299–302.
25. Refahee SM, Aboulhassan MA, Abdel Aziz O, et al. Is PRP Effective in Reducing the Scar Width of Primary Cleft Lip Repair? A Randomized Controlled Clinical Study. *Cleft Palate-Craniofacial J Off Publ Am Cleft Palate-Craniofacial Assoc*, 2019, 57(5):581–8.
26. Pathak H, Mohanty S, Urs AB, Dabas J. Treatment of Oral Mucosal Lesions by Scalpel Excision and Platelet-Rich Fibrin Membrane Grafting: A Review of 26 Sites. *J Oral Maxillofac Surg*, 2015, 73(9):1865–74.
27. Mahajan M, Gupta MK, Bande C, Meshram V. Comparative Evaluation of Healing Pattern After Surgical Excision of Oral Mucosal Lesions by Using Platelet-Rich Fibrin (PRF) Membrane and Collagen Membrane as Grafting Materials—A Randomized Clinical Trial. *J Oral Maxillofac Surg*, 2018, 76(7):1469.e1-1469.e9.
28. EL-Komy MHM, Saleh NA, Saleh MA. Autologous platelet-rich plasma and triamcinolone acetonide intralesional injection in the treatment of oral erosions of pemphigus vulgaris: a pilot study. *Arch Dermatol Res*, 2018, 310(4):375–81.
29. Scala M, Gipponi M, Mereu P, et al. Regeneration of mandibular osteoradionecrosis defect with platelet rich plasma gel. *Vivo Athens Greece*, 2010, 24(6):889–93.

30. Elkahwagi M, Elokda M, Elghannam D, Elsobki A. Role of autologous platelet-rich fibrin in relocation pharyngoplasty for obstructive sleep apnoea. *Int J Oral Maxillofac Surg*, 2020, 49(2):200–6.
31. Joudi M, Hamidi Alamdari D, Hyradfar M, et al. Lateral Traumatic Esophago-Cutaneous fistula in a Child; Platelet-Rich Fibrin Glue Challenge. *Iran Red Crescent Med J*, 2013, 15(3):256–9.
32. Ricci E, Riva G, Dagna F, Cavalot AL. The use of platelet-rich plasma gel in superficial parotidectomy. *Acta Otorhinolaryngol Ital Organo Uff Della Soc Ital Otorinolaringol E Chir Cerv-facc*, 2019, 39(6):363–6.
33. Scala M, Mereu P, Spagnolo F, et al. The use of platelet-rich plasma gel in patients with mixed tumour undergoing superficial parotidectomy: a randomised study. *Vivo Athens Greece*, 2014, 28(1):121–4.
34. Lee SK, Lim YM, Lew DH, Song SY. Salvage of Unilateral Complete Ear Amputation with Continuous Local Hyperbaric Oxygen, Platelet-Rich Plasma and Polydeoxyribonucleotide without Micro-Revascularization. *Arch Plast Surg*, 2017, 44(6):554–8.
35. Habesoglu M, Oysu C, Sahin S, et al. Platelet-Rich Fibrin Plays a Role on Healing of Acute-Traumatic Ear Drum Perforation. *J Craniofac Surg*, 2014, 25(6):2056–8.
36. Yadav SPS, Malik JS, Malik P, Sehgal PK, Gulia JS, Ranga RK. Studying the result of underlay myringoplasty using platelet-rich plasma. *J Laryngol Otol*, 2018, 132(11):990–4.
37. Sharma D, Mohindroo S, Azad RK. Efficacy of platelet rich fibrin in myringoplasty. *Int J Otorhinolaryngol Head Neck Surg*, 2018, 4(3):677–81.
38. Sankaranarayanan G, Prithiviraj V, Kumar RV. A Study on Efficacy of Autologous Platelet Rich Plasma in Myringoplasty. *Otolaryngol Online J*, 2013, 3(3):1–15.
39. Saeedi M, Ajalloueian M, Zare E, et al. The Effect of PRP-enriched Gelfoam on Chronic Tympanic Membrane Perforation: A Double-blind Randomised Clinical Trial. *Int Tinnitus J*, 2017, 21(2):108–11.
40. Fawzy T, Hussein M, Eid S, Guindi S. Effect of adding platelet-rich plasma to fat grafts in myringoplasty. *Egypt J Otolaryngol*, 2018, 34(4):224–8.
41. El-Anwar MW, Elnashar I, Foad YA. Platelet-rich plasma myringoplasty: A new office procedure for the repair of small tympanic membrane perforations. *Ear Nose Throat J*, 2017, 96(8):312–26.
42. Nair NP, Alexander A, Abhishekh B, Hegde JS, Ganesan S, Saxena SK. Safety and Efficacy of Autologous Platelet-rich Fibrin on Graft Uptake in Myringoplasty: A Randomized Controlled Trial. *Int Arch Otorhinolaryngol*, 2019, 23(1):77–82.
43. El-Anwar MW, El-Ahl MAS, Zidan AA, Yacoup MA-RA-S. Topical use of autologous platelet rich plasma in myringoplasty. *Auris Nasus Larynx*, 2015, 42(5):365–8.
44. Ersözlü T, Gultekin E. A Comparison of the Autologous Platelet-Rich Plasma Gel Fat Graft Myringoplasty and the Fat Graft Myringoplasty for the Closure of Different Sizes of Tympanic Membrane Perforations. *Ear Nose Throat J*, 2020, 145561319900388.
45. Shiomi Y, Shiomi Y. Surgical outcomes of myringoplasty using platelet-rich plasma and evaluation of the outcome-associated factors. *Auris Nasus Larynx*, 2020, 47(2):191–7.
46. Elbary M, Nasr W, Sorour S. Platelet-Rich Plasma in Reconstruction of Posterior Meatal Wall after Canal Wall Down Mastoidectomy. *Int Arch Otorhinolaryngol*, 2018, 22(2):103–7.
47. Jang CH, Choi CH, Cho YB. Effect of BMP2–Platelet-rich Plasma–Biphasic Calcium Phosphate Scaffold on Accelerated Osteogenesis in Mastoid Obliteration, *In Vivo*, 2016 30(6):835–40.

48. Askar SM, Saber IM, Omar M. Mastoid Reconstruction With Platelet-Rich Plasma and Bone Pate After Canal Wall Down Mastoidectomy: A Preliminary Report. *Ear Nose Throat J*, 2019, 145561319879789.
49. Vasilikos I, Beck J, Ghanaati S, et al. Integrity of dural closure after autologous platelet rich fibrin augmentation: an in vitro study. *Acta Neurochir (Wien)*, 2020, 162(4):737–43.
50. Kim T-H, Kim S-H, Sándor GK, Kim Y-D. Comparison of platelet-rich plasma (PRP), platelet-rich fibrin (PRF), and concentrated growth factor (CGF) in rabbit-skull defect healing. *Arch Oral Biol*, 2014, 59(5):550–8.
51. Banks WA, Sharma P, Bullock KM, Hansen KM, Ludwig N, Whiteside TL. Transport of Extracellular Vesicles across the Blood-Brain Barrier: Brain Pharmacokinetics and Effects of Inflammation. *Int J Mol Sci*, 2020, 21(12):4407.
52. György B, Sage C, Indzhukulian AA, et al. Rescue of Hearing by Gene Delivery to Inner-Ear Hair Cells Using Exosome-Associated AAV. *Mol Ther*, 2017, 25(2):379–91.
53. Steiner N, Battelino S, Extracellular vesicles and their use in the inner ear, In Kralj-Iglič V ed., *Proceeding of the 4th Symposium Socratic Lectures*, Ljubljana, 2021, P



Evaluation the effect of frequency modulated transcutaneous electrical nerve stimulation on postural sway in healthy young adults. A pilot study.

Rugelj D^{1,*}, Vidovič M²

¹University of Ljubljana, Faculty of Health Sciences, Biomechanical laboratory, Ljubljana, Slovenia

²University Institute of Rehabilitation - Soča, Ljubljana, Slovenia

*darja.rugelj@zf.uni-lj.si

Abstract

Transcutaneous electrical nerve stimulation (TENS) is a therapeutic modality that can elicit afferent flow from somatosensory afferents. There are ambiguous results of previous research on TENS effect on postural sway. Some authors have reported the effect while others found no effect. **Purpose** of the study was to evaluate the effect of frequency modulated TENS applied through the soles and posterior aspect of shanks on postural sway. **Methods:** In a group of 13 young adults postural sway was measured with force platform during 60 s standing balance task in four conditions (eyes opened and eyes closed with TENS and with sham TENS). Sub-sensory threshold TENS with sweep of frequencies between 5 and 180 Hz was delivered to the soles and shanks of both legs. **Results** indicated that TENS with the chosen frequencies and electrode positions had no immediate effect on postural sway in both vision and no vision conditions. **Conclusion:** within the setup used (regarding type of stimuli parameters and type of electrode placement) we observed no attenuation of postural sway in a group of young persons with no balance impairments. A further research with different stimulation frequencies and intensities as well as different electrodes placements is needed.

1. Introduction

Regulation of human postural control depends on accurate processing of visual, vestibular and various somatosensory stimuli [1, 2]. During standing and purposeful movements persons constantly and subconsciously use this information for the correction of posture or ongoing movements. Additional somatosensory stimuli from skin mechanoreceptors are believed to enhance the signals coming from muscle and joint proprioceptors, thus enabling better perception and integration of stimuli into the ongoing movement [2]. There are different methods that specifically enhance somatosensory flow, among them light touch by fingertip of stationary [3] or movable surface [2] or even self-touching [4] have been shown to decrease postural sway in elderly as well as in young persons [3]. Other types of sensory stimulations that were used for the enhancement of sensory information are stochastic resonance stimulation, textured material stimulation and garment stimulation usually applied over lower limbs. They all exhibit stabilising effect on postural sway resulting in decrease of the centre of pressure (CoP) path length or its mean velocity [5].

Transcutaneous electrical nerve stimulation (TENS) is a therapeutic modality with the main purpose to modulate pain intensity and is routinely used in physiotherapy. With TENS additional somatosensory flow can be provided. It is of importance to investigate whether TENS can add information to the sensory processing to attenuate postural sway similarly to other somatosensory stimulation. These signals are usually composed of short pulses (50-200 μ s) administered with fixed or varying frequency in the range of 50 to 200 Hz.

To date, few investigators have studied the effect of conventional TENS on postural sway and reported inconclusive results. For instance, Dickstein et al. [6] and Laufer and Dickstein [7] used conventional TENS with constant frequency of 100 Hz and reported a decrease of one of five CoP variables in a group of young healthy persons. While Saadat et al. [8] found no effect of TENS stimulation in the knee region in a group of diabetic neuropathy patients. The disagreement between the results of the previous reports of TENS on the postural sway led to the purpose of the present work which is to evaluate the effect of sensory sub-threshold TENS applied directly on the soles of the feet and on the posterior aspect of the shanks below the knee on postural sway in a group of healthy young persons. We hypothesised that sub-threshold TENS would attenuate postural sway.

2. Methods

13 young persons (21 ± 2 years; body mass 67.1 ± 14.7 ; body height 168.1 ± 7.5) were invited to participate in the study. Inclusion criteria were no prior lower leg injuries or conditions, which could affect their balance. The study was approved by the Slovenian National Medical Ethic Committee (0120-309/2018/3) and prior to any measurements, all participants read the information about the testing protocol, received additional verbal explanations when required, and provided written informed consent.

2.1 Sensory threshold testing

Before the application of the TENS and measurements of postural sway the sensory threshold of the soles was measured with Sammens-Weinstein mono-filaments (Baseline Tactile Sensory evaluator, USA) ranging from 0,007g to 300g. The sensory threshold testing is valid and reliable procedure for evaluating the cutaneous threshold sensitivity [9,10]. A point beneath the first metatarsal was tested. The initial side of the body was randomly chosen. To determine the sensory threshold a stepping algorithm was used according to testing protocol described by Snyder et al. [10].

2.2. Experimental procedure

Participants were instructed to stand barefooted as still as possible with their feet close together on the force platform, with their eyes opened or closed with or without sub-threshold TENS. Arms were relaxed beside the body, head was held upright with gaze forward to the anchor point at the eye height approximately 2 metres away.

Measurements of postural sway were performed under four different conditions during standing on force platform: eyes opened without TENS, eyes opened with sub-threshold TENS, eyes closed without TENS, eyes closed with sub-threshold TENS. The order of testing was randomised in two blocks: first eyes opened or closed and then in each vision condition the sub-sensory TENS or sham TENS. The random number generator was used to determine the order of tests. The participants and the assessor were blinded for the presence or absence of the sub-threshold electrical stimulation. Electrical stimulation was operated by research assistant.

2.3. Instrumentation and data processing

The force platform Kistler 9286AA (Winthertur, Switzerland), with the corresponding data acquisition software BioWare was used for data acquisition. A non-slip insulating rubber pad was installed on the force platform to avoid electrical interference. Data acquisition lasted 60 seconds at 200 Hz sampling rate. All the analysis was later done on a Linux server (Fedora 24) with a StabDat-V2.0 software [11].

Four sway parameters in the time domain were chosen for the analysis of postural sway: (1) CoP velocity (2), medio-lateral (3) and antero-posterior path lengths, (4), sway area calculated as the best area outline represented by the first 20 Fourier coefficients (FAO) as described elsewhere [12]. The fractal dimensions of the ML and AP CoP positions time series were determined by the Higutchi method [13] described in detail previously [14]. The fractal dimensions were calculated from the unfiltered ML and AP time series of the CoP positions for the two time intervals from 0 to 0.3 s and from 0.8 to 12 s. These short and long time intervals were chosen to exclude the transition region and to assure two predominantly linear regions in the log/log plot of the curve length vs. sampling time. The fractal

dimensions were then determined by linear regression from the slopes of these two lines. The test-retest reliability of the used postural sway measurements on the force platform in opened and closed eyes has been established for older and young group as excellent to very good (ICC from 0.68 – 0.85 and 0.61 – 0.93 respectively [15]).

For the electrical stimulation, Sono Plus 6920 (Enraf Nonius, the Netherlands) device was used. The self-adhesive electrodes (9 x 5 cm Axelgaard PALS, Axelgaard Manufacturing Co. Ltd., CA, USA) were placed on the soles over distal heads of metatarsals (-) and posterior shanks below the knee (+) to stimulate direct skin receptors on the soles and posterior aspect of the shanks. Before applying the electrodes, the skin of the soles and shanks was cleaned with alcohol to decrease the surface impedance. The stimulation parameters were set at 300 μ s pulse duration, frequency range from 5 to 180 Hz in a 12 seconds ramp up and 12 seconds ramp down sweeping between the two set frequencies. Detailed testing protocol is described elsewhere (16).

2.4. Statistical analysis

The Statistical Package for Social Sciences (SPSS 26, SPSS Inc., Chicago, IL USA) was used for the statistical analysis. A 2 x 2 repeated measures analysis of variance (ANOVA) was performed to identify the effect of the vision conditions and TENS on postural sway dependent variables in time and fractal domain. The significance level was set at $p < 0.05$.

3. Results

3.1. Pressure threshold test

The median value for the pressure threshold test was at monofilament no. 3.61 or 0.4g. This result revealed that all participants were slightly more pressure sensitive compared to normative values [17].

3.2. Postural sway

Data distribution was assessed for normality using histograms of the raw data and with the Kolmogorov-Smirnov test. Since data showed normal distribution, data was analysed using parametric tests. Postural sway variables were analysed in two domains, firstly the time domain followed by the fractal dimension.

3.3. Time domain

A repeated measures 2 x 2 ANOVA was calculated comparing the postural sway variables for the four different experimental conditions. A significant main effect for the vision condition was found for all the analysed postural sway variables: mean CoP velocity ($F_1 = 32.491$, $p < 0.001$); medio-lateral path length ($F_1 = 32.765$, $p < 0.001$), antero-posterior path length ($F_1 = 21.682$, $p = 0.001$), and sway area ($F_1 = 20.76$, $p = 0.001$) indicating an increase of postural sway in no vision conditions. The main effect of TENS was not significant for all the analysed

postural sway variables: mean CoP velocity ($F_1 = 0.267$, $p = 0.615$), medio-lateral path length ($F_1 = 0.458$, $p = 0.511$), antero-posterior path length ($F_1 = 0.006$, $p = 0.940$), and sway area ($F_1 = 2.121$, $p = 0.171$) indicating no effect of TENS on postural sway variables. Also the interaction between eyes open or closed with TENS and no TENS condition was not significant for all four postural sway variables p ranged between 0.155 and 0.506.

Table 1. The mean values of the time domain variables of postural sway for different sensory conditions.

	Mean velocity (SD) (cm/s)	ML path (SD) (cm)	AP path (SD) (cm)	Sway area (SD) (cm ²)
Opened eyes	1.14 (0.18)	46.96 (7.06)	39.88 (7.11)	3.05 (1.09)
Opened eyes with TENS	1.12 (0.20)	46.37 (8.36)	38.48 (8.03)	3.32 (12.29)
Closed eyes	1.68 (0.43)	68.26 (16.87)	59.47 (17.98)	4.94 (1.85)
Closed eyes with TENS	1.74 (0.56)	71.45 (22.41)	61.09 (22.89)	5.40 (2.40)

ML – medio-lateral, AP – antero-posterior, SD – standard deviation

Table 2. The mean values of the fractal dimensions of medio-lateral and antero-posterior time series in four different sensory conditions.

	ML-short (SD)	ML-long (SD)	AP-short (SD)	AP-long (SD)
Opened eyes	1.21 (0.03)	1.83 (0.12)	1.39 (0.10)	1.78 (0.09)
Opened eyes with TENS	1.21 (0.04)	1.78 (0.14)	1.38 (0.10)	1.73 (0.15)
Closed eyes	1.16 (0.04)	1.92 (0.07)	1.29 (0.07)	1.89 (0.75)
Closed eyes with TENS	1.17 (0.04)	1.89 (0.10)	1.29 (0.08)	1.86 (0.09)

ML - medio-lateral, AP - antero-posterior, SD – standard deviation

3.4. Fractal dimension

A 2 x 2 repeated measures ANOVA was calculated comparing the fractal dimension of time series for the four different experimental conditions. A significant main effect for the vision condition was found for all the analysed time series: medio-lateral short ($F_1 = 53.581$, $p < 0.001$) medio-lateral long ($F_1 = 22.736$, $p < 0.001$), antero-posterior short ($F_1 = 27.511$, $p = 0.001$), and antero-posterior long ($F_1 = 19.028$, $p = 0.001$) indicating an increase in fractal dimension in eyes closed conditions. The main effect of TENS was not significant for all the analysed time series: medio-lateral short ($F_1 = 0.590$, $p = 0.457$), medio-lateral long ($F_1 = 2.786$, $p = 0.121$), antero-posterior short ($F_1 = 0.211$, $p = 0.653$), and antero-posterior long ($F_1 = 2.494$, $p = 0.140$) indicating no effect of TENS on postural sway.

The interaction between eyes open or closed with TENS and no TENS condition was not significant for all analysed time series p ranged between 0.421 and 0.782.

4. Discussion

The purpose of the present work was to evaluate the effect of TENS applied through the soles and posterior aspect of shanks on postural sway for the variables in time and fractal domain. Our results indicated that TENS with chosen frequencies and electrode positions had no statistically significant effect on postural sway in the group of young adults in both vision and no vision conditions. We investigated the response to TENS in time domain and in fractal dimensions of postural sway time series of the acquired postural sway data. The results showed that dynamic complexity of measured data did not change with added somatosensory stimuli.

The reports regarding the effect of TENS on postural sway are inconclusive. In the present study, no influence of TENS on postural sway variables was found. This is in agreement with Saadat et al [8]. On the other hand, Dicksten et al. [6] and Laufer and Dickstein [15] reported the influence of TENS on one of the three reported postural sway variables. In those two studies the reported difference between stimulation and no stimulation was in a range of 5%, which is very small and probably not clinically important.

There are several features of the TENS such as intensity, frequency settings, irregularity of the stimuli and targeted tissue that contribute to the efficacy of TENS and offer possible explanations for the obtained results. Additionally, TENS used as a pain control tool has a high placebo effect [18], therefore sham stimulation and double blind design is required to control for the placebo effect. In our study care was taken to apply sub-threshold intensity to produce stimuli to elicit noise-like frequency-modulated stimulation instead of perceivable stimuli. It could be that the intensity of the stimuli was too low to be able to attenuate the postural sway response.

Breen et al. [19] reported an optimal level of stimulation intensity where subjects demonstrated the highest percentage of the improvement of vibratory threshold perception. Only one of the previous studies had a placebo group [20] and TENS had no effect on postural sway whereas studies without control group or sham TENS [6,7] reported a mild effect on postural sway. We can conclude that the stimulation intensity could play a role for the effect of TENS on postural sway. The other possible explanation for the differences between the studies with perceivable ES and sub-threshold ES might be the effect of stiffening of the posture as a consequence of the perceived stimulation. Increased stiffness as a result of environmental conditions and perception [21] indicates an anticipatory motor control strategy.

TENS frequency settings could have also play a role. In our study the frequency sweep between 5 – 180 Hz was used to avoid adaptation to regular stimuli, while Saadat et al. [8] reported applying constant frequency of 100 Hz as well as Dickstein et al., and Laufer et al. [6,7]. Since there was no response in our study and no response in the study of Saadat et al. [8] we might conclude that low frequencies in the range up to 200 Hz are not sufficient to enhance detection or processing of pressure stimuli. Furthermore, the irregularity of the

stimuli could play an important role in the sub threshold stimulation. For TENS it is known that the nervous system habituates to constant stimuli [22]. To avoid habituation to TENS stimuli, we introduced frequency modulation from 5 to 180 Hz in a 12 seconds ramp up and 12 seconds ramp down interval. The sweep of different frequencies (5 – 1000 Hz) was used also by Kimura et al. [20] to produce noise like stimuli with much higher frequencies and resulted in decrease in three of eight CoP variables. While noise stimulation such as stochastic resonance with irregular pulses reported a decrease of postural sway [23,24] and Toledo et al., [25] reported a decrease of postural sway only in more demanding conditions. The chosen stimulation area in our study was the sole and posterior aspect of the shank. We assumed that the stimulation applied directly over the target tissue (in our case the skin of the sole) could contribute to the processing of the cutaneous afferents as well as proprioceptive ones arising from soleus muscle. The enhanced sensory flow could support faster response to the small changes in the pressure on the sole skin and/or soleus muscle length that are a consequence of the postural sway and thus detection of smaller changes.

5. Conclusion

In conclusion, the basic assumption for the use of TENS-type of electrical stimulation for facilitation of information processing was that regular or frequency modulated signal produced by low frequency TENS could alter the regulatory mechanisms of postural sway. The electrical stimulation was expected to improve the information processing and thus allow the detection of weaker signals and respective responses.

We can conclude that low frequencies and predictable sweep of frequencies with sub-threshold intensity are not the type of stimuli to improve the detection of movements on the soles or around ankle joint in response to postural sway in a group of young participants. Although our results did not support the hypothesis we recommend further investigation of different parameters as well as intensities of TENS along with different electrode placements.

Acknowledgements

Authors acknowledge support of ARRS, grant P3-0388.

References

1. Maurer C, Mergner T, Peterka RJ, Multisensory control of human upright stance. *Exp Brain Res* 2006, 171: 231-250. DOI: 10.1007/s00221-005-0256-y.
2. Albertsen IM, Temprado JJ, Berton E, Effect of haptic supplementation on postural stabilization: A combination of fixed and mobile support conditions. *Hum Mov Sci* 2010, 29: 999–1010. Doi: 10.1016/j.humov.2010.07.013.
3. Jeka JJ, Lackner JR, Fingertip contact influences human postural control. *Exp Brain Res* 1994, 100: 495–502. Doi: 10.1007/bf02738408.
4. Nagano A, Yoshioka S, Hay DC, Fukashiro S, Light finger touch on the upper legs reduces postural sway during quasi static standing. *Motor Control*, 2006, 10: 348–358. Doi: 10.1123/mcj.10.4.348.

5. Woo MT, Davids K, Liukkonen J, Orth D, Chow JY, Jaakkola T, Effects of different lower-limb sensory stimulation strategies on postural regulation-A systematic review and meta-analysis. *PLoS One* 2017, 12: e0174522. Doi: 10.1371/journal.pone.0174522.
6. Dickstein R, Laufer Y, Katz M, TENS to the posterior aspect of the legs decreases postural sway during stance. *Neurosci Lett*, 2006, 393: 51-55. Doi: 10.1016/j.neulet.2005.09.039.
7. Laufer Y, Dickstein R, TENS to the lateral aspect of the knees during stance attenuates postural sway in young adults. *ScientificWorldJournal* 2007, 7: 1904-1911. Doi: 10.1100/tsw.2007.279.
8. Saadat Z, Rojhani-Shirazi Z, Abbasi L, Dose postural control improve following application of transcutaneous electrical nerve stimulation in diabetic peripheral neuropathic patients? A randomized placebo control trial. *Diabetes Metab Syndr* 2017, 11: S755-S757. Doi: 10.1016/j.dsx.2017.05.011.
9. Collins A, Visscher P, de Vet HC, Zuurmond W, Perez R, Reliability of the Semmes Weinstein Monofilaments measure coetaneous sensibility in the feet of healthy subjects. *Disabil Rehabil* 2010, 32: 2019 – 2027. Doi: 10.3109/09638281003797406.
10. Snyder BA, Munter AD, Houston MN, Hoch JM, Hoch MC, Interrater and intrarater reliability of the Semmes-Weinstein monofilament 4-2-1 stepping algorithm. *Muscle Nerve*, 2016; 53: 918 – 924. Doi: 10.1002/mus.24944.
11. Sevšek F. StabDat V 2.0. 2014, Faculty of health sciences, Ljubljana. Accessed 18.1.2021. Available from <http://manus.zf.uni-lj.si/stabdat>.
12. Rugelj D, Sevšek F, The effect of load mass and its placement on postural sway. *Appl Erg* 2011, 42: 860-866. Doi: 10.1016/j.apergo.2011.02.002.
13. Higuchi T, Approach to an irregular time series of the basis of the fractal theory. *Phys D* 1988, 31: 277–283. [https://doi.org/10.1016/0167-2789\(88\)90081-4](https://doi.org/10.1016/0167-2789(88)90081-4).
14. Rugelj D, Gomišček G, Sevšek F, The influence of very low illumination on the postural sway of young and elderly Adults. *PLoS One* 2014, 9:e103903. Doi: 10.1371/journal.pone.0103903.
15. Rugelj D, Hrastnik A, Sevšek F, Vauhnik R, Reliability of modified sensory interaction test as measured with force platform. *Med Biol Eng Comput* 2015, 53:525–534. Doi: 10.1007/s11517-015-1259-x.
16. Rugelj D, Vidovič M, Vauhnik R, Sensory Sub- and Suprathreshold TENS Exhibit No Immediate Effect on Postural Steadiness in Older Adults with No Balance Impairments. *Biomed Res Int* 2020, 2020:2451291. Doi: 10.1155/2020/2451291.
17. Rinkel WD, Aziz MH, Van Deelen MJM, Willemsen SP, Cabezas MC, Van Neck JW, et al. Normative data for cutaneous threshold and spatial discrimination in the feet. *Muscle Nerve* 2017, 56: 399-407. Doi: 10.1002/mus.25512.
18. Daguet I, Bergeron-Vézina K, Harvey MP, Martel M, Léonard G, Transcutaneous electrical nerve stimulation and placebo analgesia: is the effect the same for young and older individuals? *Clin Interv Aging* 2018, 13: 335-342.
19. Breen PP, O'Laighin G, McIntosh C, Dinneen SF, Quinlan LR, Serrador JM, A new paradigm of electrical stimulation to enhance sensory neural function. *Med Eng Phys*, 2014, 36: 1088-1091. Doi: 10.2147/CIA.S152906.
20. Kimura T, Kouzaki M, Electrical noise to a knee joint stabilizes quiet bipedal stance. *Gait & posture* 2013, 37: 634-636. Doi: 10.1016/j.gaitpost.2012.09.013

21. Stins JF, Roerdink M, Beek P. To freeze or not to freeze? Affective and cognitive perturbations have markedly different effects on postural control. *Hum Mov Sci.* 2011; 30: 190–202. Doi: 10.1016/j.humov.2010.05.013
22. Spielholz NI, Nolan MF, Conventional TENS and the phenomena of accommodation, adaptation, habituation, and electrode polarization. *J Clin Electrophysiol* 1995, 7: 16-19.
23. Magalhaes FH, Kohn AF, Imperceptible electrical noise attenuates isometric plantar flexion force fluctuations with correlated reductions in postural sway. *Exp Brain Res* 2012, 217: 175-186. Doi: 10.1007/s00221-011-2983-6.
24. Magalhaes FH, Kohn AF, Effectiveness of electrical noise in reducing postural sway: a comparison between imperceptible stimulation applied to the anterior and to the posterior leg muscles. *Eur J Appl Physiol* 2014, 114: 1129-1141. Doi: 10.1007/s00421-014-2846-5.
25. Toledo DR, Barela JA, Kohn AF, Improved proprioceptive function by application of subsensory electrical noise: effects of aging and task-demand. *Neuroscience* 2017, 358: 103-114. Doi: 10.1016/j.neuroscience.2017.06.045.





Routine coagulation parameters in brachycephalic dogs with brachycephalic obstructive airway syndrome

Svete AN¹, Erjavec V^{1*}

¹ University of Ljubljana, Veterinary Faculty, Small Animal Clinic, Ljubljana, Slovenia

*vladimira.erjavec@vf.uni-lj.si

Abstract

Brachycephalic dogs, such as English and French Bulldogs, Boston Terriers, and Pugs, are prone to a conformation-related respiratory disorder known as brachycephalic obstructive airway syndrome (BOAS), which is associated with a variety of clinical signs and dysfunction of other systems (e.g., pulmonary, digestive, cardiovascular, coagulation, and immune). The results of routine coagulation tests, such as prothrombin time (PT), activated partial thromboplastin time (aPTT), and D-dimer concentration, have not been reported in BOAS patients. Therefore, the aim of the present study was to determine these parameters in dogs with different grades of BOAS and a group of healthy non-brachycephalic dogs (control group). All BOAS patients were client-owned dogs admitted to the small animal clinic for surgical treatment of BOAS. We included 74 patients with BOAS and 8 healthy age-matched non-brachycephalic dogs. According to the severity of the disease, BOAS patients were classified into grade 1 (13 dogs), grade 2 (28 dogs), and grade 3 (33 dogs). The median values of PT were slightly above the upper value of the reference range in the grade 1 patients and control dogs; however, the dogs were clinically healthy. Other parameters remained within the reference ranges in all grades of BOAS and the control dogs. We did not find a significant difference between BOAS patients and control dogs in any of the coagulation parameters measured. We can conclude that routine coagulation parameters are not altered in BOAS patients. However, further studies including larger groups of BOAS patients and control dogs and other haemostatic parameters are warranted.

1. Introduction

Brachycephaly, or foreshortening of the facial skeleton, is a common condition in dogs that is aggravated by selective breeding. In recent years, brachycephalic dogs have become increasingly popular, possibly due to the similarity between the head shape of brachycephalic dogs and that of human infants and their generally less fearful nature toward strangers compared to dolichocephalic breeds [1,2,3].

Brachycephalic dogs, such as English and French Bulldogs, Pugs and Boston Terriers, belong to a group of breeds characterized by a severe shortening of the muzzle and thus of the underlying bones, as well as a more modest shortening and widening of the skull.

Brachycephalic dogs are prone to a conformation-related respiratory disorder known as brachycephalic obstructive airway syndrome (BOAS) [2-7]. Breeding selection for extreme brachycephaly has resulted in the deformation of the upper airway tract leading to obstruction because the soft tissues have not reduced proportionally with the length of the skull. Affected dogs show clinical signs that may include inspiratory dyspnoea, snoring, stertor and stridor, panting, stress, exercise and heat intolerance, cyanosis, and even syncopal episodes, respiratory distress, gastrointestinal problems, and disturbed sleep patterns [2-8]. Due to skull conformation, several other medical complications occur in brachycephalic dogs, including skin fold dermatitis, malocclusion, hydrocephalus, globe proptosis, and facial nerve paralysis [4]. In addition, BOAS is associated with dysfunction of other systems (e.g., pulmonary, digestive, cardiovascular, coagulation, and immune) and should be considered a systemic disorder [4,9]. Furthermore, BOAS has potentially serious welfare consequences [3,8].

Most systemic consequences of BOAS are similar to those of obstructive sleep apnoea syndrome (OSAS) [9]. Brachycephalic obstructive airway syndrome shares features of OSAS (10,11), which is the most common type of sleep-disordered breathing in humans [12]. A useful animal model for OSAS is the English Bulldog, as no surgical interventions or genetic manipulation is required [10]. Obstructive sleep apnoea syndrome is caused by repetitive collapse of the narrow upper airway during sleep. Patients with OSAS experience repeated episodes of cessation of breathing, leading to hypoxia and reoxygenation. These events can cause increased formation of reactive oxygen species/reactive nitrogen species and thus oxidative stress. The latter may further lead to endothelial dysfunction, vascular inflammation, and atherosclerosis, which plays an important role in the progression of cardiovascular disease in OSAS patients [12,13,17].

A hypercoagulable or prothrombotic state is characterized by an imbalance between procoagulant and anticoagulant molecules that occurs before the appearance of thrombotic phenomena [14]. Epidemiological studies have shown that OSAS is associated with hypercoagulability. Moreover, hypercoagulability has been proposed as a link between OSAS and cardiovascular complications, as it contributes to both inflammation and thrombosis [15,16,17,18]. In human OSAS patients, the presence of a hypercoagulable state has been

assessed using global coagulation assays (thromboelastography), which reflect the dynamics of the complete coagulation process in whole blood [19], as well as traditional (routine) coagulation tests (coagulation times: prothrombin time (PT) in seconds and as International Normalized Ratio (INR) and activated partial thromboplastin time (aPTT); D-dimer, a final degradation product of cross-linked fibrin) [15,16,17,18]. On the other hand, there is a lack of data on coagulation abnormalities in brachycephalic dogs with BOAS. Only two studies have been published reporting hypercoagulability in small groups of clinically healthy Bulldogs [20] and severely affected BOAS patients [21] using a global coagulation assay, thromboelastography.

In veterinary medicine, the availability of thromboelastography for the diagnosis of hypercoagulability is often limited to academic institutions and large referral centres because of the expense of equipment and the time sensitivity of sample processing [22]. Widely used routine coagulation parameters such as PT, aPTT and D-dimer concentration have not been reported in brachycephalic dogs with BOAS. However, shortened PT and aPTT and increased D-dimer concentrations have been found to be associated with a hypercoagulable state in dogs [23]. We were interested in whether there are similar changes in routine coagulation parameters in BOAS patients as in OSAS patients. Therefore, our study aimed to determine PT, aPTT and D-dimer concentration in brachycephalic dogs with different severity of BOAS and healthy non-brachycephalic dogs.

2. Material and Methods

2.1. Dogs

A total of 74 client-owned dogs diagnosed with BOAS and 8 healthy dogs of non-brachycephalic breeds that served as controls were included in the study. The control dogs were considered healthy based on normal history, normal clinical examination, and results of haematological and biochemical analyses.

All BOAS patients were admitted to the Small Animal Clinic for surgical treatment of BOAS. At initial presentation, the history of BOAS patients was obtained using a questionnaire about behaviour, health, and lifestyle. All dogs that showed signs of concurrent disease or had received any type of therapy or vaccination within the last month were excluded from evaluation. A preoperative owner questionnaire was completed for each dog with BOAS to investigate a wide range of clinical signs, i.e., respiratory signs, gastrointestinal signs, exercise intolerance, and sleep disorders. The health status of the patients was assessed by history, physical examination, and results of blood tests including complete blood count with white blood cell differential count (data not shown) and serum biochemical analyses (data not shown).

The diagnosis of BOAS was based on clinical signs of upper airway obstruction and anatomical anomalies, as described elsewhere [5,24]. According to the severity of the disease, BOAS patients were classified into grade 1 (13 dogs), grade 2 (28 dogs), and grade 3 (33 dogs). The severity of the disease was classified based on the anatomical anomalies of

the airways. Patients were classified as grade 1, grade 2, and grade 3 based on the decrease in the radius of the airway at the level of the nasopharynx, oropharynx, laryngopharynx, and larynx after soft palate surgery. Grade 1 patients had no or very mild narrowing of the airways, grade 2 patients had 50% decrease in airways radius, and grade 3 patients had almost complete airway obstruction at the level of nasopharynx, oropharynx, laryngopharynx, and larynx.

Formal written informed consent was obtained from the owner. All procedures complied with the relevant Slovenian governmental regulations (Animal Protection Act, Official Gazette of the Republic of Slovenia, 43/2007). The study was evaluated and approved by the Ethical Committee on Animal Research of the Veterinary Faculty, University of Ljubljana.

2.2. Blood samples collection and coagulation analyses

Venous blood samples for coagulation profile determination and other routine blood analyses were collected once from the cephalic vein on the day of surgical treatment in BOAS patients and at the time of inclusion in the study in control dogs. Blood samples for determination of coagulation parameters were collected into tubes containing the anticoagulant sodium citrate (Sarstedt, Germany). The tubes were centrifuged immediately after blood collection at $2000 \times g$ for 15 minutes at room temperature (21°C). The obtained citrated plasma was harvested and stored at -80°C until batch analysis. The coagulation parameters, PT, aPTT and D-dimer concentration, were determined using an automated coagulation analyser STA Satellite (Diagnostica Stago, France) and commercially available reagents (all Diagnostica Stago, France), NeoPTimal[®] (PT), Cephascreen[®] (aPTT) and Liatest[®] (D-dimer concentration) according to the manufacturer's instructions.

2.3. Statistical analysis

Data were analysed using commercial software (IBM[®] SPSS 25.0, USA). The Shapiro-Wilk test was performed to test whether the data were normally distributed. According to the results of the normality test, a non-parametric test, the Kruskal-Wallis test, followed by multiple comparisons, was used to compare the coagulation parameters as well as age and weight between the dog groups. The significance level was set at 5%.

3. Results

The demographic data of the brachycephalic and non-brachycephalic dogs are shown in **Table 1**. There were no significant weight differences between non-brachycephalic dogs and BOAS patients; however, patients in BOAS grade 3 were significantly ($p = 0.028$) older than patients in BOAS grade 1. Regardless of BOAS grade, French Bulldogs were the most common breed. These dogs accounted for 38 of the 74 cases.

Table 1: Demographic data of brachycephalic dogs with different grades of brachycephalic obstructive airway syndrome (BOAS) and healthy non-brachycephalic dogs (Control)

	Grade 1	Grade 2	Grade 3	Control
Number	13	28	33	8
Sex (F/M)	6/7	12/16	11/22	5/3
Age (months)				
Median (IQR)	13 (8.5 – 28.5)	33.5 (16.5 – 52.8)	36.0 (19.5 – 67.0)*	45.0 (27.0 – 55.5)
Weight (kg)				
Median (IQR)	8.5 (6.5 – 12.1)	10.0 (8.5 – 12.6)	12.2 (9.5 – 15.3)	12.2 (9.5 – 15.3)

*grade 3 patients significantly older than grade 1 ($p = 0.028$); IQR: interquartile range (interval from 25th quartile to 75th quartile); F: female; M: male

Table 2: Coagulation parameters of brachycephalic dogs with different grades of BOAS and healthy non-brachycephalic dogs (control)

	Grade 1	Grade 2	Grade 3	Control	Reference ranges
PT (s)					6.9 – 9.0^a
Median	9.35	8.90	8.70	9.25	
IQR	8.93 – 9.85	8.50 – 9.25	8.35 – 9.05	8.63 – 9.60	
APTT (s)					13.1 – 17.7^a
Median	15.5	14.3	13.6	14.3	
IQR	14.3 – 17.3	13.5 – 17.5	12.9 – 15.5	13.5 – 15.5	
D-dimer (µg/L)					23 – 654^b
Median	120	175	190	150	
IQR	98 – 165	120 – 210	120 – 240	140 – 180	

^a reference ranges of the Diagnostic laboratory, Small Animal Clinic, Veterinary Faculty, University of Ljubljana; ^b Reference range for D-dimer concentration in dogs (25); IQR: interquartile range (interval from 25th quartile to 75th quartile)

The coagulation parameters are shown in **Table 2**. The median values of coagulation parameters were within the reference ranges except PT in grade 1 of BOAS and control dogs. The median values of PT were slightly above the upper value of the reference range for grade 1 of BOAS patients and control dogs; however, the dogs were clinically healthy. We found no significant difference in any of the coagulation parameters between the different grades of BOAS and control group. In addition, there was no significant difference in any of the coagulation parameters when comparing three grades of BOAS.

4. Discussion

In this study, routine coagulation parameters, PT, aPTT and D-dimer concentration, were determined in brachycephalic dogs with different severity of BOAS and healthy non-brachycephalic dogs. Our results cannot be compared with the results of similar studies performed in BOAS patients because no such papers have been published. Therefore, our results were partially discussed with the results obtained in OSAS patients, as the two syndromes are similar [10,11].

Contrary to our expectations, we found no alteration in any of the measured coagulation parameters in brachycephalic dogs with different grades of BOAS and no significant difference between BOAS patients and control dogs. Because prolongation of coagulation times, PT and aPTT, is an indicator of coagulation factor deficiencies and a hypocoagulable state, it has been suggested that shortening of these same times indicates a hypercoagulable state [23]. There is no single conventional test for hypercoagulability, so current diagnostics also focus on measuring D-dimer, a final degradation product of cross-linked fibrin [23]. Hypercoagulability [26] has been detected in clinically healthy Bulldogs [20] and severely affected BOAS patients [21] using the thromboelastography method. Therefore, we expected a shortened PT and aPTT and increased D-dimer concentration in BOAS patients, as such changes have been associated with a hypercoagulable state in dogs [23]. In severe and moderate OSAS patients, a significantly shortened PT, but not a shortened aPTT was found compared with the control group (18) or patients with mild OSAS (27), which is partly in agreement with our results. In the study by Hong and colleagues (18), the shortening of PT in OSAS patients was attributed to underlying chronic inflammatory processes. The latter are also present in BOAS patients (28). D-dimer concentration is commonly used as hypercoagulability marker. Since D-dimers are formed secondary to fibrinolysis after thrombus formation, it is expected that hypercoagulable dogs would have increased thrombus formation and consequently increased D-dimer concentration (23,26). In addition, Song and colleagues (23) reported that dogs with shortened coagulation times were significantly more likely to have increased D-dimer concentration than normal dogs. As mentioned above, we found no significant difference in D-dimer concentration in BOAS patients compared with control dogs. In OSAS patients, hypoxic challenge increased D-dimer concentration (16); however, it has been reported that D-dimer concentration at baseline was lower in OSAS patients than in healthy subjects (29).

In interpreting our results, some limitations must be taken into account. The most important limitation of our study is the lack of thromboelastography measurements, which would allow comparison of the results obtained by two different methods. The next limitation is the fact that patients in BOAS grade 3 were significantly older than patients in BOAS grade 1 and that more of the BOAS patients were male dogs.

5. Conclusion

We may conclude that in BOAS patients the routine coagulation parameters, PT, aPTT and D-dimer concentration, are not altered. However, further studies that include larger groups of BOAS patients and control dogs as well as other haemostasis parameters are warranted.

Acknowledgments

The authors acknowledge the financial support of the Slovenian Research Agency (research program P4-0053). The authors also thank Rebeka Turk and Luka Šparaš, undergraduate students, for the processing of the collected blood samples.

References

1. McGreevy PD, Georgevsky D, Carrasco J, Valenzuela M, Duffy DL, Serpell JA. Dog behavior co-varies with height, bodyweight and skull shape. *PlosOne*. 2013;8(12):e80529. doi: 10.1371/journal.pone.0080529.
2. O'Neill DG, Jackson C, Guy JH, Church DB, McGreevy PD, et al. Epidemiological associations between brachycephaly and upper respiratory tract disorders in dogs attending veterinary practices in England. *Canine Genet Epidemiol*. 2015;2:10.
3. Packer RM, Hendricks A, Tivers MS, Burn CC. Impact of Facial Conformation on Canine Health: Brachycephalic Obstructive Airway Syndrome. *PLoS One*. 2015;10(10):e0137496. <https://doi.org/10.1371/journal.pone.0137496>.
4. Meola SD. Brachycephalic airway syndrome. *Top Companion Anim Med*. 2013;28:91-96. doi: 10.1053/j.tcam.2013.06.004.
5. Dupre G, Heidenreich D. Brachycephalic Syndrome. *Vet Clin North Am Small Anim Pract*. 2016;46:691–707. doi: 10.1016/j.cvsm.2016.02.002.
6. Fasanella FJ, Shivley JM, Wardlaw JL, Givaruangsawat S. (2010) Brachycephalic airway obstructive syndrome in dogs: 90 cases (1991-2008). *J Am Vet Med Assoc*. 2010;237:1048–1051. doi: 10.2460/javma.237.9.1048.
7. Liu NC, Troconis EL, Kalmar L, Kalmar L, Price DJ, et al. Conformational risk factors of brachycephalic obstructive airway syndrome (BOAS) in pugs, French bulldogs, and bulldogs. *PLoS One*. 2017;12:e0181928. <https://doi.org/10.1371/journal.pone.0181928>.
8. Roedler FS, Pohl S, Oechtering GU. How does severe brachycephaly affect dog's lives? Results of a structured preoperative owner questionnaire. *Vet J*. 2013;198:606–610. doi: 10.1016/j.tvjl.2013.09.009
9. Mellema MS, Hoareau GL. Brachycephalic syndrome. In: Silverstein DC, Hopper K, eds. *Small animal critical care medicine*. 2nd ED. St. Louis: Elsevier, 2014:104–106.
10. Hendricks JC, Kline LR, Kovalski RJ, O'Brien JA, Morrison AR, et al. The English bulldog: a natural model of sleep-disordered breathing. *J Appl Physiol*. 1987 (1985);63:1344–1350. doi: 10.1152/jappl.1987.63.4.1344.
11. Hendricks JC (1992) Brachycephalic airway syndrome. *Vet Clin North Am Small Anim Pract*. 1992;22:1145–1153. [https://doi.org/10.1016/S0195-5616\(92\)50306-0](https://doi.org/10.1016/S0195-5616(92)50306-0).
12. Eisele HJ, Markart P, Schulz R. Obstructive Sleep Apnea, Oxidative Stress, and Cardiovascular Disease: Evidence from Human Studies. *Oxid Med Cell Longev*. 2015:608438. doi: 10.1155/2015/608438.
13. Lavie L. Oxidative stress in obstructive sleep apnea and intermittent hypoxia--revisited--the bad ugly and good: implications to the heart and brain. *Sleep Med Rev*. 2015;20:27–45. doi: 10.1016/j.smrv.2014.07.003.

14. Bauer KA, Rosenberg RD. The pathophysiology of the prethrombotic state in humans: insights gained from studies using markers of hemostatic system activation. *Blood*. 1987;70:343–350. <https://pubmed.ncbi.nlm.nih.gov/3607275/>.
15. Guardiola JJ, Matheson PJ, Clavijo LC, Wilson MA, Fletcher EC. Hypercoagulability in patients with obstructive sleep apnea. *Slepp Med*. 2001;2(6):517–523. doi: 10.1016/s1389-9457(01)00088-0
16. von Känel R, Le DT, Nelesen RA, Mills PJ, Ancoli-Israel S, Dimsdale JE. The hypercoagulable state in sleep apnea is related to comorbid hypertension. *J Hypertens*. 2001;19(8):1445–51. doi: 10.1097/00004872-200108000-00013.
17. Toraldo DM, De Benedetto M, Scoditti E, De Nuccio F. Obstructive sleep apnea syndrome: coagulation anomalies and treatment with continuous positive airway pressure. *Sleep Breath*. 2016;20(2):457–65. Doi: 10.1007/s11325-015-1227-6.
18. Hong SN, Yun HC, Yoo JH, Lee SH. Association between hypercoagulability and severe obstructive sleep apnea. *JAMA Otolaryngol Head Neck Surg*. 2017;143(10):996–1002. doi: 10.1001/jamaoto.2017.1367.
19. Lancé MD. A general review of major global coagulation assays: thrombelastography, thrombin generation test and clot waveform analysis. *Thromb J*. 2015;13:1. doi:10.1186/1477-9560-13-1.
20. Hoareau GL, Mellema M. Pro-coagulant thromboelastographic features in the bulldog. *J Small Anim Pract*. 2015;56(2):103–107. <https://doi.org/10.1111/jsap.12299>.
21. Crane C, Rozanski EA, Abelson AL, deLaforcade A. Severe brachycephalic obstructive airway syndrome is associated with hypercoagulability in dogs. *J Vet Diagn Invest*. 2017;29 (4):570–573. doi: 10.1177/1040638717703434.
22. Wiinberg B, Kristensen AT. Thromboelastography in veterinary medicine. *Semin Thromb Hemost*. 2010;36(7):747–756. doi: 10.1055/s-0030-1265291.
23. Song J, Drobotz KJ, Silverstein DC. Retrospective evaluation of shortened prothrombin time or activated partial thromboplastin time for the diagnosis of hypercoagulability in dogs: 25 cases (2006–2011). *J Vet Emerg Crit Care*. 2016;26:398–405. doi: 10.1111/vec.12478.
24. Hedlund CS. Surgery of the upper respiratory system. In: Fossum TW, ed, *Small animal surgery*. Mosby, St.Luis, USA, 2007, pp: 817–866. doi:10.1016/j.cvfa.2008.02.003.
25. Bauer N, Eralp O, Moritz A. Reference intervals and method optimization for variables reflecting hypocoagulatory and hypercoagulatory states in dogs using the STA Compact automated analyzer. *J Vet Diagn Invest*. 2009;21:803–814. doi: 10.1177/104063870902100606.
26. Kittrell D, Berkwitz L. Hypercoagulability in dogs: pathophysiology. *Compend Contin Educ Pract Vet*. 2012;34(4):E1–5. <https://pubmed.ncbi.nlm.nih.gov/22488600/>.
27. Basavaraj PB, Tejaswini JS, Samanvaya S. Hemostatic alterations in patients with obstructive sleep apnea: an observational study. *Int J Otorhinolaryngol Head Neck Surg*. 2019;5(4):990–96. doi: 10.18203/issn.2454-5929.ijohns20192718.
28. Rancan L, Romussi S, Garcia P, Albertini M, Vara E, et al. Assessment of circulating concentrations of proinflammatory and anti-inflammatory cytokines and nitric oxide in dogs with brachycephalic airway obstruction syndrome. *Am J Vet Res*. 2013;74:155–160. doi: 10.2460/ajvr.74.1.155.
29. von Kanel R, Natarajan L, Ancoli-Israel S, Mills PJ, Loredó JS, Dimsdale JE. Day/night rhythm of hemostatic factors in obstructive sleep apnea. *Sleep*. 2010;33:371–7. doi: 10.1093/sleep/33.3.371.



NON-DESTRUCTIVE CHARACTERISATION OF NATURAL MATERIALS: QUANTITATIVE DETERMINATION OF BORNEOL AND LIMONENE IN EUROPEAN SPRUCE NEEDLES (*PICEA ABIES*) BY FTIR SPECTROSCOPY

Jeran M^{1,2,*}, Barrios-Francisco R³, Sedušak Kljakič A⁴, Remškar H⁴, Novak U⁵

¹University of Ljubljana, Faculty of Health Sciences, Laboratory of Clinical Biophysics, Ljubljana, Slovenia

²University of Ljubljana, Faculty of Electrical Engineering, Laboratory of Physics, Ljubljana, Slovenia

³División Ingeniería Química, Tecnológico Nacional de México/TES de San Felipe del Progreso, San Felipe del Progreso, Mexico

⁴University of Ljubljana, Biotechnical Faculty, Department of Agronomy, Slovenia

⁵National Institute of Chemistry, Laboratory for Biomolecular Structure, Ljubljana, Slovenia

[*marko.jeran@fe.uni-lj.si](mailto:marko.jeran@fe.uni-lj.si)

Abstract

Plants have an incredible power ability to synthesize many of the active ingredients on which today's medicines and therapies are based. They are able to defend themselves against external influences (enemies) by releasing the appropriate molecules into individual parts of plants. In this work we studied the maceration process of isolation and quantitative identification of biologically active compounds limonene and borneol from European spruce (*Picea abies*) needles. Ethanol and *n*-hexane macerate was prepared from needles of healthy spruce. Limonene and borneol were quantitatively determined by FTIR spectroscopy. The results have shown the high yield of limonene and borneol in the isolate. It was interpreted that high yield was achieved also due to polarity of the solvent (ethanol). Limonene was macerated better in *n*-hexane while borneol was macerated better in ethanol. It was concluded that the solvent (and its chemical and physical properties) plays key role in maceration process.

1. Introduction

In many natural sources, a variety of chemical compounds showing desirable biological properties such as antimicrobial, antitumor, antioxidants activity, etc, can be found. One of them is spruce (*Picea Abies*), which it is an abundant and common tree. The spruce tree contains different composition of biologically active and complex substances. The composition of such substances depends on several factors (e.g. climate, period of collection in the year, accessibility to nutrients, etc.).

1.1 European spruce (*Picea abies*)

The European spruce (*Picea abies*) belongs to the pine family (Pinaceae), the most numerous family of conifers with more than 200 species. Home of origin is the European mountains of the central and northern regions [1,2].

The spruce is a versatile plant. In the past, it was used for heating, for example. Its light-coloured, relatively light and soft wood is mainly used in construction, in the furniture, paper industry and manufacturing musical instruments. Many spruce preparations have served in medicinal purposes. It is worthy to note its particular its essential oils from needles and resin as an ointment. Needles and tips are mainly used for the preparation of teas, baths and vitaminated drinks. The active substances contained in spruce help for coughing up phlegm in colds, and they have an antibacterial effect and relieve rheumatism [1].

1.2 Biologically active substances in European spruce (*P. abies*)

We focused on substances that have effects on model organisms or produce effects that could later be used for further applications. The activity of the target substance itself depends on the dose (amount) of a substance we use. The active substance must comply with the rules of ADME (absorption, distribution, metabolism and excretion) to be truly biologically active [3].

Biologically active substances in spruce known so far are: *p*-hydroxybenzoic acid (PHBA) and its glucosides, piceol (and its glucoside picein): which is used in the pharmaceutical industry for the production of active ingredients, piceatannol (and astringin who is stilbenoid, the 3- β -*D*-glucoside of piceatannol), ferulic acid, which is the basis for the production of aromatic compounds, isorhapontin, catechin: which is a natural antioxidant and a secondary metabolite of plants. Vitamin C, which is one of the most important antioxidants in the extracellular fluid and taken orally, is also present in spruce tops [1, 4-7]. Limonene (by IUPAC nomenclature 1-methyl-4-(1-methylethenyl)-cyclohexene), is a liquid and colorless hydrocarbon at room temperature. It is classified as a cyclic terpene with a ring (**Figure 1A**). Its name comes from from its considerable content in lemon peel, and peel of other citrus fruits, which also gives their characteristic aroma. The most common form of limonene is *D*-limonene, an enantiomer with a strong orange odor. This compound is extracted from the peel of citrus fruits by centrifugation and steam distillation.

The primary natural source of limonene is citrus fruits, where *D*-limonene can be easily obtained. Racemic mixture of limonene is known as dipentene. Limonene as an active ingredient is also found in resin of coniferous trees, and it is used to repel insects. In addition

to carvone production, limonene is also used in cosmetics as a citrus fragrance additive. *D*-limonene is used in the food industry and in some medicines to mask the bitter taste of alkaloids and as a fragrance in perfumes, detergents, and hand sanitizers. Lemon is also a natural plant insecticide [8,10].



Figure1. Structure of the borneol (A) and limonene (B).

Borneol (Figure 1B) exists under normal conditions in the form of partially transparent white crystals, which smell strongly of camphor and spruce resin. Due to its non-polarity, it is relatively insoluble in water, slightly soluble in ethers and related non-polar solvents such as chloroform, toluene, *n*-hexane and dichloromethane. It has a higher density compared to water, a boiling point of 212 °C, a melting point of 202 °C, and an ignition temperature or flash point of 60 °C. Due to its flammability, it can ignite by friction or heat. Borneol is used as a flavouring agent for food, fragrances, and for conversion into chemicals. It is also used in traditional Chinese medicine. Contact with the skin and eyes can cause irritation. Some people may also develop skin allergies. Headaches, shortness of breath, vomiting, dizziness, and unconsciousness may occur if high amounts of borneol are inhaled. Inhalation of extremely high concentrations may cause restlessness, difficulty concentrating, irritability and seizures [11-14].

2. Isolation of biological agents from plants

Like most other plants, the essential oils of spruce are complex mixtures of many compounds. There are several methods of distillation for making essential oils: with water, with steam, with both water and steam, and distillation with steam under pressure. Many of the essential oils have a boiling point between 150 and 200 °C, so they must be heated to the boiling point to separate them from the rest of the non-volatile plant material. Since the plant would burn at such high temperatures, the plant material is not heated directly, but with hot water or steam. The active ingredients must be stable enough to withstand heating processes at operating temperatures and must not react chemically with water. The simplest and most common process for obtaining plant extracts is maceration or "solid-liquid" extraction [1,15]. The crushed plant material is mixed with the solvent in a specific ratio and allowed to stand at room temperature, with occasional shaking or stirring. After a few days, the mixture is drained or filtered.

The process of isolation on an industrial scale is often carried out with some modifications: increased temperature, constant stirring and/or shorter time. The main disadvantages of the method are the long periods of the process and the entrapment of the active ingredient in the plant material. Maceration is most commonly used to obtain tinctures and oil extracts. This group of extracts can also include infusions and decoctions prepared with water, but much shorter than classical macerations: the whole or crushed plant is covered with boiling water for 5 to 15 minutes (infusion) or crushed is covered with cold water and brought to a boil, then boiled for another 15 to 30 minutes [1,15].

3. Aim and hypothesis of research work

The aim of the research work in hands consists on describing a method to carry out the maceration or "solid/liquid" extraction technique of extraction from a large amount of needles of spruce and to study the role of two maceration solvents – ethanol and *n*-hexane. Then followed quantitative analysis/characterization of macerates and evaluation of limonene and borneol content by means of FTIR spectroscopy (IR spectroscopy with Fourier transform).

A larger amount of the extract is quantified in a polar solvent (ethanol), since we expect that many other components of the real sample are also isolated. In *n*-hexane, the mass of the extract will be lower, since hexane is a weakly polar (non-polar) solvent. In characterizing the macerates, quantitative FTIR spectroscopy will show a higher content of limonene isolated in *n*-hexane and a higher content of borneol in ethanol.

4. Methods

4.1 Preparation of macerate from spruce needles

50.0 g of dried needles of healthy spruce were weighed into a 1000 mL conical flask (Erlenmeyer flask). 500 mL of the selected solvent was then added to each conical flask. For the needles in the first Erlenmeyer flask, 500 mL of ethanol was added and for the needles in the second Erlenmeyer flask, the same amount of *n*-hexane was added. The samples were heated at 50 °C for 30 minutes and then allowed to cool spontaneously. The mixture in the Erlenmeyer flasks was then shaken on a laboratory shaker at room temperature (22 °C) at 250 rpm for 7 days (168 hours). The procedure is shown in **Figure 2**.



Figure 2. (A) Maceration mixture in solvents. (B) Mixture on the laboratory shaker. (C) Maceration mixture after filtration. (D) Evaporation of solvent on rotary evaporator.

At the end of the procedure, the contents were filtered. The solid plant residue was washed with 3 times 80 mL each one of the respective solvent and the contents were quantitatively transferred into a weighing flask. The solvent was removed under reduced pressure and the solid residue was weighed. The isolated material was stored in an airtight flask in a refrigerator at 5 °C until analysis and use.

4.2 Quantitative determination of limonene and borneol in spruce macerates by FTIR-spectroscopy

FTIR spectra were recorded on a Bruker Tensor 27 FTIR spectrometer with Specac's Golden Gate ATR (Attenuated Total Reflection method) cell (**Figure 3**). The spectral range of the recorded spectra was between 4000 and 600 cm^{-1} , spectra resolution was 4 cm^{-1} . Each final spectrum was averaged from 64 individual spectra, improving the spectral signal and noise ratio. Using the same measurement parameters, the background was subtracted from each individual spectrum. The concentration of limonene and borneol in macerates was determined by the difference between the individual macerate spectra and standard spectra of limonene/borneol.

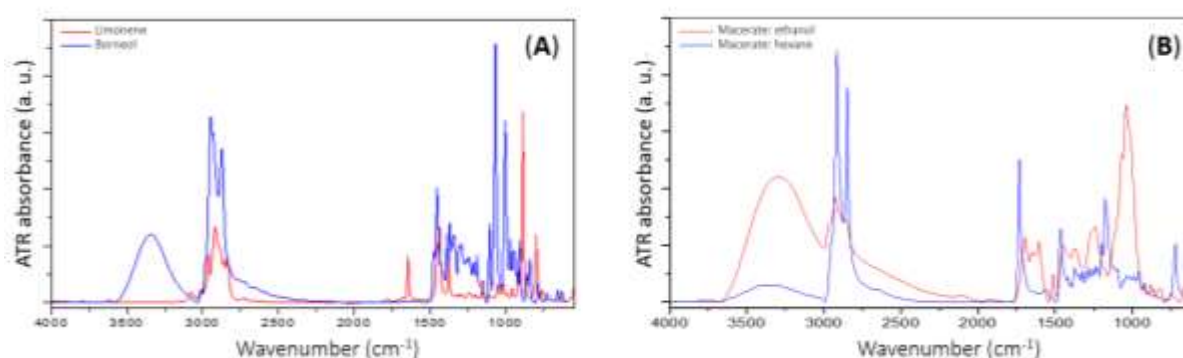


Figure 3. FTIR spectra: (A) Standard spectra of limonene and borneol. (B) Spectra of macerated samples – isolates.

4. Results and Discussion

4.1 Results of the maceration of spruce needles

Table 1 presents the masses of the extracts obtained after separating the plant material from the maceration solvent with the sample components. The yield was better when ethanol instead of *n*-hexane was used as a solvent. We interpreted this as a consequence of polarity of solvent molecules, namely, ethanol has a higher dielectric constant (ϵ) [16] – a measure of polarity ($\epsilon = 22.4$) compared to *n*-hexane ($\epsilon = 1.9$).

Table 1. Macerate quantities.

Solvent	Macerate Mass [g]	Isolated Oily Yield (%)
Ethanol	5.75	11.5
<i>n</i> -Hexane	0.23	0.46

4.2 Results of the quantitative determinations of limonene and borneol by FTIR spectroscopy

Using FTIR spectroscopy, we quantified the content of two biologically active components that we expected to be present in the sample (Table 2). Borneol and limonene could be defined as integral parts of the aromatic components of the sample.

Table 2. Quantitative contents of components in macerates by FTIR spectroscopy.

Solvent	Limonene (%)	Borneol (%)
Ethanol	<i>n. d.</i>	4.0
<i>n</i> -Hexane	3.5	1.0

Quantitative evaluation of limonene and borneol in the isolates was performed by subtracting the spectrum of pure limonene and borneol from the spectrum of the isolate. The bands at 1644 cm^{-1} and 886 cm^{-1} were used as an indicator of limonene. The band at 1644 cm^{-1} is attributed to the stretching vibration of cyclic C=C groups. The band at 886 cm^{-1} belongs to the out of plane bending vibrations of the C-H and CH₂ groups in the cyclohexane ring. As an indicator of borneol, we have used bands at 1068 and 1004 cm^{-1} attributed to C-O stretching vibration. It can be seen in Table 2 that limonene was not detected in ethanol macerate. In *n*-hexane macerate, both substances were detected and the sample was rich with limonene. Limonene was macerated better in *n*-hexane and borneol in ethanol. Spruce needles were macerated in two kinds of solvents. In polar ethanol, a higher mass of the final macerate was obtained. Ethanol leached from plant tissue ethanol-soluble substances, which can be salts of organic compounds, dyes, and alike. A more selective solvent was reflected in the lower polarity of *n*-hexane. The mass of macerate is expected to be low, as it selectively leached only non-polar components. The difference between the maceration process can be seen in the colour of the solvent. Ethanol has a distinctly darker shade, and the *n*-hexane phase has a lighter shade.

The characterization was performed using FTIR spectroscopy, which proved to be fast, easy to use and efficient. It is also a non-destructive technique, with which samples in all aggregate states can be analysed. In addition when measuring solids or liquids only small amount of sample is needed (the top of lab spatula is already sufficient).

We found that ethanol macerate is enriched in borneol because this compound is readily soluble in ethanol. As we can see, the solvents (and their chemical and physical properties) play key role in maceration process.

Acknowledgements

This research work was supported by the Slovenian Research Agency (ARRS) (Grants P3-0388, P1-0010, L3-2621, J3-9262, J1-9162, J1-1705).

References

1. Jeran M, Navadna smreka (*Picea abies*) kot vir aktivnih učinkovin/ Engl. European Spruce (*Picea abies*) as biologically active compounds source. Bilten Trdoživ, 2020, IX(2): 22-24.
2. Skrøppa T (2003), Euforgen technical guidelines for genetic conservation and use for Norway spruce (*Picea abies*). International Plant Genetic Resources Institute, Rome, Italy. Accessed 10.1.2021. Available from: http://www.euforgen.org/uploads/tx_news/856_Technical_guidelines_for_genetic_conservation_and_use_for_Norway_spruce_Picea_abies.pdf
3. Balani SK, Miwa GT, Gan L-S, et al. Strategy of utilizing *in vitro* and *in vivo* ADME tools for lead optimization and drug candidate selection. Curr Top Med Chem, 2005, 5: 1033-1038. DOI: <https://doi.org/10.2174/156802605774297038>
4. Metsämuuronen S, Sirén H, Bioactive phenolic compounds, metabolism and properties: a review on valuable chemical compounds in Scots pine and Norway spruce. Phytochem Rev, 2019, 18: 623-664. DOI: <https://doi.org/10.1007/s11101-019-09630-2>
5. Løkke H, Picein and piceol concentrations in Norway spruce. Ecotoxicol Environ Saf, 1990, 19: 301-309. DOI: [https://doi.org/10.1016/0147-6513\(90\)90032-Z](https://doi.org/10.1016/0147-6513(90)90032-Z)
6. Gabaston J, Richard T, Biais B, Stilbenes from common spruce (*Picea abies*) bark as natural antifungal agent against downy mildew (*Plasmopara viticola*). Ind Crops Prod, 2017, 103: 267-273. DOI: <https://doi.org/10.1016/j.indcrop.2017.04.009>
7. Osswald WF, Senger H, Elstner EF, Ascorbic acid and glutathione contents of spruce needles from different locations in Bavaria. Z Naturforsch C, 1987, 42: 879-884. DOI: <https://doi.org/10.1515/znc-1987-7-825>
8. Fahlbusch K-G, Hammerschmidt F-J, Panten J at al. Flavors and fragrances. Ullmann's Encyclopedia of Industrial Chemistry, 2003, 15: 73-198. Wiley-VCH Verlag GmbH & Co. KGaA. DOI: https://doi.org/10.1002/14356007.a11_141
9. Burnham PM, Limonene (2008): The industrial degreasing agent found in orange peel (Molecule of the month – March 2008). Updated 2017. Accessed 19.1.2020. Available from: https://figshare.com/articles/online_resource/Limonene_-_Molecule_of_the_Month_March_2008_Archived_version_/5427154 DOI: 10.6084/m9.figshare.5427154
10. Ciriminna R, Lomeli-Rodrigues M, Demma Carà P, et al. Limonene: a versatile chemical of the bioeconomy. Chem Comm, 2014, 50: 15288-15296. DOI: <https://doi.org/10.1039/C4CC06147K>

11. Gril M, Šivavec J (menthorsk: Jeran M, Susič R, Kralj-Cigić), Priprava ekstraktov navadne smreke (*Picea abies*), bogatih z aktivnim borneolom ter njihova aktivnost in delovanje na kvasovke (*Saccharomyces cerevisiae*) / Engl. Preparation of the Norway Spruce extracts (*Picea abies*), rich with active borneol and its effect on yeast (*Saccharomyces cerevisiae*). Research work, 2019. Ljubljana, Faculty of Health Sciences and Faculty of Electrical Engineering, University of Ljubljana, Slovenia, and General Upper Secondary School and Veterinary Technician School, Biotechnical Educational Centre Ljubljana.
12. Sheng LS, Du LD, Qiang GF, et al. Borneol. In: Natural small molecule drugs from plants. Springer, Singapore, 2018. DOI: https://doi.org/10.1007/978-981-10-8022-7_30
13. Sedušak Kljakič A, Remškar H (menthorsk: Jeran M, Oder M), Protimikrobno delovanje macerata iglic navadne smreke (*Picea abies*) na bakterije *Legionella pneumophila* / Engl. Antimicrobial activity of Norway spruce (*Picea abies*) needles macerate on baceteria *Legionella pneumophila*. Research work, 2020. Ljubljana, Faculty of Health Sciences and Faculty of Electrical Engineering, University of Ljubljana, Slovenia, and General Upper Secondary School and Veterinary Technician School, Biotechnical Educational Centre Ljubljana.
14. Wang Y, Wang A, Tian H, et al. Determination of (-)-borneol, camphor and isoborneol in *Blumea balsamifera* (L.) DC. Leaves by simultaneous ultrasonic and microwave assisted extraction and gas chromatography. Asian J Chem, 2014, 26: 997-1001. DOI: <http://dx.doi.org/10.14233/ajchem.2014.15737>
15. Kočevkar Glavač N., Pridobivanje in vrednotenje rastlinskih izvlečkov / Engl. Production and evaluation of herbal extracts. Farm Vestn, 2018, 69: 259-264. Available from http://www.sfd.si/uploads/datoteke/kocevar_glavac.pdf
16. Smallwood IM, Handbook of organic solvent properties. Arnold, London, 1996 (1st edition).



Removal process optimisation for emerging pollutants onto two biochars synthesised with classic and microwave induced pyrolysis

Paunovic O^{1,*}; Pap S^{1,2}; Prosen H³; Krasevec I³; Trebše P⁴; Turk Sekulic M¹

¹ University of Novi Sad, Faculty of Technical Sciences, Novi Sad, Serbia

² Environmental Research Institute, North Highland College, University of the Highlands and Islands, Thurso, UK

³ University of Ljubljana, Faculty of Chemistry and Chemical Technology, Ljubljana, Slovenia

⁴ University of Ljubljana, Faculty of Health Sciences, Ljubljana, Slovenia

[*o.paunovic88@gmail.com](mailto:o.paunovic88@gmail.com)

Abstract

Emerging pollutants, such as benzotriazole and its derivatives 4-hydroxy-1*H*-benzotriazole (OHBZ), 4-methyl-1*H*-benzotriazole (4MBZ), 5-methyl-1*H*-benzotriazole (5MBZ), 5-chloro-1*H*-benzotriazole (ClBZ), 5,6-dimethyl-1*H*-benzotriazole (DMBZ) are usually present in trace concentrations in industrial and municipal wastewater effluents. This study shows the removal efficiencies of adsorption of these pollutants onto two functionalised biochars with the variation of different process parameters (e.g., pH, contact time, and initial concentration). Microwave induced and classic pyrolysis were used to synthesise the biochars from wild plum (WpOH) and apricot kernels (AsPhA), respectively. Removal efficiency was optimal at pH 4 for WpOH and at pH 6 for AsPhA and equilibrium was reached for both adsorbents after 240 min. Maximum adsorption capacity showed ClBZ (98.1 mg/g) for WpOH and DMBZ (120.41 mg/g) for AsPhA. It was shown that both adsorbents were efficient for the removal of benzotriazole and its derivatives. AsPhA was more suitable at neutral pH conditions.

1. Introduction

Due to the intensive development of industry and civilization in recent decades, there is a growing problem created by wastewaters. Emerging pollutants, usually present in trace concentrations in industrial and municipal wastewater effluents, have become subject of interest due to potentially toxic effects on the environment and human health [1].

Benzotriazole and its derivatives are heterocyclic compounds that are produced in high volumes and widely used in different products and industrial applications [2,3]. Considering their polar character and solubility in water, they easily reach different environmental compartments and can be found in different concentrations: in surface and ground water in ng/L levels, while in wastewater up to $\mu\text{g/L}$ [4]. Adsorption with low-cost adsorbents is an economical, simple method, that does not require expensive equipment and does not generate toxic or harmful by-products.

Efficiency of adsorption has been shown as very high, with numerous advantages [5]. The aim of this study is to compare the efficiency of two different alternative low-cost biochars for removal of benzotriazole (1*H*-benzotriazole, BTZ) and its derivatives 4-hydroxy-1*H*-benzotriazole (OHBZ), 4-methyl-1*H*-benzotriazole (4MBZ), 5-methyl-1*H*-benzotriazole (5MBZ), 5-chloro-1*H*-benzotriazole (ClBZ), 5,6-dimethyl-1*H*-benzotriazole (DMBZ), and to optimise the operational parameters.

2. Methods

2.1. Materials and chemicals

Solid standards of the analytes in this study were purchased from Sigma-Aldrich, USA (OHBZ, ClBZ, and BTZ), or from Fluka, Switzerland (4MBZ, 5MBZ, and DMBZ). Ultrapure (MQ) water was prepared by Milli-Q water system (Millipore, USA). HPLC grade solvents acetonitrile (Fisher Chemical, UK) and methanol (J. T. Baker, UK) were used. All other chemicals were of *p.a.* or higher purity. Wild plum kernels were collected from Zrenjanin city, Serbia. Apricot kernels came from private orchard in Novi Becej, Serbia.

2.2. Biochar preparation

Synthesis of wild plum biochar (WpOH) was done in few steps. First, the wild plum kernels were washed in water and after that they were crushed in a mechanical mill. Ground biomass was placed in ceramic crucibles and then into an electric furnace, where pyrolysis was performed. There were two phases of pyrolysis: heating the raw material on 180 °C for 35 min (rate of 10 °C min⁻¹) and then the temperature was set up on 500 °C for 60 min (rate of 10 °C min⁻¹). After pyrolysis, the material was crushed to <2 mm and impregnated with a KOH aqueous solution (50% w/v), the impregnation ratio was 0.4 g KOH/g biochar. Material was soaked for 24 h at a room temperature and then it was dried in an oven at 110 °C for 2 h. After that, it was placed in ceramic crucibles and introduced into a microwave oven (Samsung ME71A) for 12 min at 700 W. Obtained product was rinsed several times with an acidic solution (0.1 mol/L HCl) and then with MQ water until the filtrate pH was 7. Finally,

the prepared biochar was dried in an oven at 110 °C for at least 3 h. The final biochar is referred to as WpOH.

First step of apricot kernel biochar (AsPhA) preparation was the raw material pre-treatment. Apricot kernels were washed and crushed in mechanical mill. Milled material was washed with water and dried at 105 °C in electrical furnace. Dried material (<2 mm) was soaked in 50% w/v phosphoric acid with the aim of chemical activation. After 24 h of impregnation the material was filtered to remove excess acid, placed in ceramic crucibles and introduced into an electric furnace. Pyrolysis was done in two phases, likewise as with WpOH. Thereafter, the material was cooled in a desiccator to the room temperature and washed with MQ water until the filtrate pH was above 4. The adsorbent thus prepared was dried in an oven at 110 °C for at least 3 h to obtain biochar AsPhA.

2.3. Adsorption experiment

Experiment was begun with four different biochars: the two mentioned biochars (WpOH and AsPhA) and biochars synthesised from plum and mixed cherry and sweet cherry kernels (PPhA [6] and CScPhA [7], respectively). PPhA and CScPhA were prepared in the same way as AsPhA. Removal of benzotriazole and its derivatives was performed in batch experiments. Specified mass of biochar was mixed with 50 mL aqueous solution of mixed OHBZ, BTZ, 4MBZ, 5MBZ, CIBZ and DMBZ in an Erlenmeyer flask with a stopper. For this purpose, a mechanical shaker was used at 90 rpm at 22 ± 1 °C. Initial screening was done under the same conditions: pH 6-7, concentration of benzotriazoles was 0.01 mg/L, adsorbent mass was 20 mg. The effect of initial pH (2-9), contact time (5-420 min) and initial concentration of compounds (1-50 mg/L) were studied. pH was adjusted using 0.1 mol/L HCl or 0.1 mol/L $\text{NH}_{3(\text{aq})}$. When the initial concentrations were lower than 10 mg/L, an extraction step was implemented using the method described in chapter 2.4.

The removal efficiency, R (%), and the adsorption capacity of OHBZ, BTZ, 4MBZ, 5MBZ, CIBZ, and DMBZ, q_e (mg/g), were calculated using equations:

$$R (\%) = \frac{C_0 - C_e}{C_0} \cdot 100 \quad , \quad (1)$$

$$q_e = \frac{C_0 - C_e}{m} \cdot V \quad , \quad (2)$$

where C_0 is the initial and C_e is the residual concentration of OHBZ, BTZ, 4MBZ, 5MBZ, CIBZ and DMBZ (mg/L), V is the volume of solution (L) and m is the mass of the biochar (g).

2.4. Solid-phase extraction

For the purpose of solid-phase extraction Oasis MAX cartridges (500 mg) supplied by Waters (Milford, MA, USA) were used. The optimal conditions were: loading volume of sample from adsorption experiment was 50 mL. Oasis MAX cartridges were conditioned with 10 mL of MeOH, followed by 10 mL of MQ water. After conditioning, cartridges were loaded with

sample, and then washed first with 5 mL of 5% solution of NH_3 in methanol and dried for 5 min, until they were completely dry. At the end, elution was done with 5 mL of 5% HCOOH in MeOH . Eluates were evaporated and taken to a final volume of 0.5 mL with MQ water.

2.5. Benzotriazoles analysis

Benzotriazoles solutions from the adsorption experiments with concentrations above 10 mg/L were quantified by High Performance Liquid Chromatography (HPLC) coupled to a diode-array detector (DAD). Conditions were optimised using an HPLC-DAD method with the following parameters: an Agilent 1100 Series HPLC-DAD instrument (Agilent, USA) equipped with autosampler. LC separation was performed on a Kinetex XB-C18 column (Phenomenex, USA, 150×4.6 mm, $5 \mu\text{m}$) at room temperature and flow rate of 0.7 mL/min. The mobile phase was composed of acetonitrile (A) and 0.1% HCOOH in MQ water (B), with the following gradient profile: 5% A, increased to 15% A in 0.5 min, then to 35% A in 12.5 min, then to 100% A in next 7 min. The injection volume was 10 μL . UV spectra were recorded in 200–400 nm range, and detection wavelengths for quantification were set at 260, 304, and 350 nm.

Samples with concentrations lower than 10 mg/L were quantified by LC-MS/MS method where Perkin Elmer LC system, coupled with TurboSpray ESI ionisation and 3200 QTRAP mass analyser (Sciex, USA) was used. Same column and parameters as previously described for HPLC-DAD were used for LC separation, except for the mobile phase gradient. Mobile phase gradient was as follows: 5% A, increased to 15% A in 0.5 min, then to 35% A in 12.5 min, then to 100% A in next 7 min. The injection volume was 10 μL .

Ionisation was performed with the electrospray in positive mode with the curtain gas pressure at 30 psi, ion spray voltage of 4 kV, drying gas temperature at 450°C , sheath gas 1 at 50 psi and sheath gas 2 at 50 psi. Nitrogen, supplied by Messer (Germany), was used both as drying and collision cell gas. The mass spectrometer was operated in selected reaction monitoring (SRM) mode; the declustering potential, entrance potential and collision cell exit potential were fixed at 40 V, 10 V, and 3 V, respectively. Transition parameters were optimised for each analyte separately by injecting separate solutions directly into the ion source by flow-injection; two fragment ions were monitored for each compound.

Quantification was performed as analyte signal, using the first transition for each analyte, while the second transition and the fragment ion ratio were used for identity confirmation. During sample analysis, the calibration standard at 0.1 mg/L level and a MQ blank were injected every 12 samples to check for drift in response and carryover effect.

3. Results

3.1. Initial screening

At the beginning, four different biochars were tested. Their characteristics are shown in Table 1.

Table 1. Characteristics of four biochars used in the initial screening

Biochar	Activation process	S_{BET} (m^2/g)	pH_{pzc}	Total pore volume (cm^3/g)
AsPhA	Chemical (H_3PO_4 , 500 °C, 2 h)	1098.9	3.98	0.505
PPhA	Chemical (H_3PO_4 , 500 °C, 2 h)	829.0	4.12	0.418
WpOH	Chemical (KOH, 500 °C 2 h, 700 W MW 12 min)	601.9	7.20	0.260
CScPA	Chemical (H_3PO_4 , 500 °C, 2 h)	657.1	3.14	0.315

Figure 1 shows efficiency of the removal of benzotriazole and its derivatives under the uniform conditions. It can be noticed that all biochars have efficiency over 50%, some of them even over 90%. As might be expected, considering the highest S_{BET} value, AsPhA was the most efficient.

Efficiency of the removal was over 90% for all pollutants, except for CIBZ, where it was over 85%. CScPA was also highly efficient with high percentage of pollutant removal, while PPhA was the least efficient, but still had over 70% efficiency. WpOH had the lowest efficiency, but was still considered as satisfactory because of over 60% removal of most pollutants. Only OHBZ was adsorbed around 50%. AsPhA, PPhA and CScPA were considered as similar, because of the same activation process, so AsPhA was chosen for further experiments, as the most efficient. WpOH, although the least efficient, was studied further because of different impregnation agent and activation process.

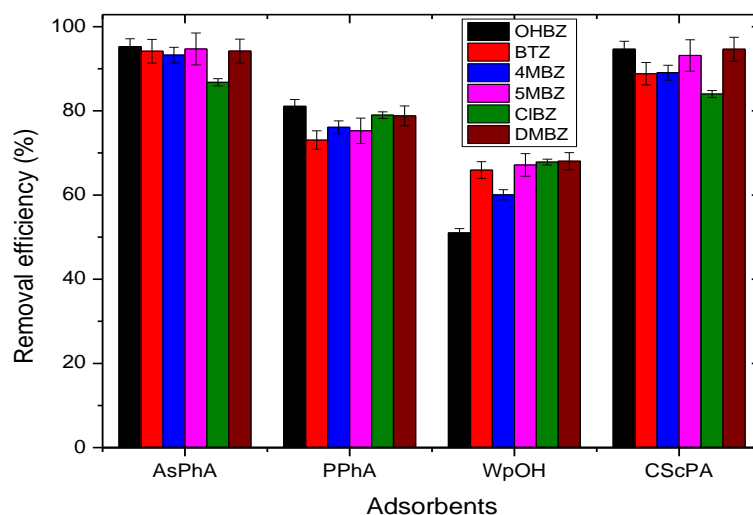


Figure 1. Initial screening of removal of mixed OHBZ, BTZ, 4MBZ, 5MBZ, CIBZ, and DMBZ with AsPhA, PPhA, WpOH, and CScPA

3.2. pH influence on adsorption

The influence of pH on adsorption was demonstrated as a function of adsorption capacity (in mg/g) with respect to the solution pH (**Figure 2**). Very high removal efficiency can be noticed at lower pH values. For WpOH the efficiency is very high (65% to over 90%) at pH value 2-4, and then decreases rapidly; except for OHBZ, where it is around 70% at pH 2, then decreases until pH 5 and increases again until pH 9. As it was shown in a previously study [8], pH_{pzc} of WpOH is neutral or slightly basic (7.2). Since pK_A of studied compounds ranges between 7.25 and 8.92, electrostatic interaction is not expected to occur, but adsorption is still present. Although the removal efficiency at these pH values is very high, pH 4 was decided to be used in the further experiments due to the less extreme acidity of the medium, in order to create a matrix closest to the realistic conditions.

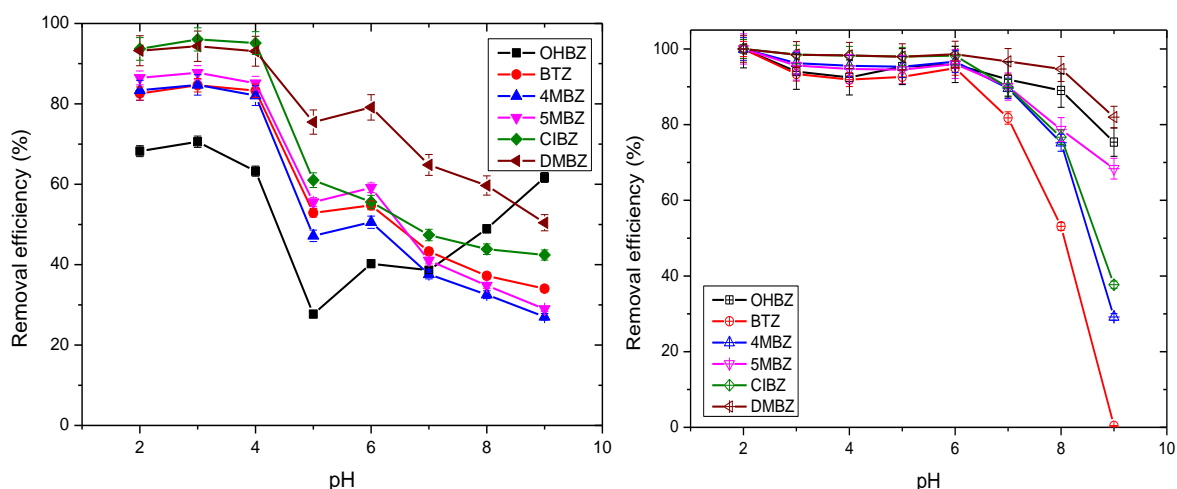


Figure 2. Influence of pH on removal efficiency for mixed compounds OHBZ, BTZ, 4MBZ, 5MBZ, CIBZ, and DMBZ with adsorbent WpOH (left) and AsPhA (right).

For the other adsorbent, AsPhA, the situation is a little bit different. Efficiency is very high (over 90%) at a low pH (2-4), but it does not decrease until pH 6. At neutral pH efficiency is still high (over 80%), but after that it decreases rapidly down to 70% to even less than 5%. pH_{pzc} of AsPhA is 3.98 [5], so strong electrostatic interactions may be present, since between 4 and 7 biochar is negatively charged and pollutants are positively charged. In the further experiments for AsPhA, pH 6 was decided to be used due to the highest efficiency and almost neutral medium.

3.3. Contact time influence

The data regarding contact time and adsorption are presented in **Figure 3** (WpOH and AsPhA dose 0.4 g/L, pH 4 and pH 6, respectively, for contact time of 5, 10, 15, 30, 60, 120, 180, 240, and 300 min).

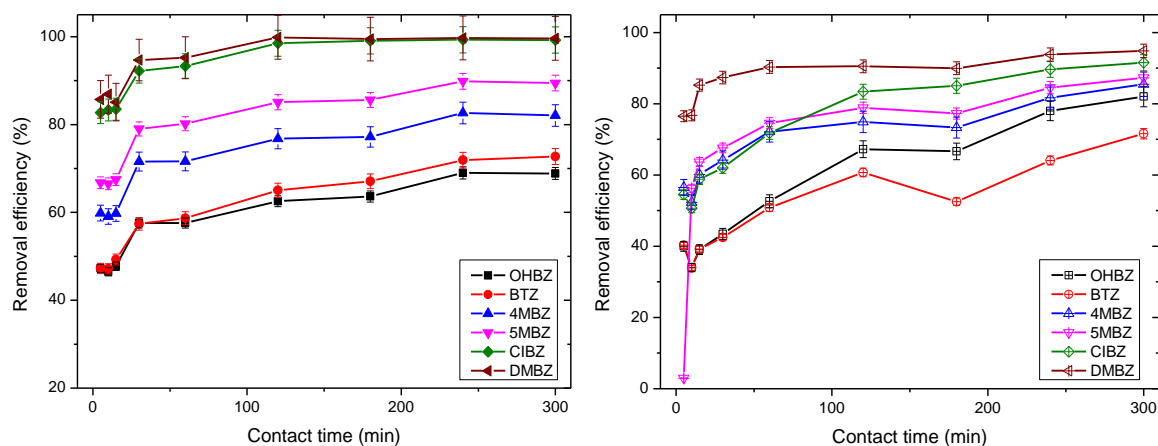


Figure 3. Contact time influence on removal efficiency for mixed compounds OHBZ, BTZ, 4MBZ, 5MBZ, CIBZ, and DMBZ with adsorbent WpOH (left) and AsPhA (right).

At first, adsorption was rapid and spontaneous (during first 60 min) for both adsorbents. After that, adsorption became slower, and reached the equilibrium at 240 min. Processes like diffusion and physical adsorption may need extended time needed to establish the equilibrium.

3.4. Initial adsorbate concentration influence

Adsorption of benzotriazole and its derivatives onto WpOH and AsPhA was investigated for individual compounds OHBZ, BTZ, 4MBZ, 5MBZ, CIBZ, and DMBZ separately at various initial concentrations, from 1 to 50 mg/L (at pH 4 for WpOH and pH 6 for AsPhA, dose 0.4 g/L, reaction temperature 22 ± 1 °C and contact time 240 min). Results of this study are shown on **Figure 4**. Adsorption capacity was highly dependent on initial concentration of compounds for both adsorbents. Maximum adsorption capacity is different for every compound, but it is highest for initial concentration 50 mg/L. For the adsorption with WpOH the highest adsorption capacity was for CIBZ (98.10 mg/g) with removal efficiency of 78.4% and the lowest was for 4MBZ (34.62 mg/g), efficiency 27.7%. AsPhA was shown as more efficient so far, so it was expected to have higher maximum adsorption capacity. The highest adsorption capacity was for DMBZ (120.41 mg/g) with very high efficiency of 96.3%, while the lowest was for OHBZ (72.24 mg/g) with removal efficiency of 57.6%. Compared to other study[9], maximum adsorption capacity of metal-organic framework, MAF-5(Co) for BTZ was higher (175,00 mg/g) than it was achieved with WpOH and AsPhA, but this adsorbent was synthesized from commercial activated carbon, which is not economic. Compared to a different type of adsorbent (surfactant modified Ca-montmorillonite) [10], where adsorption capacity for BTZ and 5MBZ was 18.31 and 16.24 mg/g, respectively, results obtained for WpOH and AsPhA were much higher.

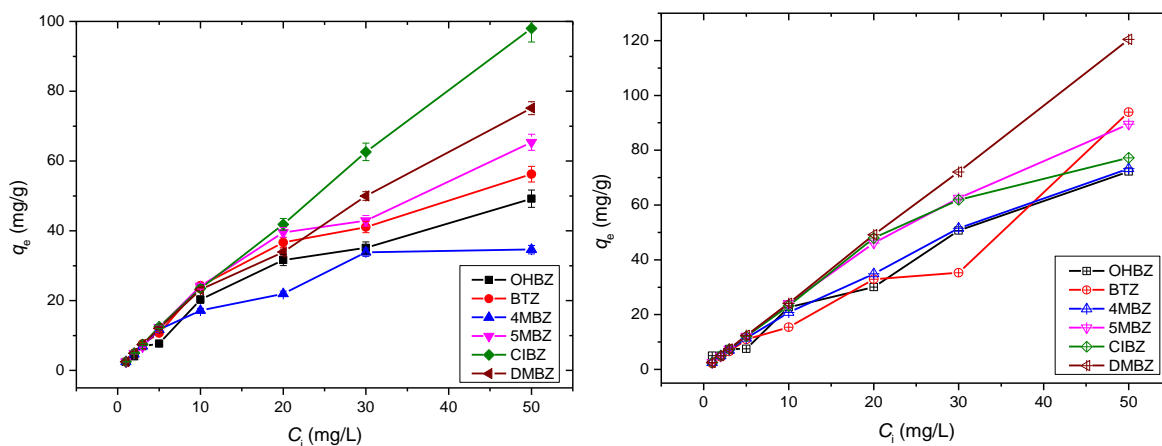


Figure 4. Initial adsorbate concentration influence for individual compounds OHBZ, BTZ, 4MBZ, 5MBZ, CIBZ, and DMBZ with adsorbent WpOH (left) and AsPhA (right).

4. Conclusion

We investigated the adsorption of emerging pollutants benzotriazole and its derivatives (OHBZ, 4MBZ, 5MBZ, CIBZ, and DMBZ) onto two novel functionalised biochars WpOH and AsPhA made from wild plum and apricot kernels, respectively. Removal was the most efficient at lower pH values (2-4), but optimal pH values for the process were 4 and 6 for WpOH and AsPhA, respectively. Adsorption was faster and more spontaneous for the first 60 min, and then it started to be slower until equilibrium. Equilibrium was reached after 240 min for both adsorbents. Maximum adsorption capacity was shown for CIBZ (98.1 mg/g) on WpOH and for DMBZ (120.41 mg/g) on AsPhA. This study showed that both adsorbents were efficient for removal of benzotriazole and its derivatives, especially in acidic environment. AsPhA was more efficient and suitable for neutral environment. Both of these biochars should be investigated further on real wastewater samples and pilot-scale, so they can be implemented in a real wastewater treatment systems.

Acknowledgements

This study has been financially supported by CEEPUS student exchange program and by the Ministry of Education, Science and Technological Development through the project no. 451-03-68/2020-14/200156: "Innovative scientific and artistic research from the FTS (activity) domain". The financial support of the Slovenian Research Agency, namely Programme Group P1-0153, is acknowledged as well.

References

1. Rueda-Marquez J, Levchuk I, Fernandez Ibanez P, Sillanpaa M, A critical review on application of photocatalysis for toxicity reduction of real wastewaters. *Journal of Cleaner Production*, 2020, 258: 120694. <https://doi.org/10.1016/j.jclepro.2020.120694>.
2. Maceira A, Marce RM, Borrull F, Occurrence of benzothiazole, benzotriazole and benzenesulfonamide derivatives in outdoor air particulate matter samples and human exposure assessment. *Chemosphere* 2020, 193: 557-566.
3. Doi: 10.1016/j.chemosphere.2017.11.073.
4. Shi ZQ, Liu YS, Xiong Q, Cai WW, Ying GG, Occurrence, toxicity and transformation of six typical benzotriazoles in the environment: A review. *Science of the Total Environment* 2020, 661: 407-421. Doi: 10.1016/j.scitotenv.2019.01.138.
5. Kraševc I, Prosen H, Development of a Dispersive Liquid-Liquid Microextraction Followed by LC-MS/MS for Determination of Benzotriazoles in Environmental Waters, *Acta Chim. Slov.* 2019, 66: 247–254. Doi: 10.17344/acsi.2018.4914.
6. Turk Sekulić M, Pap S, Stojanović Z, Bošković N, Radonić J, Šolević Knudsen T, Efficient removal of priority, hazardous priority and emerging pollutants with *Prunus armeniaca* functionalized biochar from aqueous wastes: Experimental optimization and modelling. *Science of the Total Environment* 2018, 613–614: 736–750. Doi:10.1016/j.scitotenv.2017.09.082.
7. Turk Sekulic M, Boskovic N, Slavkovic A, Garunovic J, Kolakovic S, Pap S, Surface functionalised adsorbent for emerging pharmaceutical removal: Adsorption performance and mechanisms. *Process Safety and Environmental Protection* 2016, 125: 50-63.
8. Doi: 10.1016/j.psep.2019.03.007.
9. Pap S, Radonic J, Trifunovic S, Adamovic D, Mihajlovic I, Vojinovic Miloradov M, Turk Sekulic M, Evaluation of the adsorption potential of eco-friendly activated carbon prepared from cherry kernels for the removal of Pb^{2+} , Cd^{2+} and Ni^{2+} from aqueous wastes. *Journal of Environmental Management* 2016, 184: 279-306. Doi: 10.1016/j.jenvman.2016.09.089.
10. Paunovic O, Pap S, Maletic S, Taggart M, Boskovic N, Turk Sekulic M, Ionisable emerging pharmaceutical adsorption onto microwave functionalised biochar derived from novel lignocellulosic waste biomass. *Journal of Colloid and Interface Science* 2019, 547: 350–360. Doi: 10.1016/j.jcis.2019.04.011.
11. Sarker M, Bhadra BN, Seo PW, Jhung SH, Adsorption of benzotriazole and benzimidazole from water over a Co-based metal azolate framework MAF-5(Co). *Journal of Hazardous Materials* 2017, 324: 131–138. Doi: 10.1016/j.jhazmat.2016.10.042.
12. Li P, Khan MA, Xia M, Lei W, ZHU S, Wang F, Efficient preparation and molecular dynamic (MD) simulations of Gemini surfactant modified layered montmorillonite to potentially remove emerging organic contaminants from wastewater. *Ceramics International* 2019, 45: 10782–10791. Doi: 10.1016/j.ceramint.2019.02.152.



Challenges in removal of emerging contaminants from the wastewater through hybrid treatment system: An eco-friendly approach

Radović S^{1,*}, Pap S^{1,2}, Jelena Prodanović³, Bremner B³, Turk Sekulic M¹

¹University of Novi Sad, Faculty of Technical Sciences, Department of Environmental Engineering and Occupational Safety and Health, Trg Dositeja Obradovica 6, 21 000 Novi Sad, Serbia

²Environmental Research Institute, North Highland College, University of the Highlands and Islands, Thurso, Scotland, KW14 7JD, UK

³University of Novi Sad, Faculty of Technology Novi Sad, Bulevar Cara Lazara 1, 21 000 Novi Sad, Serbia

[*sanjaradovic@uns.ac.rs](mailto:sanjaradovic@uns.ac.rs)

Abstract

In order to improve performances and reduce negative effects of the sole technologies effective for the removal of different pollutants from wastewater, hybrid processes have been investigated. This work proposes an eco-friendly hybrid technology for the removal of target emerging water pollutants, namely non-steroidal anti-inflammatory drugs (NSAIDs) – diclofenac (DCF) and naproxen (NPX). Hybrid technology consists of coagulation and adsorption processes, successively applied in the mentioned order. Eco-friendly coagulant obtained from the common bean seeds (*Phaseolus vulgaris*) was used as an alternative coagulant (prepared by conventional solid/liquid and ultrasound extraction and spray drying process), whereas low-cost adsorbent obtained from apricot kernels additionally magnetised with FeSO₄ was used in adsorption process. Coagulation alone achieved promising results in terms of turbidity removal (over 60%), but it insignificantly reduced DCF and NPX concentrations within defined conditions (pH 6, coagulant dose: 0.4 mL/L, turbidity: 200 NTU, DCF and NPX initial concentration: 1 mg/L). However, after hybrid process, removal of DCF and NPX was upgraded to 27.5-99.9% and 15.7-99.9%, respectively. The results variation originated from the type of coagulant and adsorbent dose (1.25 to 12.5 mg/mL). Additionally, potential benefits of the hybrid technology as well as suggestions for the process optimisation were discussed in the paper. An importance and justification for the application of hybrid systems in wastewater treatment was also emphasised.

1. Introduction

Non-steroidal anti-inflammatory drugs (NSAIDs) are a group of pharmaceuticals (PhCs) that became popular for treating inflammatory and painful conditions [1]. Among NSAID group, diclofenac (DCF) and naproxen (NPX) were detected as highly consumed NSAIDs that are abundantly found in water and wastewater streams [2]. In such aquatic environments they could pose a serious health and environmental issue, even in small but constantly present concentrations (ranging from ng/L to several $\mu\text{g/L}$) [3]. The main source of NSAIDs in aquatic environments is inadequate treatment by conventional technologies in wastewater treatment plants (WWTPs) [4]. Advanced technologies were tested for the removal of different PhCs and although they achieved high removal rates, they were proved to be economically demanding. Their high cost makes large scale application cost-prohibitive which is a problem especially in poor regions. In order to overcome the economical barrier and make wastewater treatment more affordable to all countries, alternative, cost-beneficial technologies have been investigated [5].

Adsorption is recognised as one of the most widely used technologies for the reduction of organic and inorganic pollutants from wastewater. It could be attributed to its easy operation, simple design, low-cost, high efficiency and absence of hazardous products [6]. In order to further lower the cost of adsorption, adsorbent produced from low-cost precursors could be used instead of commercially used adsorbent (i.e., activated carbon). Low-cost adsorbents utilised for the PhCs removal were made from different precursors such as agricultural waste (e.g., lignocellulosic biomass) [7,8], industrial waste, chitosan, clays, fly ash, organic resins etc. [9,6]. Difficult segregation of adsorbent from the treated medium is one of the obstacles that should be overcome so that the adsorption process would be unconditionally adopted by the industries. This could be done by adsorbent magnetisation [10]. In order to magnetise adsorbent, magnetic particles (i.e., oxides of different metals such as Fe, Mg, etc.) are incorporated in the adsorbent structure [11]. Hence, their magnetic properties would facilitate separation and recovery of spent adsorbent which will further reduce capital investments [10].

Although adsorption was proved as an efficient method, their material and energy demand could be optimised by coupling adsorption with a different technology. Integration of technologies could be implemented to achieve the treatment goals by utilising the strength of each process, while minimising the shortcoming of others [12]. One potential promising technology that could be coupled with adsorption in order to enhance reduction of different pollutants from wastewater is coagulation. Previous studies on such hybrid processes included removal of NPX, acetaminophen [13], caffeine, benzophenone, benzophenone-3 [14] and dyes [15].

As the primal role of coagulation is to remove colloid and suspended solids, it could be assumed that in hybrid system coagulation it would enhance adsorption of target pollutants by removing potentially interfering impurities (adsorption barriers) from the treated water [13].

Additionally, conventional coagulants (aluminium (Al) and ferrous (Fe) salts), which are problematic because of the potential negative effects of Al and Fe on human health, could be replaced by safer coagulants of "green" origin [16]. Conventional coagulants could increase ionic strength and hinder reduction of PhCs in hybrid (coagulation-adsorption) system [13], hence, application of natural coagulants could be beneficial in this area. Justification for natural coagulant implementation could also be found in their numerous advantages such as their non-toxicity, biodegradability, less sludge production, non-corrosivity etc. [17]. Precursors for natural coagulant production such as chitosan and different plants (e.g. *Moringa Oleifera*, cactus) are renewable and abundantly available which is another benefit of their utilisation [12].

In this work hybrid system, which consists of coagulation and adsorption technology, the removal of DCF and NPX was tested from the model water in lab-conditions. For that purpose, novel eco-friendly coagulant made from the common bean was introduced, whereas apricot kernels were utilised as precursors for low-cost magnetised adsorbent preparation. The novelty of this work comparing to the others published in this area of research is that it includes a completely alternative and eco-friendly approach for the design of treatment technology.

2. Methods

DCF and NPX standards (VWR Chemicals) were used for preparing 500 mg/L stock solution of each pollutant. NaCl (Centrohem, Stara Pazova) was used as an extracting agent. HCl and 33% NaOH (Sigma Aldrich) were used for adjusting pH. Iron (II) sulphate heptahydrate ($\text{FeSO}_4 \times 7\text{H}_2\text{O}$) (Sigma Aldrich) was utilised for the adsorbent magnetisation.

Seeds from the common bean (*Phaseolus vulgaris*) were purchased from the local market and used as a precursor for an eco-friendly coagulant production. The coagulant was produced by a three-step procedure, including: mechanical treatment (milling and sieving), extraction phase and spray drying. After milling, bean seeds were sieved and a smaller fraction (<0.4 mm in diameter) was collected and used in extraction step. Two types of the coagulant from the same precursor were obtained. The difference was in the extraction step. The one produced by conventional solid/liquid extraction (10 min stirring on magnetic stirrer at room temperature, followed by filtration on Büchner's funnel) will be denoted in further text as KNO. The other coagulant produced by ultrasound extraction (50 min treatment in ultrasonic bath at 25°C, followed by filtration in Büchner's funnel) will be denoted as UNO. The extraction agent in both cases was 0.5 mol/L NaCl aqueous solution. Obtained liquid extracts were dried in a spray dryer at 120°C.

Powdered coagulants were kept in well-sealed plastic tubes in an exicator until further use. Apricot kernels used as starting material for adsorbent production were obtained from the local plantation in Novi Becej, province of Vojvodina, Serbia. First of all, the impurities were removed from obtained kernels by washing in distilled water. After washing, kernels were milled in a mechanical mill and then dried for 2 h at 105°C. 20 g of $\text{FeSO}_4 \times 7\text{H}_2\text{O}$ was diluted

in 100 mL of Milli-Q distilled water. Apricot kernels were immersed in FeSO₄ solution and the obtained suspension was treated in ultrasonic bath (30 min in ultrasonic bath followed by 10 min of mixing on magnetic stirrer – the procedure repeated four times). The treated suspension was left in a dryer on 105°C overnight. Following that, the drying material was placed in crucibles and heated in a furnace at 500°C for 1 h. The cooled adsorbent was washed until pH 7 was achieved. Recommendation is to wash adsorbent under a digestor, because of the strong ferrous smell. Adsorbents were dried at 105°C overnight and packed in zip-bags until further use.

For the experiments, model water made from previously prepared 1% kaolin suspension, was made on the day of experiments. To obtain turbidity of 200 NTU, kaolin suspension was diluted with tap water. pH 6 was adjusted by HCl and 33% NaOH. 1 mg/L of each DCF and NPX were spiked in model water. For that purpose, stock solution of 500 mg/L for DCF and NPX were used.

Based on the previously conducted coagulation/flocculation experiments, a coagulant dose of 0.4 mL/L was determined as an optimal dose for turbidity reduction. Hence, this dose was used in hybrid experiments. Coagulation/flocculation experiments were done in Jar Tester. Firstly 200 mL of model water was divided in the glass beakers of 600 mL in volume. The experiments were done in the following dynamic/regime: 1 min of rapid mixing (200 rpm) and 30 min of slow mixing (60 rpm). This was followed by 1 h of settling after which 50 mL of precipitate was decanted and prepared for HPLC-MS/MS and turbidity measurements.

Preparation for HPLC-MS/MS included filtration through PTFE filter (0.45 µm pore diameter, Fisherbrand). Samples were additionally diluted (2x) before HPLC/MS/MS analysis.

For adsorption experiments, model water was divided into plastic tubes of 20 mL in volume and prepared for the adsorption experiments. In each sample different mass of adsorbent was added so that the final adsorbent concentration would be 0, 1.25, 2.5 and 12.5 mg/mL. Adsorption experiments were done on pH 6 in batch mode (2 h mixing on magnetic stirrer, room temperature, 150 rpm). After adsorption, samples were prepared for the HPLC-MS/MS analysis in the previously described method.

Hybrid experiments consisted of described technologies in the mentioned order (coagulation followed by adsorption). Precipitate from the coagulation experiments was, in hybrid experiments, used for the adsorption phase. Except from the type of water used as a medium for adsorption process, everything else was the same in separate as well as within hybrid systems. pH, DCF and NPX concentrations were measured after each process.

The removal efficiency (%) was estimated using the equation below:

$$Removal (\%) = \frac{(C_0 - C_e)}{C_0} \times 100\% \quad , \quad (1)$$

where C₀ and C_e (mg/L) represent initial and final concentration of the PhCs, respectively, in the treated model water.

3. Results

Preliminary results showed promising potential of hybrid coagulation-adsorption system for the removal of relatively low initial DCF and NPX concentrations. The system had the highest efficiency (>98%) when higher adsorbent dosages (5 and 12.5 mg/mL) are applied.

Additionally, application of UVO coagulant was preferable. However, on lower adsorbent dosages (1.25 and 2.5 mg/mL) efficiency dropped significantly. This trend can also be noticed in the results of sole adsorption experiments, but to a lesser extent.

Coagulation alone did not present any significant removal of DCF and NPX under applied conditions, hence, the results were not graphically presented herein. On the other hand, adsorption was effective (>60% of removal rate for all applied dosages). Removal efficiency was increased with adsorbent dosage and showed best efficiency (99.86±0.13 and 99.76±0.07 % for DCF and NPX, respectively) for the dose of 12.5 mg/L (**Figure 1**).

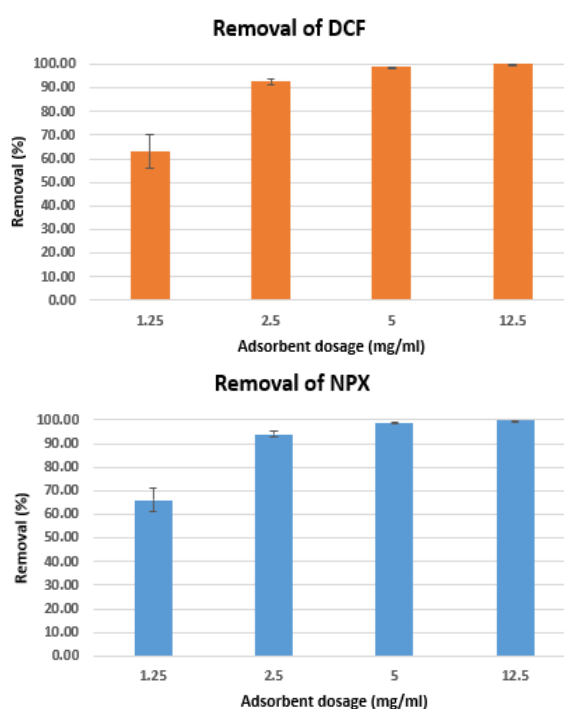


Figure 1. Removal of DCF and NPX under batch adsorption experiments (pH 6, 120 min contact time, 180 rpm, initial DCF and NPX concentration: 1 mg/L)

Concerning DCF and NPX removal within the hybrid system, it could be seen from **Figure 2** that combination of coagulant obtained by ultrasound extraction and magnetised adsorbent (UVO&FeSO₄) achieved higher removal of both compounds compared to experiments where coagulant obtained by conventional solid/liquid extraction was combined with magnetised adsorbent (KNO&FeSO₄). The largest difference could be observed for the adsorbent dose of 2.5 mg/mL (removal was around 20% lower for DCF and around 10% lower for NPX). The mentioned differences could be attributed to higher efficiency of UVO coagulant for turbidity removal. From the previously conducted experiments it was proved that for the same coagulant dose (0.4 mL/L), UVO reduced turbidity for 68.29%, whereas KNO removed

44.04%. However, differences in DCF and NPX removal were significant only for lower doses of adsorbent (1.25 and 2.5 mg/mL). DCF and NPX removal rates were not hindered by different coagulants on higher adsorbent doses (5 and 12.5 mg/mL). As for the adsorption alone, the highest removal by hybrid system was achieved at the highest adsorbent doses (removal rate was >99.9 and >99.8% for DCF and NPX, respectively). The similar can be observed for the adsorbent dose of 5 mg/mL. Adsorption alone and hybrid system were almost equally efficient for the DCF and NPX removal on mentioned higher doses. However, for lower adsorbent doses, DCF and NPX removal was higher in adsorption experiments compared to experiments with hybrid system.

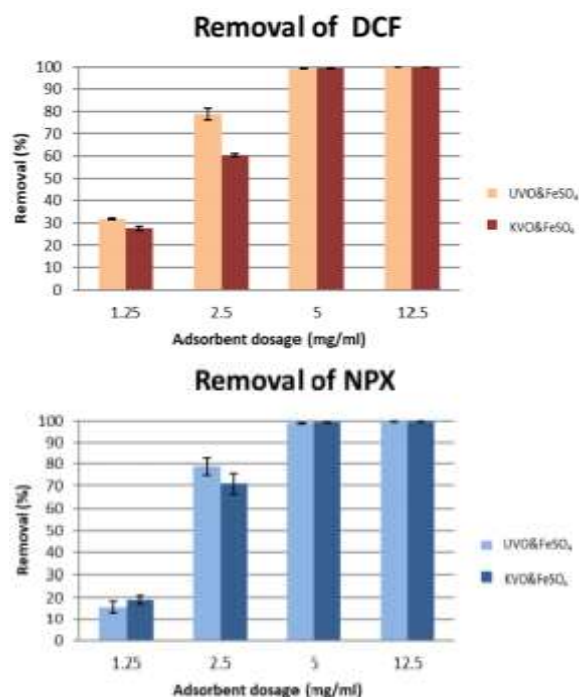


Figure 2. Removal of DCF and NPX by successively applied coagulation and adsorption process (hybrid system)

4. Discussion

The differences between adsorption and hybrid system (successive coagulation and regime) were in accordance with previous study conducted by Jung et al. (2015). They assumed that failure of hybrid system to remove acetaminophen and NPX was due to the increase in ionic strength. Furthermore, they emphasised the difference between the experiments where coagulation and adsorption were conducted simultaneously and successive regime. Successive coagulation-adsorption was more efficient for the pollutant removal as pre coagulation removed adsorption barriers and in that way facilitate adsorption of targeted compounds (Jung et al., 2015). Similar results can be observed in the study of Ivančev-tumbas et al. [14] who also emphasised an importance of total suspended solids (TSS) concentration in treated medium. The performances and activities of simultaneous and successive hybrid system differ with TSS concentration (<2 mg/L and equal to 68 mg/L).

Hence, it could be assumed that whether simultaneous or successive design of hybrid system would be preferable depends on TSS concentration in treated water. Bearing in mind all previously said, ionic strength should be monitored so that the system behaviour could be better understood. In order to optimise and rise an efficiency of hybrid technology in future experiments more operational parameters could be varied, with special attention on TSS content and pH of the model water. Successive and simultaneous performance of technologies should also be compared (with additional TSS concentration monitoring), in order to deduce which one is more adequate and effective for the removal of DCF and NPX under optimal conditions. Optimal conditions, for instance, could be determined or re-evaluated by response surface methodology. Hoong and Ismail (2018)[15] [used it to determine optimal operating conditions for the removal of dye from Congo red dye wastewater by simultaneous adsorption-coagulation system. The only possible drawback is that this methodology requests higher number of experiment set-ups (27) [15]. Another possible interfering factor in the evaluated research could be utilisation of kaolin for model water preparation, as kaolin as well have adsorption properties. This could be the reason for the deviations in the removal efficiencies between the sole and hybrid systems. Kaolin replacement should be taken into consideration for the future experiments. Inefficiency of sole coagulation technology for DCF and NPX removal could be explained by the model water used for the experiments. In this work coagulation was purposely used for the turbidity removal, hence experiments were set according to that. If coagulation would be investigated only for DCF and NPX removal, more explanations would be gathered by experiments on distilled water rather than kaolin suspension spiked with target pollutants. By and large, hybrid systems have advantages that should not be neglected, such as lower sludge production, lower resources and energy consumption, but to achieve them, the system must be optimised. Preliminary results could direct future research and lead toward system optimisation. In order to achieve that, more work should be done.

Acknowledgements

This research has been supported by Innovation Fund, Republic of Serbia, ID 5156 through project Proof of Concept, by the Ministry of Education, Science and Technological Development through the project no. 451-03-68/2020-14/200156: “Innovative scientific and artistic research from the FTS (activity) domain” and mobility funding which facilitated study at Environmental Research Institute in Scotland provided through ERASMUS + Higher Education International Credit Mobility - Project 2018-1_UK01-KA107-047241 between North Highland College, Thurso and Faculty of Technical Sciences, University of Novi Sad, Serbia.

References

1. Rainsford K.D, Kean W.F, Ehrlich G.E, Review of the pharmaceutical properties and clinical effects of the topical NSAID formulation, diclofenac epolamine. *Curr. Med. Res. Opin.* 2008, 24: 2967–2992. DOI: 10.1185/03007990802381364
2. Elizalde-velázquez A, Subbiah S, Anderson T.A, Green M.J, Zhao X, Cañas-carrell J.E, Sorption of three common nonsteroidal anti-inflammatory drugs (NSAIDs) to microplastics. *Sci. Total Environ.* 2020, 715: 136974. DOI: 10.1016/j.scitotenv.2020.136974
3. Wang T, Liu S, Gao G, Zhao P, Lu N, Lun X, Hou X, Magnetic solid phase extraction of non-steroidal anti-inflammatory drugs from water samples using a metal organic framework of type Fe₃O₄/MIL-101(Cr), and their quantitation by UPLC-MS/MS. *Microchim. Acta* 2017, 184: 2981–2990. DOI: 10.1007/s00604-017-2319-8
4. Stancová V, Ziková A, Svobodová Z, Kloas W, Effects of the non-steroidal anti-inflammatory drug(NSAID) naproxen on gene expression of antioxidant enzymes in zebrafish (*Danio rerio*). *Environ. Toxicol. Pharmacol.* 2015, 40: 343–348. DOI: 10.1016/j.etap.2015.07.009
5. Li Y, Zhu G, Ng W.J, Tan S.K, A review on removing pharmaceutical contaminants from wastewater by constructed wetlands: Design, performance and mechanism. *Sci. Total Environ.* 2014, 468–469, 908–932. DOI: 10.1016/j.scitotenv.2013.09.018
6. Quesada H.B, Baptista A.T.A, Cusioli L.F, Seibert D, de Oliveira Bezerra C, Bergamasco R, Surface water pollution by pharmaceuticals and an alternative of removal by low-cost adsorbents: A review. *Chemosphere* 2019, 222: 766–780. DOI: 10.1016/j.chemosphere.2019.02.009
7. Pap S, Taggart M.A, Shearer L, Li Y, Radovic S, Sekulic M.T, Removal behaviour of NSAIDs from wastewater using a P-functionalised microporous carbon. *Chemosphere* 2020, 264: 128439. DOI: 10.1016/j.chemosphere.2020.128439
8. Turk Sekulic M, Boskovic N, Slavkovic A, Garunovic J, Kolakovic S, Pap S, Surface functionalised adsorbent for emerging pharmaceutical removal: Adsorption performance and mechanisms. *Process Saf. Environ. Prot.* 2019, 125: 50–63. DOI: 10.1016/j.psep.2019.03.007
9. De Andrade J.R, Oliveira M.F, Da Silva M.G.C, Vieira M.G.A, Adsorption of Pharmaceuticals from Water and Wastewater Using Nonconventional Low-Cost Materials: A Review. *Ind. Eng. Chem. Res.* 2018, 57: 3103–3127. DOI: 10.1021/acs.iecr.7b05137
10. Mehta D, Mazumdar S, Singh S.K, Magnetic adsorbents for the treatment of water/wastewater-A review. *J. Water Process Eng.* 2015, 7: 244–265. DOI: 10.1016/j.jwpe.2015.07.001
11. Philippova O, Barabanova A, Molchanov V, Khokhlov A, Magnetic polymer beads: Recent trends and developments in synthetic design and applications. *Eur. Polym. J.* 2011, 47: 542–559. DOI: 10.1016/j.eurpolymj.2010.11.006
12. Ang W.L, Mohammad A.W, State of the art and sustainability of natural coagulants in water and wastewater treatment. *J. Clean. Prod.* 2020, 262. DOI: 10.1016/j.jclepro.2020.121267
13. Jung C, Oh J, Yoon Y, Removal of acetaminophen and naproxen by combined coagulation and adsorption using biochar: influence of combined sewer overflow components. *Environ. Sci. Pollut. Res.* 2015, 22: 10058–10069. DOI: 10.1007/s11356-015-4191-6
14. Ivančev-tumbas I, Bogunović M, Vasić Vet al., 'Green' coagulant application with activated carbon : dosing sequence and removal of selected micropollutants and effluent organic matter from municipal wastewater. *Environ. Technol.* 2020, 0: 1–7. DOI: 10.1080/09593330.2020.1821788

15. Hoong H.N.J, Ismail N, Removal of Dye in Wastewater by Adsorption-Coagulation Combined System with Hibiscus sabdariffa as the Coagulant. MATEC Web Conf. 2018, 152. DOI: 10.1051/mateconf/201815201008
16. Yin C.Y, Emerging usage of plant-based coagulants for water and wastewater treatment. Process Biochem. 2010, 45: 1437–1444. DOI: 10.1016/j.procbio.2010.05.030
17. Maurya S, Daverey A, Evaluation of plant-based natural coagulants for municipal wastewater treatment. 3 Biotech 2018, 8: 1–4. DOI: 10.1007/s13205-018-1103-8





Development of an analytical method to determine contamination of propolis with neonicotinoid pesticides

Tomšič R¹, Heath D², Heath E^{2,3}, Markelj J¹, and Prosen H^{1*}

¹ University of Ljubljana, Faculty of Chemistry and Chemical Technology, Ljubljana, Slovenia

² Jožef Stefan Institute, Department of Environmental Sciences, Ljubljana, Slovenia

³ Jožef Stefan International Postgraduate School, Ljubljana, Slovenia

[*helena.prosen@fkkt.uni-lj.si](mailto:helena.prosen@fkkt.uni-lj.si)

Abstract

Neonicotinoid insecticides in the environment are one of the possible reasons for the diminishing number of honeybees. They are frequently found in different bee products. We developed a method for the determination of five neonicotinoids in propolis samples. Two sample preparation methods were tested: solid-phase extraction (SPE) and quick, easy, cheap, effective, rugged, and safe (QuEChERS). The extracts were analysed with liquid chromatography-tandem mass spectrometry (LC-MS/MS) in selected reaction monitoring mode. Cleaner extracts were obtained by solid-phase extraction. SPE-LC-MS/MS method was validated at two spiking levels and good recoveries were obtained for all neonicotinoids (61-101%), except for clothianidin, as well as low LODs (0.2-4.4 µg/L) and LOQs (0.8-14.7 µg/L). Matrix-matched calibration was used with good accuracy and linearity ($R^2 > 0.991$). Thirty real propolis samples (raw propolis and alcohol tinctures) from Slovenia and other countries were analysed and low contamination with some neonicotinoids was detected.

1. Introduction

Neonicotinoid insecticides became commercially available by early 1990s [1] and are nowadays commonly used as systemic insecticides for the protection of economic plants during the entire growing season[2].

They show low toxicity for the mammals, but are more problematic for bees. Within plant, they are present in pollen and nectar, which are the primary food source for bees[3]. Those neonicotinoids that exhibit the lowest LD₅₀ for bees (clothianidin, imidacloprid, and thiamethoxam) are currently banned in the European Union. Even sub-lethal exposure of bees could lead to colony collapse disorder (CCS)[4].

Most often, LC-MS or LC-MS/MS in combination with a suitable extraction method are used for the determination of neonicotinoids in honeybee products, such as pollen, honey, and beeswax [5-11]. Different extraction methods are used, such as liquid-liquid extraction (LLE) [12,6], dispersive liquid-liquid microextraction (DLLME)[13,6], QuEChERS[14,7,9,10] and solid-phase extraction – SPE [15,5,16,10]. Residues of any type of pesticides are rarely determined in propolis because of its complexity. Only one study was found that included determination of thiacloprid residues along with other pesticides in propolis [17].

We developed and validated a method for the determination of five neonicotinoid pesticides in propolis. It was applied to the analysis of thirty propolis samples from Slovenia and other countries. To the best of our knowledge, this is the first study on the contamination of propolis with neonicotinoid insecticides.

2. Methods

Standard stock solutions of acetamiprid, clothianidin, imidacloprid, thiacloprid, and thiamethoxam (1 g/L) and standard stock solution of the internal standard (IS) clothianidin-d₃ (1 g/L) were prepared in acetonitrile. Multicomponent working standard (5.5 mg/L) was prepared in acetonitrile-0.1% HCOOH (1:9, V/V). Matrix-matched solutions were prepared by adding the multicomponent working standard to blank propolis extracts. Spiked propolis samples were prepared by adding multicomponent working standard and internal standard to the blank propolis sample prior to extraction.

Thirty propolis samples (18 raw propolis and 12 tinctures) were collected from Europe and Canada. Propolis tinctures were diluted with MilliQ water, while raw propolis samples were dissolved in 10% ethanol.

Solid-phase extraction was optimised using aqueous samples with approximately 10% of ethanol. Oasis HLB extraction cartridges were used.

The QuEChERS method was adapted from Anastassiades, Lehotay, Stajnbaher, and Schenck [18].

LC-MS/MS analysis was performed on a Perkin Elmer Series 200 HPLC instrument, coupled to a triple quadrupole MS (Applied Biosystems/MDS Sciex 3200 QTRAP) with TurbolonSpray (ESI) source. Electrospray ionization (ESI) with positive polarity was used. The mass analyzer was run in the selected reaction monitoring (SRM) mode.

Final SPE-LC-MS/MS method was validated at two spiking levels 10 and 50 ng/g of raw propolis. Matrix-matched calibration was used to determine LOD, LOQ, and linearity. Identification was based on a precursor and two product ions (SRM method), the ratio between the signals for product ions (product ion 1/product ion 2) and on retention time. Method accuracy was calculated as the relative error and method efficiency as average recovery. Repeatability of the method was calculated as RSD of the parallel determinations.

5. Results and Discussion

For SPE method propolis samples with different ethanol content (1-20%) were tested. Ethanol content in the above range did not significantly affect recoveries of neonicotinoids, except for clothianidin. In the final method, samples with 10% ethanol content were used. The highest sample volume to be loaded on the cartridge was 50 mL. The optimum elution solvent was acetonitrile (5 mL).

For QuEChERS, a modified and unmodified EN method [18] (Anastassiades et al., 2003) were tested with reconstitution of dried ethanol tinctures in either acetonitrile or ethanol. Higher recoveries were obtained by using acetonitrile (95-117%). However, the QuEChERS extracts were very complex and clogging of MS ion source was observed. Additional clean-up by SPE resulted in very low recoveries. For this reason, SPE was selected as the better sample preparation method.

SPE-LC-MS/MS method was validated and it was found that the method gives good linearity ($R^2 > 0.99$) for all analytes, low LODs (0.2-4.4 ng/g), and LOQs (0.7-14.7 ng/g). The LOQs were below the MRLs in honey for all analytes, while for propolis, no MRLs are currently established. Method gave satisfactory recoveries for acetamiprid, imidacloprid, and thiacloprid at both spiking levels (91-101%). Lower recovery was obtained for thiametoxam (61%) and clothianidin (10-20%). Overall accuracy (expressed as relative error) was below 11% at both spiking levels. Matrix effect was low for clothianidin and thiametoxam and higher for the other three analytes. Detailed method optimization and validation data are available in the paper by [19].

Analysis of 30 propolis samples from Europe and Canada confirmed the presence of acetamiprid, thiacloprid and imidacloprid, with concentrations between LOD and LOQ. Acetamiprid was detected in three samples, thiacloprid in two samples, and imidacloprid in two samples as well (**Figure 1**).

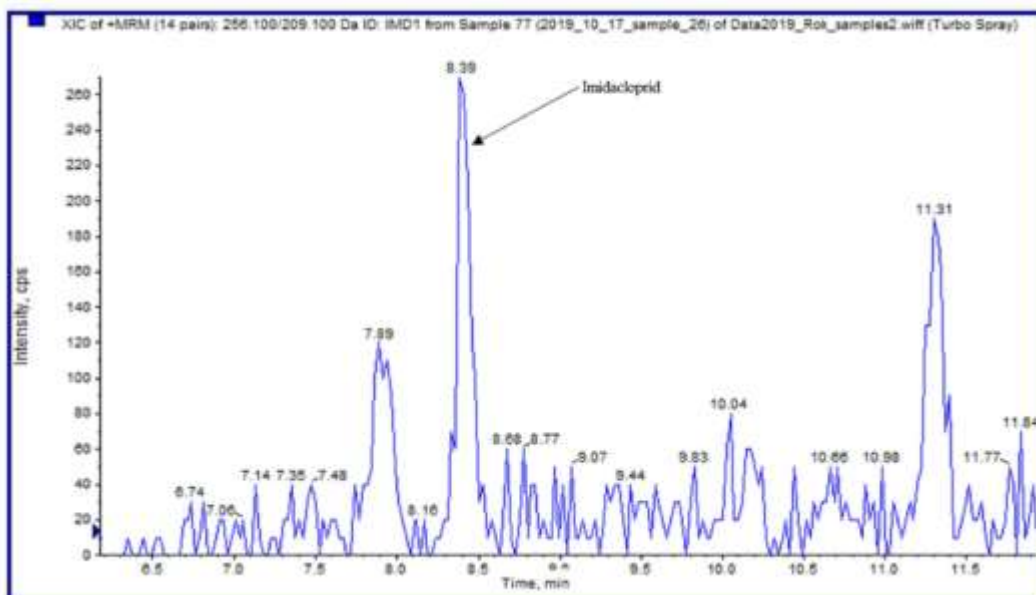


Figure 1. Chromatogram of a contaminated sample (m/z transition for imidacloprid).

Acknowledgements

The study was performed with the financial support of the Slovenian Research Agency, namely Program Groups P1-0143 and P1-0153, and Projects L1-9191 and N1-0143. This study has received funding from the EMPIR programme co-financed by the Participating States and from the European Union's Horizon 2020 research and innovation programme (18NMR01).

References

1. Lundin, O., Rundlöf, M., Smith, H. G., Fries, I., and Bommarco, R. Neonicotinoid insecticides and their impacts on bees: A systematic review of research approaches and identification of knowledge gaps. *PLoS One* 2015, 10: 1–20. DOI:10.1371/journal.pone.0136928.
2. Jeschke, P., Nauen, R., Schindler, M., and Elbert, A. Overview of the status and global strategy for neonicotinoids. *J. Agric. Food Chem.* 2011, 59: 2897–2908. DOI:10.1021/jf101303g.
3. Elbert, A., Haas, M., Springer, B., Thielert, W., and Nauen, R. Applied aspects of neonicotinoid uses in crop protection. *Pest Manag. Sci.* 2008, 64: 1099–1105. DOI:10.1002/ps.1616.
4. Lu, C., Warchol, M.-K., and Callahan, A. R. Sub-lethal exposure to neonicotinoids impaired honey bees winterization before proceeding to colony collapse disorder. *Bull. Insectology* 2014, 67: 125–130.
5. Fidente, P., Seccia, S., Vanni, F., and Morrica, P. Analysis of nicotinoid insecticides residues in honey by solid matrix partition clean-up and liquid chromatography-electrospray mass spectrometry. *J. Chromatogr. A* 2005, 1094: 175–178. DOI:10.1016/j.chroma.2005.09.012.
6. Jovanov, P., Guzsvány, V., Franko, M., et al. Multi-residue method for determination of selected neonicotinoid insecticides in honey using optimized dispersive liquid-liquid microextraction combined with liquid chromatography-tandem mass spectrometry. *Talanta* 2013, 111: 125–133. DOI:10.1016/j.talanta.2013.02.059.

7. Jovanov, P., Guzsány, V., Franko, M., et al. Development of multiresidue DLLME and QuEChERS based LC-MS/MS method for determination of selected neonicotinoid insecticides in honey liqueur. *Food Res. Int.* 2014, 55: 11–19. DOI:10.1016/j.foodres.2013.10.031.
8. Gbylik-Sikorska, M., Sniegocki, T., and Posyniak, A. Determination of neonicotinoid insecticides and their metabolites in honey bee and honey by liquid chromatography tandem mass spectrometry. *J. Chromatogr. B Anal. Technol. Biomed. Life Sci.* 2015, 990: 132–140. DOI:10.1016/j.jchromb.2015.03.016.
9. Daniele, G., Giroud, B., Jabot, C., and Vulliet, E. Exposure assessment of honeybees through study of hive matrices: analysis of selected pesticide residues in honeybees, beebread, and beeswax from French beehives by LC-MS/MS. *Environ. Sci. Pollut. Res.* 2018, 25: 6145–6153. DOI:10.1007/s11356-017-9227-7.
10. Mrzlikar, M., Heath, D., Heath, E., Markelj, J., Kandolf, A., and Prosen, H. LWT - Food Science and Technology Investigation of neonicotinoid pesticides in Slovenian honey by LC-MS/MS. *LWT* 2015, 104: 45–52. DOI:10.1016/j.lwt.2019.01.017.
11. Yáñez, K. P., Martín, M. T., Bernal, J. L., Nozal, M. J., and Bernal, J. Trace Analysis of Seven Neonicotinoid Insecticides in Bee Pollen by Solid-Liquid Extraction and Liquid Chromatography Coupled to Electrospray Ionization Mass Spectrometry. *Food Anal. Methods* 2014, 7: 490–499. DOI:10.1007/s12161-013-9710-9.
12. Liu, S., Zheng, Z., Wei, F., et al. Simultaneous determination of seven neonicotinoid pesticide residues in food by ultraperformance liquid chromatography tandem mass spectrometry. *J. Agric. Food Chem.* 2010, 58: 3271–3278. DOI:10.1021/jf904045j.
13. Campillo, N., Viñas, P., Férrez-Melgarejo, G., and Hernández-Córdoba, M. Liquid chromatography with diode array detection and tandem mass spectrometry for the determination of neonicotinoid insecticides in honey samples using dispersive liquid-liquid microextraction. *J. Agric. Food Chem.* 2013, 61: 4799–4805. DOI:10.1021/jf400669b.
14. Kamel, A. Refined methodology for the determination of neonicotinoid pesticides and their metabolites in honey bees and bee products by liquid chromatography-tandem mass spectrometry (LC-MS/MS). *J. Agric. Food Chem.* 2010, 58: 5926–5931. DOI:10.1021/jf904120n.
15. Albero, B., Sánchez-Brunete, C., and Tadeo, J. L. Analysis of pesticides in honey by solid-phase extraction and gas chromatography-mass spectrometry. *J. Agric. Food Chem.* 2004, 52: 5828–5835. DOI:10.1021/jf049470t.
16. Jones, A., and Turnbull, G. Neonicotinoid concentrations in UK honey from 2013. *Pest Manag. Sci.* 2016, 72: 1897–1900. DOI:10.1002/ps.4227.
17. Oellig, C. Acetonitrile extraction and dual-layer solid phase extraction clean-up for pesticide residue analysis in propolis. *J. Chromatogr. A* 2016, 1445: 19–26. DOI:10.1016/j.chroma.2016.03.082.
18. Anastassiades, M., Lehotay, S. J., Štajnbaher, D., and Schenck, F. J. Fast and easy multiresidue method employing acetonitrile extraction/partitioning and “dispersive solid-phase extraction” for the determination of pesticide residues in produce. *J. AOAC Int.* 2003, 86: 412–431. DOI:10.1093/jaoac/86.2.412.
19. Tomšič, R., Heath, D., Heath E., Markelj, J., Kandolf Borovšak, A., and Prosen, H. Determination of neonicotinoid pesticides in propolis with liquid chromatography coupled to tandem mass spectrometry. *Molecules* 2020, 25: 5870. DOI:10.3390/molecules25245870



PHARMACEUTICAL AND FINANCIAL ASPECT OF RESEARCH AND DEVELOPMENT IN NINE PHARMACEUTICAL INDUSTRY GIANTS

Tršek A¹, Smerkolj N², Jeran M^{3,4,*}

¹University of Ljubljana, Faculty of Pharmacy, Ljubljana, Slovenia

²University of Ljubljana, Faculty of Economics, Ljubljana, Slovenia

³University of Ljubljana, Faculty of Electrical Engineering, Laboratory of Physics, Ljubljana, Slovenia

⁴University of Ljubljana, Faculty of Health Sciences, Laboratory of Clinical Biophysics, Ljubljana, Slovenia

* marko.jeran@fe.uni-lj.si

Abstract

In the time of writing this article, the first dosages of vaccine against COVID-19 are being redistributed around Europe. Although much desired and needed, the vaccine had to go through a number of processes before it was approved by the overseeing authorities. However, the development of a regular medicine is considerably longer. In this article, we describe the research and development process that pharmaceutical companies have to go through in order to register a new drug. The article shows just how crucial it is for the companies to invest proper amounts in R&D and it further illustrates what some of the most well-known companies have achieved in the last twenty years. The article also includes financial data and analysis with the focus on so-called R&D intensity.

1. Drug discovery and development

Industrial research and development (R&D) is a fundamental segment of innovation-led growth as it helps generate higher value-added products, processes and services [1]. Studies suggest that there is a positive correlation between the expenditure for R&D and productivity (output per unit of input) [2,3]. High-tech industries have a stronger correlation between R&D spending and productivity; however, low-tech industries likewise enjoy the benefits of R&D spending, but to a smaller degree [2]. In sectors where R&D is especially important, investments also have a positive correlation with sales growth and share price, moreover, with sustained R&D investment, businesses can more easily achieve and maintain a competitive advantage on the market, *ceteris paribus* [1]. Johansson and Lööf demonstrated that firms with a continual R&D investing outperform companies with irregular or no R&D investment program [4]. Among industries with known high R&D intensity (R&D expenses as a ratio of total revenue) are IT hardware, Automotive, Biotechnology, Aerospace and defence, Electronics, Engineering and chemicals and Pharmaceuticals [1].

In the pharmaceutical industry drug discovery and development is a lengthy, complex and expensive process. The journey from when a new drug molecule is discovered to when an innovative medical product is available on the market for treating a medical condition may take up to 15 years [5,6]. The average R&D costs for each drug ranges from \$900 million to \$2 billion and comprises the cost of all failures [5].

The process of drug discovery and development is presented in Figure 1. Before a drug is approved for use, rigorous testing is performed to determine its safety, efficacy, the correct dosage and the optimum administration route [6,7]. Firstly, scientists identify and validate an enzyme, receptor, ion channel, protein or another biological target in the human body, related to a certain disease [8,9]. The ultimate goal of drug discovery is to find molecules that elicit the desired activity on the target [7]. With the help of high throughput screening assays, this wide range of candidates is narrowed down to the most promising ones. Identified hits are then validated and optimized to achieve adequate target selectivity, absorption, distribution, metabolism and excretion properties. Their pharmacokinetics and toxicity must also be evaluated [9]. All of these studies are performed *in vitro* and/or in animal models, simulating *in vivo* conditions [6]. At this stage, companies also have to consider cost-effectiveness, as it impacts the long-term profitability of the drug [6]. Companies seek to find more than just one candidate molecule, since many of them fail further down in the development process on account of factors such as safety and potency issues [8]. Detailed research methods are needed in order to eliminate unsuitable candidates, since gaps in knowledge at this stage often lead to difficulties later on [8]. Both *in vitro* and *in vivo* tests are usually used for exploring the drugs' pharmacodynamics, pharmacokinetics and safety [6,10]. The purpose of formulation is to deliver the drug to the target site at the right time and in the right concentration. Formulation optimization begins in preclinical testing and continues throughout clinical research [11].

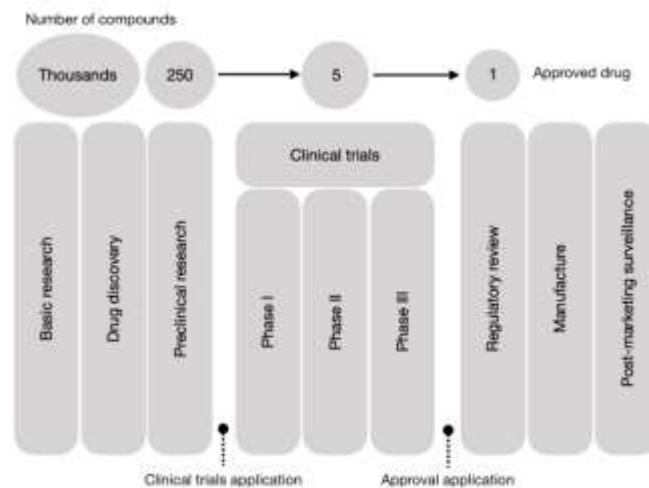


Figure 1. The process of drug discovery and development in the pharmaceutical industry. Adapted from [6, 10].

After the viable candidates are defined, regulatory authorities, such as Food and Drug Administration (FDA) in the U. S. and European Medicines Agency (EMA) in the European Union, require the submission of a clinical trials application [9]. If the regulatory agency deems the information gathered during preliminary testing suitable, clinical trials may begin. The objective of clinical trials is to answer specific research questions. All four phases must follow a protocol [6]. Phase I trials are performed on 20-100 healthy volunteers and take several months [10]. They are intended to determine the drug's safety in humans and gather information on the best administration route [6,10]. At least half of compounds exhibit adequate safety to progress [7]. Phase II trials are conducted on the patient population and include several hundred volunteers with the disease the drug is intended to treat. These trials last from several months to two years and gather additional data on safety as well as determine efficacy and the appropriate therapeutic dose [6]. This is the stage in which most clinical candidates fail due to lack of efficacy or safety [9,10]. Larger scale phase III trials include 300-3000 patients and last from one to four years. They further discover the drug's efficacy and acquire the greatest amount of safety information [6,10].

The greater number of participants enables the detection of long-term and rarer side effects [6]. Clinical trials account for a large share of the drug development budget. Originating from the complexity of medical conditions new drugs are being developed for, the extent and duration of clinical trials is increasing. This of course also contributes to the growth of R&D costs [12].

If clinical research is successful in terms of drug's efficacy and safety, the pharmaceutical company submits an application for marketing authorization. For FDA, the application is called New Drug Application (NDA), whereas EMA requests a Marketing Authorization Application (MAA) [6]. The regulatory authority scientifically evaluates the submitted documentation and decides to approve or not to approve the drug [6]. If the application is

granted, the company will then take steps towards manufacturing and launching the product [6,7]. The drug development process, however, does not stop here. After the drug reaches the market and is being widely used among the patient population, post-marketing surveillance is performed. Phase IV clinical trials obtain information on the drug's long-term advantages and disadvantages [6,10]. The scope for further development of the drug may be determined. On the other hand, if the drug's risks outweigh the benefits, more severe measures are taken and the drug may even be taken off the market [9].

R&D clearly plays a significant role in drug discovery and development, as it allows scientists to gain information on the safety, efficacy and quality of the drug, which are the basic requirements for every medical product. R&D costs differ substantially, depending on the kind of drug being developed and the prospect of failure [12]. Furthermore, all R&D investments bear a high risk and no guarantee of positive returns. Therefore, companies need to alter their R&D strategies and costs with respect to the expected profit from future drug sales [12].

2. Financial Analysis

In this paper, we analyze the R&D expenses of nine pharmaceutical groups (for the purpose of objective and unaffiliated research work we changed their names to letters A to I). They were specifically selected based on financial criteria, such as market share (they are among the biggest companies in the industry), generated revenue and reliance of their financial reports (compliance with International Accounting Standards). The article does not analyze trends of the pharmaceutical industry as a whole, but solely focuses on the aforementioned nine giants. The selected timeframe for the analysis is the period from 2000-2019 and all financial data was taken from the official consolidated financial statements. Whole statements are available online on respective websites of the company. Data used for the analysis is available in the Appendix.

In the observed period the aforementioned companies invested a total of 1014,3 billion USD in R&D¹. In the analysis 158 values were taken into consideration, as some companies were created by a merger or were founded later than in 2000. The mean value of R&D intensity for the selected companies and period is 16.737 percentage points with a standard deviation of 3.57 percentage points². In **Figure 2** we present revenue (in millions), net income (in millions) and research and development expenditure (in millions) for each selected companies individually. Additionally, RD intensity (represented by the red line) is added to each graph.

- 1.Sum of all R&D investments was calculated using the USD values in the reported year. For companies reporting in foreign currency, the annual mean value of exchange rate was used to determine the USD value of their investments.
2. There were two major mergers in the selected companies, namely company E and G. One company was founded later than the beginning of our selected period (company H).

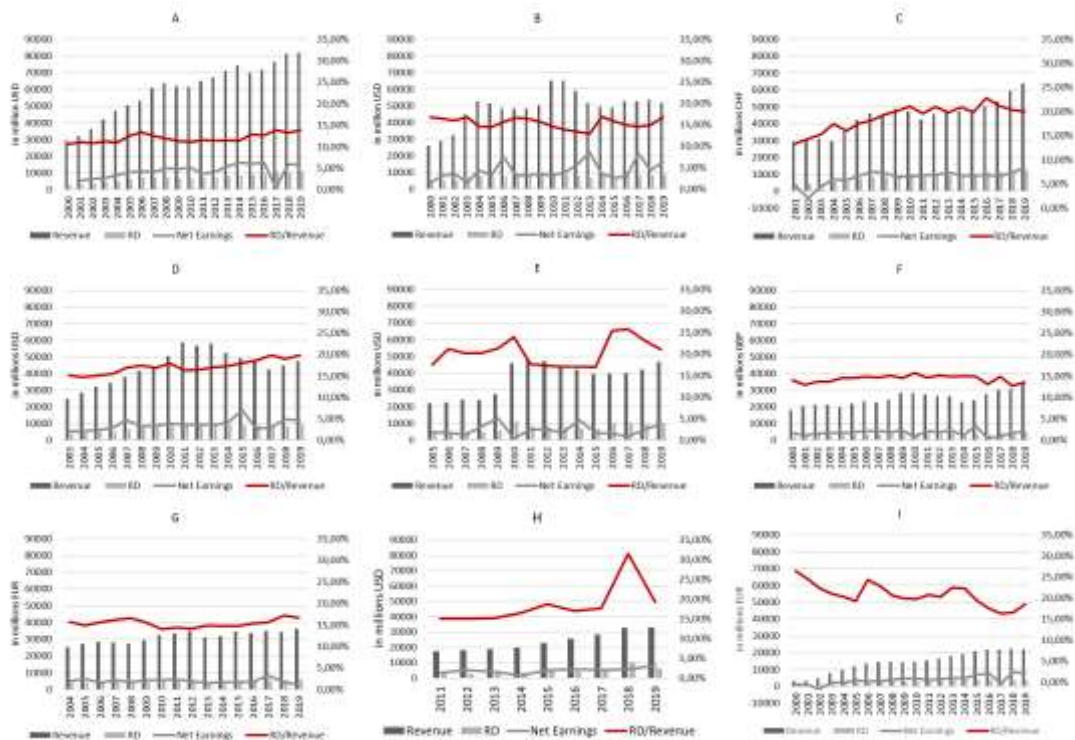


Figure 2. Operating revenue, R&D Investments, Net earnings and R&D Intensity for the selected companies.

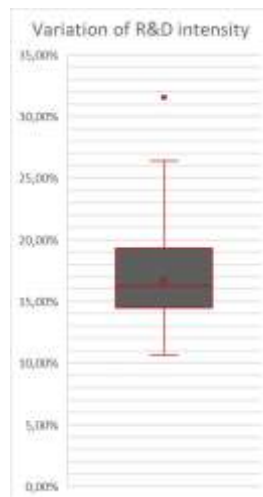


Figure 3. Variation of R&D Intensity. For the analysis of absolute values invested in R&D we divided the total expenditure by the number of companies (since not all were operating during the whole selected period). The mean value of R&D expenditure in 2000 was 3037.7 million USD, while the mean value of R&D expenditure in 2019 was 8359.3 million USD. The slope of our model linear regression function is positive, meaning that the absolute values of R&D investments are increasing over time. In absolute terms, throughout the last 20 years, company C and company B contributed the most to the R&D with investments of 156 and 150 billion USD (see footnote 1 in previous page) respectively. If we compare yearly absolute investments in R&D over the years, companies C, A and E invested the most (7.8, 7.7 and 7.5 billion USD (see footnote 1 in previous page) per year).

We can observe an increasing trend of RD intensity in the majority of companies, however, the differences between individual companies are present (see **Figure 3**). A joint graph of all RD intensities of the selected companies is presented in **Figure 4**.

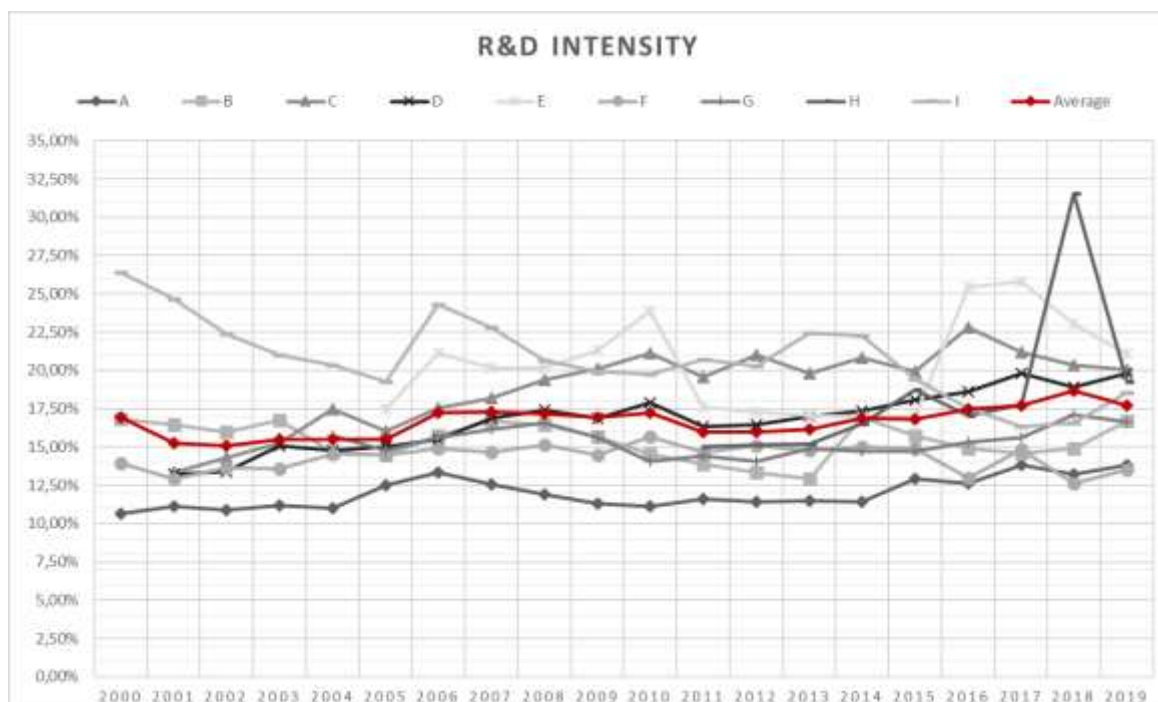


Figure 4. R&D Intensity for the selected companies and period with mean values added.

In the observed period three companies stand out with the high R&D intensity. Companies E, C and I had above-average investments in R&D for 15, 16 and 18 years, respectively. In our model we also analyzed the changes of R&D intensity over the observed period. The slope of the linear regression line is positive, meaning that throughout the years, the mean R&D intensity was increasing. Periods 2006-2010 and 2014-2019 were above-average in R&D intensity, with the highest value in 2018 (18.70 %).

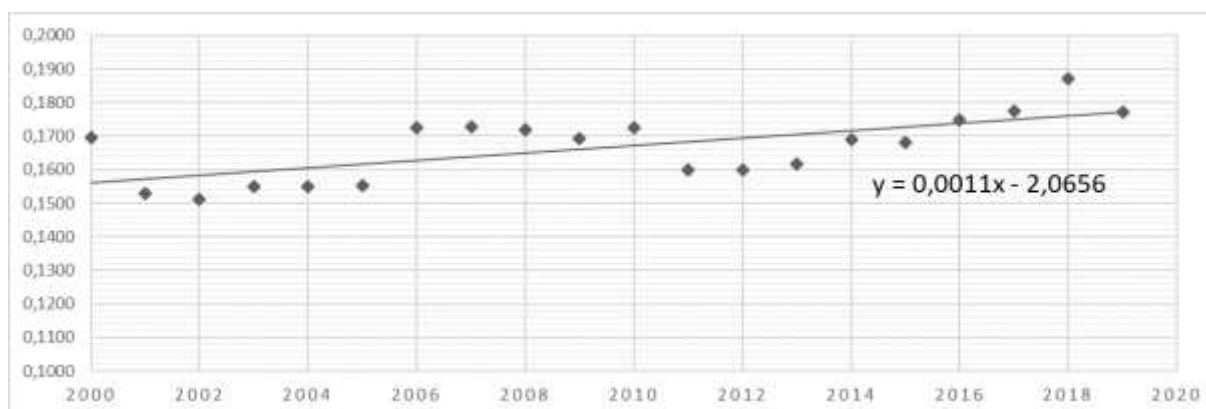


Figure 5. Mean value of yearly R&D intensity for the selected nine companies.

Although this financial analysis has its limitations, namely the usage of data gathered from consolidated yearly reports, it still offers an interesting insight into the finances of big pharmaceutical companies. With increasing absolute and relative R&D investments, companies will be able to adapt to the market demands and will provide better and safer products for the consumers.

Acknowledgements

The authors are in no way connected to the below-mentioned companies nor they hold any personal interest in them. The article's purpose is solely to illustrate research and development expenditure. Nothing in the article constitutes financial advice.

This research work was supported by the Slovenian Research Agency (ARRS) (Grants P3-0388, L3-2621, J3-9262, J1-9162).

References

1. The Department of Trade and Industry UK (2004), Research & Development. Updated 6. 3. 2011. Accessed 7. 1 .2021. Available from <https://web.archive.org/web/20051016024614/http://www.innovation.gov.uk/randd/index.asp?lvl1=1&lvl2=1&lvl3=0&lvl4=0>
2. Ortega-Argilés R, Potters L, Vivarelli M, R&D and productivity: testing sectoral peculiarities using micro data. *Empir Econ*, 2011, 41: 817–839. DOI: <https://doi.org/10.1007/s00181-010-0406-3>
3. Ortega-Argilés R, Piva M, Vivarelli M, The productivity impact of R&D investment: are high-tech sectors still ahead?. *Econ Innov New Technol*, 24: 204-222. DOI: <https://doi.org/10.1080/10438599.2014.918440>
4. Johansson B, Löf H, The impact of firm's R&D strategy on profit and productivity. Working Paper Series in Economics and Institutions of Innovation (CESIS Electronic Working Paper Series), 2008, 156: 1-28. Accessed 25.12.2019. Available from <https://static.sys.kth.se/itm/wp/cesis/cesiswp156.pdf>
5. Deore AB, Dhumane JR, Wagh R, et al. The Stages of drug discovery and development process. *Asian J Pharm Res Develop*, 2019, 7: 62-67. DOI: <https://doi.org/10.22270/ajprd.v7i6.616>
6. Lansdowne LE (2020), Exploring the Drug Development Process. Updated 13. 3. 2020. Accessed 1. 12. 2020. Available from <https://www.technologynetworks.com/drug-discovery/articles/exploring-the-drug-development-process-331894>
7. Torjesen I (2015), Drug development: the journey of a medicine from lab to shelf. Updated 12. 5. 2015. Accessed 1. 12. 2020. Available from <https://www.pharmaceutical-journal.com/publications/tomorrows-pharmacist/drug-development-the-journey-of-a-medicine-from-lab-to-shelf/20068196.article?firstPass=false>
8. Mohs RC, Greig NH, Drug discovery and development: Role of basic biological research. *Alzheimer's Dement* 2017, 3: 651-57. DOI: <https://doi.org/10.1016/j.trci.2017.10.005>
9. Sinha S, Vohora D, Drug discovery and development: an overview (Chapter 2). In: Vohora D, Singh G, editors. *Pharmaceutical Medicine and Translational Clinical Research*. Amsterdam, The Netherlands, Elsevier, 2018, pp. 19-32. DOI: <https://doi.org/10.1016/B978-0-12-802103-3.00002-X>

10. U. S. Food and Drug Administration (2018), The Drug Development Process. Updated 4. 1. 2018. Accessed 1. 12. 2020 Available from <https://www.fda.gov/patients/learn-about-drug-and-device-approvals/drug-development-process>
11. Padney A (2020). Drug Discovery and Development Process. Updated 2020. Accessed 2. 12. 2020. Available from <https://www.nebiolab.com/drug-discovery-and-development-process/>
12. Austin DH (2006), Research and Development in the Pharmaceutical Industry. The Congress of the United States, Congressional Budget Office. Updated 2006. Accessed 7. 12. 2020. Available from <https://www.cbo.gov/sites/default/files/109th-congress-2005-2006/reports/10-02-drugr-d.pdf>



APPENDIX

Table A1

	2019	2018	2017	2016	2015	2014	2013	2012	2011	2010	2009	2008	2007	2006	2005	2004	2003	2002	2001	2000
A - millions USD																				
Revenue	82059	81581	76450	71890	70074	74331	71312	67224	65030	61587	61897	63747	61095	53324	50514	47348	41862	36298	32317	29172
RD	11355	10775	10554	9095	9046	8494	8183	7665	7548	6844	6986	7577	7680	7125	6312	5203	4684	3957	3591	3105
Net Earnings	15119	15297	1300	16540	15409	16323	13831	10853	9672	13334	12266	12949	10576	11053	10411	8509	7197	6597	5668	
RD/Revenue	13.84%	13.21%	13.81%	12.65%	12.91%	11.43%	11.47%	11.40%	11.61%	11.11%	11.29%	11.89%	12.57%	13.36%	12.50%	10.99%	11.19%	10.90%	11.11%	10.64%
B - millions USD																				
Revenue	51750	53647	52546	52824	48851	49605	51584	58986	65259	65165	50009	48296	48418	48371	51298	52516	44736	32373	29024	26045
RD	8650	8006	7657	7872	7690	8393	6678	7870	9074	9483	7845	7945	8089	7599	7442	7684	7487	5176	4776	4374
Net Earnings	16273	11153	21308	7215	6960	9135	22003	14570	10009	8257	8635	8104	8144	19337	8085	11361	3910	9126	7788	3726
RD/Revenue	16.71%	14.92%	14.57%	14.90%	15.74%	16.92%	12.95%	13.34%	13.90%	14.55%	15.69%	16.45%	16.71%	15.71%	14.51%	14.63%	16.74%	15.99%	16.46%	16.79%
C - millions CHF																				
Revenue	63751	59497	53299	50576	48145	47462	46780	45499	42531	47473	49051	45617	46133	42041	35511	29522	31220	29725	29163	
RD	12774	12092	11292	11532	9581	9895	9270	9552	8326	10026	9874	8845	8385	7365	5705	5154	4766	4257	3893	
Net Earnings	14108	10865	8825	9733	9056	9535	11373	9660	9544	8891	8510	10844	11437	9171	6730	7063	3069	-4026	3697	
RD/Revenue	20.04%	20.32%	21.19%	22.80%	19.90%	20.85%	19.82%	20.99%	19.58%	21.12%	20.13%	19.39%	18.18%	17.52%	16.07%	17.46%	15.27%	14.32%	13.35%	
D - millions USD																				
Revenue	47498	44833	42381	48518	49440	52419	57920	56673	58566	50624	44267	41459	38072	34393	32212	28247	24864	32412	31643	
RD	9402	8489	8389	9039	8935	9086	9852	9332	9583	9070	7469	7217	6430	5321	4846	4171	3756	4339	4189	
Net Earnings	11737	12614	7703	6698	17794	10280	9292	9383	9245	9969	8454	8233	11968	7202	6141	5380	5016	7313	7024	
RD/Revenue	19.79%	18.93%	19.79%	18.63%	18.07%	17.33%	17.01%	16.47%	16.36%	17.92%	16.87%	17.41%	16.89%	15.47%	15.04%	14.77%	15.11%	13.39%	13.24%	
E - millions USD																				
Revenue	46840	42294	40122	39807	39498	42237	44033	47267	48047	45987	27428	23850	24197.7	22636	22011.9					
RD	9872	9752	10339	10124	6704	7180	7503	8168	8467	10991	5845	4805	4882.8	4782.9	3848					
Net Earnings	9843	6220	2394	3920	4442	11920	4404	6168	6272	982	13022	7932	3275.4	4433.8	4631.3					
RD/Revenue	21.08%	23.06%	25.77%	25.43%	16.97%	17.00%	17.04%	17.28%	17.62%	23.90%	21.31%	20.15%	20.18%	21.13%	17.48%					
F - millions GBP																				
Revenue	33754	30821	30186	27889	23923	23006	26505	26431	27387	28392	28368	24352	22716	23225	21660	19986	21070	21212	20489	18079
RD	4568	3893	4476	3628	3560	3450	3923	3979	4009	4457	4106	3681	3327	3457	3136	2904	2865	2900	2651	2526
Net Earnings	5268	4046	2169	1062	8372	2831	5628	4678	5458	1853	5669	4712	5310	5498	4816	4022	4308	3915	3053	4106
RD/Revenue	13.53%	12.63%	14.83%	13.01%	14.88%	15.00%	14.80%	15.05%	14.64%	15.70%	14.47%	15.12%	14.65%	14.88%	14.48%	14.53%	13.60%	13.67%	12.94%	13.97%
G - millions EUR																				
Revenue	36126	34463	35072	33809	34542	31694	30966	34947	33389	32367	29306	27568	28052	28373	27311	25199				
RD	6018	5894	5472	5172	5082	4667	4605	4922	4811	4547	4583	4575	4537	4430	4044	3964				
Net Earnings	2837	4410	8537	4800	4388	4509	3874	5136	5934	5721	5691	4292	5682	4006	6335	5025				
RD/Revenue	16.66%	17.10%	15.60%	15.30%	14.71%	14.73%	14.87%	14.08%	14.41%	14.05%	15.64%	16.60%	16.17%	15.61%	14.81%	15.73%				
H - millions USD																				
Revenue	33266	32753	28216	25638	22859	19960	18790	18380	17444											
RD	6407	10329	5007	4366	4285	3297	2855	2778	2618											
Net Earnings	7882	5687	5309	5953	5144	1774	4128	5275	3433											
RD/Revenue	19.26%	31.54%	17.75%	17.03%	18.75%	16.52%	15.19%	15.11%	15.01%											
I - millions USD																				
Revenue	22204	22533	21795	21892	20944	19327	18192	16639	15295	14660	14351	14687	14311	13858	12022	9977	7868	4991.2	3511	3202.2
RD	4116	3737	3562	3840	4070	4297	4083	3380	3167	2894	2864	3030	3266	3366	2314	2028	1655	1116.6	865	845
Net Earnings	7842	8394	1979	7722	6939	5158	5081	4345	3683	4627	4605	4196	3166	2950	3674	2363	2259	-1391.9	1119.7	1138.5
RD/Revenue	18.54%	16.58%	16.34%	17.54%	19.43%	22.23%	22.44%	20.31%	20.71%	19.74%	19.96%	20.63%	22.82%	24.29%	19.25%	20.33%	21.03%	22.37%	24.64%	26.39%





Review

Mental health during COVID-19

Šuligoj Ariana^{1*}

¹Faculty of Medicine, University of Ljubljana, Ljubljana, Slovenia

*soncek.mavrica@gmail.com

Abstract

Outbreaks of infectious diseases remain a major problem worldwide. They have substantial impacts not only on medical treatment, the economy, and society, but also on the psychological health of healthcare workers and people, which has become a prominent public health problem. In this article, we review some of the studies conducted during the epidemic of COVID-19 regarding mental health issues of different population groups. We believe that it is essential to introduce time-oriented policy, and implement care monitoring plans, which may help managing the pandemic as well as nurturing the public mental health to combat COVID-19 related psychological challenges. Governments must address public health needs by developing and implementing strategic plans to meet these needs during the COVID-19 pandemic and for any other pandemic outbreaks in the future.

1. Introduction

Outbreaks of infectious diseases remain a major problem worldwide. They have substantial impact not only on medical treatment, the economy, and society, but also on the psychological health of healthcare workers, which has become a prominent public health problem [1]. The novel coronavirus designated COVID-19, is one of the most challenging threats to public health around the world. Due to its high incidence, strong risk of contagion and asymptomatic transmission, the epidemic situation is severe, and control is difficult, leading to the strictest prevention and control measures [2]. With widespread work stop-offs, school suspensions and the shortage of protective materials, this COVID-19 epidemic exceeds the coping ability of individuals and society, causing anxiety and panic around the world [3].

2. Recent studies

The COVID-19 pandemic has aggregated mental health sufferings throughout the entire world. Suicide completions are the extreme consequences of COVID-19 related psychological burdens, which was reported in many countries. However, there is a lack of studies assessing COVID-19 related human stress and its associations with other relevant factors affecting quality of life [4]. Some groups may be more vulnerable than others to the psychosocial effects of pandemics. In particular, people who contract the disease, those at heightened risk for it (including the elderly, people with compromised immune function, and those living or receiving care in congregate settings), and people with pre-existing medical, psychiatric, or substance use problems are at increased risk for adverse psychosocial outcomes. Health care providers are also particularly vulnerable to emotional distress in the current pandemic, given their risk of exposure to the virus, concern about infecting and caring for their loved ones, shortages of personal protective equipment (PPE), longer work hours, and involvement in emotionally and ethically fraught resource-allocation decisions. Prevention efforts such as screening for mental health problems, psychoeducation, and psychosocial support should focus on these and other groups at risk for adverse psychosocial outcomes [5].

2.1 University students

University students may constitute a particularly vulnerable population for mental health problems in light of challenges commonly associated with transitions to adulthood and the frequent economic and material difficulties of this population. French respondents to a World mental Health survey of university students completed questions concerning COVID-19 confinement. The sample experienced increased anxiety as well as moderate to severe stress during confinement.

Respondents who did not relocate to live with parents were disproportionately affected. Knowledge of confinement effects may be used to reduce its negative impact in vulnerable populations. However, very recent research conducted in China among medical school

undergraduates demonstrated that only a minority of students reported moderate (2.7%) or severe anxiety (0.9%), although the specific timing of data collection is unclear. This latter study further reported that living with parents was associated with significantly lower rates of severe anxiety in students, while living in rural areas, not having a steady income and knowing someone infected with COVID-19 increased the risk of severe anxiety.

Nevertheless, the important differences between the cultural and political characteristics in China compared with those of western nations requires information concerning country-specific data addressing this question [6].

Nearly half of the present student sample from the French respondents to a World mental Health survey were relocated from their usual place of residence to more rural areas immediately before confinement began. Individuals who changed residences were more likely to be living in a house, to share their living quarters with their parents, and to have access to an exterior space such as a yard or garden compared to students who did not exhibit mobility. The overall sample also experienced significant psychological distress, with the majority of participants reporting that an increase in anxiety since the beginning of the confinement period as well as moderate to severe levels of stress. These findings are in stark contrast with the recent statistics reporters for medical school students in China [7] where less than 4% reported at least moderate levels of anxiety during the COVID-19 pandemic. While methodological and cultural factors may explain a portion of differences relative to the current findings, it is notable that these reported rates for psychological distress in Chinese university students are also far below estimates for this same population observed just before the pandemic began [8]. No differences in alcohol use were noted, consistent with prior reports that invoked restrictions in the access to alcohol during quarantine as one possible explanation [9]. However, it remained possible in France to purchase alcohol at any supermarket or liquor store for the duration of confinement, although restaurants, bars and nightclubs were closed [6].

The differences in estimates for university students who relocated versus those who did not suggest how public health crises may magnify inequalities that exist within specific populations, as a function of the individual's financial situation, family resources or other factors. These inequalities are well-documented risk factors for mental disorder onset and symptom severity. Importantly, the transition from high school to university is a major life transition in itself and source of stress that can be associated with adjustment problems [10, 6]. However, the present findings should be interpreted in light of several limitations of the methodology, notably the inability and no information was collected concerning their housing conditions prior to changing locations. The specific nature of the sample may also restrict the generalization of conclusions.

The findings nevertheless suggest that public health strategies used to combat COVID-19, as well as specific psychological interventions (e.g. cognitive behaviour therapy, mindfulness-based therapy) may correlate with mental health indicators [11, 6].

2.2 Medical staff and medical students

In China, a study was aimed to investigate the mental state of medical staff and medical students in the early stages of the COVID-19 outbreak, as well as analyse the risk factors of serious mental illness (SMI), to provide a scientific basis for further psychological intervention and management [3].

In total, 505 respondents completed the online survey. Only 7.90% of all respondents showed relaxed in current mental state. Respectively, 14.14% of 304 medical staff and 72.14% of 201 medical students reported high risk of SMI. At the same time, those at high risk spent more time watching outbreaks per day and were younger and more likely to be medical students, to have a history of contact with people from Wuhan, to have experienced an outbreak in their residential community, and to have suspected that they themselves or their relatives were infected with the new coronavirus. High-risk individuals were also more likely to report difficulty in controlling their emotions during the epidemic, to have dreams related to the SARS.Cov-2, to be more concerned about media reports of the epidemic, to experience more anxiety about the epidemic, and to agree with the idea that mental state is important in dealing with the epidemic [3].

These findings highlight that medical staff and medical students were vulnerable to SMI during the early stages of COVID-19 outbreak and identify the factors associated with SMI, which can be used to formulate psychological interventions to improve the mental health. The independent risk factors for SMI among them are suspicion that they or relatives were infected with the COVID-19, greater interest in media reports about the epidemic, frequency of recent dreams related to COVID-19, difficulty in controlling emotions during the epidemic, and hours spent watching outbreaks per day. This suggests that medical students and staff, especially who pay more attention to the epidemic, should be taught active coping strategies [3].

2.3 Population research

In Bangladesh an online survey was carried out among 340 Bangladesh adult populations (65.90 % male; mean age 26.23 +- 6.39) by utilizing the socio-demographics, possible human stress due to COVID-19 pandemic and its consequences. About 85.60% of the participants are in COVID-19-related stress, which results in sleep shortness, short temper, and chaos in family. Fear of COVID-19 infection (i.e., self and/or family members, and/or relatives), hampering scheduled study plan and future career, and financial difficulties are identified as the main cause of human stress [4].

In America, concern was raised about how people will react individually and collectively because beyond stresses inherent in the illness itself, mass home-confinement directives (including stay-at-home orders, quarantine, and isolation) are new to Americans. A recent review of psychological sequelae in samples of quarantined people and of health care providers may be instructive. It revealed numerous emotional outcomes, including stress, depression, irritability, insomnia, fear, confusion, anger, frustration, boredom, and stigma

associated with quarantine, some of which persisted after the quarantine was lifted. Specific stressors included greater duration of confinement, having inadequate supplies, difficulty securing medical care and medications, and resulting financial losses. In the current pandemic, the home confinement of large swaths of the population for indefinite periods, differences among the stay-at-home orders issued by various jurisdictions, and conflicting messages from government and public health authorities will most likely intensify distress. A study conducted in communities affected by severe acute respiratory syndrome (SARS) in the early 2000s revealed that although community members, affected individuals, and health care workers were motivated to comply with quarantine to reduce the risk of infecting others and to protect the community's health, emotional distress tempted some to consider violating their orders [5].

An online survey of a representative sample of Canadian adults (n = 1055) was also made, in which they explored whether perceptions of threat from COVID-19 and efficacy to follow government recommendations for preventing COVID-19 would mediate the relationships between personality traits (e.g., neuroticism, conscientiousness-goal-striving, extroversion-activity and sociability) and perceived stress. They found that higher neuroticism and extroversion were associated with higher levels of stress during the pandemic and a greater increase in stress levels compared to levels before the pandemic. Individuals with higher neuroticism experienced higher levels of stress due to higher levels of perceived threat and lower levels of efficacy. Perceived threat did not mediate the relationship between extroverts and stress, like between the neuroticism and stress, which suggested that the source of stress might stem from elsewhere (e.g., inability to socialize). This study highlighted that personality traits could be an important factor in identifying stress-prone individuals during a pandemic and that stress management interventions need to be personality-specific [12].

3. Stressors

Along with the fear of infection of this highly contagious virus, fear of losing beloved ones, the COVID-19 related misinformation spreading, the lack of medical treatment, and the shortage of properly equipped units to treat the patients, the lockdown-related issues (e.g. prolonged home isolation, social distancing, food insecurity, fear of unemployment, loss of income etc.) are being sought to be associated with mental distresses like depression, anxiety, phobia, insomnia, trauma etc [13]. But, as the world is being arguably failed to combat with the physical treatments of the COVID-19, the mental health portion is somewhat being neglected or overseen [14]. Consequently, suicide rate increment is common during and aftermath of the pandemics that was also reported in the COVID-19 pandemic context, where the mental health problems and its mediators aggravate the suicide risk [15].

Individual physical performance as well as immunological stability are somewhat correlated with psychological states [16]. But studies reported elevated psychological problems and

decreased quality of life across nations and occupations, which are reflecting the forthcoming worst mental as well physical health situations to the risky people. Besides, most of the global COVID-19 studies are arguably concerned with infection control, effective vaccine or treatment, its spread, and forecasting [17].

While still largely undocumented, the COVID-19 pandemic may affect mental health through direct threats to the individual's health but also through indirect effects of public health policies and containment efforts. It is important to note that the most common strategies applied to combat the spread of COVID-19 involve travel restriction, social distancing and confinement to one's residence. While necessary from a public health standpoint, understanding their impact on vulnerable individuals requires extensive investigation [6]. Uncertain prognoses, looming severe shortages of resources for testing and treatment and for protecting responders and health care providers from infection, imposition of unfamiliar public health measures that infringe on personal freedoms, large and growing financial losses, and conflicting messages from authorities are among the major stressors that undoubtedly will contribute to widespread emotional distress and increased risk for psychiatric illness associated with COVID-19. Health care providers have an important role in addressing these emotional outcomes as part of the pandemic response [5].

Public health emergencies may affect the health, safety, and well-being of both individuals (causing, for example, insecurity, confusion, emotional isolation, and stigma) and communities (e.g. owing to economic loss, work and school closures, inadequate resources for medical response, and deficient distribution of necessities). These effects may translate into a range of emotional reactions (e.g. distress or psychiatric conditions), unhealthy behaviours (such as excessive substance use), and noncompliance with public health directives (e.g. home confinement and vaccination) in people who contract the disease and in the general population. Extensive research in disaster mental health has established that emotional distress is ubiquitous in affected populations – a finding certain to be echoed in populations affected by the COVID-19 pandemic [5].

4. How to cope?

After disasters, most people are resilient and do not succumb to psychopathology. Indeed, some people find new strengths. Nevertheless, in “conventional” natural disasters, technological accidents, and intentional acts of mass destruction, a primary concern is post-traumatic stress disorder (PTSD) arising from exposure to trauma. Medical conditions from natural causes such as life-threatening viral infection do not meet the current criteria for trauma required for a diagnosis of PTSD, but other psychopathologies, such as depressive and anxiety disorders, may ensue [5].

Opportunities to monitor psychosocial needs and deliver support during direct patient encounters in clinical practice are greatly curtailed in this crisis by large-scale home confinement. Psychosocial services, which are increasingly delivered in primary care

settings, are being offered by means of telemedicine. In the context of COVID-19, psychosocial assessment and monitoring should include queries about COVID-19 related stressors, such as exposures to infected sources, infected family members, loss of loved ones, and physical distancing; secondary adversities, i.e. economic loss, psychosocial effects, i.e. depression, anxiety, psychosomatic preoccupations, insomnia, increased substance use, and domestic violence, and indicators of vulnerability, i.e. pre-existing physical or psychological conditions. Some patients will need referral for formal mental health evaluation and care, while others may benefit from supportive interventions designed to promote wellness and enhance coping, i.e. psychoeducation or cognitive behavioural techniques. In light of the widening economic crisis and numerous uncertainties surrounding this pandemic, suicidal ideation may emerge and necessitate immediate consultation with a mental health professional or referral for possible emergency psychiatric hospitalization [5].

5. Conclusion

Considering the present findings, it is essential to introduce time-oriented policy, and implement care monitoring plans, which may help managing the pandemic as well as nurturing the public mental health to combat COVID-19 related psychological challenges [4]. During any outbreak of an infectious disease, the population's psychological reactions play a critical role in shaping both spread of the disease and the occurrence of emotional distress and social disorder during and after the outbreak [18]. Given lessons learned from past outbreaks in the world, public mental health interventions should be formally integrated into public health preparedness and emergency response plans to effectively curb all outbreaks. The World Health Organization's strategic preparedness and response plan for COVID-19, however, has not yet specified any strategies to address mental health needs of any kind [19]. Governments must address public health needs by developing and implementing strategic plans to meet these needs during the COVID-19 pandemic and for any other pandemic outbreaks in the future.

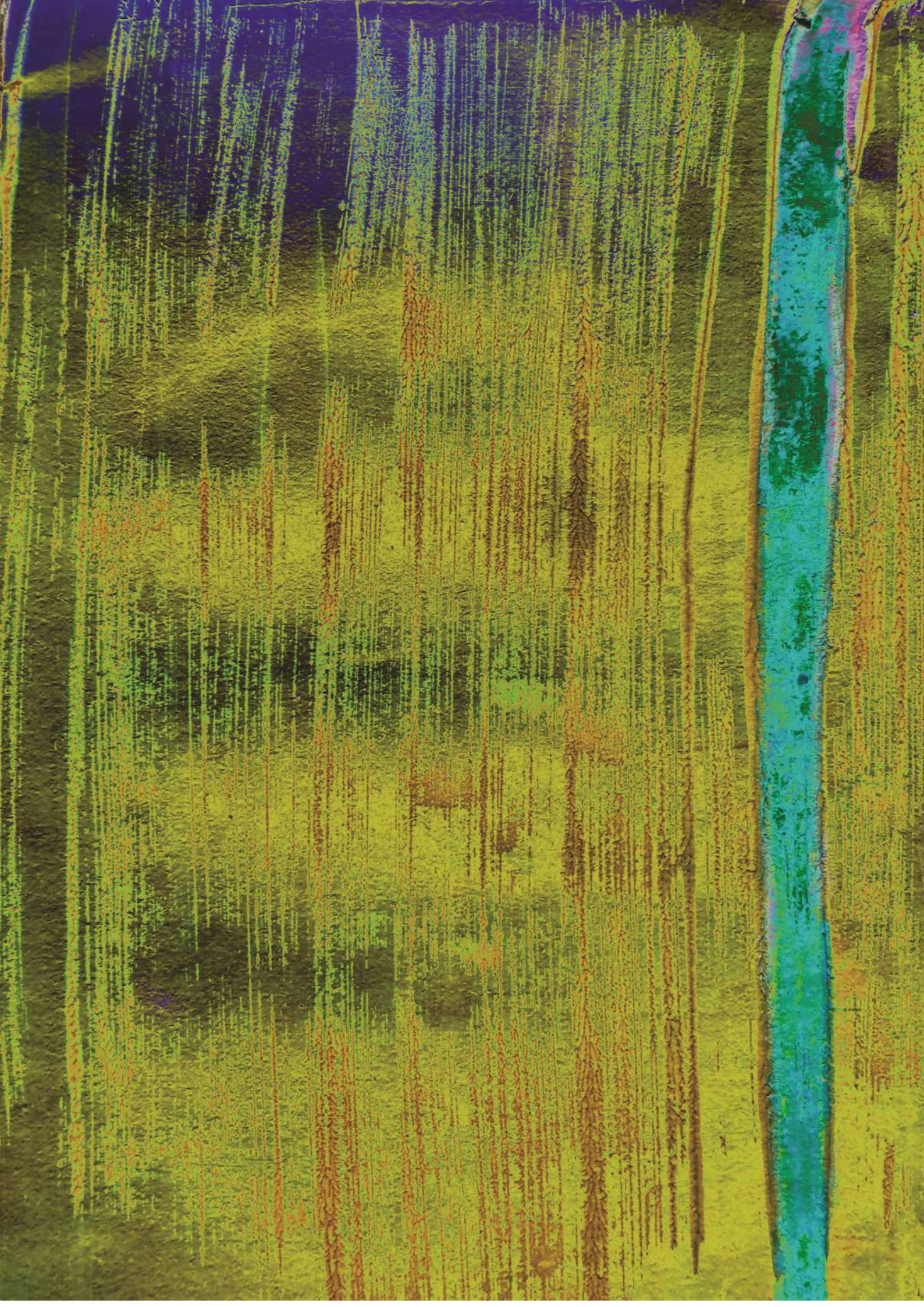
References

1. Holloway HC, Norwood AE, Fullerton CS, Engel CC, Ursano RJ. The threat of biological weapons: prophylaxis and mitigation of psychological and social consequences. *Jama*, 1997. 278(5), 425-427. doi:10.1001/jama.1997.03550050087038
2. Xiang YT, Yang Y, Li W, Zhang L, Zhang Q, et al. Timely mental health care for the 2019 novel coronavirus outbreak is urgently needed. *The Lancet Psychiatry*, 2020. 7(3), 228-229. doi: 10.1016/S2215-0366(20)30046-8
3. Wu S, Li Z, Li Z, Xiang W, Yuan Y, et al. The mental state and risk factors of Chinese medical staff and medical students in early stages of the COVID-19 epidemic. *Comprehensive psychiatry*, 2020. 102, 152202. doi: 10.1016/j.comppsy.2020.152202
4. Islam SDU, Bodrud-Doza M, Khan RM, Haque MA, Mamun MA. Exploring COVID-19 stress and its factors in Bangladesh: a perception-based study. *Heliyon*, 2020. 6(7), e04399. doi: 10.1016/j.heliyon.2020.e04399

5. Pfefferbaum B, North C S . Mental health and the Covid-19 pandemic. *New England Journal of Medicine*, 2020. 383(6), 510-512. doi: 10.1056/NEJMp2008017
6. Husky MM, Kovess-Masfety V, Swendsen JD. Stress and anxiety among university students in France during Covid-19 mandatory confinement. *Comprehensive Psychiatry*, 2020. 102, 152191. doi: 10.1016/j.comppsy.2020.152191
7. Cao W, Fang Z, Hou G, Han M, Xu X, et al. The psychological impact of the COVID-19 epidemic on college students in China. *Psychiatry research*, 2020. 287, 112934. doi: 10.1016/j.psychres.2020.112934
8. Chau S W, Lewis T, Ng R, Chen JY, Farrell S M, et al. Wellbeing and mental health amongst medical students from Hong Kong. *International Review of Psychiatry*, 2019. 31(7-8), 626-629. doi: 10.1080/09540261.2019.1679976
9. Hao F, Tan W, Jiang L, Zhang L, Zhao X, et al. Do psychiatric patients experience more psychiatric symptoms during COVID-19 pandemic and lockdown? A case-control study with service and research implications for immunopsychiatry. *Brain, behavior, and immunity*, 2020. 87, 100-106. doi: 10.1016/j.bbi.2020.04.069
10. Fisher S, Hood B. The stress of the transition to university: A longitudinal study of psychological disturbance, absent-mindedness and vulnerability to homesickness. *British journal of psychology*, 1987. 78(4), 425-441. doi: 10.1111/j.2044-8295.1987.tb02260.x
11. Ho CS, Chee CY, Ho RC. Mental health strategies to combat the psychological impact of COVID-19 beyond paranoia and panic. *Ann Acad Med Singapore*, 2020. 49(1), 1-3. <https://pubmed.ncbi.nlm.nih.gov/32200399/>
12. Liu S, Lithopoulos A, Zhang CQ, Garcia-Barrera MA, Rhodes RE. Personality and perceived stress during COVID-19 pandemic: Testing the mediating role of perceived threat and efficacy. *Personality and individual differences*, 2021. 168, 110351. doi: 10.1016/j.paid.2020.110351
13. Tasnim S, Rahman M, Pawar P, Chi X, Yu Q, et al. Epidemiology of sleep disorders during COVID-19 pandemic: A systematic scoping review. *MedRxiv*, 2020. doi: 10.1101/2020.05.17.20104794
14. Usman N, Mamun MA, Ullah I. COVID-19 infection risk in pakistani health-care workers: The cost-effective safety measures for developing countries. *Social Health and Behavior*, 2020. 3(3), 75. doi: 10.4103/SHB.SHB_26_20
15. Jahan S, Araf K, Gozal D, Griffiths MD, Mamun MA. Depression and suicidal behaviors among Bangladeshi mothers of children with Autistic Spectrum Disorder: a comparative study. *Asian journal of psychiatry*, 2020. doi: 10.1016/j.ajp.2020.101994
16. Naser AY, Dahmash EZ, Al-Rousan R, Alwafi H, Alrawashdeh HM, et al. Mental health status of the general population, healthcare professionals, and university students during 2019 coronavirus disease outbreak in Jordan: A cross-sectional study. *Brain and behavior*, 2020. 10(8), e01730. doi: 10.1002/brb3.1730
17. Ahorsu DK, Lin CY, Imani V, Saffari M, Griffiths MD, Pakpour AH. The fear of COVID-19 scale: development and initial validation. *International journal of mental health and addiction*, 2020. 1-9. doi: 10.1007/s11469-020-00270-8
18. Cullen W, Gulati G, Kelly BD. Mental health in the Covid-19 pandemic. *QJM: An International Journal of Medicine*, 2020. 113(5), 311-312. doi: 10.1093/qjmed/hcaa110

19. World Health Organization. (2019). Novel coronavirus (2019-nCoV): strategic preparedness and response plan Feb 3, 2020 [cited 2020 Feb 7].
<https://www.who.int/publications/i/item/strategic-preparedness-and-response-plan-for-the-new-coronavirus>





Review

Testing for SARS-CoV-2: A review of current methods

Maša Smajila¹, Desiree Celin¹, Domen Kovačič¹.

¹ University of Ljubljana, Faculty of Medicine, Ljubljana, Slovenia

masa.smajila@gmail.com

Abstract

More than a year ago a quick-spreading respiratory virus emerged in Wuhan, China. After sequencing its genome it was named severe acute respiratory syndrome-coronavirus type 2 or SARS-CoV-2. Due to its quick spread and mortality, scientists designed several tests for identifying a SARS-CoV-2 infection as well as post-infection immunity and its duration. These include RT-qPCR, antigen and serological tests. In this article we aimed to briefly explain these testing methods, which are currently being used in the clinical environment, their advantages and their disadvantages.

1. Introduction

In December 2019, a newly emerged respiratory virus began spreading in Wuhan city, Hubei Province, China. The causal agent was initially called 2019-novel coronavirus and the associative respiratory illness Coronavirus Disease 2019 (COVID-19). After sequencing its genome, the virus was then renamed to severe acute respiratory syndrome-coronavirus type 2 (SARS-CoV-2). This virus is a positive-sense, single-stranded RNA virus in the genus *Betacoronavirus*, family *Coronaviridae* [1]. As of 21 January, 2021, there have been 101.378.379 confirmed cases and 2.188.287 global deaths due to COVID-19 [2].

Because the infection spreads quickly, there have been established protective measures to limit the spread, e.g. social distancing and wearing face masks. Furthermore, scientists have designed several tests aimed at diagnosing a SARS-CoV-2 infection as quickly and accurately as possible to limit its spread. There are three major groups of test currently available. The first one is the real-time reverse transcriptase-polymerase chain reaction (RT-qPCR) test, the second are antigen tests and the third are serological tests. The first two detect viral RNA or viral protein(s) in the sample, whereas the third measures a person's immune response to the virus. In this review we will briefly explain each test and their use in the clinical environment.

2. RT-qPCR testing

When performing a test, we must consider its specificity and its sensitivity. Sensitivity is the percentage of persons with the disease who are correctly identified by the test. This means that all persons with the disease get a positive result on the test. Specificity is the percentage of persons without the disease who are correctly excluded by the test. Ideally, we want a test with both high sensitivity and high specificity [3].

The gold standard in diagnosing COVID-19 is a nucleic acid test (NAT) using reverse-transcriptase polymerase-chain-reaction (RT-PCR) technology. This test detects SARS-CoV-2 RNA in the specimen using PCR technology [4]. The RNA is first reversely transcribed into cDNA (complimentary DNA sequence) and then amplified using primer sets and detected using specific probes. These are unique to SARS-CoV-2 in order to evade a positive result with other closely related coronaviruses [5].

A positive PCR result indicates the presence of SARS-CoV-2 nucleic acid. To interpret it, we need to combine it with patient clinical history and additional diagnostic tools. It is important to note that even though this test is highly specific, its sensitivity is not ideal [5]. The sensitivity differs between different testing kits. Furthermore, the reporting of positive results is not unified.

The cycle threshold value (Ct), which is the number of the amplification cycle in which viral RNA becomes detectable, is used to differentiate between a positive and a negative result. Ct values below 40 are generally recommended as a positive result, although some reports consider values greater than 35 as negative because a detection of non-specifically precipitated sequences could occur [1]. To add, this also means that if there is not enough

viral RNA in the specimen, the test will not detect it and will be falsely negative [6]. A negative PCR result therefore does not rule out a SARS-CoV-2 infection. It is also important to note that viral RNA can be present after the virus fragments, therefore the results can continue to be positive after the resolution of symptoms [5].

Due to low viral load specimens and previously described limitations of RT-qPCR, we are confronted with false negative results, which are inevitable. Because they impose a risk due to failure in timely diagnosing the disease and cutting off transmission, there is another method being tested. It is called droplet digital PCR (ddPCR). In ddPCR, the sample is randomly distributed into thousands of droplets or partitions, some of which contain no template and other contain one or more of them. These partitions or droplets are then amplified and a droplet reader afterwards determines the number of positive partitions. An estimated concentration is then calculated by modelling as a Poisson distribution. In ddPCR, the quantification is therefore less affected by poor amplification efficiency and inhibitors of amplification that may be present in the samples. This method is not only applicable to analysing absolute viral loads from clinical samples, but also to analyse gene copy number variations, gene expressions, microRNA analysis and so on [7].

When comparing the limit of detection (LoD) between ddPCR and RT-qPCR, Suo et al (2020) [7] found that ddPCR is 500 times more sensitive than RT-qPCR in a low level analyte. This means that the use of ddPCR could help in early treatment and control of viral transmission, when the viral load is still too low for RT-qPCR to detect [7].

Even though ddPCR provides a number of clear advantages over RT-qPCR, there are also a few technical disadvantages to the method. These include limited sample volume per reaction, small dynamic range due to a limited number of partitions, and falsely low quantification due to molecular dropout, in which not all templates in a partition are amplified. The workflow is also more complex, requires more time with multiple steps, which increases the time to result [8].

3. Antigen testing

In contrast to reverse transcription polymerase chain reaction (RT-PCR), which amplifies the virus target sequences, rapid antigen tests detect the presence of a viral antigen in the patient's specimen without amplification. As a result, most currently available rapid antigen tests show a lower sensitivity compared to the standard RT-PCR test, while their specificity is generally reported to be high (above 98%). It is important to note that rapid antigen tests may be sensitive enough to detect cases with a high viral load, i.e. pre-symptomatic and early symptomatic cases (up to five days from symptom onset; or low RT-PCR cycle threshold (Ct) value <25), which likely account for a significant proportion of transmissions [9]. Most antigen-detecting rapid diagnostic tests (Ag-RDTs) for COVID-19 use a sandwich immunodetection method employing a simple-to-use lateral flow test format commonly used for HIV, malaria, and influenza testing. Lateral flow tests use capillary action in order to spread the specimen containing liquid along the pad, which has a test line and a control line.

Ag-RDTs are usually comprised of a plastic cassette with sample and buffer wells, a nitrocellulose matrix strip with a test line with bound antibody specific for conjugated target antigen-antibody complexes and a control line with bound antibody specific for conjugated-antibody. Antibodies are conjugated with larger molecules to allow the visualization of the results. In the case of SARS-CoV-2 rapid diagnostic tests the target analyte is often the virus' nucleocapsid (N) protein, preferred because of its relative abundance. Typically, all materials that are required to perform the test, including sample collection materials, are provided in the commercial kit, except for a timer (specialized type of clock used for measuring specific time intervals). After collecting the respiratory specimen and applying it to the test strip, results are read by the operator within 10 to 30 minutes with or without the aid of a reader instrument. The use of a reader standardizes interpretation of test results, reducing variance in assay interpretation by different operators, but requires ancillary equipment. Most of the currently manufactured tests require nasal or nasopharyngeal swab samples, but companies are carrying out studies to assess the performance of their tests using alternative sample types such as saliva, oral fluid and sample collection systems to potentially expand options for use and to facilitate safe and efficient testing [10].

Rapid antigen tests are easy to use and offer rapid results at low cost but show a sensitivity of 80%, which is lower than the 98% sensitivity of the RT-PCR test. Rapid antigen tests offer multiple benefits in comparison to RT-PCR tests for the detection of SARS-CoV-2. They have been developed as both laboratory-based tests and for near-patient use (point-of-care or PoC), and results are normally generated in 10 to 30 minutes after the start of the analysis, and at low cost. Due to the timeliness of results, rapid antigen tests can provide added value e.g. in the patient triage process in healthcare settings at admission. In the context of contact tracing, rapid antigen tests can allow for a more rapid identification of infectious contacts [9].

4. Serological testing

Even though the forementioned PCR testing is considered a gold standard in detecting SARS-CoV-2 infection, serological and antigen testing are also used in laboratory and point-of-care (PoC) testing.

As with other infections in non-immunocompromised patients, the immunity against a pathogen consists of innate immunity (rapid response), adaptive immunity (slow response) and passive immunity [11].

Serological, or antibody, tests detect immunoglobulins produced by the host's plasma B cells following exposure to foreign antigens, which is part of adaptive immunity. In a SARS-CoV-2 infection the antigens that we are exposed to are approximately 25 proteins that are required for its infection and replication [12]. The main structural proteins are spike (S) membrane (M), envelope (E) and nucleocapsid (N) proteins [13].

When a person starts producing antibodies against these proteins, they seroconvert. Most patients with COVID-19 seroconvert by day 10–14 (~80%) following the onset of symptoms, with almost 100% seroconversion by day 20 [14].

The evidence suggests that seroconversion in SARS-CoV-2 is similar to other acute viral infections. IgM antibodies are the first to form, whereas IgG concentration begins to rise as IgM levels reach a plateau [13]. IgMs are therefore interpreted as an indicator of acute infection, whereas IgG represent previous infection and possible immunity [15]. There are also IgA, predominantly present in the mucosal tissue, which may also play an important role in the immune response and disease progression in COVID-19 [12]. Antibodies primarily neutralize SARS-CoV-2 cell fusion and entry and facilitate recognition and phagocytosis. It has been suggested that host-neutralising antibodies primarily work against SARS-CoV-2 S (spike) and N (nucleocapsid) proteins [12].

When testing for host antibodies, we can use different serological tests. They can be vaguely divided into (I) point-of-care tests (PoCTs), (II) tests, that can be performed in routine diagnostic laboratories and (III) those, that can only be performed in specialised reference laboratories [14].

The PoCT is a rapid diagnostic test based on lateral flow immunoassay (LFIA) technology, that is used also in pregnancy test kits for home use. In this test, we have an adhesive membrane (e. g. nitrocellulose), in which host antibodies migrate across due to capillary forces. On this membrane, we have two lines, one consisting of conjugated SARS-CoV-2-specific antigens and the other of secondary antibodies (antihuman IgG/IgM antibodies). We also have a control line using rabbit IgG conjugates and their corresponding anti-rabbit IgG antibodies. The test is valid, when we have a positive result in the control line. The test is positive, when the positive result appears in the IgM or IgG line as well [12]. Tests that can be routinely performed in diagnostic laboratories, include ELISA (enzyme-linked immunosorbent assay) and CLIA (chemiluminescence immunoassay). ELISA has a test-to-result time of 2.5 hours. It uses a surface coated with specific viral antigens on which bind the corresponding patient antibodies (IgG, IgM, IgA). The antigen-antibody complex is then detected using a second antibody and a substrate that produces a color- or fluorescent-based signal. It is important to note we have different formats of ELISA, including direct, competitive and sandwich ELISA tests [12]. CLIA uses a similar concept to ELISA but uses chemical probes that yield light emission through a chemical reaction to generate a positive signal. An average time-to-result is 1-2 hours [12]. Due to longer time-to-result time and specific reagents and steps that need to be followed, this test can not be used as a PoCT. Neutralisation tests can only be performed in specialised reference laboratories.

Neutralisation tests determine the ability of antibodies to inhibit live virus replication. This test is highly specific but technically demanding and involves a live virus, hence it needs special handling and protective equipment. It has a slow turnaround time [14].

If we compare all the tests described above, we can see that PoCTs are the least technically demanding, give results in 10 to 30 minutes and can be therefore deployed in large-scale serological surveys. They may be less sensitive and specific than laboratory-based assays, but are the only ones that can be taken by non-laboratory staff. The most demanding are of course neutralisation tests, whereas CLIA and ELISA tests represent a midpoint between the PoCT and neutralisation considering the time-to-result and required expertise to perform. As given in the COVID-19 Testing Toolkit, developed by The Johns Hopkins Center for Health Security, most PoCT tests have a sensitivity of above 98 % 15 days after symptom onset and a specificity above 98%. It is important to note that sensitivity is much lower in the earliest days of symptom onset, which is expected due to seroconversion time. Reported CLIA and ELISA test specificities and sensitivities 15 days after symptom onset are above 99% for the majority of tests. It is important to note that these are specificities and sensitivities as stated by the manufacturers [16]. Neutralisation assays are used to establish the ability of detected antibodies to neutralize the virus itself in a cell culture, hence we don't talk about specificity and sensitivity.

5. Conclusions

With the pandemic still emerging, the use of previously described tests is of great importance not only in determining SARS-CoV-2 infection but in evaluating population immunity and its duration as well. This is why apart from COVID-19 vaccines, which are already being used and distributed, the use of specific tests in different environments equally contributes to limiting the pandemic. Rapid antigen tests are of great value in screening testing of critical staff and people of greater risk of infection, whereas RT-qPCR and especially ddPCR enable confirmation of results given by rapid antigen tests if needed. RT-qPCR tests are still the gold standard in diagnosing infection due to their specificity and greater sensitivity than antigen tests. With the use of vaccines, serological tests are not only used to evaluate immune response after infection, but after vaccination as well. We see a future in an even broader and synchronised use of the forementioned tests, possibly enabling the use of rapid antigen tests by the general population as well. We also hope for an implementation of ddPCR tests for negative RT-qPCR samples that have a great epidemiological and clinical risk of having the infection and might have a false negative result due to low viral load.

References

1. Sule WF, Oluwayelu DO, Real-time RT-PCR for COVID-19 diagnosis: challenges and prospects. *Pan Afr Med J.* 2020, 35(Suppl 2): 121. DOI: 10.11604/pamj.supp.2020.35.24258
2. Dong E, Du H, Gardner L, An interactive web-based dashboard to track COVID-19 in real time. *Lancet Infect Dis*, Published online 2020. Updated 28. 1. 2021. Accessed 28. 1. 2021. Available from: [https://doi.org/10.1016/S1473-3099\(20\)30120-1](https://doi.org/10.1016/S1473-3099(20)30120-1)

3. Boyce D, Orthopaedic Physical Therapy Secrets, Third Edition. In: Placzek J, Boyce D, editors. Evaluation of Medical Laboratory Tests. St Louis, United states, Elsevier, 2017. pp. 125–134.
4. Li X, Zeng W, Li X, Chen H, et al. CT imaging changes of corona virus disease 2019(COVID-19): a multi-center study in Southwest China. J Transl Med. 2020, 18: 154. DOI: [10.1186/s12967-020-02324-w](https://doi.org/10.1186/s12967-020-02324-w)
5. Ward S, Lindsley A, Courter J, Assa'ad A, Clinical testing for COVID-19. J Allergy Clin Immunol. 2020, 1: 23-34. DOI: 10.1016/j.jaci.2020.05.012
6. Liu C, Shi Q, Peng M, et al. Evaluation of droplet digital PCR for quantification of SARS-CoV-2 virus in discharged COVID-19 patients. Aging (Albany NY). 2020, 12: 20997-21003. DOI: [10.18632/aging.104020](https://doi.org/10.18632/aging.104020)
7. Suo T, Liu X, Feng J, et al. ddPCR: a more accurate tool for SARS-CoV-2 detection in low viral load specimens. Emerg Microbes Infect. 2020, 9: 1259–1268. DOI: 10.1080/22221751.2020.1772678
8. Kuypers J, Jerome KR, Applications of Digital PCR for Clinical Microbiology. J Clin Microbiol. 2017, 55: 1621–1628. DOI: [10.1128/JCM.00211-17](https://doi.org/10.1128/JCM.00211-17)
9. ECDC (European centre for disease prevention and control), Options for the use of rapid antigen tests for COVID-19 in the EU/EEA and the UK [internet]. Accessed 3. 1. 2021. Available from: <https://www.ecdc.europa.eu/sites/default/files/documents/Options-use-of-rapid-antigen-tests-for-COVID-19.pdf>
10. WHO (World Health Organization), Antigen-detection in the diagnosis of SARS-CoV-2 infection using rapid immunoassays [internet]. Accessed 3. 1. 2021. Available from: <https://apps.who.int/iris/rest/bitstreams/1302653/retrieve>
11. Chowdhury MA, Hossain N, Kashem MA, Shahid MA, Alam A, Immune response in COVID-19: A review. J Infect Public Health. 2020, 13(11): 1619-1629. DOI: 10.1016/j.jiph.2020.07.001
12. Ghaffari A, Meurant R, Ardakani A, COVID-19 serological tests: how well do they actually perform?. Diagnostics (Basel). 2020, 10(7): 453. DOI: 10.3390/diagnostics10070453
13. La Marca A, Capuzzo M, Paglia T, Roli L, Trenti T, Nelson S, Testing for SARS-CoV-2 (COVID-19): a systematic review and clinical guide to molecular and serological in-vitro diagnostic assays. Reproductive BioMedicine Online. 2020, 41(3): 483–499 DOI: [10.1016/j.rbmo.2020.06.001](https://doi.org/10.1016/j.rbmo.2020.06.001)
14. Bond K, Williams E, Howden BP, Williamson DA, Serological tests for COVID-19. Med. J. Aust. 2020, 213: 397-399.e1. DOI: [10.5694/mja2.50766](https://doi.org/10.5694/mja2.50766)
15. Moura D, McCarty T, Ribeiro IB, et al. Diagnostic characteristics of serological-based COVID-19 testing: a systematic review and meta-analysis. Clinics, 75, e2212. Epub. 2020 Aug 10. DOI: [10.6061/clinics/2020/e2212](https://doi.org/10.6061/clinics/2020/e2212)
16. Kobokovich A, West R, Gronvall G, Serology-based tests for COVID-19. COVID-19 Testing Toolkit. Johns Hopkins Center for Health Security. Published online 2020. Updated 27. 1. 2021. Accessed 28. 1. 2021. Available from: <https://www.centerforhealthsecurity.org/covid-19TestingToolkit/serology/Serology-based-tests-for-COVID-19.html>



Review

Experience with glucocorticoids and other treatments on COVID-19 so far

Pevec V¹, Černe ŽP¹, Dobrin E¹, Beović B^{1,2}

¹University of Ljubljana, Faculty of Medicine, Ljubljana, Slovenia

²University Medical Centre Ljubljana, Department for Infectious Diseases, Ljubljana, Slovenia

*valentina.pevec@icloud.com

Abstract

The Coronavirus disease 2019 (COVID-19) is an infectious respiratory disease caused by a newly discovered coronavirus which was recognized in December 2019 and quickly spread around the world causing a global pandemic by March of 2020. There is currently no cure for the infection with the virus as there is not enough knowledge. However, many treatments are being studied and a lot of physicians are working on their own clinical trials. There are quite a few different hypotheses of how to proceed with the treatment, yet none of them have been conclusively approved. Currently corticosteroids, remdesivir, monoclonal antibodies and some other agents are being used, mostly in the context of various clinical trials. Intravenous methylprednisolone pulse as a treatment of patients receiving supplemental oxygen showed to be significantly beneficial as treatment of the disease. The RECOVERY study used dexamethasone, hydroxychloroquine or lopinavir-ritonavir at random and the results were in favor of the corticosteroid for the patients who were also on invasive mechanical ventilation. However, data on the side effects are sparse. Further studies are needed, corticosteroids have been shown as the most effective therapy in COVID-19, but we are still far from effective antiviral treatment.

1. Introduction

In late December 2020, Severe acute respiratory syndrome coronavirus 2 (SARS-CoV-2) first appeared in Wuhan, Hubei province, China [1]. It is most likely the origin is Wuhan's wet animal wholesale market, where viruses could be transferred from a bat to humans [2]. SARS-CoV-2 is the cause of Coronavirus disease 2019 (COVID-19), which has, in a matter of few months, become a global problem due to its high transmissibility [3]. In most cases the disease is asymptomatic or shows as a mild upper respiratory tract infection, however, an important percentage of infected individuals develop more severe form of the disease, which requires a hospital care. Approximately 10 percent of the infected require hospital care and approximately 10 percent of those require admission to Intensive care unit (ICU), including mechanical ventilation [4]. Morbidity of hospitalized patients is high, 26% of all patients admitted to hospitals in UK died and the percentage was even higher among those in ICU receiving mechanical ventilation, 37% of them died. Independent risk factors for terminal outcome appear to be increasing age, male sex, and chronic comorbidity, including obesity [5].

Pathological findings in patients who died as a result of COVID-19 are similar to those found in SARS and MERS; apart from clinical and radiological signs of interstitial pneumonia, autopsies revealed diffuse alveolar damage, inflammatory infiltrate, and microvascular thrombosis [6]. Highly elevated inflammation markers such as C-reactive protein, ferritin, interleukin-1, and interleukin-6 were observed in patients with severe form of the disease, meaning Cytokine release syndrome (CRS) could be the cause behind ARDS, therefore the search for potential drugs targeting exaggerated immune response was addressed [7]. Several drugs that do not target patient's immune response, but rather aim directly at virions or their replication pathway, were also considered and some of them still have not been ruled out as ineffective [8].

2. Review of different pharmacological treatment options on COVID-19

Hydroxychloroquine was considered as a treatment option due to its various immunomodulatory effects and even in vitro inhibition of SARS-Cov-19 [9,10]. However the clinical trials have failed to show any significant decrease in mortality, moreover, adverse effects such as arrhythmias were more frequent among individuals receiving hydroxychloroquine [8]. There were also considerations of treatment, combining hydroxychloroquine with azithromycin, an antibiotic which has in-vitro antiviral effect and same anti-inflammatory activity [11, 12]. Again, treatment did not manage to provide significant improvement of patients' outcomes and therefore is not advised [8]. One of the most promising therapeutic agents is broad spectrum antiviral remdesivir, which has shown its efficacy against various coronaviruses, such as SARS-CoV both in-vitro as in animal models [10, 13].

Significant results were observed in a trial regarding hospitalized patients with saturation under 94% on room air, including ones receiving supplemental oxygen, mechanical ventilation or ECMO, group receiving remdesivir had statistically significant shorter time of

recovery and lower need for mechanical ventilation compared to patients that did not receive remdesivir, the difference was most apparent in the group only receiving supplemental oxygen [14]. Other trials failed to prove that remdesivir reduces mortality, however they did, as well as the trial mentioned before, prove patients receiving remdesivir did not experience significantly more side effects than patients in the placebo groups [14,15]. No statistically significant data was obtained from trials regarding patients with oxygen saturation over 94% on room air [8]. Therefore, usage of remdesivir is advised in hospitalized patients with saturation under 94% on room air, receiving supplemental oxygen, rather than in ones receiving mechanical ventilation or ECMO [8].

Convalescent plasma has been successfully used as a passive immunization therapy for over 100 years and was therefore also considered as a treatment option, its main mechanism of action is supposed to be neutralization of virions via antibodies [8,16]. The treatment has shown to be more effective if administered shortly after the initial diagnosis, effect also varied depending on titre level of transfused plasma [17]. Naturally, transfusion can cause serious complications such as thrombosis, thromboembolism and cardiac events, however, most of the described events in COVID-19 patients occurring after transfusion do not seem to be connected to convalescent plasma therapy [18]. Due to lack of evidence, usage of convalescent plasma is only advised in a context of clinical trials [8].

As mentioned above, cytokine storm plays an important role in pathogenesis of COVID-19 and as IL-6 is associated with it the storm could potentially be suppressed by monoclonal antibody against IL-6 receptor, tocilizumab [7, 8]. Clinical studies did not show decreased mortality among patients receiving tocilizumab compared to patients that received standard care, however, number of patients that experienced clinical deterioration, need for mechanical ventilation or admission to ICU was significantly lower among those who received tocilizumab [8, 19-23]. However, a recent study including tocilizumab and sarilumab, another IL-6 receptor antagonist showed that both drugs significantly decrease duration of respiratory or cardiovascular organ support as well as decrease mortality among critically ill patients, though the described trial still awaits for peer review (24). Routine usage of tocilizumab is still not advised, as some of the studies have a serious risk of bias, since CRP levels in patients receiving treatment were significantly lower, which could have effect on assessment of patient's outcomes, nonetheless recommendations could change shortly due to new evidence [8, 24].

Another way of using antibodies could be by directly blocking SARS-CoV-2 spike protein, for this purpose, antibodies targeting different parts of the receptor binding domain of spike protein were identified [8, 25-26].

Compared to convalescent plasma, commercial products containing monoclonal antibodies offer significantly better control over administered dosage, which may vary greatly in case of convalescent plasma [8]. Bamlanivimab did show to reduce frequency of hospitalization and reduce the burden of symptoms among non-hospitalized patients with recently diagnosed mild or moderate disease, however another study among hospitalized patients without end organ failure showed that bamlanivimab offers no significant effect when combined with

standard care [27, 28]. Casirivimab and Imdevimab, which must be administered together in a combined cocktail REGN-COV2, did show to reduce viral load compared to the placebo group, especially in seronegative patients with higher viral loads, side effects reported in the test group were similar to those reported in placebo group [26, 29]. Both Bamlanivimab and REGN-COV2 are currently authorised by FDA under Emergency Use Authorisation (EUA) for treatment of mild to moderate COVID-19 in adults and children at least 12 years old weighing at least 40 kg [30, 31]. In order to give clear recommendation on usage of monoclonal antibodies against COVID-19, again, further clinical trials need to be carried out [8].

Surprisingly, famotidine, a H2 histamine receptor antagonist, usually used in conditions such as GERD, is also being considered as a potential treatment for COVID-19 [8, 32, 33]. An analysis of potential therapeutic targets showed that famotidine may successfully inhibit one of the viral enzymes crucial for its replication [34]. Till now, only one clinical trial was completed, results showed that usage of famotidine was associated with lower chance for clinical deterioration, proceeding to death or mechanical ventilation, however the study was designed as a retrospective cohort study, therefore further research is needed in order to ensure effectiveness of famotidine and advise its usage [8, 33].

A protease inhibitor lopinavir was also studied as a possible treatment for COVID-19, alongside with ritonavir, which enhances lopinavir's effect by inhibiting cytochrome P450 3A4 metabolic pathway, described combination is usually prescribed to HIV-1 positive patients [35]. The described combination has even shown to be efficient in treatment of SARS-CoV-1 and MERS induced illness [36-38]. Randomized controlled trials failed to prove combination of lopinavir and ritonavir as effective treatment against COVID-19, mortality or need for mechanical ventilation, although it might enhance clinical improvement, however evidence remains uncertain [8, 15, 39, 40]. There are also some concerns regarding side effects such as anorexia, diarrhoea, abdominal discomfort and acute gastritis, these findings raised concerns about higher dosages in potential future trials [8, 39, 40]. Due to all noted data, usage of lopinavir and ritonavir against COVID-19 is not advised [8].

Routinely used antiparasitic ivermectin is another candidate drug which might be suitable for treatment of COVID-19, as it has been proven to inhibit viral replication in-vitro [41]. Nevertheless the drug concentrations in-vitro were 50 fold higher than concentrations achieved in the standard administration regime used against parasites such as strongyloides [42].

Currently available results from trials using standard dosing regimes offer diverse results, from failing to show any significant data at all, to statistically significant earlier viral clearance or even decrease in mortality, unfortunately these trials were all relatively small and mostly retrospective [42- 44]. These results call for additional research, and with a fair number of trials underway, we should expect more reliable information about ivermectin effectiveness in the following months, however at the moment, the evidence for it's usage against COVID-19 are insufficient [45, 46].

In the study in Iran they did a single-blind, randomized, controlled clinical trial randomly on 68 patients in the early pulmonary phase of the illness from April to June 2020. They

investigated the methylprednisolone pulse effects as a glucocorticoid therapy on the treatment, clinical symptoms, and laboratory signs of hospitalized severe COVID-19 patients since in the phase of the severe inflammatory response there is a cytokine storm which glucocorticoid administration suppresses. All patients received oxygen support and neither of them received mechanical ventilation. Half the patients received standard care with methylprednisolone pulse, intravenous injection of 250mg/day for 3 days and the other half the standard care alone (Hydroxychloroquine sulfate, Lopinavir, and Naproxen). The improvement was higher in the methylprednisolone group to the standard care group (94.1% vs 57.1%; median, 11.84 ± 4.88 days vs 16.44 ± 6.93 days; $P=0.003$), they had reduced time to event (discharge, or death) compared to patients assigned to the standard care group (median, 11.62 ± 4.81 days vs 17.61 ± 9.84 days; $P=0.006$). The mortality rate was also lower (5.9% vs 42.9%; $P<0.001$). The patients with methylprednisolone treatment had a significantly increased survival time compared with the standard care group (Log rank test: $P<0.001$; Hazard ratio: 0.293; 95% CI: 0.154-0.555). Other measurements: blood saturation O₂ level, BORG score, blood oxygen saturation level, heart rate, temperature, respiratory rate, other clinical characteristics of COVID-19 patients and the CT scan were also significantly better in the treated group. The laboratory findings showed significantly better results for white blood cells, hemoglobin and lymphocytes and the platelet count, inflammatory markers such as CRP and IL-6 serum levels in the treated group. The administration time and pulmonary phase of patients are key factors in the corticosteroid treatment efficacy. The patients in the methylprednisolone group were less likely to receive invasive ventilation. Nevertheless, there are several limitations in this study, including the possible existing bias, single-blind design of the study, lack of follow-up to identify late adverse events, such as hip osteonecrosis or tuberculosis reactivation, and limited sample size [47].

The RECOVERY is a controlled, open-label Randomized Evaluation of COVID-19 Therapy trial of dexamethasone in patients hospitalized with COVID-19 in the United Kingdom where the hospitalized patients (6425) with no other medical history that could cause risk received dexamethasone, hydroxychloroquine, or lopinavir–ritonavir at random from March to June 2020. 2:1 patients received the usual standard of care alone or the usual standard of care plus oral or intravenous dexamethasone (at a dose of 6 mg once daily) for up to 10 days (or until hospital discharge if sooner) or to receive one of the other suitable and available treatments that were being evaluated in the trial. Mortality at 28 days was significantly lower in the dexamethasone group than in the usual care group, with deaths reported in 482 of 2104 patients (22.9%) and in 1110 of 4321 patients (25.7%), respectively (rate ratio, 0.83; 95% confidence interval [CI], 0.75 to 0.93; $P<0.001$). In the dexamethasone group, the incidence of death was lower than that in the usual care group among patients receiving invasive mechanical ventilation (29.3% vs. 41.4%; rate ratio, 0.64; 95% CI, 0.51 to 0.81) and in those receiving oxygen without invasive mechanical ventilation (23.3% vs. 26.2%; rate ratio, 0.82; 95% CI, 0.72 to 0.94). However, there was no clear effect of dexamethasone among patients who were not receiving any respiratory support at randomization (17.8% vs. 14.0%; rate ratio, 1.19; 95% CI, 0.91 to 1.55). Patients with a longer duration of symptoms

had a greater mortality benefit in response to treatment with dexamethasone. The receipt of dexamethasone was associated with a reduction in 28-day mortality among those with symptoms for more than 7 days but not among those with a more recent symptom onset who are receiving respiratory support. Patients in the dexamethasone group had a shorter duration of hospitalization than those in the usual care group (median, 12 days vs. 13 days) and a greater probability of discharge alive within 28 days (rate ratio, 1.10; 95% CI, 1.03 to 1.17). The greatest effect regarding discharge within 28 days was seen among patients who were receiving invasive mechanical ventilation at randomization. The risk of progression to invasive mechanical ventilation was lower in the dexamethasone group than in the usual care group. They also continue to check for cause-specific mortality, the need for renal hemodialysis or hemofiltration, major cardiac arrhythmia, and the duration of ventilation. They did not collect information on physiologic, laboratory, or virologic measures [48]. The data also indicated that dexamethasone might increase mortality in hospitalised patients who were not receiving oxygen. Because the design of the largest trial, RECOVERY, was pragmatic, data were scarce in some domains. The benefit–risk profile of corticosteroids across the full spectrum of patients with critical COVID-19 and a range of comorbidities remains uncertain. There is no data available on the level of oxygen support, the need for higher levels of oxygen might have been a good indicator that SARS-CoV-2 infection had caused some degree of lung injury and that these patients were likely to benefit from dexamethasone therapy. A third limitation is that the vast majority of patients in these trials were not receiving remdesivir. A fourth limitation is the lack of any data on viral clearance, which is likely to be an important factor in determining harm versus benefit of dexamethasone [49].

3. Guidelines for the treatment of patients infected with SARS-CoV-2

Countries have different guidelines for the treatment of patients infected with SARS-CoV-2. We sum up some of the available guidelines for the USA, UK and the World Health Organisation. Usually the recommendations in guidelines are based on evidence from the best available clinical studies with patient-important endpoints.

During the pandemic, there is a need to frequently update practice guidelines, based on critical evaluation of rapidly emerging publications. It is important to know that guidelines cannot always account for individual variation among patients [8].

In hospitalized critically ill patients with COVID-19, the Infectious Diseases Society of America (IDSA) guideline panel recommends dexamethasone rather than no dexamethasone – graded as strong recommendation, moderate certainty of evidence. IDSA guideline panel made a remark that if dexamethasone is unavailable, equivalent total daily doses of alternative glucocorticoids may be used. Physicians should prescribe 6 mg of dexamethasone IV or PO for 10 days or until discharge. Equivalent total daily doses of alternative glucocorticoids to dexamethasone 6 mg daily are methylprednisolone 32 mg and prednisone 40 mg.

Among hospitalized patients with severe, but non-critical, COVID-19, the IDSA guideline panel suggests dexamethasone rather than no dexamethasone – graded as conditional

recommendation, moderate certainty of evidence. Physicians should prescribe 6 mg of dexamethasone IV or PO for 10 days or until discharge or equivalent glucocorticoid dose may be substituted if dexamethasone is unavailable. Equivalent total daily doses of alternative glucocorticoids to dexamethasone 6 mg daily are methylprednisolone 32 mg and prednisone 40 mg.

Among hospitalized patients with non-severe COVID-19 without hypoxemia requiring supplemental oxygen, the IDSA guideline panel suggests against the use of glucocorticoids – graded as conditional recommendation, low certainty of evidence [8].

Guidelines published by National Institute for Health and Care Excellence (NICE) recommend to offer dexamethasone or hydrocortisone to people with severe or critical COVID-19 (this is also in line with updated WHO guidance). Recommended use of dexamethasone is 6 mg once a day orally (tablets or oral solution) or intravenously for 7 to 10 days. For hydrocortisone the recommended dosage is 50 mg every 8 hours intravenously (solution, powder for solution for injection/infusion is also available). The treatment may be continued for up to 28 days for patients with septic shock and it should stop if the person is discharged from hospital before the 10 day course is completed. Treated should be people with ARDS, sepsis or septic shock, other conditions that would normally need life- sustaining therapies such as ventilation or vasopressor therapy, sign of severe respiratory distress, oxygen saturation <90% (or deteriorating) on room air and increased respiratory rate (more than 30 breaths per minute in adults and children over 5 years). They emphasised that corticosteroids should not normally be used in people with COVID-19 that is not severe or critical, because there is the possibility of harm to such people. They also stated that you should consider following local policies on gastroprotection during treatment with corticosteroids and that if a person is pregnant or breastfeeding, the benefits of treatment with corticosteroids outweigh the risk [50].

The WHO in their recommendations, they recommend systemic corticosteroids rather than no systemic corticosteroids for the treatment of patients with severe and critical COVID-19 (graded as strong recommendation, based on moderate certainty evidence). This recommendation was achieved after a vote, which concerned the strength of the recommendation in favour of systemic corticosteroids. Of the 23 voting panel members, 19 (83%) voted in favour of a strong recommendation, and 4 (17%) voted in favour of a conditional recommendation.

They also suggest not to use corticosteroids in the treatment of patients with non-severe COVID-19 (graded as conditional recommendation, based on low certainty evidence). This recommendation they achieved by consensus.

Systemic corticosteroids may be administered both orally and intravenously. When considering the use of systemic corticosteroids, it is important to keep in mind that the bio-availability of dexamethasone is very high (i.e. similar concentrations are achieved in plasma after oral and intravenous intake), however critically ill patients may be unable to absorb any nutrients or medications due to intestinal dysfunction. Clinicians therefore may consider administering systemic corticosteroids intravenously rather than orally if intestinal dysfunction is suspected. In terms of glucocorticoid effect, a dose of 6 mg of dexamethasone

is equivalent to 150 mg of hydrocortisone (e.g. 50 mg every 8 hours), or 40 mg of prednisone, or 32 mg of methylprednisolone (e.g. 8 mg every 6 hours or 16 mg every 12 hours). It would be reasonable to monitor glucose levels in patients with severe and critical COVID-19, regardless of whether the patient is known to have diabetes [51].

Published literature described important side-effects of drugs used, for example azithromycin and hydroxychloroquine can cause QT prolongation and potentially life threatening arrhythmias. Corticosteroids may increase the risk of death when used in non-severe COVID-19 patients. The RECOVERY trial suggests that the relative effects of systemic corticosteroids varied as a function of the level of respiratory support received at randomization. The studies showed that the therapy is likely to increase the incidence of hyperglycemia (moderate certainty evidence; absolute effect estimate 46 more per 1000 patients, 95% confidence interval 23 more to 72 more) and hypernatraemia (moderate certainty evidence; 26 more per 1000 patients, 95% confidence interval 13 more to 41 more) [51]. Patients receiving a short course of steroids may experience hyperglycemia, neurological side effects (e.g., agitation/confusion), adrenal suppression, and risk of bacterial and fungal infection. Steroids can be immunosuppressive and potentially increase risk of secondary infections (e.g., hepatitis B virus, herpesvirus infections, strongyloidiasis, tuberculosis [52]. Steroids may produce long term side effect such as osteonecrosis [8]. Prolonged use of dexamethasone (i.e., used for more than two weeks) may be associated with adverse events such as glaucoma, cataract, fluid retention, hypertension, psychological effects (e.g., mood swings, memory issues, confusion or irritation), weight gain, or increased risk of infections and osteoporosis [53].

Dexamethasone is a moderate cytochrome P450 (CYP) 3A4 inducer. As such, it may reduce the concentration and potential efficacy of concomitant medications that are CYP3A4 substrates [54]. One study suggested that corticosteroid might have a negative effect on lung injury recovery, as patients in the corticosteroid group were estimated to have a lower CT score than in non-corticosteroid group on day 7 after admission [55]. The dexamethasone dose was chosen based on a previous trial showing the benefit of dexamethasone to patients with non-COVID-19 ARDS. Previous data suggest that high doses of corticosteroids (the equivalent of 30 mg/d of dexamethasone) in viral pneumonia may be associated with unfavorable outcomes. However, there is no currently available data from patients with COVID-19 to determine if higher doses are harmful. There are no written protocols on how to proceed when patients experience any of the side effects, whether the steroid treatment was terminated or gradually reduced. We did not find any cases where they would explain in the study how they managed the side effects. It could be that the studies are focused on benefits and the usage of steroids and there has not been enough time to focus on. Common practice with steroid treatment is to slowly lower the dosage administered for the patient to prevent withdrawal side effects. It is also important to acknowledge that the side effects of steroids take time to show so researchers should perform monitoring of their patients for a few months after the discharge and make a record of any possible side effects that may occur.

4. Discussion

During epidemics like the current, caused by SARS-CoV-2, a major challenge is that for rapid information on best treatment for patients there are no clinically proven treatments. Physicians are most likely to be instructed to use drugs based on in vitro studies, in this case their antiviral activity or on anti-inflammatory effects or based on observational studies. For example, in vitro activity of hydroxychloroquine, its use for multiple other conditions and widespread availability made it one of the first possible treatments for COVID-19. In the end studies can show that such promising drugs for treatment can be clinically ineffective. Rapid information comes first from observational studies that are not necessarily objectively and thoroughly made [8]. Observational studies were reported that were not conducted sufficiently well, for example included analyses without adjustment, had no proper control group, and used cases and controls from different patient populations [56]. Some factors that can influence the trustworthiness of evidence are avoidance of some of the usual research steps, limited peer-review and increased potential for publication bias. There is increased potential for publication bias because there may be added inclination to publish positive results and disregard negative ones [8]. On the other hand, randomized control trial (RCTs) require considerable advance planning and approval processes and are expensive. Performing RCTs is thus reserved for the pharmaceutical industry and research institutions with strong funding. This poses a problem during the COVID-19 pandemic.

The economic crisis that will be the result of a pandemic may cause a reduction of research funding. However, the RCTs provide reliable evidence and should be the preferred method of study design [57].

Due to the understandable urgency in producing, synthesizing and disseminating data during the current pandemic, there has been an evident increase in fast track publication of studies. This process is not based on the usual thoroughness from editors and reviewers and this could lead to unnoticed errors in data and calculations, incomplete reporting of methods and results. It's also important that the study limitations could be underestimated [8]. As the term pandemic suggests, SARS-CoV2 is causing damage in both developed and undeveloped parts of the world. Large proportion of patients requiring hospitalization or even admission to the ICU will without any doubt significantly increase operating costs of healthcare systems [58, 59]. Nevertheless, chances for reducing treatment costs still haven't been completely exploited, for example, minimal estimated generic production costs and actual prices for dexamethasone have already varied greatly in years prior to pandemic [60]. However even with that data in mind, corticosteroids are still considered as an affordable treatment option. Newer repurposed agents such as remdesivir are far more problematic, with estimated cost of daily dose under 1 dollar and actual cost of five days treatment at 2 340 dollars in the US [61, 62]. Luckily, Gilead Sciences allowed several other pharmaceutical companies to produce generic remdesivir for mostly low income countries without paying any royalties until WHO declares end of the pandemic, a new drug or vaccine is developed for treatment or prevention of COVID-19, whichever comes first [63]. Hopefully, other producers will also decide to add their share to the ongoing fight against global COVID pandemic.

The clinical effects of systemic corticosteroids in patients with non-severe COVID-19 (i.e. pneumonia without hypoxaemia) remain unclear and may be studied further. The impact of the treatment on immunity and the risk of a subsequent infection, which may impact the risk of death after 28 days, remains uncertain [51]. In instances where the doctors could not make a determination whether the benefits outweigh harms, it is ethical and prudent to enroll patients with COVID-19 in clinical trials, rather than use clinically unproven therapies. There are multiple ongoing trials, some with adaptive designs, which potentially can quickly answer pressing questions on efficacy and safety of drugs in the treatment of patients with COVID-19 [8]. The benefit–risk profile of corticosteroids across the full spectrum of patients with critical COVID-19 and a range of comorbidities remains uncertain as they excluded certain patients with the conditions on which dexamethasone has effect on in The RECOVERY trial [49]. Co-administration of remdesivir and dexamethasone has not been formally studied, but a clinically significant pharmacokinetic interaction is not predicted. Very few pediatric or pregnant patients with COVID-19 were included in the RECOVERY trial; therefore, the safety and efficacy of dexamethasone for the treatment of COVID-19 in children or in pregnant individuals are unknown [52].

There are still many limitations to the studies about side effects of steroids as treatment for COVID-19 so far. Some studies use retrospective methods which resulted in few missing values despite the effort in data collection, and might also bring many confounders, such as confounding by indications of corticosteroid treatment. Future analyses of evidence will consider long-term effects of systemic corticosteroids on functional outcomes and mortality in COVID-19 survivors and the clinical effects of systemic corticosteroids in patients with non-severe COVID-19. It would be very valuable if researchers compared all investigational therapies for severe and critical COVID-19 with systemic corticosteroids or evaluated in combination with systemic corticosteroids vs. systemic corticosteroids alone. It is also necessary to evaluate how additional therapies (i.e. novel immunomodulators) interact with systemic corticosteroids [51].

Despite multiple studies made, there are still a lot of ongoing uncertainties and unanswered questions for the future. Really important is that the safety of drugs used for the treatment of COVID-19, especially in patients with cardiovascular disease and immunosuppressive conditions or those who are critically ill with multi-organ failure also needs to be studied [8]. Important issue is the generalizability of clinical study results to populations that were under-represented in the trials, especially children and immuno-compromised patients. WHO encounters difficulty in making recommendations for the low- and middle-income countries where there are limited resources to provide expensive drugs [51]. There are also unanswered questions on the effect on viral replication and viral clearance [49]. The potential of effective treatment brings high levels of publicity to the medicines and incidents of substandard and/or falsified dexamethasone products occur. The same happened when hydroxychloroquine was thought to be a potential treatment for COVID-19 and falsified chloroquine products occurred. There have been reports on the falsified dexamethasone being sold on the international market. The WHO records events like this in their Global Surveillance and Monitoring System database [64].

5. Conclusion

Our findings from reviewing many different studies confirm the beneficial effects of corticosteroids used up to 12 days on short-term mortality and a reduction in the need for mechanical ventilation. Optimal timing, dose and duration of corticosteroids, in relation to safety, remain a subject of further investigation. Since corticosteroids are affordable and easily accessible in healthcare systems quivering under the pressure of the global outbreak of this rapidly spreading coronavirus, this field of research should be a universal priority. It is important to emphasise that until there is sufficient evidence, physicians and medical associations should not recommend or administer unproven treatments to patients with COVID-19 or people self-medicate with them. There are still many aspects to the best treatment of COVID-19 to be studied and hopefully we get there soon and stop this world pandemic.

Acknowledgements

Authors acknowledge kind support of prof. Veronika Kralj-Iglič. Special thanks to Tanja Kunej for English language editing.

References

1. Zhu N, Zhang D, Wang W, et al. A Novel Coronavirus from Patients with Pneumonia in China, 2019. *N Engl J Med*. 2020;382(8):727-733. doi:10.1056/NEJMoa2001017
2. Andersen KG, Rambaut A, Lipkin WI, Holmes EC, Garry RF. The proximal origin of SARS-CoV-2. *Nat Med*. 2020;26(4):450-452. doi:10.1038/s41591-020-0820-9
3. World Health Organization. Coronavirus disease 2019 (COVID-19) Situation Report - 75. Geneva: World Health Organization, 2020 4 April.
4. Wu Z, McGoogan JM. Characteristics of and Important Lessons From the Coronavirus Disease 2019 (COVID-19) Outbreak in China: Summary of a Report of 72 314 Cases From the Chinese Center for Disease Control and Prevention. *JAMA*. 2020;323(13):1239-1242. doi:10.1001/jama.2020.2648
5. Docherty AB, Harrison EM, Green CA, et al. Features of 20 133 UK patients in hospital with covid-19 using the ISARIC WHO Clinical Characterisation Protocol: prospective observational cohort study. *BMJ* 2020. 2020;369:m1985. doi:10.1136/bmj.m1985
6. Carsana L, Sonzogni A, Nasr A, Rossi RS, Pellegrinelli A, Zerbi P, Rech R, Colombo R, Antinori S, Corbellino M, Galli M, Catena E, Tosoni A, Gianatti A, Nebuloni M. Pulmonary post-mortem findings in a series of COVID-19 cases from northern Italy: a two-centre descriptive study. *Lancet Infect Dis*. 2020 Oct;20(10):1135-1140. doi: 10.1016/S1473-3099(20)30434-5. Epub 2020 Jun 8. PMID: 32526193; PMCID: PMC7279758.
7. Moore JB, June CH. Cytokine release syndrome in severe COVID-19. *Science*. 2020 May 1;368(6490):473-474. doi: 10.1126/science.abb8925. Epub 2020 Apr 17. PMID: 32303591.
8. Bhimraj A, Morgan RL, Shumaker AH. Infectious Diseases Society of America Guidelines on the Treatment and Management of Patients with COVID-19. IDSA 2020. Last updated January 2021. Available on: <https://www.idsociety.org/COVID19guidelines>.
9. Ben-Zvi I, Kivity S, Langevitz P, Shoenfeld Y. Hydroxychloroquine: from malaria to autoimmunity. *Clin Rev Allergy Immunol* 2012; 42(2): 145-53.

10. Wang M, Cao R, Zhang L, Yang X, Liu J, Xu M, Shi Z, Hu Z, Zhong W, Xiao G. Remdesivir and chloroquine effectively inhibit the recently emerged novel coronavirus (2019-nCoV) in vitro. *Cell Res*. 2020 Mar;30(3):269-271. doi: 10.1038/s41422-020-0282-0. Epub 2020 Feb 4. PMID: 32020029; PMCID: PMC7054408.
11. Gielen V, Johnston SL, Edwards MR. Azithromycin induces anti-viral responses in bronchial epithelial cells. *Eur Respir J*. 2010 Sep;36(3):646-54. doi: 10.1183/09031936.00095809. Epub 2010 Feb 11. PMID: 20150207.
12. Takizawa H, Desaki M, Ohtoshi T, et al. Erythromycin suppresses interleukin 6 expression by human bronchial epithelial cells: a potential mechanism of its anti-inflammatory action. *Biochem Biophys Res Commun*. 1995;210(3):781-786. doi:10.1006/bbrc.1995.1727
13. Sheahan TP, Sims AC, Graham RL, et al. Broad-spectrum antiviral GS-5734 inhibits both epidemic and zoonotic coronaviruses. *Sci Transl Med*. 2017;9(396):eaal3653. doi:10.1126/scitranslmed.aal3653
14. Beigel JH, Tomashek KM, Dodd LE, et al. Remdesivir for the Treatment of Covid-19 - Final Report. *N Engl J Med*. 2020;383(19):1813-1826. doi:10.1056/NEJMoa2007764
15. WHO Solidarity Trial Consortium, Pan H, Peto R, et al. Repurposed Antiviral Drugs for Covid-19 - Interim WHO Solidarity Trial Results [published online ahead of print, 2020 Dec 2]. *N Engl J Med*. 2020;NEJMoa2023184. doi:10.1056/NEJMoa2023184
16. Casadevall A, Dadachova E, Pirofski LA. Passive antibody therapy for infectious diseases. *Nat Rev Microbiol*. 2004;2(9):695-703. doi:10.1038/nrmicro974
17. Joyner MJ, Senefeld JW, Klassen SA, et al. Effect of Convalescent Plasma on Mortality among Hospitalized Patients with COVID-19: Initial Three-Month Experience. Preprint. *medRxiv*. 2020;2020.08.12.20169359. Published 2020 Aug 12. doi:10.1101/2020.08.12.20169359
18. Joyner MJ, Bruno KA, Klassen SA, et al. Safety Update: COVID-19 Convalescent Plasma in 20,000 Hospitalized Patients. *Mayo Clin Proc*. 2020;95(9):1888-1897. doi:10.1016/j.mayocp.2020.06.028
19. Hermine O, Mariette X, Tharaux PL, et al. Effect of Tocilizumab vs Usual Care in Adults Hospitalized With COVID-19 and Moderate or Severe Pneumonia: A Randomized Clinical Trial. *JAMA Intern Med*. 2021;181(1):32-40. doi:10.1001/jamainternmed.2020.6820
20. Rosas I, Bräu N, Waters M, et al. Tocilizumab in hospitalized patients with COVID-19 pneumonia. *MedRxiv* 2020: Available at: <https://doi.org/10.1101/2020.08.27.20183442> [Preprint 12 September 2020].
21. Salama C, Han J, Yau L, et al. Tocilizumab in Patients Hospitalized with Covid-19 Pneumonia. *N Engl J Med*. 2021;384(1):20-30. doi:10.1056/nejmoa2030340
22. Spinner CD, Gottlieb RL, Criner GJ, et al. Effect of Remdesivir vs Standard Care on Clinical Status at 11 Days in Patients With Moderate COVID-19: A Randomized Clinical Trial. *JAMA*. 2020;324(11):1048-1057. doi:10.1001/jama.2020.16349
23. Stone JH, Frigault MJ, Serling-Boyd NJ, et al. Efficacy of Tocilizumab in Patients Hospitalized with Covid-19. *N Engl J Med*. 2020;383(24):2333-2344. doi:10.1056/NEJMoa2028836
24. The REMAP-CAP Investigators, Gordon AC, Mouncey PR, et al. Interleukin-6 receptor antagonists in critically ill patients with Covid-19 – preliminary report. *bioRxiv*. Published online 2021. doi:10.1101/2021.01.07.21249390

25. Jones BE, Brown-Augsburger PL, Corbett KS, et al. LY-CoV555, a rapidly isolated potent neutralizing antibody, provides protection in a non-human primate model of SARS-CoV-2 infection. Preprint. *bioRxiv*. 2020;2020.09.30.318972. Published 2020 Oct 1. doi:10.1101/2020.09.30.318972
26. Wolf J, Abzug MJ, Wattier RL, et al. Initial Guidance on Use of Monoclonal Antibody Therapy for Treatment of COVID-19 in Children and Adolescents [published online ahead of print, 2021 Jan 3]. *J Pediatric Infect Dis Soc*. 2021;piaa175. doi:10.1093/jpids/piaa175
27. Chen P, Nirula A, Heller B, et al. SARS-CoV-2 Neutralizing Antibody LY-CoV555 in Outpatients with Covid-19. *N Engl J Med*. 2021;384(3):229-237. doi:10.1056/NEJMoa2029849
28. ACTIV-3/TICO LY-CoV555 Study Group, Lundgren JD, Grund B, et al. A Neutralizing Monoclonal Antibody for Hospitalized Patients with Covid-19 [published online ahead of print, 2020 Dec 22]. *N Engl J Med*. 2020;NEJMoa2033130. doi:10.1056/NEJMoa2033130
29. Weinreich DM, Sivapalasingam S, Norton T, et al. REGN-COV2, a Neutralizing Antibody Cocktail, in Outpatients with Covid-19. *N Engl J Med*. 2021;384(3):238-251. doi:10.1056/NEJMoa2035002
30. Food and Drug Administration. Bamlanivimab EUA Letter of Authorization. Published November 10, 2020. Available at: <https://www.fda.gov/media/143602/download>.
31. Food and Drug Administration. Casirivimab and Imdevimab EUA Letter of Authorization. Published November 21, 2020. Available at: <https://www.fda.gov/media/143891/download>.
32. Zhao F, Wang S, Liu L, Wang Y. Comparative effectiveness of histamine-2 receptor antagonists as short-term therapy for gastro-esophageal reflux disease: a network meta-analysis. *Int J Clin Pharmacol Ther*. 2016;54(10):761-770. doi:10.5414/CP202564
33. Freedberg DE, Conigliaro J, Wang TC, et al. Famotidine Use Is Associated With Improved Clinical Outcomes in Hospitalized COVID-19 Patients: A Propensity Score Matched Retrospective Cohort Study. *Gastroenterology*. 2020;159(3):1129-1131.e3. doi:10.1053/j.gastro.2020.05.053
34. Wu C, Liu Y, Yang Y, et al. Analysis of therapeutic targets for SARS-CoV-2 and discovery of potential drugs by computational methods. *Acta Pharm Sin B*. 2020;10(5):766-788. doi:10.1016/j.apsb.2020.02.008
35. Chandwani A, Shuter J. Lopinavir/ritonavir in the treatment of HIV-1 infection: a review. *Ther Clin Risk Manag*. 2008;4(5):1023-1033. doi:10.2147/tcrm.s3285
36. Chu CM, Cheng VC, Hung IF, et al. Role of lopinavir/ritonavir in the treatment of SARS: initial virological and clinical findings. *Thorax*. 2004;59(3):252-256. doi:10.1136/thorax.2003.012658
37. Spanakis N, Tsiodras S, Haagmans BL, et al. Virological and serological analysis of a recent Middle East respiratory syndrome coronavirus infection case on a triple combination antiviral regimen. *Int J Antimicrob Agents*. 2014;44(6):528-532. doi:10.1016/j.ijantimicag.2014.07.026
38. Kim UJ, Won EJ, Kee SJ, Jung SI, Jang HC. Combination therapy with lopinavir/ritonavir, ribavirin and interferon- α for Middle East respiratory syndrome. *Antivir Ther*. 2016;21(5):455-459. doi:10.3851/IMP3002
39. Cao B, Wang Y, Wen D, et al. A Trial of Lopinavir-Ritonavir in Adults Hospitalized with Severe Covid-19. *N Engl J Med*. 2020;382(19):1787-1799. doi:10.1056/NEJMoa2001282

40. RECOVERY Collaborative Group. Lopinavir-ritonavir in patients admitted to hospital with COVID-19 (RECOVERY): a randomised, controlled, open-label, platform trial [published online ahead of print, 2020 Oct 5]. *Lancet*. 2020;396(10259):1345-1352. doi:10.1016/S0140-6736(20)32013-4
41. Caly L, Druce JD, Catton MG, Jans DA, Wagstaff KM. The FDA-approved drug ivermectin inhibits the replication of SARS-CoV-2 in vitro. *Antiviral Res*. 2020;178:104787. doi:10.1016/j.antiviral.2020.104787
42. Camprubí D, Almuedo-Riera A, Martí-Soler H, et al. Lack of efficacy of standard doses of ivermectin in severe COVID-19 patients. *PLoS One*. 2020;15(11):e0242184. Published 2020 Nov 11. doi:10.1371/journal.pone.0242184
43. Ahmed S, Karim MM, Ross AG, et al. A five-day course of ivermectin for the treatment of COVID-19 may reduce the duration of illness [published online ahead of print, 2020 Dec 2]. *Int J Infect Dis*. 2020;103:214-216. doi:10.1016/j.ijid.2020.11.191
44. Rajter JC, Sherman MS, Fatteh N, et al. ICON (ivermectin in COvid nineteen) study: Use of ivermectin is associated with lower mortality in hospitalized patients with COVID19. *bioRxiv*. Published online 2020. doi:10.1101/2020.06.06.20124461
45. Pandey S, Pathak SK, Pandey A, et al. Ivermectin in COVID-19: What do we know?. *Diabetes Metab Syndr*. 2020;14(6):1921-1922. doi:10.1016/j.dsx.2020.09.027
46. COVID-19 Treatment Guidelines Panel. Coronavirus Disease 2019 (COVID-19) Treatment Guidelines. National Institutes of Health. Available at <https://www.covid19treatmentguidelines.nih.gov/>. Accessed [26.1.2021].
47. Edalatifard M, Akhtari M, Salehi M, et al. Intravenous methylprednisolone pulse as a treatment for hospitalised severe COVID-19 patients: results from a randomised controlled clinical trial. *Eur Respir J* 2020; in press (<https://doi.org/10.1183/13993003.02808-2020>).
48. RECOVERY Collaborative Group. Dexamethasone in Hospitalized Patients with Covid-19 — Preliminary Report (RECOVERY): a randomised, controlled, open-label, platform trial, published on July 17, 2020, at NEJM.org.
49. *Lancet Respir Med* 2020. Dexamethasone in hospitalised patients with COVID-19: addressing uncertainties; Published online October 29, 2020. Available from: [https://doi.org/10.1016/S2213-2600\(20\)30503-8](https://doi.org/10.1016/S2213-2600(20)30503-8)
50. Yusuf E, Maiwald M. COVID-19, equipoise and observational studies: a reminder of forgotten issues [published online ahead of print, 2020 Jun 25]. *Infection*. 2020;1-3. doi:10.1007/s15010-020-01466-9
51. Diaz J, Bertagnolio S, Emiroglu N, et al. Corticosteroids for COVID-19: Living guidance. 2 September 2020. Reference number: WHO/2019-nCoV/Corticosteroids/2020.1
52. NIH COVID-19 Treatment Guidelines. Updated 3rd November 2020. Available from: <https://www.covid19treatmentguidelines.nih.gov/immune-based-therapy/immunomodulators/corticosteroids/>
53. WHO: Solidarity” clinical trial for COVID-19 treatments. Accessed in January 2021. Available from: <https://www.who.int/emergencies/diseases/novel-coronavirus-2019/global-research-on-novel-coronavirus-2019-ncov/solidarity-clinical-trial-for-covid-19-treatments>
54. NIH COVID-19 Treatment Guidelines. Updated 3rd November 2020. Available from: <https://www.covid19treatmentguidelines.nih.gov/immune-based-therapy/immunomodulators/corticosteroids/>

55. Yuan, Mingli; Xu, Xiaoxiao; Xia, Dongping; Tao, Zhaowu; Yin, Wen; Tan, Weijun; Hu, Yi; Song, Cheng. Effects of Corticosteroid Treatment for Non-Severe COVID-19 Pneumonia: A Propensity Score-Based Analysis. *SHOCK*: November 2020 - Volume 54 - Issue 5 - p 638-643. doi: 10.1097/SHK.0000000000001574
56. Alexander PE, Debono VB, Mammen MJ, Iorio A, Aryal K, Deng D, et al. COVID-19 research has overall low methodological quality thus far: case in point for chloroquine/hydroxychloroquine. *J Clin Epidemiol*. 2020;123:120–126. doi: 10.1016/j.jclinepi.2020.04.016.
57. Yusuf E, Maiwald M. COVID-19, equipoise and observational studies: a reminder of forgotten issues [published online ahead of print, 2020 Jun 25]. *Infection*. 2020;1-3. doi:10.1007/s15010-020-01466-9
58. Bartsch SM, Ferguson MC, McKinnell JA, et al. The Potential Health Care Costs And Resource Use Associated With COVID-19 In The United States. *Health Aff (Millwood)*. 2020;39(6):927-935. doi:10.1377/hlthaff.2020.00426
59. Youngji Jo, Lise Jamieson, Ijeoma Edoaka, Lawrence Long, Sheetal Silal, Juliet R.C. Pulliam, et al. Cost-effectiveness of remdesivir and dexamethasone for COVID-19 treatment in South Africa. medRxiv 2020. Posted September 27, 2020. doi: <https://doi.org/10.1101/2020.09.24.20200196>
60. Hill AM, Barber MJ, Gotham D. Estimated costs of production and potential prices for the WHO Essential Medicines List. *BMJ Glob Health*. 2018;3(1):e000571. Published 2018 Jan 29. doi:10.1136/bmjgh-2017-000571
61. Hill A, Wang J, Levi J, Heath K, Fortunak J. Minimum costs to manufacture new treatments for COVID-19. *J Virus Erad*. 2020;6(2):61-69. Published 2020 Apr 30. doi:10.1016/S2055-6640(20)30018-2
62. O'Day D. An Open Letter from Daniel O'Day, Chairman & CEO, Gilead Sciences . Gilead Sciences. 29 June 2020. Available from: <https://www.gilead.com/news-and-press/press-room/press-releases/2020/6/an-open-letter-from-daniel-oday-chairman-ceo-gilead-sciences>
63. Voluntary Licensing Agreements for Remdesivir. Gilead Sciences. 24 May 2020. <https://www.gilead.com/purpose/advancing-global-health/covid-19/voluntary-licensi>
64. WHO: Coronavirus disease (COVID-19): Dexamethasone. Last updated 16 October 2020. Available from: <https://www.who.int/news-room/q-a-detail/coronavirus-disease-covid-19-dexamethasone#:~:text=Dexamethasone%20is%20a%20corticosteroid%20used,for%20critically%20ill%20patients>.



Review

Problem of hip dysplasia in adults

Zore LA^{1,*}, Stražar K^{1,2}

¹ University Medical Centre Ljubljana, Department for Orthopaedic Surgery, Ljubljana, Slovenia

² University of Ljubljana, Faculty of Medicine, Chair of Orthopaedics, Ljubljana, Slovenia

[*lenartzore@gmail.com](mailto:lenartzore@gmail.com)

Abstract

Hip dysplasia has long been recognized as one of main risk factors for pain and early degenerative changes in the hip joint. Therefore it is important for the patient to be diagnosed early and treated before initiation of adverse arthritic changes. In this article we present different types of hip dysplasia and its variations in diagnostic criteria. Further we discuss on timing and different options of treatment of this relatively common developmental disorder. We stress the significance of novel approach to 3D visualization of dysplastic hip joint and surgical planning which is the treatment of choice in adult population.

1. Introduction

Hip dysplasia is a developmental disorder of variable pattern predominantly of the pelvic acetabulum and can present at various time points in the developing human skeleton. It can be congenital or can develop later during skeletal growth [1]. Primary, it affects the acetabulum which is shallow, steep and often anteverted. Possible concomitant pathology on the femoral side includes femoral neck valgus and femoral head anteversion. Such pathoanatomy can result in instability and uneven transfer of weight (distribution of stress) in the hip joint, which can produce mechanical overloading of specific areas of acetabular surfaces and its edges [2]. Patients with dysplastic deformities have pathologic transfer of forces through their hip joints and are therefore more prone to develop injury and premature osteoarthritis [3].

2. Diagnosing hip dysplasia

Historically, diagnosis of hip dysplasia was made by clinical exam together with certain projections of X-ray imaging [4]. Knowledge of pathoanatomy and natural history of the hip joint has improved significantly over the last two decades due to development of advanced imaging modalities such as Computed Tomography (CT) with 3D reconstruction and high-resolution Magnetic Resonance Imaging (MRI) together with their better accessibility [5]. There are still many different definitions of hip dysplasia but most researchers and clinicians agree to consist of the clinical exam of the patient and radiological findings [6] (Bali, 2020). Clinical diagnosis can be made already in newborns when testing stability of hips (the Barlow and Ortolani tests) in which case we talk about developmental dysplasia of the hips (DDH) [7-9]. When there is suspicion of hip dysplasia (positive Barlow and Ortolani tests), diagnosis is confirmed with ultrasound screening. In later childhood and in adults it is hard to make clinical diagnosis by clinical exam alone. Patients usually seek help due to unspecific pain in the (dysplastic) hip joint which is triggered by overload injury or early degeneration. We differentiate pre-arthritis and arthritic stages. First, symptoms are usually tiredness after longer activities. Later, pain is triggered by compensation of hip movements and occurs in the surrounding soft tissues (muscles) or by the labral lesion which is usually hypertrophied in dysplastic hip due to increased axial loading [10].

Acetabular coverage is classified in the literature into borderline hip dysplasia and (true) hip dysplasia depending on the two measurements - lateral center-edge angle of Wiberg (LCEA) and acetabular index (AI) on the standing anteroposterior (AP) x-ray of the whole pelvis with both hips [11] (**Figure 1**). LCE angle of Wiberg should range from 25° to 39°. Angle less than 20° defines structural instability due to acetabular dysplasia (under-coverage), 20°–24° indicate borderline acetabular dysplasia and 40° or more indicates acetabular over coverage and diagnosis of pincer type of femoroacetabular impingement (FAI) [12].

Acetabular Index is also measured from (AP) x-ray of the whole pelvis with both hips and is normal from 0° - 10°. If angle is negative, we talk about pincer type of FAI and when the angle is more than 10°, we define the hip as dysplastic. However, both measurements, LCE

and AI on AP x-ray of the pelvis with both hips represent angles measured from two-dimensional AP images at the most cranial acetabular roof and neglect the total acetabular weight-bearing surface. Pelvis with hip joints is a very complex 3-dimensional structure. In 2-dimensional anteroposterior images lateral femoral head coverage just anterior or posterior to the AP x-ray will not be measured. In case of acetabular version, abnormalities and acetabular anterior or posterior wall deficiencies, LCEA measurement may over- or underestimate the true amount of actual femoral head coverage bearing area [6,13]. To be able to assess anterior coverage we have to make Faux profile x-ray projection of investigated hip [14]. All radiographs can be taken supine or standing, however there is discussable which manner is more appropriate. Patient's own pelvic tilt is also of great importance when assessing orientation and coverage of acetabula. According to the literature, appropriate AP x-ray the pelvic radiograph is when the distance between the pubic symphysis and the tip of coccyx is 1-3cm and the obturator foramina are symmetrical [15].



Figure 1. AP radiograph of pelvis with dysplastic hips. AI measurements (left) and LCEA measurements (right).

In dysplastic hip there is increased contact stress on the smaller weight bearing area which is found to be primary mechanical driver of the labral lesion, i.e. rupture and degeneration, and the osteoarthritis progression [16,17]. Chegini et al. (2009) [18] tested hip stresses while sitting and walking and showed that stresses increased linearly during walking with variations in femoral and acetabular version from normal reference position [18]. These authors also recognized high stress at the acetabular rim in association with insufficient head coverage (LCEA<25°) together with high contact pressures in this small coverage zone during walking [18]. Further, several authors demonstrated secondary soft tissue adaptations around the dysplastic hip joints by using Magnetic Resonance Imaging (MRI) [19-21]. Hip stress was also estimated within the HIPSTRESS method by using a mathematical model which uses as input the geometrical parameters of the hip and pelvis (reviewed in[22]).

3. Types of acetabular dysplasia

Researchers tend to differentiate three types of acetabular under coverage depending on the deficient area of acetabulum. Different types of dysplasia give different clinical pictures and radiological findings. The most common is lateral (global) type where LCEA and AI angles measured on the standard AP x-ray of pelvis show superolateral undercoverage of acetabuli [6],[23]. Anterosuperior type is measured by LCEA angle on faux profile of acetabular x-ray. Third type is the posteriorsuperior type of acetabular undercoverage [24,25]. Anterior and posterior types of dysplasia can have normal values of LCEA and AI on standard AP x-ray of pelvis [25]. Differentiating different types of dysplasia is important since each has specific clinical presentation.

4. Symptoms of different types of acetabular dysplasia

Lateral (global) dysplasia is the main type of acetabular instability with deficiency of superolateral part of acetabulum. Further it can also have different degrees of anterior or posterior acetabular deficiency at the same time [25]. Patients often have symptoms of static overload such as pain with prolonged standing and/or abductor fatigue such as pain with prolonged walking or jogging. On anterior-posterior x-ray of the whole pelvis with both hips, the LCEA will be reduced ($<25^\circ$) and there may be also features of anterior or posterior deficiency [7,23].

Anterior dysplasia represents anterior under coverage of acetabulum and can be suspected when patient has shortened stride length, anterior hip pain in late stance phase and increased pain while wearing high heels. Pain resembles to full extension and external rotation of the involved hip joint where femoral head is pushed anteriorly from behind. On physical exam, patient has increased internal rotation of the hip, may have a positive anterior apprehension test and/or pain with anterior pressure on the femur with the hip in an extended position, during so called prone apprehension-relocation test. The anterior instability may include a loss of anterior acetabular coverage or excessive anteversion of the acetabulum and/or the proximal femur. Radiographically, anterior acetabular deficiency is suggested by decreased anterior wall index (AWI), reduced anterior acetabular sector angle (AASA) by CT, and many times normal LCEA [23].

Posterior dysplasia results from posterior under coverage of the acetabulum [24]. Patients can be recognized by posterior hip pain and posterior instability symptoms (increased external rotation), however anterior symptoms does not exclude posterior dysplasia since there can be anterior impingement simultaneously due to increased acetabular retroversion [25,26]. Patients would complain of increased pain when climbing stairs or walking on an incline. Steeper the incline, bigger the pressure of femoral head towards posterior acetabular wall and greater the instability (pain). Patients may have a history of treating piriformis syndrome and may have vague neurologic symptoms in the distribution of the sciatic nerve. Clinically, the posterior apprehension test may be positive. Radiographically,

posterior acetabular deficiency is suggested by a positive posterior wall sign, positive ischial spine sign, positive crossover sign, a decreased posterior wall index (PWI), reduced posterior acetabular sector angle (PASA) by CT, and normal LCEA [23].

5. Treatment of Acetabular Dysplasia

Current treatment depends on age of the patient. Complex reorientational periacetabular osteotomies (PAOs) remain the golden standard for treatment of adult hip dysplasia. There are many types of PAOs described. The goal of PAO is to correct and to optimize acetabular alignment for improved hip biomechanics. The most commonly performed PAOs are triple pelvic osteotomy (e.g. Tönnis type PAO) rotational (curved) acetabular osteotomy (RAO) and Bernese PAO.

6. Conclusion

Hip dysplasia is a complex three-dimensional deformity. Traditional diagnostic criteria based on 2-D imaging are not optimal to accurately capture all cases of acetabular dysplasia. The future of treatment of acetabular dysplasia is to fully comprehend pathoanatomy and to make surgical plan which would provide correction of acetabular position in order to optimize the pressure distribution in the hip joint.

As the three-dimensionally-derived CT reconstruction is the new standard we can not only better understand different types of acetabular dysplasia but also make simulations of individual hip movements (**Figure 2**). In addition to 3D planning there is a great need to precisely execute the surgical plan. Intraoperative navigation is the next expected technological advance in order to provide safer osteotomies and to obtain more reliable and accurate correction. Technology is already used in some centers and enables real-time tracking of osteotomies in relation to 3-D anatomy of the pelvis followed by guided reposition of the osteotomized acetabular fragment. Surgical navigation systems have been developed for surgical treatment of hip dysplasia based on real-time biomechanical feedback (Lepistö J, 2008).

Dedicated software system provides measurement of contact surface angles in three dimensions and simultaneously estimates biomechanical loading pattern in means of joint pressure at weight bearing area during distinct activities of daily living.

Surgical navigation systems enable real-time tracking of instruments and full 3-D intraoperative assessment during execution of surgical plan. Despite limited scientific evidence, advanced 3-D planning and intraoperative navigation seem to be sufficiently reliable and accurate for clinical application in hip preservation surgery. Evolution of planning systems based on MR imaging and optimization of imageless navigation systems is expected to eliminate potential harmful effect of preoperative and intraoperative radiation exposure on patient's health. At the moment, 3-D planning and surgical navigation are time consuming, require supportive technical personnel and are relatively expensive. Before becoming widely accepted, automatization of certain steps, e.g. motion analysis and

intraoperative registration, is necessary. Ultimate intention is to incorporate elements of robotic assistance into surgical navigation systems. Robotic surgery may also enable surgeons to perform more complex and precise tasks in restricted spaces as they are already used in some other industries [5].

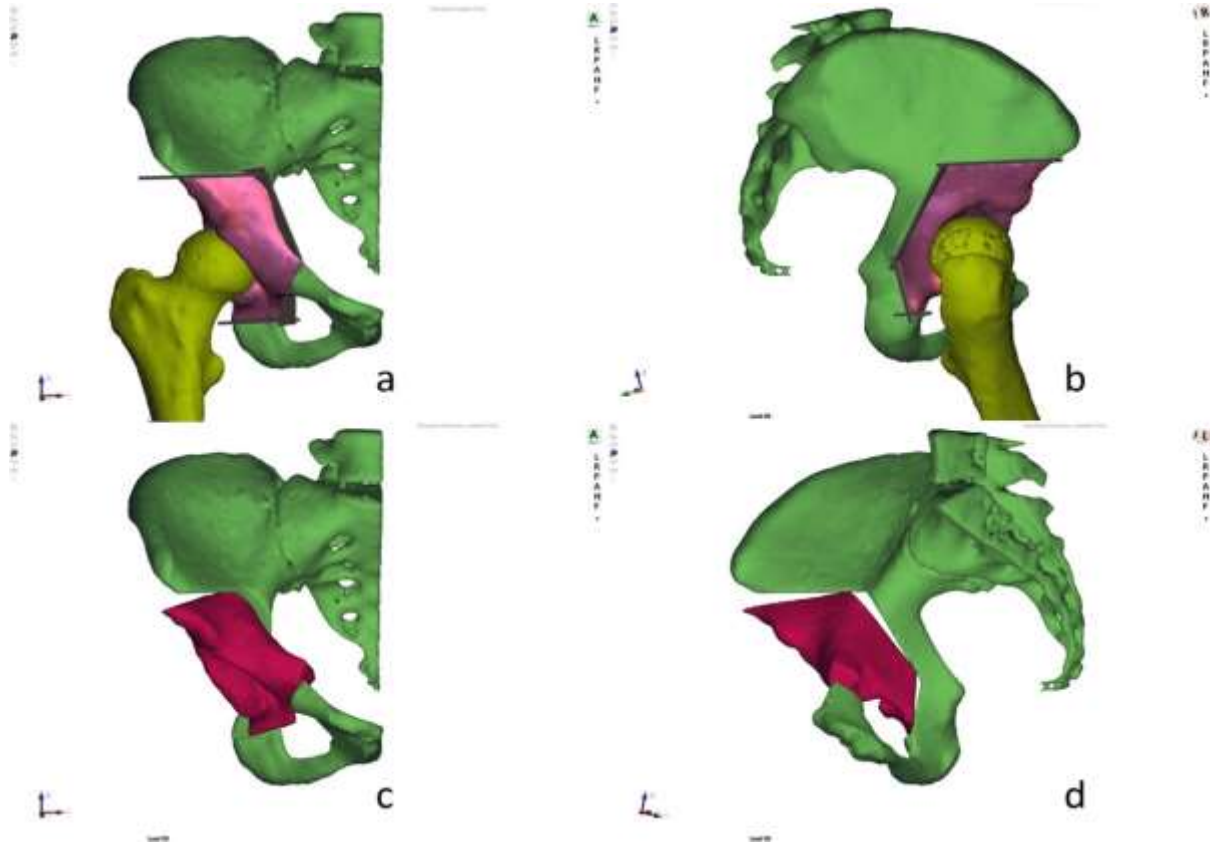


Figure 2. Planning pelvic cuts of pelvic acetabular osteotomy by on CT-based 3-D model utilizing EBS software (Ekliptik, Slovenia) From [5].

References

1. Klisic, PJ. Congenital dislocation of the hip--a misleading term: brief report. *J Bone Joint Surg [Br]* (1989), 71(1):136.
2. Mavčič, B., Antolič V., Brand R. et al. Weight bearing area during gait in normal and dysplastic hips. *Pflügers Arch* (2000), r213–r214.
3. Henak CR., Abraham CL., Anderson AE., Maas SA, Ellis BJ, Peters CL, et al. Patient-specific analysis of cartilage and labrum mechanics in human hips with acetabular dysplasia. *Osteoarthritis Cartilage* (2014), 22(2):210-7.
4. Van Bosse H., Wedge JH., Babyn P. How are dysplastic hips different? A three-dimensional CT study. *Clin Orthop Rel Res* (2015), 473(5):1712-23.
5. Stražar, K. Computer assistance in hip preservation surgery—current status and introduction of our system. *Int Orthop* (2020).

6. Bali, K., K. Smit, M. Ibrahim, S. Poitras, G. Wilkin, R. Galmiche, E. Belzile, P. E. Beaulé. Ottawa classification for symptomatic acetabular dysplasia: assessment of interobserver and intraobserver reliability. *Bone & Joint Research* (2020), 242–249.
7. TG, Barlow. Early diagnosis and treatment of congenital dislocation of the hip. *Proc Royal Soc Med* (1963), 804-6.
8. Barlow, TG. CONGENITAL DISLOCATION OF THE HIP. EARLY DIAGNOSIS AND TREATMENT. *London Clinic Med J* (1964), 47-58.
9. Ortolani, M. Congenital hip dysplasia in the light of early and very early diagnosis. *Clin Orthop Rel Res* (1976), 6-10.
10. Nunley RM, Prather H, Hunt D, Schoenecker PL, Clohisy JC. Clinical presentation of symptomatic acetabular dysplasia in skeletally mature patients. *J Bone Joint Surg [Am]* (2011), 17-21.
11. Ciglič M, Stražar K. Plain radiography in femoroacetabular impingement syndrome. *Zdravniški vestnik*, 83, 6 (2014), 475-483.
12. Tönnis, D. Normal values of the hip joint for the evaluation of X-rays in children and adults. *Clin Orthop Relat Res* (1976), 39–47.
13. Agricola R., Heijboer MP., Roze RH., Reijman M., Bierma-Zeinstra SM., Verhaar JA., et al. Pincer deformity does not lead to osteoarthritis of the hip whereas acetabular dysplasia does: acetabular coverage and development of osteoarthritis in a nationwide prospective cohort study (CHECK). *Osteoarthritis Cartilage* (2013), 1514-21.
14. Lequesne MG, Laredo JD. The faux profil (oblique view) of the hip in the standing position. Contribution to the evaluation of osteoarthritis of the adult hip. *Ann Rheum Dis*, 57 (1998), 676–81.
15. Clohisy JC, Carlisle JC, Beaulé PE, et al. A systematic approach to the plain radiographic evaluation of the young adult hip. *J Bone Joint Surg [Am]*, 90 (2008), 47-66.
16. Wyles CC, Heidenreich MJ, Jeng J, Larson DR, Trousdale RT, Sierra RJ. The John Charnley Award: redefining the natural history of osteoarthritis in patients with hip dysplasia and impingement. *Clin Orthop Rel Res* (2017), 336-50.
17. Chegini S, Beck M, Ferguson SJ. The effects of impingement and dysplasia on stress distributions in the hip joint during sitting and walking: a finite element analysis. *J Orthop Res* (2009), 195-201.
18. KS, Rakhra. Magnetic resonance imaging of acetabular labral tears. *J Bone Joint Surg [Am]* (2011), 28-34.
19. Leunig M, Podeszwa D, Beck M, Werlen S, Ganz R. Magnetic resonance arthrography of labral disorders in hips with dysplasia and impingement. *Clin Orthop Relat Res* (2004), 74-80.
20. Haefeli PC, Steppacher SD, Babst D, Siebenrock KA, Tannast M. An increased iliocapsularis-to-rectus-femoris ratio is suggestive for instability in borderline hips. *Clin Orthop Rel Res* (2015), 3725-34.
21. Kralj-Iglič V. Validation of mechanical hypothesis of hip arthritis development by HIPSTRESS method. In: *Osteoarthritis: progress in basic research and treatment*, Intech (2015), 131-156.

22. Wilkin GP, Ibrahim MM, Smit KM, Beaulé PE. A Contemporary Definition of Hip Dysplasia and Structural Instability: Toward a Comprehensive Classification for Acetabular Dysplasia. *J Arthroplasty* (2017), S20-S27.
 23. Nepple JJ, Wells J, Ross JR, Bedi A, Schoenecker PL, Clohisy JC. Three Patterns of Acetabular Deficiency Are Common in Young Adult Patients With Acetabular Dysplasia. *Clin Orthop Rel Res* (2016).
 24. Dandachli W, Islam SU, Liu M, Richards R, Hall-Craggs M, Witt J. Three-dimensional CT analysis to determine acetabular retroversion and the implications for the management of femoro- acetabular impingement. *J Bone Joint Surg [Br]* (2009), 1031-6.
 25. Cross MB, Fabricant PD, Maak TG, Kelly BT. Impingement (acetabular side). *Clin Sports Med* (2011), 379-90.
 26. Steppacher SD, Albers CE, Siebenrock KA, Tannast M, Ganz R. Femoroacetabular impingement predisposes to traumatic posterior hip dislocation. *Clin Orthop Rel Res* (2013), 1937-43.
 27. Lepistö J, Armand M, Armiger RS. Periacetabular osteotomy in adult hip dysplasia - developing a computer aided real-time bio- mechanical guiding system (BGS). *Suom Ortoped Traumatol*, 31 (2008), 186–190.
 28. Mayer SW, Abdo JC, Hill MK, Kestel LA, Pan Z, Novais EN. Femoroacetabular Impingement Is Associated With Sports-Related Posterior Hip Instability in Adolescents: A Matched-Cohort Study. *Am J Sports Med* (2016), 2299-303.
- bone 347 and joint surgery British volume (1989), 71(1):136.



EXTRACELLULAR VESICLES AND THEIR USE IN INNER EAR

Nejc Steiner^{1,*}, Saba Battelino¹

¹University Medical Centre Ljubljana, Slovenia, Department of Otorhinolaryngology and Cervicofacial Surgery

*nejc.steiner@kclj.si

Abstract

Hearing loss is a substantial health issue that affects approximately 18.5% of the world population. Currently there is no medical treatment that would cure cochlear malfunction. Once the hearing deteriorates only hearing rehabilitation with hearing aids and implantable hearing devices can be offered to the patients. To overcome this global health problem novel methods of treatment are being studied. Extracellular vesicles could have regenerative and therapeutic effect on the inner ear. Gene therapy is another new developing treatment. The delivery of therapeutic agents to the inner ear presents an obstacle and a lot of studies are investigating the best way to overcome it. Studies show that extracellular vesicles may serve as nanocarriers for the delivery of different agents that will act against preventing and treating hearing loss.

1. Introduction

Extracellular vesicles (EVs) are a heterogeneous group of nanometrically sized cell-derived membranous structures which can originate from any cell, including plant cell or bacteria. They were found in many body fluids including platelet and extracellular vesicle rich plasma (PVRP) which is a blood-derived product with immune, haemostatic and regenerative effects. PVRP is expected to contain important concentrations of EVs which could be important contributors to PVRPs effects [1].

2. Classification

Classification of EVs is done based on physical characteristics, biochemical composition and by descriptions of conditions or cell of origin. But mostly they are classified as (i) microvesicles, formed by budding, 50–500 nm in size, and (ii) exosomes, formed by exocytosis of intracellular compartments, 50–150 nm in size [1].

3. Mode of action of extracellular vesicles

Platelets and their EVs have an essential role in hemostasis, immune response and tissue regeneration. Their shape and size enable them to travel near the wall of the blood vessels and detect endothelial damage [2]. They secrete bioactive molecules contained in granules, cytoplasm or cellular organelles. The largest and the most abundant are alpha granules, which contain approximately 280 different types of proteins. Delta granules are smaller and contain smaller molecules. Lambda, the least abundant granules, are lysosomes and contain mainly enzymes. T-granules contain molecules which can be either simply translocated to the extracellular surface of the plasma membrane or they can be secreted with exocytosis [3]. EVs exert a physiological or pathological response when they reach a target cell, which can be adjacent, distant or an origin cell.

The latter implies an important role of EVs in autoregulation. There are three modes of action of EVs [1]: (i) Binding with plasma cell membranous receptors (cellular signalling), (ii): Fusion of EV and plasma membrane which causes a cytosolic release of EV cargo, (iii): Uptake of EV by plasma membrane with endocytosis.

4. Use of extracellular vesicles in inner ear

Only a few studies regarding the use of EVs in inner have been published. Platelet-derived exosomes isolated from PVRP possess a substantial role in the proliferation, migration and vessel formation. These roles are mediated by composition of exosomes, which are rich in growth factors, especially bFGF, PDGF, TGF- β and VEGF [4]. Many pathological processes, immunological or degenerative disorders cause ischemia, inflammation and cause damage to the hair cells of inner ear.

Growth factors, angiogenetic substances and immunomodulators from EVs could have positive influence on restoration of cochlear function.

In principle, EVs could also serve as potential carriers for inner ear delivery of different effectors. EVs could be delivered to the inner ear systemically, through round and oval windows which are natural openings to the cochleae or through the cochleostomy, which is an opening drilled into cochlea. [5] To access the inner ear from the external ear canal, a

tympano-meatal flap needs to be lifted, like in procedure called tympanoplasty [6]. The round window membrane is the only delivery portal to the inner ear that does not require bone perforation. Recent advances in microneedle fabrication enable the safe membrane perforation with polymeric and gold-coated metallic microneedles as a mean to enhance the rate of agent delivery from the middle ear to the inner ear [7].

The agents can be either injected into the inner ear or they could be potentially released from cochlear implant electrode which is inserted into cochlea. To our knowledge the delivery of EVs with cochlear implant electrode has not been studied yet but cochlear implant electrode has already been used for delivery of different medications such as glucocorticosteroids, antiapoptotic substances, or neurotrophins to the inner ear and thus might be used for delivery of EVs in the future [8]. Studies of delivering other agents including neurotrophins, antiapoptotics, cell therapy, gene therapy, and anti-inflammatory drugs are mostly in preclinical stages [9].

Disabling hearing loss is a big health issue that affects approximately 6.1% of the world population [10]. It can be present at birth or it can be acquired at any time afterwards. About half of all congenital hearing losses, which incidence is 1:1,000 births [11], have a defined genetic cause. Currently there is no medical treatment that would cure deafness. Once the hearing deteriorates there is not much that we can do except to offer hearing rehabilitation with hearing aids and implantable hearing devices. Novel methods of treatment are being studied to treat this global health problem. One of the new methods is gene therapy.

Cochlea is the part of inner ear involved in hearing. It is surgically accessible and local application of agents into a relatively immune-protected environment is possible, thus gene therapy using viral vectors is an attractive approach for treating hearing loss. For congenital recessive deafness, gene addition is possible and for congenital dominant forms of deafness, silencing or correcting the mutated gene should be done [10]. Gene therapy could also be used in the future for age-related hearing loss by targeting pathways involved in hair cell or spiral ganglion neuron survival (for example - neurotrophic factors [12] or antioxidant proteins [13]).

The cochlea has two types of hair cells. Inner hair cells and outer hair cells [14]. Most deafness genes that are known to affect hair cell function are expressed in both cell types, so gene therapy strategy should target both inner and outer hair cells [15].

Currently, gene therapy for hearing disorders is still not yet as advanced because the delivery of agents to the inner ear is still inefficient. The major limitation of gene therapy for the cochlea is the relative inefficiency of vectors that mediate transgene expression in hair cells. In order to achieve better delivery to the inner ear B György et. al. (2017)[5] demonstrated that a vector, exosome-associated AAV, is a potent carrier of transgenes to all inner ear hair cells and may be useful for gene therapy of deafness. They injected the agent in vivo into cochlea through round window membrane and through cochleostomy. Injection through round window membrane resulted in higher transduction of inner hair cells and injection through cochleostomy resulted in higher transduction of outer hair cells.

Cochleostomy results were more variable and there were more instances with very low

expression [5]. Promising results of gene therapy have been showed in studies regarding Usher syndrome, where not only hearing but also vision is deteriorating over time [16]. Acquired hearing loss can happen due to trauma, infection, ototoxic medication and loud noises. In the past, noise induced hearing loss was thought to be caused primarily by noise, but today more and more children and adolescents are suffering from hearing loss caused by exposure to loud music. We could say that the world we live in is getting louder. In addition to all the loud machines, the development of a louder environment was mainly influenced by the technological development of loud speakers, headphones, portable music players and smartphones. Their invention simplified the way we listen to music, but it also brought with it a great risk, namely hearing impairment among young people. Many people are unaware of the dangers posed by audio devices. They should be aware of the fact that these seemingly innocent devices can cause irreparable hearing loss [17]. Data from studies conducted in countries with a medium and high standard of living, analysed by the WHO, show that among teenagers and young adults aged 12 to 35, almost 50% are exposed to the dangerous volume of music from personal audio devices. However, around 40% are exposed to the potentially harmful intensity of music in entertainment venues [18].

Drug and noise related hearing loss are associated with inflammatory responses in the inner ear [19]. Inflammation is a normal biological reaction aimed at restoring tissue functionality and its homeostasis. It is mostly divided into two phases: initiation and resolution [20]. The start of inflammation is characterized by the up-regulation of pro-inflammatory mediators. The resolution phase, which starts at the time when the inflammatory response peaks, is an active process achieved mostly by the action of specialized protein and lipid pro-resolving mediators [21]. Stimulation of these pro-resolving pathways associated with cochlear inflammatory processes could be an important therapeutic approach for preventing drug and noise related hearing loss [22].

Kalinec et. al. (2019) [23] provided evidence that auditory hair cells generated abundant EVs that can be loaded with cocktail of molecules (a combination of pro-resolving mediators, specialized proteins and lipids) aimed at accelerating inflammation resolution and improving the organ response to inflammation damage and thus prevent or alleviate drug and noise related hearing loss [23]. They accelerate the return to homeostasis by modifying the immune response rather than by inhibiting inflammation [24].

Hair cell death and consequent hearing loss are common results of treatment with ototoxic drugs, including the widely used aminoglycoside antibiotics. Breglio et. al. (2020) [25] studied how to decrease the negative effect of ototoxic drugs. They showed that in response to heat stress, inner ear tissue releases exosomes that improved the survival of hair cells exposed to the aminoglycoside antibiotic neomycin, whereas inhibition or depletion of exosomes from the extracellular environment abolished the protective effect of heat shock [25].

5. Conclusion

EVs have a role in intercellular communication of the inner ear and can mediate nonautonomous hair cell survival. Their delivery to the inner ear currently present one of the challenges that researchers are trying to overcome. Anatomical position, microscopic dimensions and very sensitive cell structures of the inner ear present challenges that need to be faced in research. In the future, extracellular vesicles may also serve as nano-carriers for the delivery of therapeutic agents for treating hearing loss.

References

1. Vozel D, Božič D, Jeran M, Jan Z, Pajnič M, Pađen L, et al. Treatment with platelet- and extracellular vesicle-rich plasma in otorhinolaryngology-a review and future perspectives. In: *Advances in Biomembranes and Lipid Self-Assembly* [Internet]. Academic Press; 2020 [cited 2020 Sep 22]. Available from: <http://www.sciencedirect.com/science/article/pii/S2451963420300224>
2. Holinstat M. Normal platelet function. *Cancer Metastasis Rev.* 2017 Jun;36(2):195–8. doi: 10.1007/s10555-017-9677-x
3. Morrell CN, Aggrey AA, Chapman LM, Modjeski KL. Emerging roles for platelets as immune and inflammatory cells. *Blood.* 2014 May 1;123(18):2759–67. doi: 10.1182/blood-2013-11-462432
4. Guo S-C, Tao S-C, Yin W-J, Qi X, Yuan T, Zhang C-Q. Exosomes derived from platelet-rich plasma promote the re-epithelization of chronic cutaneous wounds via activation of YAP in a diabetic rat model. *Theranostics.* 2017;7(1):81–96. doi: 10.7150/thno.16803
5. György B, Sage C, Indzhukulian AA, Scheffer DI, Brisson AR, Tan S, et al. Rescue of Hearing by Gene Delivery to Inner-Ear Hair Cells Using Exosome-Associated AAV. *Mol Ther.* 2017 01;25(2):379–91. doi: 10.1016/j.ymthe.2016.12.010
6. Steiner N, Battelino S. Techniques of tympanoplasty in otorhinolaryngology. In Ljubljana; 2020 [cited 2021 Jan 30]. p. 153–4. Available from: https://www.zf.uni-lj.si/images/stories/datoteke/Zalozba/Sokratska_2020.pdf
7. Aksit A, Rastogi S, Nadal ML, Parker AM, Lalwani AK, West AC, et al. Drug delivery device for the inner ear: ultra-sharp fully metallic microneedles. *Drug Deliv Transl Res.* 2021 Feb;11(1):214–26. doi: 10.1007/s13346-020-00782-9
8. Plontke SK, Götze G, Rahne T, Liebau A. Intracochlear drug delivery in combination with cochlear implants : Current aspects. *HNO.* 2017 Jan;65(Suppl 1):19–28. doi: 10.1007/s00106-016-0285-9
9. Chin OY, Diaz RC. State-of-the-art methods in clinical intracochlear drug delivery. *Curr Opin Otolaryngol Head Neck Surg.* 2019 Oct;27(5):381–6. doi: 10.1097/MOO.0000000000000566
10. Global, regional, and national incidence, prevalence, and years lived with disability for 310 diseases and injuries, 1990–2015: a systematic analysis for the Global Burden of Disease Study 2015. *Lancet.* 2016 Oct 8;388(10053):1545–602. Doi:[https://doi.org/10.1016/S0140-6736\(16\)31678-6](https://doi.org/10.1016/S0140-6736(16)31678-6)
11. Shearer AE, Hildebrand MS, Smith RJ. Hereditary Hearing Loss and Deafness Overview. In: Adam MP, Ardinger HH, Pagon RA, Wallace SE, Bean LJ, Mirzaa G, et al., editors. *GeneReviews®* [Internet]. Seattle (WA): University of Washington, Seattle; 1993 [cited 2021 Jan 27]. Available from: <http://www.ncbi.nlm.nih.gov/books/NBK1434/>

12. Deafness | Britannica [Internet]. [cited 2021 Jan 27]. Available from: <https://www.britannica.com/science/deafness>
13. Deafness and hearing loss [Internet]. [cited 2021 Jan 27]. Available from: <https://www.who.int/news-room/fact-sheets/detail/deafness-and-hearing-loss>
14. Flint PW, Haughey BH, Robbins KT, Thomas JR, Niparko JK, Lund VJ, et al. Cummings Otolaryngology - Head and Neck Surgery. Elsevier Health Sciences; 2014. 4198 p.
15. Schilder AG, Chong LY, Ftouh S, Burton MJ. Bilateral versus unilateral hearing aids for bilateral hearing impairment in adults. Cochrane Database Syst Rev [Internet]. 2017 Dec 19 [cited 2021 Jan 27];2017(12). Available from: <https://www.ncbi.nlm.nih.gov/pmc/articles/PMC6486194/>
16. Géléoc GGS, El-Amraoui A. Disease mechanisms and gene therapy for Usher syndrome. Hearing Research. 2020 Sep 1;394:107932. doi: 10.1016/j.heares.2020.107932
17. eSiNAPSA | Kako nam lahko glasna glasba »vzame« sluh in povzroči tinitus [Internet]. [cited 2021 Jan 30]. Available from: https://www.sinapsa.org/eSinapsa/stevilke/2015-10/183/kako_nam_lahko_glasna_glasba_vzame_sluh_in_povzroci_tinitus
18. Shrivastava SR, Shrivastava PS, Ramasamy J. Joining hands with World Health Organization initiative Make Listening Safe. Noise and Health. 2015 Jan 5;17(76):173. doi: 10.4103/1463-1741.155854
19. Kaur T, Borse V, Sheth S, Sheehan K, Ghosh S, Tupal S, et al. Adenosine A1 Receptor Protects Against Cisplatin Ototoxicity by Suppressing the NOX3/STAT1 Inflammatory Pathway in the Cochlea. J Neurosci. 2016 Apr 6;36(14):3962–77. doi: 10.1523/JNEUROSCI.3111-15.2016
20. Lai P, Weng J, Guo L, Chen X, Du X. Novel insights into MSC-EVs therapy for immune diseases. Biomark Res [Internet]. 2019 Mar 18 [cited 2021 Jan 28];7. Available from: <https://www.ncbi.nlm.nih.gov/pmc/articles/PMC6423844/>
21. Perretti M, Leroy X, Bland EJ, Montero-Melendez T. Resolution Pharmacology: Opportunities for Therapeutic Innovation in Inflammation. Trends Pharmacol Sci. 2015 Nov;36(11):737–55. doi: 10.1016/j.tips.2015.07.007
22. Kalinec GM, Lomberk G, Urrutia RA, Kalinec F. Resolution of Cochlear Inflammation: Novel Target for Preventing or Ameliorating Drug-, Noise- and Age-related Hearing Loss. Front Cell Neurosci. 2017;11:192. doi: 10.3389/fncel.2017.00192
23. Kalinec GM, Gao L, Cohn W, Whitelegge JP, Faull KF, Kalinec F. Extracellular Vesicles From Auditory Cells as Nanocarriers for Anti-inflammatory Drugs and Pro-resolving Mediators. Front Cell Neurosci [Internet]. 2019 [cited 2021 Jan 26];13. Available from: <https://www.frontiersin.org/articles/10.3389/fncel.2019.00530/full>
24. Dalli J, Serhan CN. Identification and structure elucidation of the pro-resolving mediators provides novel leads for resolution pharmacology. Br J Pharmacol. 2019 Apr;176(8):1024–37. doi: 10.1111/bph.14336
25. Breglio AM, May LA, Barzik M, Welsh NC, Francis SP, Costain TQ, et al. Exosomes mediate sensory hair cell protection in the inner ear. J Clin Invest. 130(5):2657–72. doi: 10.1172/JCI128867



Review

Charcot neuroarthropathy: What lies beneath?

Schara K¹, Kralj Igljč V²

¹University Medical center Ljubljana, Department of Orthopaedic Surgery, Ljubljana, Slovenia

²University of Ljubljana, Faculty of Health Sciences, Laboratory of Clinical Biophysics, Ljubljana, Slovenia

*karin.schara@gmail.com

Abstract

This work describes the mechanisms for the development of diabetic Charcot neuroarthropathy (CNA) syndrome. CNA is a chronic, progressive disease causing severe foot and ankle deformities which present a serious and potentially limb-threatening lower-extremity complication of diabetes. One lower limb is lost to diabetes every 30 seconds in the world. It is currently believed that once the disease is triggered, it is mediated through a process of uncontrolled inflammation in the foot leading to osteolysis and progressive destruction of bone and joint structures. Until the intertwining of several interrelated factors and mechanisms initiating bone and joint destruction is confirmed, challenges of early recognition and treatment of the disease remain crucial for the limb preservation.

1. Introduction

CNA is a chronic, progressive disease causing severe foot and ankle deformities which present a serious and potentially limb-threatening lower-extremity complication of diabetes [1] It is characterized by painful or painless bone and joint destruction in limbs that have lost sensory innervation. Peripheral neuropathy in diabetes is usually presenting as a distal, symmetric polyneuropathy therefore CNA is predominately affecting the joints of the foot and ankle [2]CNA is considered a rare disease with estimated prevalence of 1 to 2% of patients with diabetic neuropathy but the true prevalence in patients with diabetes mellitus is not known because it is likely that many cases remain undiagnosed due to a lack of recognition of the disease [1].

The Charcot foot can be classified in terms of clinical stage, anatomical localization and stage of natural history. In clinical practice, the Charcot foot can be classified into the acute (active) and chronic (inactive) stage while other classifications are based on anatomical localization and staging of natural history [3].

The earliest manifestation of active, acute CNA is persistent unilateral swelling with only mild to modest pain or discomfort. On clinical examination, the foot is warm, swollen and erythematous, loss of sensation is diagnosed (**Figure 1**). This initial clinical picture resembles various conditions like cellulitis, osteomyelitis, deep vein thrombosis, lymphoedema, arthritis or acute gout and can be misdiagnosed as such [1]. Bone and joint involvement during active disease present on the X ray with a variety of changes including demineralization, joint dislocation, bone destruction, fractures, bone fragmentation and periosteal reaction [4].

All these changes can occur very rapidly with a normal x-ray deteriorating to grossly abnormal within a few weeks [3] (**Figure 2**). If the condition is correctly diagnosed and the patient is appropriately treated, the local inflammation will subside and further bony destruction can be minimized or avoided [5]. If treatment is delayed or if left untreated mechanical stress may lead to ligament strain, fractures and dislocations resulting in severe foot deformity and/or joint instability [5,1].

The mainstay of treatment of Charcot neuroarthropathy is immobilization in a total contact cast, which increases the total surface area of contact to the entire lower extremity, distributing pressure away from the foot. In order to avoid weight bearing of the affected foot in active stage of CNA, the patient should use crutches or wheelchair [6].



Figure 1. Clinical presentation of CNA (patient's left).



Figure 2. A: Early stage of CNA. On the X-ray midfoot joint anatomy is still preserved, ossifications marked in the circle indicate the disease. B: Progressive stage of CNA. Bone

anatomy is destructed, abundant ossification above the joints of dorsal midfoot can be observed. Progressive X-ray changes are marked in the circle.

2. Mechanisms of CNA disease

There is no singular cause for the development of the Charcot foot therefore our knowledge on pathogenesis and treatment options remain limited. Initially the condition was explained by neurotraumatic and neurovascular theories, recently active CNA is considered to be an uncontrolled inflammatory syndrome affecting bone metabolism [7]. CNA occurs as a consequence of an imbalance of activity of two types of cells: osteoblasts and osteoclasts [8]. This imbalance leads to enhanced bone lysis and fracture and is driven by inflammation [9,1]. Increased amounts of the pro-inflammatory cytokines TNF-alpha, IL-1 and IL-6, decreased amounts of the anti-inflammatory cytokines IL-4 and IL-10 and increased amounts of the surface molecules CD40, CD80, and CD86 were found in monocytes of patients with CNA [10]. Increased concentrations of TNF-alpha and IL-6 were found also in serum of patients with CAN [11].

CN has been associated with an increase in advanced glycation end products (AGEs) in blood that is often caused by poorly controlled diabetes and/or inflammation due to hyperglycemia and oxidative stress [9]. It was found that AGEs stimulate apoptosis of human mesenchymal stem cells [12] and osteoblasts [13] by binding to receptor for AGE (RAGE) on their membranes [9]. It was also observed that the concentration of soluble RAGE in blood plasma of patients with CN was lower than in healthy subjects and also lower than in patients with diabetes mellitus [14]. Possibly due to a deficiency of soluble RAGE, binding of AGE to soluble RAGE was decreased with a deleterious consequence of AGE binding to membrane fraction of RAGE [14]. As these processes are regulated by many pathways involving the osteoblast and the osteoclast lineages [15,16,9] it is evident that intercellular communication is crucial for bone remodeling.

Extracellular vesicles (EVs) and nanotubules were reported as important participants in cellular processes [17] (**Figure 3**). Experimental evidence indicates that EV concentration is increased in some diseases e.g. cardiovascular diseases, autoimmune disorders, inflammation and infection [18]. Increased levels of extracellular vesicles have been found in the peripheral blood of patients with diabetic neuropathy [19]. Studies confirmed that EVs derived from patients with diabetic neuropathy display a higher level of leukocytes- and monocytes-derived EVs [19].

Osteoclasts, cells responsible for bone resorption in CF are members of the monocyte and macrophage group. A high content of inflammatory cytokines G-CSF, GM-CSF, IL-1-ra and IL-2 which may enhance osteoclasts differentiation was detected in CNA disease [20]. It was shown that levels of EVs in active CNA were elevated and associated with inflammatory parameters and increased temperature of the foot [21]. Therefore it was suggested that EVs may be useful in monitoring and predicting clinical progression of the disease [21].

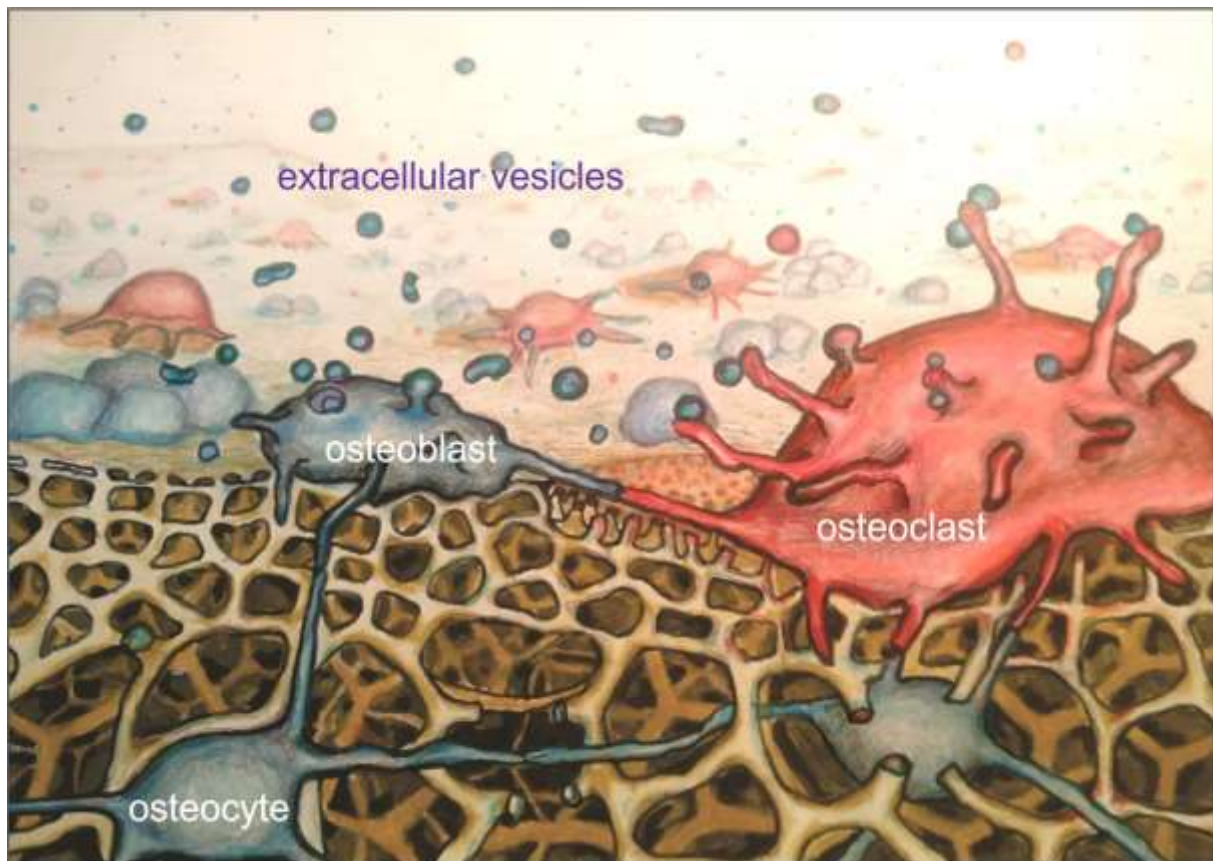


Figure 3. Cell to cell communication: EVs and nanotubules in bone remodeling process.

3. Conclusions

Few studies have included patients with active stage of CNA, therefore it is difficult to draw conclusions on causation and the relationship factors connected with the development and progression of the condition. A final common pathway for the pathogenesis of CNA is yet to be determined and promising therapeutic targets have yet to be identified. Until the intertwining of several interrelated factors and mechanisms initiating bone and joint destruction is confirmed, challenges of early recognition and treatment of the disease remain crucial for treatment and limb preservation.

Acknowledgements

Authors acknowledge support of Research Agency of the Republic Slovenia ARRS: program P3-0388 and projects J1-6728 and L3-2621.

References

1. Rogers LC, Frykberg RG, Armstrong DG, et al. The Charcot foot in diabetes. *Diabetes Care* 2011; 34:2123. DOI: 10.7547/1010437
2. Rajbhandari S, Jenkins R, Davies, C et al. Charcot neuroarthropathy in diabetes mellitus. *Diabetologia*, 2002, 45: 1085–1096. DOI:10.1007/s00125-002-0885-7

3. Armstrong DG, Todd WF, Lavery LA, Harkless LB, Bushman TR, The natural history of acute Charcot's arthropathy in a diabetic foot specialty clinic. *Diabet Med*. 1997;14(5):357–363. DOI: 10.1002/(SICI)1096-9136(199705)14:5<357::AID-DIA341>3.0.CO;2-8
4. Marmolejo VS, Arnold JF, Ponticello M, Anderson CA, Charcot Foot: Clinical clues, diagnostic strategies, and treatment principles. *Am Fam Physician*. 2018, 97: 594-599.
5. Papanas N, Maltezos E, Etiology, pathophysiology and classifications of the diabetic Charcot foot, *Diabetic Foot & Ankle*, 2013, 4: 1-5. DOI:10.3402/dfa.v4i0.20872
6. Frykberg RG, Eneroth M, Principles of conservative management. In *The Diabetic Charcot Foot: Principles and Management*. Frykberg RG, Ed. Brooklandville, MD, Data Trace Publishing Company, 2010, p. 93–116.
7. Jeffcoate WJ. Charcot neuro-osteoarthropathy. *Diabetes Metab Res Rev*. 2008, 24: S62-S65. DOI: 10.1002/dmrr.837
8. Jeffcoate WJ. Charcot foot syndrome. *Diabetic Medicine*. 2015, 32: 760–770. DOI: 10.1111/dme.12754
9. Petrova NL, Shanahan CM, Neuropathy and the vascular-bone axis in diabetes: lessons from Charcot osteoarthropathy. *Osteoporos Int* 2014, 25: 1197–1207. DOI: 10.1007/s00198-013-2511-6
10. Uccioli L, Sinistro A, Almerighi C, et al., Pro-inflammatory modulation of the surface and cytokine phenotype of monocytes in patients with acute Charcot foot. *Diabetes Care* 2010, 33: 350–355. DOI:10.2337/dc09-1141
11. Petrova NL, Dew TK, Musto RL, et al., Inflammatory and bone turnover markers in a cross-sectional and prospective study of acute Charcot osteoarthropathy. *Diabet Med* 2015, 32: 267-273. DOI:10.1111/dme.12590
12. Kume S, Kato S, Yamagishi S, et al., Advanced glycation end-products attenuate human mesenchymal stem cells and prevent cognate differentiation into adipose tissue, cartilage, and bone. *J Bone Miner Res* 2005, 20: 1647–1658. DOI:10.1359/JBMR.050514
13. Alikhani M, Alikhani Z, Boyd C, et al., Advanced glycation end products stimulate osteoblast apoptosis via the MAP kinase and cytosolic apoptotic pathways. *Bone* 2007, 40: 345–353. DOI: [10.1016/j.bone.2006.09.011](https://doi.org/10.1016/j.bone.2006.09.011)
14. Witzke KA, Vinik AI, Grant LM, Loss of RAGE Defense: A Cause of Charcot Neuroarthropathy? *Diabetes Care* 2011, 34: 1617–1621. DOI:10.2337/dc10-2315
15. Nomura S, Significance of chemokines and activated platelets in patients with diabetes. *Clin Exp Immunol* 2000, 121: 437-443. DOI: 10.1046/j.1365-2249.2000.01324.x
16. Schmidt AM, Yan SD, Yan SF, Stern DM, The multiligand receptor RAGE as a progression factor amplifying immune and inflammatory responses. *J Clin Invest* 2001, 108: 949–955. DOI: 10.1172/JCI14002
17. Schara K, Janša V, Šuštar V, et al., Mechanisms for the formation of membranous nanostructures in cell-to-cell communication. *Cell Mol Biol Lett* 2009, 14: 636-656. DOI: 10.2478/s11658-009-0018-0

18. Boulanger CM, Amabile N, Tedgui A, Circulating microparticles: a potential prognostic marker for atherosclerotic vascular disease. *Hypertension* 2006, 48: 180 -186. DOI: 10.1161/01.HYP.0000259667.22309.df
19. Wang Y, Chen L, Liu M, Microvesicles and diabetic complications — novel mediators, potential biomarkers and therapeutic targets. *Acta Pharmacol Sin* 2014, 35: 433–443. DOI:10.1038/aps.2013.188
20. Pasquier J, Thomas B, Hoarau-Véchet, J et al., Circulating microparticles in acute diabetic Charcot foot exhibit a high content of inflammatory cytokines, and support monocyte-to-osteoclast cell induction. *Sci Rep* 2017, 7, 16450. DOI: 10.1038/s41598-017-16365-7
21. Schara K, Štukelj R, Krek JL et al., A study of extracellular vesicle concentration in active diabetic Charcot neuroarthropathy, *European Journal of Pharmaceutical Sciences*, 2017, 98: 58-63. DOI: 10.1016/j.ejps.2016.09.009



Laudate
Dominum

Reflection

POST-COVID-19 EXPERIENCES

Romolo A^{1*}

¹University of Ljubljana, Faculty of Electrical Engineering, Laboratory of Physics, Ljubljana, Slovenia,

*annaromolo@gmail.com

Abstract

A year since the outbreak of the Corona Virus Disease 2019 (COVID-19) pandemic, the epidemiological and clinical characteristics, pathogenesis and complications of acute stage of the disease have been described extensively in the scientific literature. However, the disease might have long-term effects on patients, in those that underwent severe disease as well as in those with milder forms. In this contribution, we explored the existing evidences of the post-COVID-19 one year after the outbreak. A search was performed in the Google Scholar base, using selected keywords. Both patients that were hospitalized and those that were not hospitalized may show persistent symptoms such as fatigue, wheezing and reduced lung function at the 6-months follow-up after infection with SARS-CoV-2 indicating that in some cases COVID-19 is not a disease from which one heals quickly.

Survey of the literature

SARS-CoV-2 virus affects different organs and systems in the body [1]. The underlying mechanisms are not yet completely understood. Its long-term consequences after the acute phase of infection exhibited in COVID-19 are now the subject of scientific research by following up of those who seem to be cured. We surveyed the literature by searching through the Google Scholar database. Inserting the keyword Effect long term COVID-19 into the browser returned 2565 articles. Changing the keyword to Consequence effect long term COVID-19 shrank the number of articles to 383. After screening the abstracts of these articles we modified the keyword to: Consequences pulmonary long term COVID-19. We obtained 48 articles. We screened the articles and outlined 6 articles which in our opinion represented best the hitherto gathered evidences on post-COVID effects.

The outlined reports

One of the first published works on the post-COVID-19 effects was a study by Cortinovis et al., (2020) [2]. These authors found that the clinical spectrum of SARS-CoV-2 infection is wide: from asymptomatic infection, fever, fatigue, myalgias, mild upper respiratory tract illness to severe life-threatening viral pneumonia and death. Persisting symptoms as well as unexpected ones were observed after the disease similar to organ dysfunction after infection with SARS-CoV-2 [2]. This was supported by the findings of the physicians from the Policlinico Gemelli in Rome (2020)[3] and by Huang et al.,(2021) [4] who showed that many people infected with SARS-Cov-2, those were hospitalized and those who were not hospitalized, had different disorders for weeks and even six months after the disease. Carfi et al. (2020) [3] described the outcome of 143 patients in a period of time ranging from 21 April to 29 May 2020. The average hospital stay was 13.5 days; 21 patients (15%) received non-invasive ventilation and 7 patients (5%) received invasive ventilation. During hospitalization, 72.7% of participants had evidence of interstitial pneumonia. Patients meeting the World Health Organisation criteria for the cessation of quarantine (absence of fever for 3 consecutive days, improvement of other symptoms and 2 negative test results taken 24 hours apart) were included in the follow-up. At the release from the hospital, patients were subjected to a full medical evaluation with detailed medical history and physical examination. Data on all clinical features, including clinical and pharmacological history, lifestyle factors, vaccination status and body measurements have been grouped together in a structured electronic data collection system. In particular, data on specific symptoms potentially related to COVID-19 were obtained using a standardised questionnaire administered to enlistment. In the waning phase of the pandemic, starting April 21, 2020, the Fondazione Policlinico Universitario Agostino Gemelli IRCCS in Rome, Italy, established an outpatient post office service for patients dismissed from the hospital after recovery from COVID-19. Patients were asked to report retrospectively the presence or absence of symptoms during the acute phase of COVID-19 and whether each symptom persisted at the time of the examination.

Patients were rated at an average of 60.3 days after the start of the first COVID-19 symptom; at the time of evaluation, only 18 (12.6%) were completely free of any COVID-19 related symptom, while 32% had 1 or 2 symptoms and 55% had 3 or more. None of the patients had a fever or any signs or symptoms of acute illness. A deterioration in the quality of life was observed in 44.1% of patients: a high percentage of individuals reported fatigue (53.1%), dyspnoea (43.4%), joint pain (27.3%) and chest pain (21.7%). The study found that in patients who recovered from COVID-19, 87.4% reported persistence of at least 1 symptom, particularly fatigue and wheezing.

Huang et al., (2021) [4] conducted the study focused on the course of 1733 patients (average age 57, 52 percent male) that were hospitalized due to COVID-19 in the Jinyintan Hospital in Wuhan between January 7 and May 29, 2020. Six months after the onset of the first symptoms, 76 percent of patients released from the hospital reported that they still had at least one symptom that have persisted longer in women. The most frequently reported symptoms were fatigue and muscle pain (63 percent) and sleep disorders (26 percent). Nearly a quarter of patients (23 percent) said that they experienced anxiety or depression [4]. In addition, changes in lung function persisting as long as six months after the onset of the symptoms were more frequent in patients with more severe forms of the. Persistent kidney disorders were also observed which were not detected during the hospitalization. The most severely ill patients have also achieved worse results in a six-minute walking test. Almost a quarter failed to walk at least 5 minutes [4]. The study also considered the antibody load at the time of maximum infection in 94 patients. Six months later, the level of antibodies against the virus was split to less than half. To our best knowledge the study of Huang et al. (2021) [3] considered the largest cohort of hospitalized patients. However the authors suggested that "It is necessary to have a larger sample to better study these postums and to measure the rate of antibodies against SARS-CoV-2".

Greenhalgh T. et al. (2020) [5] highlighted in an article published in British Medical Journal that the consequences of COVID-19 can be extremely varied. They created an infographic entitled "Long COVID in primary care" (<https://www.bmj.com/content/370/bmj.m3026>) for assessment and initial management of patients with persistent problems after COVID-19. They illustrated the symptoms with lots of drawings in a detailed summary with indications for physicians as well as for patients.

More specifically, evidences on autoimmune diseases (often atypical) arising after the acute phase are multiplying. Reyes Gil M. et al. (2020)[6] from Montefiore Medical Center in New York, have observed, on a hundred patients hospitalized that in 44% the presence of markers of systemic Lupus erythematosus greatly increased in those who were previously positive for these markers. In addition, the presence of Lupus Anticoagulant antibodies was associated with incidence of thrombosis in patients with COVID-19 [6].

Restivo et al., (2020) [7] reported that some patients infected with SARS-CoV-2 later exhibited neurologic symptoms. The authors argued that these symptoms were caused by autoimmune mechanisms. They described 3 cases without previous neurologic or autoimmune disorders (a 64-year-old male, a 68-year-old male and a 71-year old female) who developed diplopia and muscular fatigability some days after having high fever. The chest CT was normal in males while in female, it revealed bilateral interstitial pneumonia. Repetitive stimulation showed less than 60% of the neuromuscular transmission of the facial/ulnar nerve indicating involvement of the postsynaptic neuromuscular junction. Serum AChR antibody levels were elevated in all three patients and the diagnosis of myasthenia gravis was indicated.

Conclusions

Although there are many patients recovered from COVID-19, systematic reports on post-COVID-19 manifestations are yet scarce. The existing ones focus mostly on patients who were dismissed from the hospital, as there exist records of their disease. Many cases that were cured at home and were not subjected to testing are missing from the records. As COVID-19 involves different organs and systems, caution is necessary that multiple and complex symptoms may occur after the symptoms of the primary disease have ceased and that post-COVID-19 rehabilitation is indicated [8].

References

1. Kralj-Iglič V, Gošnak Dahmane R, Griessler Bulc T, et al., From extracellular vesicles to global environment: A cosmopolite SARS-CoV-2 Virus. *Int J Clin Stud Med Case Rep* 2020. 4:1-23. <https://ijclinmedcasereports.com/pdf/IJCMCR-CR-00079.pdf>
2. Cortinovis M, Perico N, Remuzzi G. Long-term follow-up of recovered patients with COVID-19. *Lancet* 2021. 16;397(10270):173-175. doi: 10.1016/S0140-6736(21)00039-8
3. Carfi A, Bernabei R, Landi F, et al. Persistent symptoms in patients after acute COVID-19. *JAMA*, 2020. 324(6):603-605. doi:10.1001/jama.2020.12603
4. Huang C, Huang L, Wang Y, Li X, Ren L, Gu X, Kang L, et al. 6-month consequences of COVID-19 in patients discharged from hospital: a cohort study. *The Lancet* 2021. 397(10270):220-232. doi: 10.1016/S0140-6736(20)32656-8.
5. Greenhalgh T, Knight M, A'Court C, Buxton M, Husain L. Management of post-acute COVID-19 in primary care. *BMJ* 2020; 370 doi: <https://doi.org/10.1136/bmj.m3026>
6. Reyes Gil M, Barouqa M, Szymanski J, et al. Assessment of lupus anticoagulant positivity in patients with coronavirus disease 2019 (COVID-19). *JAMA Netw Open* 2020 3(8):e2017539. doi:10.1001/jamanetworkopen.2020.17539.
7. Restivo DA, Centonze D, Alesina A, Marchese-Ragona R, Myasthenia gravis associated with SARS-CoV-2 infection. *Ann Intern Med* 2020. 73(12):1027-1028. <https://doi.org/10.7326/L20-0845>
8. Romolo A, Kralj-Iglič V, Rehabilitation after COVID-19 : A review of recent experiences. *Physis* 2020. 1: 11-18.

УЧИЩЕ ГORIZОНТИ



Reflection

COVID-19 Health consequences management: proposed health rehabilitation of long-term care for older adults

¹Amon Mojca*, Friderika Kresal

¹Institution of Higher Education Fizioterapevtika, Ljubljana, Slovenia

*amon.mojca@gmail.com

Abstract

Healthcare professionals must work in a balance of sustainable development with a comprehensive way of working that emphasizes a systemic approach. The pandemic situation underscores the need for health promotion in public health. An appropriate integrated health strategy, which includes intensive preventive interventions at all levels of health care, represents an opportunity to reduce health absenteeism and strengthen bio-psycho-social health. The improved uniform health explanation and understanding can contribute to the awareness of the individual and society. Unity of action is achieved through common understanding and action, which can also successfully contribute to limit the expansion of pandemic disease. The purpose of the investigated content is to encourage social development through rehabilitation as a physiotherapeutic long-term support, which will enable and connect long-term conditions for human health, well-being and quality of life. The strategy of the proposal is to unite at least two or three generations and can contribute to maintaining intergenerational understanding, empathy and coexistence. Appropriate targeted development and research-educational activities are needed, which can encourage a development of society that enables the preservation of the living environment and functional independence of older adults. To conclude, the proposal can contribute to the development of future generations in rural areas and rural development.

1. Introduction

Protecting the environment from increasing burdens is the fundamental condition for a sustainable development of society. The sustainable development strategy has three pillars, namely, environmental protection, economic development and social development. The central element of the development of society is human. The health status of society is also closely linked to the potential of environmental, economic and social development.

Sustainable development is the idea of developing a human society based on the preservation of the environment and biodiversity. The concept of sustainable development encompasses several aspects, but above all the possibility of developing each person or society in a way that does not harm others. The oft-cited definition is that sustainable development meets the needs of the current generations without compromising the ability of future generations to meet their own needs [1]. The exceptional global health situation in the COVID-19 (SARS-CoV-2) period 2019-2021 reminds us of the importance of health. The basic factors with which we can influence health are, above all, clean air, food, proper exercise, recreation and the overall bio-psycho-social quality of life.

The aging process is accompanied by an increased risk of functional limitations, disability and handicaps, social isolation and dependence on the help of others. Strengthening health status with increasing longevity is essential and also a decisive factor in maintaining the activities of several generations. The proposed measures are therefore focused on solutions to strengthen the physical capacity of the rural population, strengthen long-term rehabilitation physiotherapy support and intergenerational associations to maintain a physically active lifestyle.

Over the years, the immune system changes and this affects the acquired and innate response of the immune system. Infections, cancers and autoimmune diseases are more common in older adults (over 65 years of age) and many factors are responsible for this phenomenon. Age-related changes and the weakening of the innate and acquired immune systems play the greatest role.

Stable health in old age is not only the result of inflammatory mechanisms, but also the effectiveness of the entire system acquired over a lifetime. For this reason, fragility is also the result of an inflammatory condition. Together with hormonal changes, nutritional deficiencies and physical inactivity, it can lead to an essential element of aging - fragility or sarcopenia. Immunity plays an important role in the regulation of aging mechanisms and the occurrence of age-related diseases [2]. The immune system is associated with the aging of the endocrine, nervous, digestive, cardiovascular, and musculoskeletal systems. New infectious diseases may shape the way of life in the future, as many epidemics and pandemics have done in the past. Controlling this danger depends on understanding how to make the most of the potential of our immune system. A fundamental property of the immune system is that it has control over the whole body. An effective immune system adapts to changes in the environment [3].

The literature indisputably describes in detail the many advantages of physical activity in the period of growth and adolescence, as the movement has an exceptional educational and developmental potential [4].

Health is also a reflection of time and space. The living quality and bio-psycho-social condition of the individual in the home environment are important. We assume that helping older adults usually means an unexpected change in the way of life of the entire living structure or that it is completely focused on the female members of the family.

Dissemination of the conclusions of rehabilitation geriatrics can be a starting point for proposals for bio-psycho-social rehabilitation assistance to older adults.

2. Methods

The purpose of the studied content is to present the importance of promoting the prevention of disease, illness and health discomfort as a form of long-term rehabilitation and the deinstitutionalization of older adults.

2.1 Suggested methods

Many adult individuals may be overwhelmed due to constant activities and sudden involvement in additional nursing or rehabilitation support for older adults. In case of sudden health weakness, movement impairment and incapacity, they take care of elderly relatives without prior education. We assume that the proposed measures of long-term health rehabilitation support may lead to a change that significantly affects the health of the wider society.

2.2 Educational and developmental support of long-term rehabilitation support

To develop an appropriate strategy, it will be necessary to study the field situation, examples of good practices, long-term care options and examples of pilot projects for the formalization of long-term care in Slovenia. Based on the joint assessment, we will examine the obstacles and possibilities of long-term care in terms of the development of new staff, employment opportunities, additional knowledge and, last but not least, intergenerational coexistence.

In the proposal of measures for long-term rehabilitation support, we propose the creation of educational and developmental support for long-term rehabilitation care. Physiotherapists are obliged to contribute to the development of those activities that strengthen and improve physical performance and motor skills and quality of life. In addition, the weakened ability to communicate and cooperate between three different generations is increasingly present in Slovenia. The ability to recognize and express oneself in relationships and empathize with others is also insufficiently developed, which undermines the development of healthy, cooperative and satisfied relationships, which are crucial for living together and well-being.

Such mutual bio-psycho-social expert assistance can contribute to improving the understanding, empathy and cooperation of several generations.

Results

Expected results – the possibilities of formal health rehabilitation care for older adults
We believe that the form of formal long-term health rehabilitation support for older adults can significantly affect the quality of aging of many individuals.

3. Discussion

The exceptional global health situation in the period 2019-2021 [5] reminds us of the importance of maintaining a healthy narrower and wider living environment for health promotion. The basic factors with which we can influence health are, above all, clean air, food and proper exercise or recreation. The basics of clinical physiotherapy exercise emphasize the laws of therapeutically safe exercise [6,7]. The evolution of rehabilitation exercise shifts the boundaries of rehabilitation spaces to the external environment. Fresh air, regardless of weather conditions, with the right equipment, is the optimal choice for physical activity, which can contribute to maintaining bio-psycho-social capacity and quality of life [8]. After all, home is home. Usually, the attachment to the home environment only deepens with age. Changing the living environment is burdensome or even fatal for many.

3.1 Educational and support options for long-term health rehabilitation support

Geriatrics is a demanding medical science due to its multimorbidity. It is right that older adults have the help they really need. The informal long-term care does not allow a professional help that a person would really need. Lower secondary health education can offer certain knowledge and health care options in the form of formal long-term care. Post-vocational additional education would provide additional realistic solutions to the problem. Moreover, the possibilities are promising in the development of special health conditions that individuals could gain through shorter forms of education to provide some non-essential health services. Healthcare requires medical education, but it is not necessarily present or feasible. It is worth considering the possibilities of developing short-term education in terms of maintaining functional support that can be provided by individuals with or without health education to help older adults. The nature of work in this area is not defined and it is necessary to draw clear boundaries between what is medical, clinical, physiotherapeutic, rehabilitation, therapeutic or long-term nursing care at home and to express the individual guidelines. In the future, it is necessary to study the duties and rights and the way of work of individual care.

Implementation options are probably allowed by contract work or a form of additional / supplementary work. It is also important for the field to create minimum needs either for the implementation of nursing or rehabilitation activities at home (home study, standards, equipment) or the need for field work (work at home for older adults). Field analyses and case studies can be the basis for proposals for the measure of “deinstitutionalisation” of older adults and intergenerational participation of young and older adults on farms.

3.2 Promotion of clinical physical activity for all generations

Morbidity prevention also includes the responsibility of maintaining a physically active society [9-13]. The mission of the health professions is to restore, maintain and strengthen the health of the individual. Improving society's health can contribute to efficiency, safety and quality of life. The purpose of the studied content was to present the importance of promoting the prevention of disease, illness and health discomfort as a form of long-term rehabilitation or deinstitutionalization of older adults. The content of the proposal refers to educational and developmental opportunities and activities that highlight physical activity as a central component for maintaining the health of the wider community.

The starting point of the proposal initiates from the legality of clinical exercise, which is a central element of rehabilitation physiotherapy [6,7,12-14]. We believe that the health promotion of physical activity is an exceptional opportunity to develop the intergenerational understanding that conditions the bio-psycho-social health of society and rural development. Historical records describe disease as the result of mystical forces and according to early scientific descriptions disease encompasses environmental factors and living habits in life (Hippocrates, 460-370 BC; Galen, 129-210 AD). Hippocrates emphasized the benefits of physical activity by stating, *"If we can devote an adequate amount of nutrients and physical activity to an individual, not too much and not too little, we will find a safe path to health."* Current epidemiological data suggest that adolescents are already insufficiently physically active[15]. The prevalence of overweight individuals and the presence of obesity is becoming a widespread public health problem [16-18]. The irreversible pathological effects of physical inactivity, especially during development and adolescence, call for the importance of tracking physical activity. The sedentary lifestyle is becoming a widespread health problem, so health promotion also includes measures to prevent the consequences of the sedentary lifestyle of modern society. The scientific conclusions were the basis for health awareness of the wider social environment from kindergartens, schools to young and older adults about the importance of health. The central proposal of measures for the medical rehabilitation of older adults relates to the education of young adults for the preservation of motor abilities and abilities of older adults in the home living environment.

4.3 Intergenerational connection and strengthening of physically active everyday life in the wider environment

Children as well as adults are not immune to the dangers of the modern sedentary lifestyle and the consequences of physical inactivity. Therefore, we emphasize the importance of promoting health promotion as an opportunity for identification and initial encouragement for an active way of life, which directly or indirectly includes a group of older adults. We agree with researchers[19,7,12] that physical activity must be suitable for the individual and consistent with medical and health guidelines.

As part of health promotion, we emphasize the central measure, which includes the importance of physical activity in childhood and adulthood, as it is an important window of opportunity that opens opportunities for greater interest in a physically active lifestyle and the associated lower risk of many diseases. Furthermore, we point out that in many cases there is a need for wider professional cooperation of medical and health professions with experts in the field of sports science in the focused development of integrated strategic programs for health quality and well-being of society. We emphasize the sustainable development of optimal effectiveness of health prevention in the broader context and structure of work to strengthen community health, relieve the health system, prevent health absenteeism or absence from work due to health problems and increase work efficiency. The proposed health rehabilitation of long-term care for older adults can also contribute to new staff development and employment opportunities. Furthermore, if we start from health as a whole, health promotion can connect intergenerationally, ensure empathetic cooperation and sober decisions of young and older adults.

4. Conclusion

The mission of health professions is to restore, maintain and strengthen the health of the individual. Improving society's health can contribute to efficiency, safety and quality of life. The aim of the proposed project is to examine the promotion of health promotion and highlight physical activity as a central component for maintaining the health of the general population. We believe that the proposal of long-term physiotherapeutical care as a form of deinstitutionalization assistance to older adults is an exceptional opportunity to develop intergenerational understanding that conditions the bio-psycho-social health of society and rural development.

Prevention of illness, injury and health discomfort includes the responsibility of maintaining a physically active society. To address the consequences of the COVID-19 health emergency, an increased need for appropriate clinical activity is expected as a rehabilitation of individuals' weakness after infection.

To conclude, we strongly agree with the numerous researchers that suggested physical exercise as a type of therapy to fight the mental and physical consequences of COVID-19 [20].

References

1. Brundtland GH (1987), Brundtland Report (admin.ch). Accessed 12.11.2020. Available from <https://www.who.admin.ch/are/en/home/sustainable-development/international-cooperation/2030agenda/un-milestones-in-sustainable-development/1987--brundtland-report.html>
2. Soo-Jin O, Lee JK, Shin OS, Aging and the Immune System: the Impact of Immunosenescence on Viral Infection, Immunity and Vaccine Immunogenicity. *Immune Netw* 2019, 19(6):e37. DOI: 10.4110/in.2019.19.e37.
3. Nicholson LB, The immune system. *Essays Biochem* 2016, 31;60(3):275-301. DOI: 10.1042/EBC20160017

4. Škof B, Bočanac L, Bratina N, et al. Šport po meri otrok in mladostnikov. Pedagoški, didaktični, psiho-socialni, biološki in zdravstveni vidiki športne vadbe mladih, Fakulteta za šport Univerze v Ljubljani, Inštitut za kineziologijo, 2016, pp. (1-50) (1st Chapter in a book).
5. WHO, 2020. Available from: <https://covid19.who.int/>, Accessed: 16.09.2020)
6. Dean E, et al., 2009. Exercise specialists and the health priorities of the 21st century: A new perspective on knowledge translation for the physical therapist. *Physiotherapy* 16: 3–7. DOI: 10.1080/09593980802668027
7. Dean E, et al., 2019. Health Competency Standards in Physical Therapist Practice. *Phys Ther.* Sep 1;99(9):1242-1254. DOI: 10.1093/ptj/pzz087
8. Pedersen BK, Saltin B, Exercise as medicine—Evidence for prescribing exercise as therapy in 26 different chronic diseases. *Scand J Med Sci Sport* 2015, 25: 1–72. 10.1111/sms.12581 DOI: 10.1111/sms.12581
9. Hubley J, Copeman J, Woodall J, Practical Health Promotion Paperback. 2013, pp. 14-50.
10. World Health Organization, Final draft of the NCD action plan 2013–2020, 2013. Accessed: 10.11.2020, Available from: <http://www.ncdalliance.org/final-draft-global-ncd-actionplan-2013-2020>
11. Porta M, A Dictionary of Epidemiology. 6th ed, New York: Oxford University Press 2014, ISBN 978-0-19-997673-7.
12. Bezner JR, 2015. Promoting health and wellness: implications for physical therapist practice. *Phys Ther.* 95:1433-1444. *Phys Ther.* 2016 Jan;96(1):123. DOI: 10.2522/ptj.20140271
13. Magnusson DM, Eisenhart Gorman MI, Kennedy VK, Davenport TE, 2019. Adopting Population Health Frameworks in Physical Therapist Practice, Research, and Education: The Urgency of Now. *Physical Therapy*, 2019, Volume 99, Issue 8, August, Pages 1039–1047. DOI:10.1093/PTJ/PZZ048
14. Fizioterapija, 2017. Kodeks etike fizioterapevtov. 25(1): 75-8. Available from: <https://www.physio.si/kodeks-etike/>
15. Faigenbaum A, Myer G, Exercise deficit disorder in youth: Play now or pay later. *Curr Sports Med Reports* 2012, 11:196–200. DOI: 10.1249/JSR.0b013e31825da961
16. Nader P, Bradley R, Houts R, McRitchie S, O'Brien M, Moderate to vigorous physical activity from ages 9 to 15 years. *JAMA* 2008, 300:295–305. DOI: 10.1001/jama.300.3.295
17. Belcher B, Berrigan D, Dodd K, Emken A, Chou C, Spruijt-Metz D, Physical activity in US youth: Effect of race/ethnicity, age, gender, and weight status. *Med Sci Sports Exerc* 2010, 42:2211–2221. . DOI: 10.1249/MSS.0b013e3181e1fba9
18. Tudor-Locke C, Bassett DR Jr, How many steps/day are enough? Preliminary pedometer indices for public health. *Sports Med* 2004, 34(1):1-8. DOI: 10.2165/00007256-200434010-00001
19. Kruk J, Physical activity and health, *Asian Pac J Cancer Prev* 2009, 10(5):721-8.
20. Jimenez-Pavon D, Carborell-Baeza A, Physical exercise as a therapy to fight the mental and physical consequences of COVID-19 quarantine: Special focus in older people, *Progress in Cardiovascular Diseases* 2020, 63:386-388. DOI: 10.1016/j.pcad.2020.03.00



Reflection

REGULATION OF GENDER VERIFICATION IN SPORT AND FUTURE SUSTAINABLE DEVELOPMENT

Mustar E^{1,*}, Trofenik D¹

¹ Physiotherapeutics, Ljubljana, Slovenia

*evi.mustar@gmail.com

Abstract

Regulations concerning gender verification in sport is still a controversial topic. For the last 30 years legislators and scientists have been trying different types of testing that could be least discomfiting. The IAAF's (International Association of Athletics Federation) policy requires testosterone levels below 5 nmol/L for continuous period of at least six months (that could be achieved e.g. by use of hormonal contraceptives) which can present bias as regards human rights and ethics. These regulations have hostile impact on female dignity and right to compete in a body they are born in. The following article deals with historical view on gender verification regulation development and classification of athletes with differences in sex development.

Introduction

Gender verification in sport was first implemented in 1900 at the Olympic Games in Paris. Before that time in many cultures, women were prohibited from competing in sport. Women athletes started participating in grass tennis and golf, even though they had actively been involved as participants or supporters by the end of the 20th century [1]. According to the International Olympic Committee (IOC), first full gender-balanced Olympic games took place in Buenos Aires in 2018 (Youth Olympic Games) [2].

1. Barr body chromosomal test

In respect to the eliminated extremely discomforting visual test to verify the gender, where women were exposed nude in front of a group of doctors, the IOC enforced new type of testing, the so-called Barr body chromosomal test, also known as buccal smear [3]. To put it into more simple terms, cells are collected by scraping the cheek with cotton swab. It is a painless procedure and much less embarrassing than physical verification of the gender, which was earlier in practice [4]. The Barr body test was introduced in 1968 during the City Olympic Games in Mexico City and it has been used until 1992. Besides the test results that show only chromosomal state of the individual (XX for female or XY for male) and categorize person as man or woman, it is not practical. Information about chromosomal pictures does not give us details about hormone levels and body sensitivity on hormonal state. Polish sprinter, Ewa Klobukowska was the first woman who failed the test and was disqualified from the competition for having an “extra” chromosome and “internal, man-like characteristics” [5]. Analyses showed that the Barr body test did not take into consideration complexity of sex determination itself. Despite the fact that women have an XY chromosome, they could still have entirely female physique because of the Androgen Insensitive Syndrome (AIS) [6]. AIS was discovered after a sex verification in Maria Jose Martinez Patio at World University Games in Kobe, Japan in 1985. The athlete found out that she lacked a second X chromosome. Spanish Athletic Federation released the results to the press and made her condition public. The discovery devastated the Spanish athlete, who felt embarrassed and humiliated [7]. According to the author, it was documented that spreading the news into the public ruined her personal life [7].

2. Polymerase chain reaction (PCR) test

After 1992, the IAAF adopted a fairer, PCR (Polymerase Chain Reaction) test of the SYR gene. The buccal smears samples were taken by female officials from both side of the mouth of each women competitor with sterile filtered tip and deposited in 100ml of sterile water [21]. During the Summer Olympics in Atlanta, 8 out of 3000 female athletes were tested positive for the Y chromosome, however, they were allowed to compete [3]. Information about the positive athletes were confidential and they never came out in public [6]. The results were given to the team physicians, and in some cases, some further medical research has been

recommended after the Games. Further, researches showed AIS (Androgen insensitivity syndrome) or other syndromes lower production of the testosterone. During Atlanta Summer Olympics, 4 out of 8 athletes had an incomplete while 3 of them had a complete AIS [5].

3. Gender verification test; “suspicious” athletes only

By the year 2000 most of the international sport associations suspended gender verification test. However, the IOC still had the authority to verify the gender if there were any suspicions of determining the gender identity. In 2006 IAAF’s policy on gender verification worked similarly as IOC’s [8]. Gender verification was not mandatory. In a paper written by the IAAF in 2006 called “Medical and Anti-doping Commission” it was stated that “There will be no compulsory, standard or regular gender verification during IAAF sanctioned championships. But, if there is any ‘suspicion’ or if there is a ‘challenge’ then the athlete concerned can be asked to attend a medical evaluation before a panel comprising gynecologist, endocrinologist, psychologist, internal medicine specialist, expert on gender/transgender issues. The medical delegate can do an initial check”. In the same paper IAAF allows certain conditions that have no advantages over the female athletes such as AIS, gonadal dysgenesis or Turner’s syndrome, and examples of conditions that may cause some advantages but are, nevertheless, acceptable. New regulations and policies by the IAAF came into force in 2011, the so-called regulations governing the eligibility of females with hyperandrogenism (the term describes the excessive production of androgen). According to these rules, if an individual is recognized as a female by law, she is able to compete if her androgen level is below the male range or has androgen level within the male range. The androgen resistance is not a condition for exclusion from one’s own gender [9]. These guidelines were challenged by Indian sprinter Dutee Chand. She filed a lawsuit at the Court of Arbitration for Sport (CAS), because she was not able to compete in 2014 Commonwealth Games in Glasgow due to her natural testosterone levels, which were in the male range. She would have been allowed to return to track only if she had lowered her testosterone levels below the male level. In other words, she could have been taking hormone-suppressing drugs or had surgery that would affect body’s testosterone production [10]. CAS gave IAAF 2 years to provide evidence that would show testosterone level in females which would increase their athletic performance [4].

4. Open letter to IAAF criticizing their new regulations

IAAF changed the rules in April 2018 and developed new document Eligibility regulations for The Female Classification – Athletes with Differences of Sex Development [11]. In the same year the United Nation adept for human rights wrote an open letter to the president of IAAF, expressing serious concerns related to the new regulations [12]. Special Procedure of the Human Rights Council criticized IAAF for violation of “human rights norms and standards

including the right to equality and non-discrimination, the right to the highest attainable standard of physical and mental health, the right to physical and bodily integrity and the right to freedom from torture, and other cruel, inhuman or degrading treatments and harmful practices.” [13].

5. IAAF regulations at the european court of human rights

Caster Semenya, the 800 meters runner from South Africa, winner of two gold medals (the World Championship, 2009 and the Olympic Games in London, 2012) filed a lawsuit against the World Athletics at the Court of Arbitration, and also at the Swiss Federal Supreme Court in September 2020 [14]. Since she lost both lawsuits, she disputed IAAF regulations at the European Court of Human Rights [15]. Her lawyer revealed the news to the public on 17 November 2020 [16]. Her lawsuit deals with IAAF’s regulations which do not allow female athletes who suffer from Differences in Sexual Development (DSD) to compete in a race from 400m to 1600m without reducing the testosterone levels below 5 nmol/L for continuous period of at least six months (e.g. by use of hormonal contraceptives) [11]. The final ECHR’s decision is expected to exert an impact on further development of IAAF rules. Eventually, it could even bring the annulment of gender verification in sport.

Female athletes with high blood testosterone levels are basically left with only two decisions – to undergo hormonal treatment or to suspend their sport career. In general, physicians are expected to value the patients’ well-being over exposing them to unnecessary hormonal therapy (which can have a negative impact on a person). Moreover, it is not necessary that athletes with high levels of testosterone have changes in physical composition. The president of WMA (World Medical Association) dr. Leonid Eidelman said that: “They have strong reservation about the ethical validity of these regulations. They are based on weak evidence from a single study, which is currently being widely debated by the scientific community” [17]. According to WMA Declaration of Geneva, the modern equivalent of the Hippocratic Oath, physicians shall take the patient health as their first consideration and provide medical service in full technical and moral independence, even though there are affiliated with some other commercial entities [18].

In addition, it would be interesting to analyze athletes with particularities in sex development and advantages they have upon the other competitors in their gender group. DSD (Disorders of Sex Development) can be classified into several different types of disorders including chromosomal, anatomic or gonadal abnormalities. Those individuals have atypical development of internal and external genital structures [19]. The IAAF decision to control women athletes’ testosterone level in 400m, 800m and 1500m races is based on unverified assumption that higher testosterone level is huge advantage for women. Jurisdiction is discriminatory towards athletes with disorder of androgen insensitivity. Regardless of significantly elevated testosterone it may not be functional and does not necessarily affect body development [20].

It can be interpreted that some individuals are privileged. They can be born with a privilege or can develop it during maturation. For example, some basketball players are being taller than everyone else which is, also, another advantage towards the others.

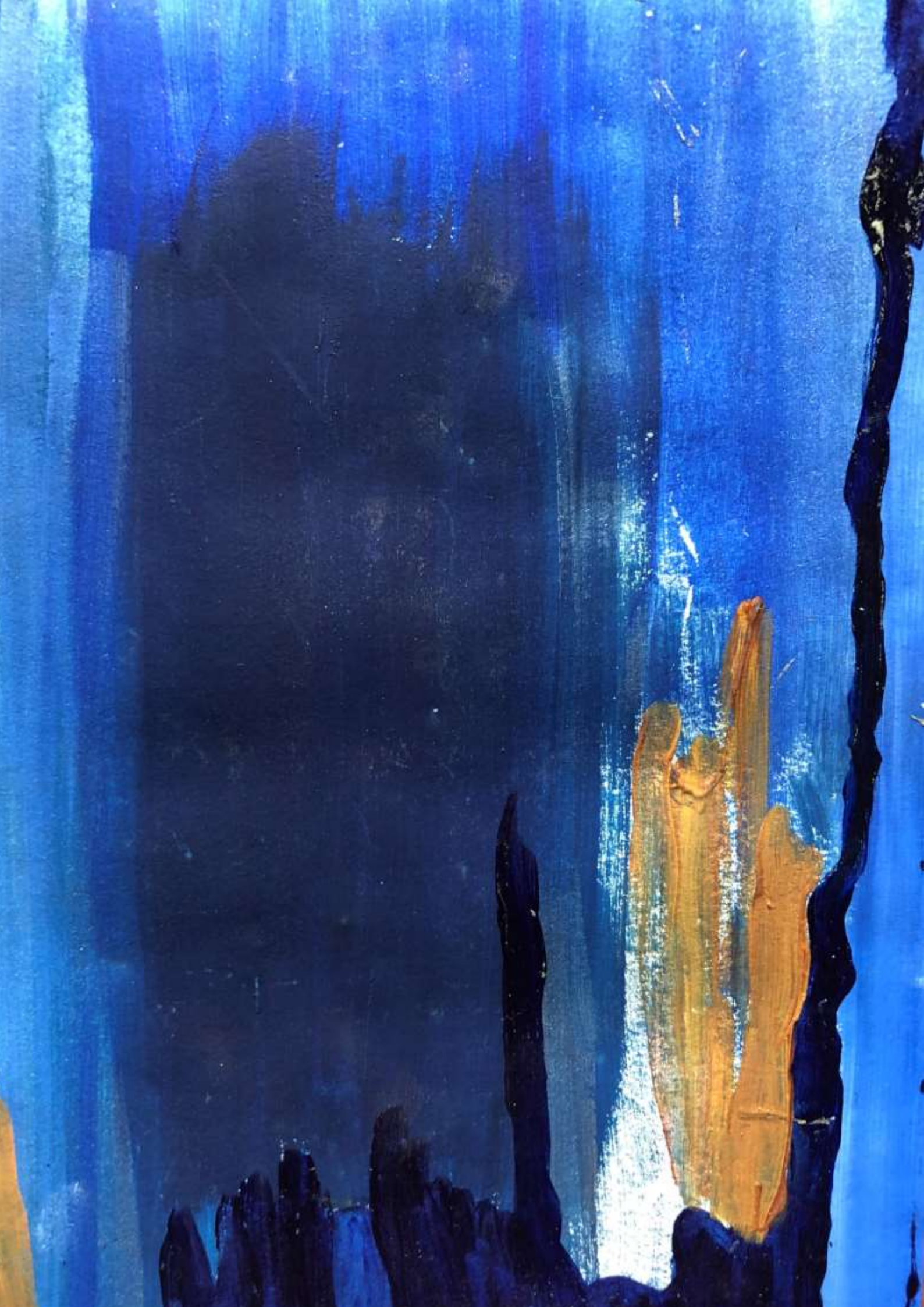
6. Conclusion

After taking everything into consideration, sport institutions are being active in developing fairer and more human regulations in order to determine athlete's gender and eligibility to compete in a competition. Rules are important for sport integrity and the entire sport community and should not be discriminating towards the athletes. However current rules stigmatize women instead of empower them for being different and celebrate their naturally occurring diversity [20]. Total abandonment of eligibility regulations is not a solution. In conclusion, the ECHR's ruling in Caster Semenya's case is a monumental milestone when gender verification is concerned [16].

References

1. Anastasovski, I. The beginnings of the participation of women in sport. 2019. <https://www.sportanddev.org/en/article/news/beginnings-participation-women-sport>
2. Promotion of women in sport through time. (b. d.). Olympic. <https://www.olympic.org/women-in-sport/background>
3. Cooky C and Dworkin SL. (Policing the Boundaries of Sex: A Critical Examination of Gender Verification and the Caster Semenya Controversy. Journal of Sex Research, 2013. 50:2, 103-111.
4. Mohamed S and Dhai A. Global injustice in sport: The Caster Semenya ordeal prejudice, discrimination and racial bias. SAMJ, 2019. Vol. 109, No. 8.
5. Elsas Lj, Ljungqvist AR, Ferguson-Smith MA, Simpson JI, Genel M, Carlson AS, Ferris E, Chapelle A and Ehrhardt AA. (2000). Gender Verification of female athletes. Genetics in Medicine, Vol. 2, No. 4, 249-254.
6. Ritchie R, Reynard J, Lewis T. Intersex and the Olympic Games. Journal of the Royal Society of Medicine, 2008. Vol. 101, No. 8.
7. Transas city. (b. d.). Cross-Training- The History and Future od Transgender and Intersex Athletes. <http://transascity.org/cross-training-the-history-and-future-of-transgender-and-intersex-athletes-3/>
8. International Association of Athletics Federations. (2006). IAAF policy on gender verification. <http://bolandathletics.com/sitefiles/wp-content/uploads/2015/11/IAAF-Gender-Verification-Policy.pdf>
9. World Athletics. (b. d). IAAF to introduce eligibility rules for females with hyperandrogenism. <https://www.worldathletics.org/news/iaaf-news/iaaf-to-introduce-eligibility-rules-for-femal-1>
10. Macur J. (6. 10. 2014). Fighting for the Body She Was Born With. <https://www.nytimes.com/2014/10/07/sports/sprinter-dutee-chand-fights-ban-over-her-testosterone-level.html>
11. International Association of Athletics Federations. (23. 4. 2018). Eligibility regulations for the female classification - athletes with differences of sex development. http://www.femede.es/documentos/IAAF_Eligibility_Regulations_DSD-2018.pdf

12. Sports Integrity Initiative. (24. 9. 2018). UN urges IAAF to withdraw DSD Regulations. <https://www.sportsintegrityinitiative.com/un-urges-iaaf-to-withdraw-dsd-regulations/>
13. Pūras D, Melzer N, Radačić I. (18. 9. 2018). Mandates of the Special Rapporteur on the right of everyone to the enjoyment of the highest attainable standard of physical and mental health; the Special Rapporteur on torture and other cruel, inhuman or degrading treatment or punishment; and the Working Group on the issue of discrimination against women in law and in practice. https://ohchr.org/Documents/Issues/Health/Letter_IAAF_Sept2018.pdf
14. Olympic Channel. (8. 9. 2020). Caster Semenya loses Swiss Supreme Court appeal. <https://www.olympicchannel.com/en/stories/news/detail/caster-semenya-loses-swiss-supreme-court-appeal-cas-defeat/>
15. BBC. (17. 11. 2020). Caster Semenya takes appeal to European Court of Human Rights. <https://www.bbc.com/sport/athletics/54973244>
16. Goh. ZK. Caster Semenya disputing World Athletics regulations at European Court of Human Rights. Olympic Channel 2020 <https://www.olympicchannel.com/en/stories/news/detail/caster-semenya-world-athletics-dsd-regulations-european-court-human-rights/>
17. World Medical Association. (25. 4. 2019). WMA urges physicians not to implement IAAF rules on classifying women athletes. <https://www.wma.net/news-post/wma-urges-physicians-not-to-implement-iaaf-rules-on-classifying-women-athletes/>
18. Human Rights Watch. (4. 12. 2020). They're Chasing US Away from Sport. <https://www.hrw.org/node/377076/printable/print>
19. Feldman Witchel, S. Disorders of Sex Development. Best Practice & Research Clinical Obstetrics & Gynaecology, 2018. Vol. 48.
20. Khattab, A. Marshall, I. Radovick, S. Controversies surrounding female athletes with differences in sexual development. The Journal of Clinical Investigation. 2020. Vol. 130.
21. Serrat, A. Garcia de Herreros, A. Gender verification in sports by PCR amplification of SRY and DYZ1 Y chromosome specific sequences: presence of DYZ1 repeat in female athletes. Sport medicine. 1996. Vol. 30.



Reflection

Exams at Socratic lectures in the time of COVID-19

Veronika Kralj-Iglič¹

¹University of Ljubljana, Faculty of Health Sciences, Laboratory of Clinical Biophysics, Ljubljana, Slovenia

*veronika.kralj-iglic@fe.uni-lj.si

Abstract

Development of communication tools has implied changes of the university teaching and learning process. Scholars (teachers and students) have exerted resistance to changes, however, necessity of faster adjustment to lockdown due to COVID-19 has accelerated exploration of possibilities of use of internet and social interactions in problem solving. From the initiation in 2008, it was our intention to use modern communication tools and social interactions to their full extent within a course Biomechanics of hip at the Faculty of Medicine, University of Ljubljana. Socratic lectures were introduced into this course as a way of expanded examination. Here we report on performing the examination at the course Biomechanics of joints in academic year 2020/2021. Students have used internet and social interactions to their advantage and produced quality answers to emerging questions. In conclusion, including internet and social interactions hints at a next generation teaching process. Adjustment to new technologies and connections seems inevitable.

1. Examination as part of the teaching process

Exams have been shaped in the learning process to provide a milestone of proof that the student has reached a certain level of maturity in the subject. Exams may feel stressful, but success after passing the exam is encouraging (**Figure 1**). A good part of the examination is that it promotes learning and presents a possibility that the student will become subjected to the matter. Although the first objective of examination is of importance to satisfy the social system in a wide sense (to provide justification that the person is able to perform certain skills), the second objective seems even more important because it will recruit individuals with interest in the subject. It is only them who could in the future create new knowledge. Examination should therefore be designed in such way to maximize the inherent potential of the students.



Figure 1. Student at exam usually feels stressed (left), but passing the exam improves self-esteem which is favorable (right).

The subject »Biomechanics of hip« was initially designed by two chairs and one institute of the Faculty of Medicine, as an elective subject for students from 2.nd to 6.th year of study of general medicine. It was worth 5 ECTS which is rather considerable. In the first years there were no applicants. However, in 2008, 14 students have chosen the course and since then, the interest has been keeping the level over 30 students. We have designed the subject by aiming that the students will learn the HIPSTRESS method for determination of biomechanical parameters of the hip and possibly contribute to its further development. The method has been developed by the students of University of Ljubljana (the author included) and colleagues of University Medical Centre Ljubljana, from 1985 on. Although personal experience indicates that good feeling after success at the exam outweighs stress at it [1], it was our opinion that being afraid of not passing the exam does not help students to develop a positive attitude towards the subject [2,3]. Therefore we

focused more on the learning part hinting at the possibility that the students will find the subject interesting. We tried to achieve positive effects of the examination with minimally stressing the students.

The exam was designed in a way to enable recruitment of positive feelings in forming a social network for problem solving. Internet and other technical platforms (mobile phones etc.) provided excellent tools for this purpose. Instead of banning mobile phones and social networks from the examination process as cheating tools, we have encouraged their use and therefore eradicated cheating from examination to a great extent.

2. Socratic lectures as an exam

Socratic lectures were intended to present to the students excellent scientists who would talk about their own contributions to the world science. Students should consider the work of the scientists and create a dialogue at the lectures. Supporting the lecturers with their interest was the main role of the students. The foreign scientists were invited to Ljubljana within ongoing scientific collaboration and have donated their lectures to the students. Also domestic scientists donated lectures. A minisymposium was created on informal basis. In particular, because there was no funding for these teaching activities, this symposium was called Socratic lectures. The students could feel that the lecturers focused on the subject of their dedication as well as on the general idea that transmission of knowledge to the youth is essential, and have responded with equal excellence. The idea was to link examination with these positive effects. In examination, students should reconsider emergent questions and try to solve actual problems. The lecturers were available to help them find the best answers to the questions posed. At the same time, students had a possibility to devote a considerable part of the day to the problems addressed in the course.

This design of the subject proved rewarding as the method HIPSTRESS [4] has been developing to meet the needs of the students. Some students have been awarded Prešeren awards for students for the work that initiated with the subject of Biomechanics of hip and later Biomechanics of joints. Some students have been coauthors of papers published in journals with impact factor. As there was an increasing interest to publish student work, we decided to make Socratic lectures formal and enable publication of excellent student work. This was recently supported by the activities of postgraduate students as well as by scientific work of teachers of University of Ljubljana and their partners abroad, in the shape of Socratic symposium that took place a day before the lectures. In 2019, the first Proceeding of the Socratic Lectures was published. The course Biomechanics of joints was this year moved to the winter semester, therefore in 2020, the Socratic lectures took part twice.

3. Exam questions in Socratic Lectures 2020/2021

Due to the lockdown, the Socratic lectures with the exam took place online (through the Zoom platform). We were therefore unlimited as regards the travel expenses and could invite the best experts in the world. The lectures were donated by prof. Leonid Margolis, National Institute of Health, Bethesda, U.S.A., dr. Gabriella Pocsfalvi, National Research Council of Italy, Naples, Italy, Prof. Duško Spasovski, Institute of Orthopaedy, Clinics Banjica, Belgrade, Serbia, Dr. Vesna Spasovski, Institute of Molecular Biology, Belgrade, Serbia and Prof. Bojana Beović from University Medical Centre Ljubljana, Slovenia. Prof. Margolis and dr. Pocsfalvi are experts in extracellular vesicles and viruses, which was of special interest because of COVID-19, colleagues from Serbia have implemented the stem cell therapy into healing of degeneration of joints in clinical practice and prof. Beović is the Head of the COVID-19 Counseling Group at the Government of Republic Slovenia. The questions were from the subjects of their lectures as well as from the lectures that took place during the course. There were 10 questions at the exam:

1. Explain what you mean by the following terms: Extracellular vesicles; Viruses.
2. What are the common properties of viruses and extracellular vesicles?
3. Can a virus infection affect joint function? Explain the answer.
4. How can we distinguish viruses from extracellular vesicles in samples?
5. Are viruses more stable than extracellular vesicles in ultracentrifugation? Explain the answer.
6. What is the order of magnitude of the number of protein species in the membrane of extracellular vesicles?
7. Indicate at least one mechanism through which extracellular vesicles could treat joint disease. Is it introduced into clinical practice? If so, give an example.
8. How do extracellular vesicles from stem cells differ from extracellular vesicles of differentiated cells?
9. How can we distinguish extracellular vesicles from stem cells from extracellular vesicles from differentiated cells in samples?
10. Do extracellular vesicles and viruses also bud from microorganisms? Explain the answer.
11. What are the strengths and weaknesses of COVID-19 control in Slovenia?
12. How can you explain silent hypoxia with your knowledge of pathophysiology?

Students have formed their own forum to discuss the issues. They used Chat in the Zoom platform to pose questions to the lecturers. Also they posed questions directly to the lecturers who provided answers from their experiences and their opinions. Students have decided to formulate answers jointly. Below we show as an example the answer to the question no. 4: How can we distinguish viruses from extracellular vesicles in samples?

Students answered:

“Separation of viruses and extracellular vesicles (EVs) is a complex process that cannot be performed to 100% with current technology. The biggest challenge is posed by viruses whose size and density are similar to the size and density of extracellular vesicles (50-100nm and 1.13-1.18 g/L)(1). According to these parameters, the viruses most similar to EVs are from the family of Retroviruses (mostly about 100 nm in size and 1.15-1.18 g/L in density). Viruses (in the case of HIV research) are thought to migrate faster in the gradient fluid, also expressing the p24 protein on the surface while acetylcholinesterase and CD45 can be found on extracellular vesicles. Although acetylcholinesterase and CD45 are not expressed on virions, it is not known whether they are expressed on all extracellular vesicles (1),(2). Only non-encapsulated viruses can be distinguished from extracellular vesicles with great certainty, since neutralizing antibodies bind to the viruses. The same technique cannot be used in the case of encapsulated viruses, as their proteins can also be expressed on the surface of extracellular vesicles. Thus, accurate differentiation between viruses and extracellular vesicles is practically impossible. Differentiation would be possible in the future using new discoveries in the field of flow cytometry, which allows counting and description of particles of the order of 550-200m, but the technique needs to be further improved (1,2). The problem is the very definition of what is a virus and what is an extracellular vesicle that may have viral proteins (99% of HIV in an infected person are not infectious). Precisely because of this, we can reliably distinguish only e.g. vesicles that come from healthy cells and vesicles (viruses, including defective ones) that derive from infected cells and have viral proteins.

1. Nolte-t Hoen E, Cremer T, Gallo RC, Margolis LB. Extracellular vesicles and viruses: Are they close relatives? Proc Natl Acad Sci U S A. 2016; 113 (33): 9155-61.<https://pubmed.ncbi.nlm.nih.gov/27432966/>

2. Cantin R, Diou J, Bélanger D, Tremblay AM, Gilbert C. Discrimination between exosomes and HIV-1: purification of both vesicles from cell-free supernatants. J Immunol Methods. 2008 Sep 30; 338.”

As there is no decisive answer to the question that students could learn and reproduce, they were challenged with taking a standpoint. It can be seen from the answer that they were able to do this and express their standpoint in such way to participate in a scientific discourse. Also they used citations and presented the references.

New ways of teaching and new tools present challenges in the teaching process. With data easily available reproducing facts in great details could be replaced by consideration of emergent problems which are not yet well understood.

Also, new problems emerge. Allowing formation of the social network in creating the answers increases the quality of the answers to such extent that the pieces of evidence can be presented for publication, especially if the students involve their friends and relatives who are experts on the issues. A question can then be posed who is the author of possible deliverables of these activities? Should students be stating the disclosure and conflict of interest on the examination form?

Conclusions

Online university teaching challenges existing methods of examination. It can be expected that new minimally frustrating methods will be developed which will enable better motivation, increase quality of answers and promote scientific work of students and teachers.

Acknowledgements

Authors acknowledge support of EU Commission H2020, grant Ves4us 80331 and ARRS, grant P3-0388.

References

1. Zajenkowska A, Zajenkowski M, Jankowski, KS, The relationship between mood experienced during an exam, proneness to frustration and neuroticism. *Learn Ind Diff* 2015, 37: 237-240, <http://doi: 10.1016/j.lindif.2014.11.014>
2. Liu S, An Investigation into the Emotional Barriers of College Students in English Learning. In: *International symposium on engineering technology, education and management (ISETEM 2014)*, 2014: 587-597.
3. Artino AR, Hemmer PA, Durning SJ, Using self-regulated learning theory to understand the beliefs, emotions, and behaviors of struggling medical students, *Acad Med* 2011, 86: S36-S39, <http://doi: 10.1097/ACM.0b013e31822a603d>
4. Kralj-Iglič V, Understanding Hip Biomechanics: From simple equilibrium to personalized HIPSTRESS method, In: *Developmental Diseases of the Hip* (Spasovski D, ed.), InTech, 2017, <http://doi: 10.5772/66753>



Reflection

Fyodor Mikhailovich Dostoevsky and his relationship with music

¹ Prelovšek, A*

*anita.prelovsek@gmail.com

Abstract

This article describes the musical world of the great Russian writer, the bicentenary of whose birth is celebrated this year. Music played an important part in his life, and in his free time he spent much time attending concerts and operas. During the period of his forced labour in Siberia he made a collection of a number of folk songs, and his musical bent was also reflected in his literary work. The last part of the article talks of Dostoevsky's descendants' relationship with music and some of the influence his works had on later musical production.



1. Introduction

Fyodor Mikhailovich Dostoevsky, born in Moscow on 11 November 1821, is, in the opinion of the contemporary Russian writer Dmitry Bykov [1], »the most Western of the Russian writers« and therefore the most popular in Europe and America. A. Gozenpud, the author of the monography *Dostoevsky i muzyka*, says that »Dostoevsky loved and understood music and felt deeply about it« [2]. The same author adds that »Dostoevsky's literary art was closely tied to music« [2], his works frequently containing quotations from tunes he had heard in the concerts, folk songs or Russian romances he knew, but also reflecting the effect which the musical experiences and impressions of great artists had had on him. As well as literature, theatre, music and musicians; Dostoevsky also loved painting; he enjoyed visiting galleries and was equally inspired by painting.

2. Music in Dostoevsky's life and literary work

Dostoevsky considered music as a way of expressing a man's inner state and uses it to describe the emotional condition of his heroes. In his story *Another Man's Wife or The Husband under the Bed*, he articulated this statement as follows: »It is maintained that what is good in music is that musical impressions can be made to fit any mood. The man who rejoices finds joy in its strains, while he who grieves finds sorrow in it.« [3]. Further, he describes with sounds (»a tempest«) the distraction and jealousy of the hero Ivan Andreyitch: »a regular tempest was howling in Ivan Andreyitch's ears« [3].

His novel *The Insulted and Injured* includes a passage in which the heroine Katia compares her feelings to those in Beethoven's third piano concerto [4]. For Dostoevsky, Beethoven's music was all about love: in 1975 he wrote to his wife Anna Grigoryevna: »in Beethoven, there is everywhere passion and love. This is the poet of love, happiness and love's torments« [2]. Dostoevsky often connects singing with happiness. He wrote in *White Nights*: »I walked along singing, for when I am happy I am always humming to myself like every happy man who has no friend or acquaintance with whom to share his joy.« [5].

In her memoirs, Dostoevsky's daughter recalls that when he was in a good mood, the writer would sing to himself Varlamov's romance 'Na zare ty ee ne budi' ('Don't wake her up at sunrise')¹ [2]. He told his later wife that at the time when his death penalty was cancelled at the last minute before its execution and commuted to forced labour in Siberia, Dostoevsky walked around his cell in the Peter and Paul Fortress in St. Petersburg and was »singing, loudly singing, because I was so happy for the life given to me« [2].

3. Dostoevsky and Russian folk music

In his early childhood, Dostoevsky had an opportunity to hear folk songs and see folk traditions during the festivities that accompanied traditional holiday days or at fairs. Later in

¹ A Russian romance song by Aleksandr Varlamov, words by Afanasy Fet, written in 1842.

his life, when he was exiled to the Siberian town of Omsk (from 1849 to 1853), he was collecting the folklore of the Russian nation, such as texts of songs, funny stories and expressions that arrested people were using in their everyday language [2]. In *The House of the Dead* he mentioned that singing songs in the forced labour camp imbued the inmates with a sense of optimism and consolation. Some of them would sing accompanying themselves on balalaikas and a small choir was also formed. As Dostoevsky writes, some of those songs were laments but there were also songs with a humorous text [2]. In Chapter XI of the first part of the novel quoted above, Dostoevsky describes the preparations for the performance of the spectacle with music that was to be put on by the inmates. In that little improvised orchestra, about eight instruments would play dance music.

4. Dostoevsky at concerts and operas in St. Petersburg

Dostoevsky was a regular visitor to concert halls; he also loved opera and frequented the salons of St. Petersburg's aristocracy, where music was regularly performed,² but music was often present also at the meetings of the Petrashevsky Circle.³ One of the strongest musical impressions in Dostoevsky's life was his meeting with the composer Mikhail Glinka. They met at an evening organized by the Palm-Durov Circle⁴ in 1849. On this occasion, Glinka was supposed to be playing on the piano his romance 'K ney', excerpts from his opera 'Ruslan and Ludmila', his 'Kamarinskaya' and pieces by Gluck and Chopin [2]. Later in his literary work, Dostoevsky remembered Glinka: 'Kamarinskaya' is mentioned in *The House of the Dead*,⁵ while many years later, Glinka's romance 'K ney' is sung by a hero in a short story *The Eternal Husband*.

All the musical impressions which left their mark on Dostoevsky (but before the meeting with Glinka in the same year) were concentrated in his most »musical« novel, *Netochka Nezvanova*, published in 1849. The characters in this novel are a failed hero, the violinist

² In this context, the house of Prince V. Odoevsky, a writer, musician and one of the first Russian musicologists, was an important musical venue for Dostoevsky [2].

In the 1830s and 1840s, one of the centres of musical life in St. Petersburg, and one where Dostoevsky was also present, was the salon of Mikhail Vielgorsky [2]. Wikipedia [6] states that Vielgorsky, a diplomat, composer and amateur musician, was a great admirer of Beethoven and hosted at his home all the most famous Russian and foreign musicians of the time, such as Berlioz, Liszt, Rubinstein, Viardo and Glinka.

³ [7] The members of this intellectual circle, including Dostoevsky, were in 1849 condemned to death. Many of them – also Dostoevsky – were condemned only because they had disseminated the text of Belinsky's letter to Gogol.

⁴ [7] An intellectual group, a branch of the Petrashevsky Circle, from which it had become independent.

⁵ 'Kamarinskaya' is likewise mentioned in the novel *The Village of Stepanchikovo* but as a traditional Russian folk dance, not the one of Glinka.

Efimov, and his opposite, a brilliant violin player named »S.«. According to Gozenpud (1971) [2], Dostoevsky got the inspiration for this talented musician from concerts given by the leading musicians of the time which he had the opportunity to listen to, such as the pianist Franz Liszt, the Norwegian violin virtuoso Ole Bull and especially Heinrich Wilhelm Ernst - a Moravian-Jewish violinist, an outstanding virtuoso and Paganini's successor [2]. Dostoevsky was also greatly impressed by a concert in which Hector Berlioz conducted his 'Symphonie dramatique Romeo and Juliet' [2]. Concerts by internationally acclaimed musicians at that time were a real sensation: »The whole musical world of St. Petersburg was astir. Singers, actors, poets, artists, musical people, and even those who were not at all musical but with modest pride declared that they did not know one note from another, rushed with eager enthusiasm to buy tickets. The hall could not seat a tenth of the enthusiasts who were able to pay twenty-five roubles for a ticket; but the European fame of S., his old age crowned with laurels, the unflagging freshness of his talent [...] all produced an effect.« [8].

In 1846, during the period in which Dostoevsky was working on *Netochka Nezvanova*, he wrote to his brother Mikhail about his passion for the opera: »After seven p.m. I am going to the Italian opera, in the gallery, to listen to our incomparable singers.« [2]. The monography about Dostoevsky and music states that the operas Dostoevsky saw in the 1840s included 'Askold's Grave', an opera, very popular at the time, by the romantic Russian composer Alexei Verstovsky, Glinka's 'Ivan Susanin' (or 'A Life for the Tsar') and 'Ruslan and Ludmila'. This opera was a particular favourite of Dostoevsky's throughout his life and he also wanted his children to appreciate this work of art [2]. Among the operas of foreign composers, he saw and much appreciated 'Robert le diable' by Giacomo Meyerbeer and Rossini's 'The Barber of Seville'. In Meyerbeer's opera he was able to admire one of the most famous ballet dancers of the romantic era, Marie Taglioni, while in Rossini, he could hear the famous singer Pauline Viardot (the younger sister of one of the most adored opera singers of her time, Maria Malibran). In a short story he mentions Meyerbeer's cemetery scene in which he saw Marie Taglioni. In the same book, he also mentions Rosina's aria from Rossini.

As described by A. Gozenpud [2] with reference to Italian opera in St. Petersburg in the 1840s, there were two opposing ways of musical interpretation which divided the public into two parties. The first one preferred a more dramatic, expressive musical interpretation while the second one admired pure virtuosity.

The representative of the first approach was a dramatic soprano, Teresa De Giuli Borsi, and that of the second a coloratura soprano, Erminia Frezzolini. Dostoevsky favoured the supporters of De Giuli Borsi [2] and he ironically described the relationship between the two groups of opera enthusiasts and the general atmosphere in the opera theatre in that time in his story *Another Man's Wife or The Husband under the Bed*: »The following evening there was a performance of some sort at the Italian opera. [...] It was known for a positive fact, anyway, that Ivan Andreyitch used to like taking a nap for an hour or two at the Italian opera; he even declared on several occasions how sweet and pleasant it was. "Why, the prima

onna,” he used to say to his friends, “mews a lullaby to you like a little white kitten.” [...] It must be observed that there were at that time two parties, each supporting the superior claims of its favourite prima donna. They were called the -sists and the -nists. Both parties were so devoted to music that the conductors actually began to be apprehensive of some startling manifestation of the passion for the good and the beautiful embodied in the two prima donnas.« [3].

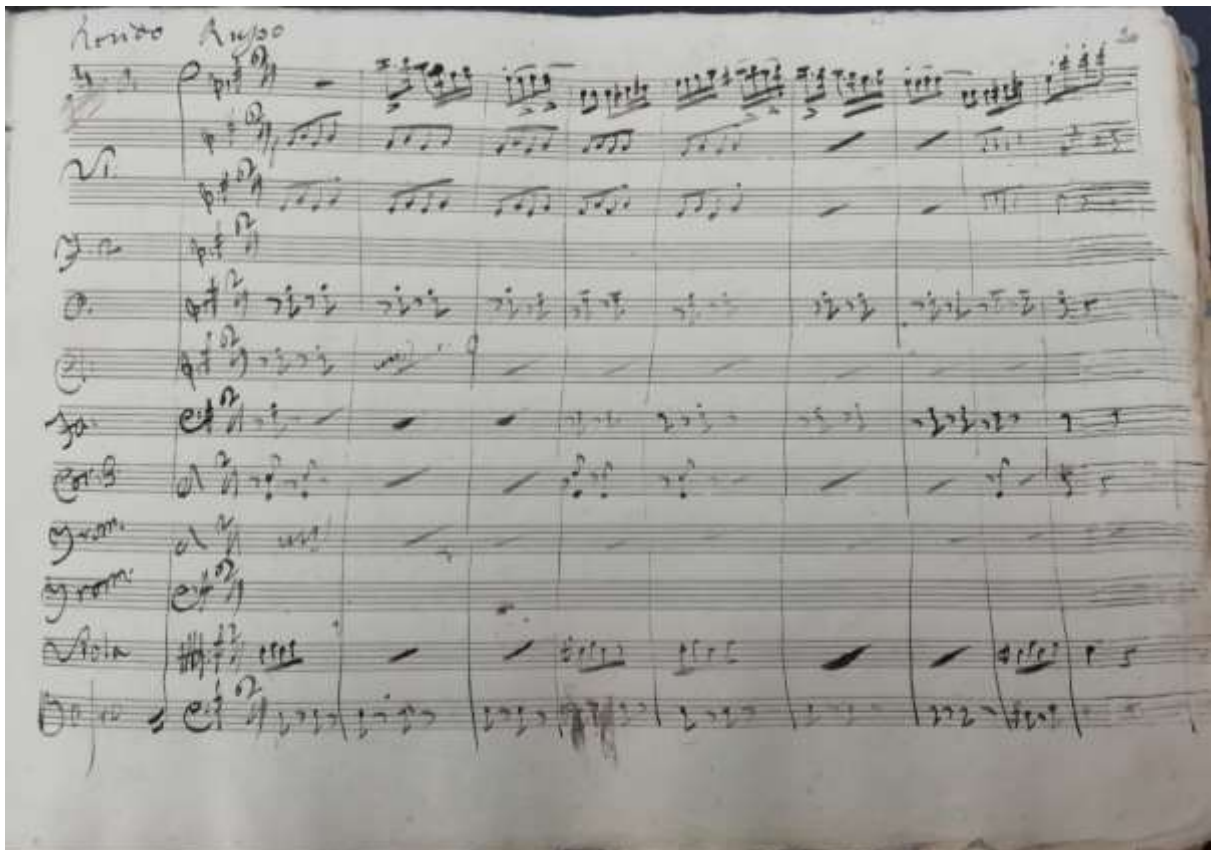


Figure 1. An excerpt (first page of 'Rondo russo') of the manuscript of Mercadante's 'Flute concerto in E minor', kept in the library of the Neapolitan Conservatory of music (photo: Anita Prelovšek).

In St. Petersburg in the 1830s and 1840s, theatrical programmes included many operas by Saverio Mercadante, an Italian composer of the Neapolitan school. Dostoevsky thought highly of his work, as can be concluded from the words he put into the mouth of his hero in The Village of Stepanchikovo. To demonstrate his wide general culture, his hero cites the names of important people who came to mind at that moment, so he puts Mercadante near to Machiavelli: »[...] perhaps Macchiavelli himself or some Mercadante was sitting before him and only to blame for being poor and nondescript...« [8]. Mercadante was a prolific composer of operas, writing more than sixty of them, but he is nowadays mainly appreciated by flute players because of his 'Concerto in E minor' (**Figure 1**). Written in 1819, when the

composer was twenty-four years old, it is faintly redolent of Russia, the last movement even being called 'Rondo russo', which also testifies to the protracted influence that Italy had on Russian music⁶.

5. Dostoevsky and music after the exile in Siberia

After ten years of exile in Siberia,⁶ he finally came back to live in St. Petersburg as a free citizen. So from the 1860s, Dostoevsky's musical impressions were again varied. He attended concerts and went to Italian and Russian operas; he went to concerts given by Anton Rubinstein and sometimes they performed at the same cultural evenings [2], Rubinstein as a pianist and Dostoevsky as a reader of literary works, in which he was known to excel. The circle of the writer's musical acquaintances was growing. As editor of the literary magazines *Vremya* and *Epoch*, he collaborated among others with the music critic and composer Alexander Serov.⁷

Music was present in Dostoevsky's home: his second wife, Anna Grigoryevna, played the piano and his library contained Mendelssohn's 'Wedding March' and Rossini's 'Stabat Mater' [2].

During his journeys abroad,⁸ Dostoevsky continued going to concerts. He couldn't afford expensive tickets and in opera-houses he had to take the cheapest, standing places. Where possible, as in Dresden and Bad Ems, he was always happy to seize the opportunity to listen to the free concerts given by symphony orchestras and brass bands in parks. The repertoire of such concerts included overtures (Mozart, Beethoven or Boieldieu,⁹ for instance) or single movements from symphonies, marches, dance music and potpourris of famous opera themes (Anna Grigoryevna mentions, among others, a potpourri on themes of Franz von Suppé [12]. Dostoevsky didn't like all the music that was being performed there. In one letter from 1875 he complained about the musical programme in Bad Ems: »They rarely play something interesting, everything is some kind of potpourri or German marches, some Strauss, Offenbach [...]« [2]. Anna Grigoryevna said that »he liked Mozart, Beethoven's 'Fidelio' and Mendelssohn's 'Wedding March', but couldn't stand Richard Wagner's music.« [12].

⁶ The first four years he spent as a prisoner in a forced labour camp in Omsk without being allowed to write and read. From 1854 he worked as a soldier, when, thanks to some influential protectors, he recovered the right to attend local intellectual circles, and later he was allowed to publish his work again.

⁷ A. Serov was known especially for his operas, which were quite successful at the time. Dostoevsky was present at the premieres of Serov's operas 'Judith' and 'Rogneda' [2].

⁸ During his first journey abroad in 1862, he visited Berlin, Dresden, Lucerne, Wiesbaden, Baden-Baden, Cologne, Paris, London, Düsseldorf, Geneva, Genoa, Livorno, Florence, Milan, Venice and Vienna. From 1867 to 1871, immediately after their marriage, Dostoevsky and his wife Anna Grigoryevna spent time in Dresden, Baden-Baden, Geneva, Vevey and Florence [11].

⁹ François Adrien Boieldieu was a French composer of operas. The overture to his comic opera 'The White Lady' was often played at concerts and Dostoevsky particularly liked it because of its attractive romantic melodies and the fact that the libretto is based on a novel by his beloved Sir Walter Scott.

His favourite composers were Mozart and Beethoven. According to his diaries, another piece he particularly loved was Rossini's 'Stabat Mater' [2].

6. Dostoevsky's heritage and music today

Among contemporary authors, Haruki Murakami, a great Japanese admirer of Dostoevsky's work who also sometimes quotes Dostoevsky in his novels, such as his reference to *The Brothers Karamazov* in the novel *18Q4*, frequently cites music of different genres, especially classical music and jazz. Music in Murakami's work is used to describe the inner state of his heroes, being related to their reminiscences, or sometimes his heroes just enjoy listening to it or it is in some way relevant to their life.

7. Dostoevsky's descendants and music

Dostoevsky's nephews Maria and Fyodor were both good pianists who studied with Anton and Nikolai Rubinstein. His niece Maria Ivanova graduated from the Moscow Conservatory in the class of N. Rubinstein [2].

A love of music has also been inherited by those of Dostoevsky's descendants who are living today. The son of a great-grandson of Fyodor Mikhailovich, Aleksei Dmitrievich Dostoevsky works for the Monastery of Valaam as a captain of the boats and boat-driver. In his free time he is also a musician, playing bass-guitar in a folk group. In an interview he gave in 2018, he said that it was thanks to this hobby that he met his wife, Natalia, who is a flautist. Their children are also musicians. Their elder daughter Anna is, as her father said in the interview, very artistic and plays the flute like her mother. Their second daughter, Vera, is studying the tamboura at the Rimsky-Korsakov musical institute and at the time of the interview was planning to enrol at the musical university. The youngest daughter, Masha, plays the cello, while their son Fyodor had taken up percussion in a music school. In 2018, daughter Vera gave a concert there on the occasion of its annual conference devoted to research into Dostoevsky's works¹⁰ [14].

8. Influence of Dostoevsky's work on music

The most famous music inspiration that Dostoevsky's novels provided for composers resulted in operas: Sergei Prokofiev adapted Dostoevsky's novel *The Gambler* [15] for the libretto of his opera of the same name, written between 1915 and 1917 and premiered in 1929.

The Czech composer Leoš Janáček adapted Dostoevsky's *The House of the Dead* for the libretto of his last opera *The House of the Dead*, [16] premiered in 1930.

There are now more recent musical adaptations of Dostoevsky's novels. For instance, 2016,

¹⁰ [13] This conference is taking place in Staraya Russa, which is home to a Dostoevsky museum. His wife Anna Grigoryevna recalled the winter of 1874-75 as being one of her most cherished memories. Dostoevsky was in good spirits and always cheerful; in the evenings he would partner her and the children in various different dances. He was particularly fond of the mazurka, which he danced enthusiastically »like a passionate Pole« [12].

the year of the 150th anniversary of the publication of Crime and Punishment, was marked by the premiere of a rock-opera of the same name by a Russian composer of mostly film music, Eduard Artemyev, [17] and the occasion of the writer's jubilee in 2021 is likely to see some new settings of his work to music.

References

1. Вуков, Д. »Открытый урок с Дмитрием Быковым. "Преступление и наказание" - странный русский детектив.« (»An open lecture with Dmitry Bykov. "Crime and Punishment" – a strange Russian detective novel.« Internet source: <https://www.youtube.com/watch?v=kxwcA9NAEcY> Accessed on 7 January 2021.
2. Gozenpud, A. Dostoevsky i muzyka. Leningrad: Muzyka, 1971.
3. Dostoevsky, F. Another Man's Wife or The Husband under the Bed. Adelaide: The University of Adelaide Library, 2016. Internet source: <https://www.holybooks.com/wp-content/uploads/Another-Mans-Wife.pdf> Accessed on 10 January 2021.
4. Dostoevsky, F. Ponižani in razžaljeni. Translation of Borut Kraševac. Ljubljana: Mladinska knjiga, 2017.
5. Dostoevsky, F. Translation by Constance Garnett. White Nights and Other Stories from Fyodor Dostoevsky. New York: The Macmillan Company, 1918. Internet source: <https://www.holybooks.com/wp-content/uploads/White-Nights-And-Other-Stories.pdf> Accessed on 9 January 2021.
6. »Vielgorsky, Mikhail« Wikipedia. Internet source: https://en.wikipedia.org/wiki/Mikhail_Vielgorsky Accessed on 11 January 2021.
7. »Petrashevsky Circle«. Wikipedia. Internet source: https://en.wikipedia.org/wiki/Petrashevsky_Circle Accessed on 12 January 2021.
8. Dostoevsky, F. Translation by Constance Garnett. Netochka Nezvanova. London: Heinemann, 1912. Internet source: <https://archive.org/details/novelsoffyodordo12dost/page/244/mode/2up> Accessed on 12 January 2021.
9. Dostoevsky, F. Translation by Constance Garnett. The Village of Stepanchikovo. (The Friend of the Family). London: Heinemann, 1912. Internet source: <https://archive.org/details/novelsoffyodordo12dost/page/106/mode/2up> Accessed on 18 January 2021.
10. Ivashkin, A. »Italiani in Russia: Presenza fisica e influenza virtuale sulla musica.« in: *Rinascimento e antirinascimento, Gabinetto scientifico letterario G. P. Vieusseux. Studi*, vol. 22: 209-218. Firenze: Casa editrice Leo S. Olschki, 2012.
11. Dostoevsky, F. Editor: Prina, S. Le notti bianche. La cronaca di Pietroburgo. Milano: Feltrinelli, 2018.
12. Dostoevskaya, A. Življenje z genijem (Spomini). Kranj: Zelolepo, 2007.
13. »Staraya Russa. Wikipedia. Internet source: «https://en.wikipedia.org/wiki/Staraya_Russa Accessed on 12 January 2021.
14. Kotov, V. and Pogodina-Kuzmina, O. »Как живут потомки Достоевского.« Internet source: <https://www.sobaka.ru/omsk/city/society/76489> August, 2018. Accessed on 12 November 2020.
15. »The Gambler.« Wikipedia. Internet source: [https://en.wikipedia.org/wiki/The_Gambler_\(Prokofiev\)](https://en.wikipedia.org/wiki/The_Gambler_(Prokofiev)) Accessed on 7 January 2021.

16. »From the House of the Dead.« Wikipedia. Internet source:
https://en.wikipedia.org/wiki/From_the_House_of_the_Dead Accessed on 7 January 2021.
17. Artemyev, E. »Ария из рок-оперы Эдуарда Артемьева "Преступление и наказание".«
(»Aria from the rock-opera »Crime and Punishment.«) Internet source:
<https://www.youtube.com/watch?v=MKJn5XX4SKk> Accessed on 7 January 2021





A GREEN WALL SYSTEM FOR LAUNDRY GREYWATER TREATMENT

Nadine Antenen, Katjuša Mežek, Ranka Junge

¹Zürich University of Applied Sciences, Wädenswil, Switzerland

Contact: ranka.junge@zhaw.ch

OUTLINE

Water shortage remains an important issue in our society (WHO & UNICEF, 2017). Poor waste management creates large quantities of wastewater, further adding to the global water shortage. Greywater represents approximately 65% of total household wastewater and is a microbiologically less-polluted category of wastewater, consisting of the outflow from sinks, laundry machines, dishwashers, showers and bathtubs (Gorgich et al., 2020; Vuppaladadiyam et al., 2019). The use of vegetated systems offers a cheap and sustainable option for greywater treatment and reuse. During a series of experiments, we tested the efficiency of a green wall system (Figure 1) for laundry greywater treatment.

METHODS

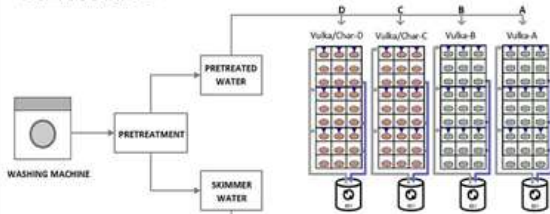


Figure 1: Experiment design

The laundry greywater was treated using the green wall treatment system (Figure 1). The pretreatment consisted of a recirculating sedimentation tank with an included skimmer. The 4 green walls were a modified NatureUP! system (Gardena, Germany) with an adapted top-down irrigation system. They had 2 substrate configurations:

- Walls A and B contained a 100% Vulkaponic substrate (Vulka-AB)
- Walls C and D contained a substrate mixture of 75% Vulkaponic and 25% plant-based Biochar (Vulka/Char-CD)

Water parameters (pH, water temperature, dissolved oxygen and electric conductivity) were measured with a Hach Lange HQ40d Multisonde and turbidity was measured with a Hach Lange 2100Qis Portable Turbidimeter. Water samples were analyzed for chemical oxygen demand (COD) ammonium-nitrogen ($\text{NH}_4\text{-N}$), nitrite-nitrogen ($\text{NO}_2\text{-N}$), nitrate-nitrogen ($\text{NO}_3\text{-N}$) and orthophosphate phosphorus ($\text{PO}_4\text{-P}$), using HachLange cuvette tests. Further analysis has been done on the microplastic fiber and microbiological pollutant removal potential.

RESULTS

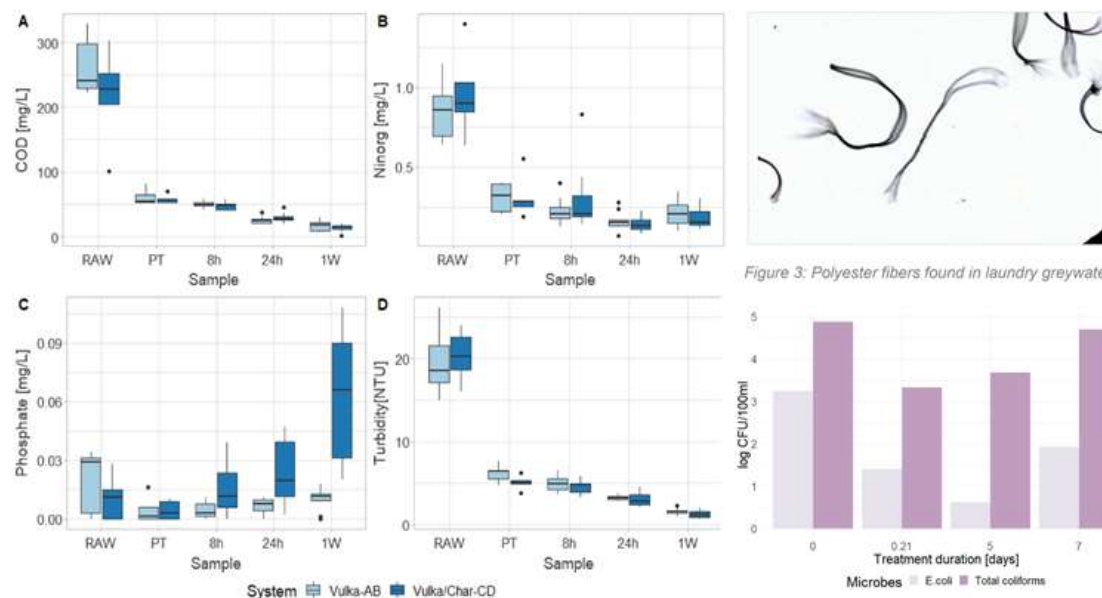


Figure 2: Average COD, N=5 (A); Ninorg, N=5 (B); $\text{PO}_4\text{-P}$, N=5 (C) and turbidity, N=5 (D) measured in two different systems (Vulka-AB and Vulka/Char-CD). Measured in raw greywater (RAW), pre-treated greywater (PT), after 8h, 24h and 1 week (1W) of recirculation in the green wall.

Figure 4: E.coli and total coliforms (log CFU/100ml) measured in greywater treated in a green wall system (Vulka/Char substrate) from raw (0), 5 hours (0.21 days), 5 and 7 days of recirculation

	Vulka-AB				Vulka/Char-CD			
	PT	8h	24h	1w	PT	8h	24h	1w
COD	76.9	81.2	90.4	93.9	73.4	78.0	86.6	93.8
$\text{NH}_4\text{-N}$	45.1	45.1	51.2	-116.5	75.2	11.8	75.2	70.3
$\text{NO}_2\text{-N}$	98.2	91.4	94.1	84.2	95.7	88.8	94.7	88.3
$\text{NO}_3\text{-N}$	63.5	73.7	81.2	78.5	66.5	70.7	85.3	81.8
$\text{PO}_4\text{-P}$	76.3	78.4	66.5	47.9	59.3	-36.1	-123.1	-477.8
Turbidity	68.6	74.6	83.5	92.0	75.0	77.8	85.1	93.7
Ninorg	64.0	73.6	81.0	74.9	67.3	69.0	85.1	81.6

Table 1: The removal rates (%) of COD, $\text{NH}_4\text{-N}$, $\text{NO}_2\text{-N}$, $\text{NO}_3\text{-N}$, $\text{PO}_4\text{-P}$, Turbidity and inorganic nitrogen (N_{inorg}) in systems with two different substrates (Vulka-AB, Vulka/Char-CD). The removal rate was calculated after the pretreatment (PT) of the raw greywater and after 8h, 24h and 1 week of recirculation in the green walls. Negative values indicate the increase of the value.

CONCLUSIONS

The green wall system was effective for the treatment of the laundry greywater, achieving a treatment efficiency of 94% for COD, 80% for Ninorg and 92% for Turbidity.

On the other hand, the $\text{PO}_4\text{-P}$ concentrations increased with prolonged recirculation, especially in the Vulka/Char-CD. This was possibly due to desorption of accumulated $\text{PO}_4\text{-P}$ in the biochar.

According to Kruskal-Wallis with Post-hoc test ($p < 0.05$) the removal of COD, Ninorg and turbidity does not differ significantly between the two different substrates, meaning that both were equally effective in nutrient removal from greywater. Vulkaponic substrate was more effective for PO_4 removal.

Later experiments indicated a potential for green wall microbial contamination treatment and microplastic fiber removal. More tests will be done to confirm these findings.

REFERENCES

- Organisation mondiale de la santé, & UNICEF. (2017). Progress on drinking water, sanitation and hygiene: 2017 update and SDG baselines.
- Gorgich, M., Mata, T. M., Martins, A., Caetano, N. S., & Formigo, N. (2020). Application of domestic greywater for irrigating agricultural products: A brief study. Energy Reports, 6, 811–817. <https://doi.org/10.1016/j.egy.2019.11.007>
- Vuppaladadiyam, A. K., Merayo, N., Prinsén, P., Luque, R., Blanco, A., & Zhao, M. (2019). A review on greywater reuse: Quality, risks, barriers and global scenarios. Reviews in Environmental Science and Bio/Technology, 18(1), 77–99. <https://doi.org/10.1007/s11557-018-9487-9>

ACKNOWLEDGEMENTS

This work was done during my internship at ZHAW, Wädenswil, Switzerland. I would like to thank everybody in the Ecotechnology Research Group for making these experiments possible and for the help and support in the execution of this experiment.

Pathways of microplastics from inland polluters in the Gulf of Trieste: determining the beaches for deposition

Ajda Kranjc Požar¹, Darja Istenič², Dušan Žagar^{1*}

¹University of Ljubljana, Faculty of Civil and Geodetic Engineering, Jamova 2, Ljubljana

²University of Ljubljana, Faculty for Health Sciences, Zdravstvena pot 5, Ljubljana

*ajda.kranjcp@gmail.com

INTRODUCTION

Microplastics (MP) in the oceans pose an increasing environmental problem since it negatively affects marine biota (Syberg et al., 2015). The main goal of our research is to determine the coastlines in the Slovenian part of the Gulf of Trieste that are most probable points for deposition of MP from inland sources (e.g. wastewater treatment plants (WWTP), rivers) by applying a numerical particle-tracking based model (PTM).

METHODS

Simulations of MP pathways from three different sources (the Dragonja River outflow, WWTP Piran and the Rižana River outflow) were performed with the Nafta3d PTM model, where MP particles were treated as conservative contaminant with density of 0,92 g/cm³ (e.g. polyethylene), thus floating in the surface layers. Previously computed daily averaged velocity fields for the entire year 2012 (NAPOM model, North Adriatic Princeton Ocean Model) were used to simulate advection, while the turbulent diffusion was modelled as a stochastic process (Ostaneč Jurina et al., 2015). For each source we simulated spreading in typical meteorological conditions with the lowest variability of wind direction over one-week duration in four selected quartiles.

Wind direction	Quartiles (wind direction) [°]	Period	Average wind speed [m/s]	Average wind direction [°]
North (N)	33-49	28.1-4.2	15.5	20
East (E)	45-135	17.1-24.1	2.7	134
South (S)	135-225	38.6-3.7	2	149
West (W)	225-315	20.4-27.8	3.6	262

The obtained MP concentrations (84 images; 3 sources, 4 directions, 7 days) were graphically displayed using a Matlab routine, showing the distribution of different MP concentrations after each day in each weather situation for each discharge

RESULTS AND DISCUSSION

The simulations showed relatively high spatial variability in spreading of the MP using the selected velocity fields and sources. In cases of the Dragonja and the Rižana River the MP hits the coast in all selected conditions, while in some simulations for WWTP Piran, MP travels towards the open sea. In case of E and W winds the MP from the Dragonja River was deposited at the highest concentration at Portorož beach, while in the case of N winds the majority of MP hit Bernardin after 3 days. In case of S winds, the majority of MP from the Dragonja River travels further to Strunjan, as does also the MP from WWTP Piran after 7 days. Furthermore, the simulations showed that MP from the Rižana River is mainly accumulated at Ankaran beach in case of E and W winds, while in case of N and S winds the MP is mainly deposited in the Port of Koper. In extremely strong wind MP from selected sources sails towards Italy (e.g. MP from WWTP Piran) or towards Croatia (e.g. MP from Dragonja River). In such wind conditions it is likely that MP hits the Slovenian coast from other sources.

The results indicated the beaches where MP from terrestrial polluters is most probably deposited. Among those, the sandy beaches of Portorož, Strunjan and Ankaran have been selected for MP sampling. The sampling will be done before and after typical events, similar to simulated. The samples will be analysed in the laboratory for the quantity of MP and samples before and after event will be compared.

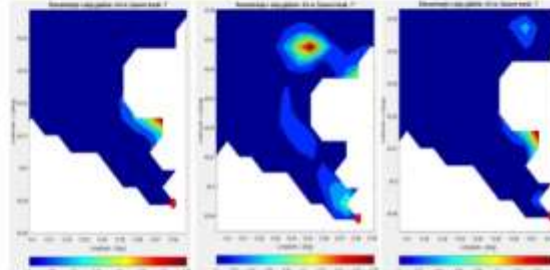


Figure 1: Distribution of MP concentrations from the Dragonja River in cases of E (left), S (middle) and W winds (right)

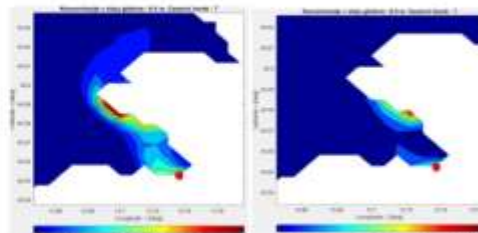


Figure 3: Distribution of MP concentrations from the Rižana River in cases of E (left) and W wind (right)

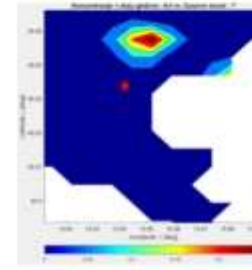


Figure 2: Distribution of MP concentrations from the WWTP Piran in case of S wind

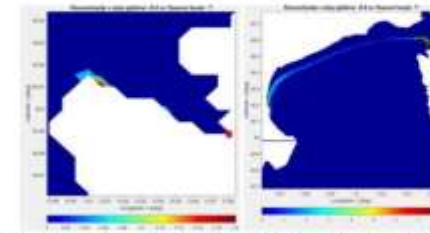


Figure 4: Distribution of MP concentrations from the Dragonja River (left), and WWTP Piran (right) in case of N wind

CONCLUSIONS

- In various weather (wind) conditions typical patterns of MP pathways exist;
- In some cases of strong steady wind MP from selected sources can be deposited at the coastline closer to and in the other cases far from the MP source;
- MP from the selected inland sources is most probably deposited at the sandy beaches of Portorož, Strunjan and Ankaran.

REFERENCES

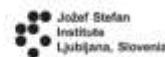
- Ostaneč Jurina T., Soško H., Žagar D. 2015. Primerjava modelov širjenja nafte na morju po metodah trajektorij in koncentracij. Acta hydrotechnica 27/46: 43-56.
- Syberg K, Khan FR, Selck H, Palmqvist A, Banta GT, Daley J, Sano L, Duhaime MB. 2015. Microplastics: Addressing ecological risk through lessons learned. Environ Toxicol Chem. 34(5):945-953. doi:10.1002/etc.2914.

Development of an analytical method to determine contamination of propolis with neonicotinoid pesticides



University of Ljubljana
Faculty of Chemistry and
Chemical Technology

Tomšič R¹, Heath D², Heath E^{2,3}, Markelj J¹, and Prosen H¹
¹ Faculty of Chemistry and Chemical Technology, University of Ljubljana, Ljubljana, Slovenia
² Department of Environmental Sciences, Jožef Stefan Institute, Ljubljana, Slovenia
³ Jožef Stefan International Postgraduate School, Ljubljana, Slovenia



Jožef Stefan
Institute
Ljubljana, Slovenia

INTRODUCTION

Neonicotinoid insecticides are commonly used as systemic insecticides for the protection of economic plants during the entire growing season [1]. They show low toxicity for the mammals, but are more problematic for bees. Within plants, they are present in pollen and nectar, which are the primary food source for bees [2]. Even sub-lethal exposure of bees could lead to colony collapse disorder (CCD) [3]. Most often, LC-MS or LC-MS/MS in combination with a suitable extraction method are used for the determination of neonicotinoids in honeybee products, such as pollen, honey, and beeswax [4,5,6]. Different extraction methods are used, such as liquid-liquid extraction (LLE) [4], dispersive liquid-liquid microextraction (DLLME) [4], QuEChERS [6] and solid-phase extraction - SPE [6]. Propolis is a very complex sample and its contamination with pesticides is seldom determined [7].



Figure 1: Raw propolis.

EXPERIMENTAL

We developed and validated a method for the determination of five neonicotinoid pesticides in propolis. It was applied to the analysis of thirty propolis samples from Slovenia and other countries. To the best of our knowledge, this is the first study on the contamination of propolis with neonicotinoid insecticides. Samples were first extracted either with SPE or QuEChERS. The extracts were further analysed with LC-MS/MS in selected reaction monitoring mode using an Agilent C8 column (150 mm x 4.6 mm x 3.5 µm) with a flow rate of 0.8 ml/min and injection volume of 20 µL. Mobile phase consisting of 0.1% HCOOH and acetonitrile was used in a gradient mode. Positive electrospray ionization was used. Cleaner extracts were obtained by SPE extraction, therefore SPE-LC-MS/MS method was applied to 30 real propolis samples.

Solid-phase extraction (SPE)

OASIS HLB cartridge (Waters) with 200 mg of sorbent with Visiprep vacuum manifold (Supelco) was used.

Method:

- Cartridge conditioning: 5 mL MeOH, followed by 5 mL MQ;
 - Sample loading (sample volume: 50 mL; ethanol content: 10%);
 - Washing: 10 mL of 25% NH₃ aqueous solution and MeOH (pH=11);
 - Elution: 5 mL of acetonitrile, eluate was spiked with internal standard and evaporated to dryness;
 - The residue was dissolved in 0.5 mL of acetonitrile.
- In order to obtain the best extraction efficiency, the following parameters were optimized:
- Different ethanol content: 1, 5, 10, 20%;
 - Sample volume load: 50 and 100 mL;
 - Elution solvent: acetonitrile, ethyl acetate, and methanol;
 - Volume of solvent for elution: 4 fractions of 5 mL.

QuEChERS

The QuEChERS method was adapted from Anastassiades et al. [8]. Propolis tincture was first evaporated to dryness and redissolved in 10 mL of acetonitrile. The method was as follows:

- 10 mL of acetonitrile tincture + 10 mL of MQW + MgSO₄ (6 g), NaCl (1 g), sodium citrate (1 g), and disodium citrate sesquihydrate (0.5 g) was shaken for 15 min at 300 rpm and centrifuged for 10 min at 3000 rpm.
- 6 mL of supernatant + 900 mg of anhydrous MgSO₄ + 150 mg of the primary-secondary amine (PSA) sorbent was shaken for 2 min and centrifuged for 5 min at 3000 rpm.
- 1.5 mL of the final supernatant was transferred into LC vial and analysed by LC-MS/MS.

Due to complexity of QuEChERS extracts, second step of QuEChERS method was modified with addition of 100 mg C18 sorbent and 100 mg of graphitized carbon black.

Sample collection and preparation

- 30 propolis samples (18 raw and 12 tinctures).
- Tincture: 5 mL of ethanol tincture was diluted with 45 mL of MQW.
- Raw: 0.5 g of sample was ground and dissolved in 50 mL of 10% ethanol in MQW. Then the mixture was shaken on orbital shaker at 300 rpm for 5 h (50 °C). Afterwards samples were stored in dark place for 5 days. Prior to SPE extraction all samples were centrifuged at 5000 rpm.

Method validation

Method was validated at two spiking levels (10 and 50 ng/g), with three parallel determinations on each level. Matrix-matched calibration was used to determine LOD, LOQ, linearity, and matrix effect. Method efficiency, accuracy, and repeatability were determined.

RESULTS AND DISCUSSION

SPE and QuEChERS optimisation

In order to obtain maximum recoveries, samples with different ethanol content were tested (1, 5, 10, 20%). Recoveries of acetamiprid, imidacloprid, and thiacloprid were not significantly affected by ethanol content. Recovery of thiamethoxam was decreased at 20% of ethanol, while clothianidin recoveries were below 20% with every ethanol content. Further experiments were performed with samples in 10% ethanol. Different sample volumes were tested in order to determine the break-through volume of cartridge, which was 50 mL. From the different elution solvents tested (each solvent 20 mL in 4 aliquots), the most efficient elution was achieved with acetonitrile, whereby 98% of analytes were eluted within the first fraction. Therefore, 5 mL of acetonitrile was used as elution solvent.

For QuEChERS, a modified and unmodified EN method [8] were tested with reconstitution of dried ethanol tinctures in either acetonitrile or ethanol (5 mL). Higher recoveries were obtained by using acetonitrile (95-117%). However, the QuEChERS extracts were very complex and we noticed frequent clogging of MS ion source. Additional clean-up by SPE resulted in very low recoveries.

Taking into account the above results, SPE was selected as the sample preparation method for further work.

SPE-LC-MS/MS method validation

Results of SPE-LC-MS/MS method validation are listed in Table 1.

Table 1: Validation results of SPE-LC-MS/MS method.

Analyte	Linearity	LOD (ng/g)	LOQ (ng/g)	Matrix effect (Peak/Peak)	Recovery (%)		Accuracy (%)		Repeatability (SD (%))	
					L	H	L	H	L	H
Acetamiprid	0.994	0.2	0.7	0.49	95	91	7.1	8.8	27	8
Clothianidin	0.991	4.4	14.7	0.99	10	20	2.8	9.5	5	6
Imidacloprid	0.996	0.7	2.2	0.54	99	95	9.6	4.5	29	12
Thiacloprid	0.991	0.2	0.8	0.3	101	96	1.9	10.4	20	13
Thiamethoxam	0.994	0.3	1.0	0.81	61	61	7.2	8.3	21	3

Analysis of samples

We used the optimised method to analyse 30 propolis samples from Europe and Canada. In a few samples (raw propolis or tinctures) the presence of analytes was confirmed, although below LOQ of the method:

- Raw (Slovenia) - acetamiprid (0.35 ng/g)*
- Raw (Slovenia) - acetamiprid (0.41 ng/g)*
- Tincture (Bulgaria) - acetamiprid (0.39 µg/L)*
- Tincture (Czech R.) - thiacloprid (0.45 µg/L)*
- Tincture (Serbia) - thiacloprid (0.39 µg/L)*
- Tincture (Czech R.) - imidacloprid (0.97 µg/L)*
- Tincture (Canada) - imidacloprid (0.99 µg/L)*

*Estimated concentration (between LOD and LOQ)

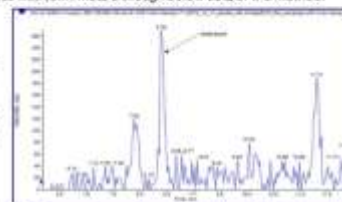


Figure 2: Chromatogram of a contaminated sample (m/z transition for imidacloprid).

ACKNOWLEDGEMENTS

The study was performed with the financial support of the Slovenian Research Agency, namely Program Groups P1-0143 and P1-0153, and Projects L1-9191 and N1-0143. This study has received funding from the EMER programme co-financed by the Participating States and from the European Union's Horizon 2020 research and innovation programme [18888831].

REFERENCES

- [1] Sevelin, P., Stevan, R., Schindler, M., and Elbert, A. Overview of the status and global strategy for neonicotinoids. 1. Egn. Pestic. Chem. 2011, 30: 2067-2069.
- [2] Elbert, A., Haas, M., Springer, B., Thaler, M., and Haauer, R. Applied aspects of neonicotinoid use in crop protection. Pest Manag. Sci. 2008, 64: 1099-1103.
- [3] Li, L., Harshbarger, M. L., and Callahan, A. R. Sub-lethal exposure to neonicotinoids impairs honey bee winter survival before proceeding to colony collapse disorder. Biol. Insectology 2014, 67: 121-136.
- [4] Ivanova, P., Gostinova, V., Frank, M., et al. Multi-residue method for determination of selected neonicotinoid insecticides in honey using optimized dispersive liquid-liquid microextraction combined with liquid chromatography tandem mass spectrometry. Talanta 2013, 131: 125-133.
- [5] Dimitrova, R., Simova, R., Jelic, C., and Vlahov, B. Exposure assessment of honeybees through study of five neonicotinoid pesticide residues in honeydew, bee pollen, and bee larvae from French territories by LC-MS/MS. Environ. Sci. Pollut. Res. 2018, 25: 6149-6204.
- [6] Mihalič, M., Heath, D., Heath, E., Markelj, J., Karabuč, K., and Prosen, H. GW - Food Science and Technology investigations of neonicotinoid pesticides in Slovenian honey by LC-MS/MS. GW 2020, 134: 44-52.
- [7] Ollig, C. Neonicotinoid extraction and fast-flow solid-phase extraction clean-up for pesticide residue analysis in propolis. J. Chromatogr. A 2020, 1445: 19-26.
- [8] Anastassiades, M., Lehmann, S. J., Bilkova, D., and Schreyer, P. Fast and easy multiresidue method employing acetonitrile extraction/partitioning and "dispersive solid-phase extraction" for the determination of pesticide residues in produce. J. Agric. Sci. 2003, 140: 413-415.



DOES MICROPLASTICS IN WASTE BIOLOGICAL SLUDGE IMPACT BIOGAS PRODUCTION?

Nina Resnik^{1*}, Tjaša Griessler Bulc², Andreja Žgajnar Gotvajn¹

¹University of Ljubljana, Faculty of Chemistry and Chemical Technology, Večna pot 114, SI-1000, Ljubljana, Slovenia,

²University of Ljubljana, Faculty of Health Sciences, Zdravstvena pot 5, SI-1000, Ljubljana, Slovenia

Contact*: Nina Resnik, nina.resnik@gmail.com

OUTLINE

WWTPs (Wastewater Treatment Plants) as major source of MP (microplastics) could retain over 90 % of MP in the sludge. Sludge can be used as fertilizer, co-incinerated or used for production of biogas using anaerobic digestion. Positive and negative impacts of MP on anaerobic digestion were found. The process can be inhibited due to the presence of toxic compounds.

Positive effects of anaerobic digestion are:



METHOD

SIST EN ISO 11734:1999

Analysis with OxiTop Control system was used to follow anaerobic degradation processes to evaluate biogas production in terms of increased pressure (hPa). Bottles were filled with mixture of anaerobic sludge ($c = 1,5 \text{ g}_{\text{VSS}}/\text{L}$), easily biodegradable substrate (glucose; $c = 0,833 \text{ mol/L}$), buffer solution for maintaining constant pH and MP (fibers: PES, PA and Polyacryl and particles PET and PP; $c = 3 \text{ g/L}$). After 7 days, NaOH was added to remove formed CO_2 . The remained pressure was attained to CH_4 in the system. The next day, after 8 days of starting, experiment was terminated. Simultaneously experiments with anaerobic sludge and glucose were run to determine the impact of added MP on biogas production.

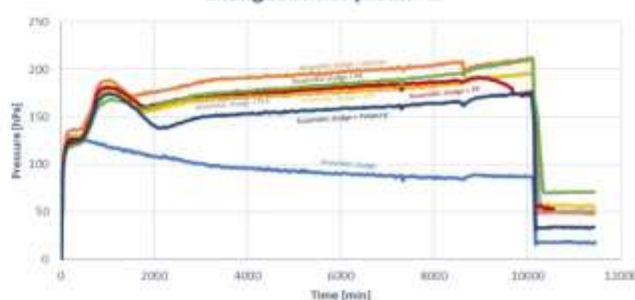


CONCLUSIONS

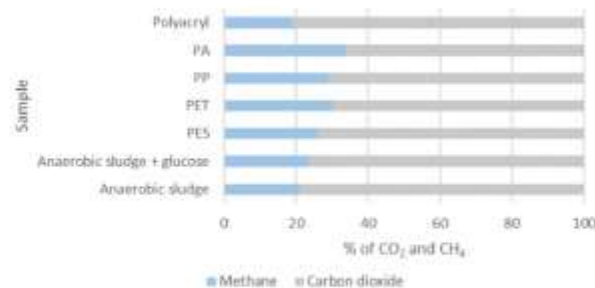
Impact of MP on biogas production was determined. Further research will be carried out with different types, sizes and concentration of MP.

RESULTS

Changes of the pressure



CO_2 and CH_4 yield dependency on type of the MP



Measurement of biogas production with OxyTop system

Impact on biogas production was noticed.

Positive effect of added MP on methane production was noticed with most of added MP types.

Types of MP with positive effect on methane production (listed from most to least effect):

- PA,
- PET
- PP
- PES

Polyacryl negatively affected methane production.

For every added type of MP, samples were prepared in two or three parallels, graphs show average results for each type of MP

REFERENCES

- Sun, J., et al., Microplastics in wastewater treatment plants: Detection, occurrence and removal. *Water Res.* 2019. **152**: p. 21-37.
- Mahon, A.M., et al., Microplastics in Sewage Sludge: Effects of Treatment. *Environ Sci Technol.* 2017. **51**(2): p. 810-818.
- Wei, W., et al., Polyethylene terephthalate microplastics affect hydrogen production from alkaline anaerobic fermentation of waste activated sludge through altering viability and activity of anaerobic microorganisms. *Water Res.* 2019. **163**: p. 114881.
- Caruso, G., Microplastics as vectors of contaminants. *Mar Pollut Bull.* 2019. **146**: p. 921-924.
- Liu, F.F., et al., Interactions between microplastics and phthalate esters as affected by microplastics characteristics and solution chemistry. *Chemosphere.* 2019. **214**: p. 688-694.
- Luo, J., et al., Potential influences of exogenous pollutants occurred in waste activated sludge on anaerobic digestion: A review. *J Hazard Mater.* 2020. **383**: p. 121176.
- Fu, S.F., et al., Exposure to polystyrene nanoplastic leads to inhibition of anaerobic digestion system. *Sci Total Environ.* 2018. **625**: p. 64-70.
- Hidayaturrahman, H. and T.G. Lee, A study on characteristics of microplastic in wastewater of South Korea: Identification, quantification, and fate of microplastics during treatment process. *Mar Pollut Bull.* 2019. **146**: p. 696-702.
- Bayo, J., S. Olmos, and J. López-Castellano, Microplastics in an urban wastewater treatment plant: The influence of physicochemical parameters and environmental factors. *Chemosphere.* 2020. **238**: p. 124593.

This work was financed by the Slovenian Research Agency (ARRS), the research programme of Chemical Engineering (P2-0191) and Mechanisms of health maintenance (P3-0388).

INHIBITION OF GROWTH OF CYANOBACTERIA *ANABAENA VARIABILIS* AND *MICROCYSTIS AERUGINOSA* BY SINGLE AND MIXED BISPHENOL A ANALOGUES

Karolina Czarny¹, Barbara Krawczyk¹, Dominik Szczukocki¹

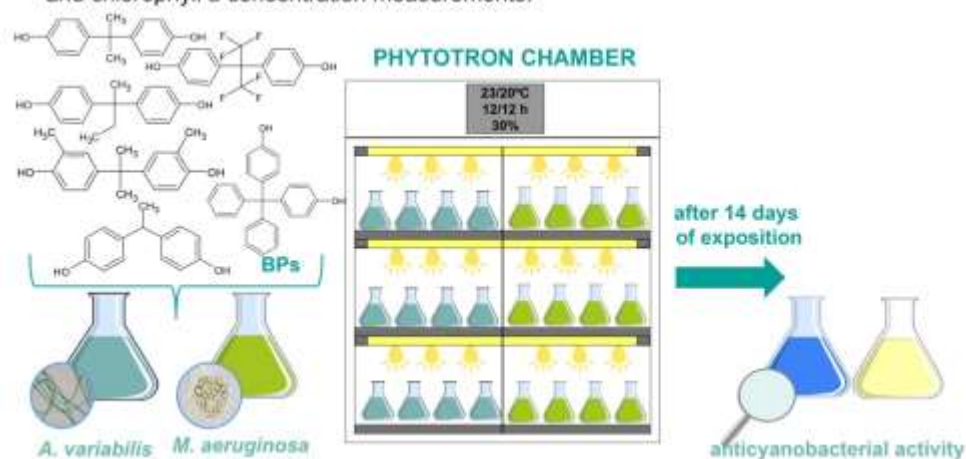
¹Laboratory of Environmental Threats, Department of Inorganic and Analytical Chemistry, Faculty of Chemistry, University of Lodz, Lodz, Poland;
Contact: Karolina Czarny: karolina.czarny@chemia.uni.lodz.pl

OUTLINE

In the last decades, the use of bisphenol A has attracted global attention resulting from its actions as an endocrine disrupting compound. In this regard, various bisphenol analogues have been manufactured as a replacement for this compound in consumer products. As a result of the high production volumes, different bisphenol analogues are entered into the terrestrial and aquatic environment, which consequently leads to their increasing contamination and may pose serious risk to organisms.

EXPERIMENTAL METHODS

To study the toxic effects of bisphenols on *Anabaena variabilis* and *Microcystis aeruginosa*, exponentially growing cyanobacteria species were exposed to different concentration of BPA and its five analogues (BPAF, BPB, BPBP, BPC, BPE). Mixture (MIX) was prepared with 1/6 of each bisphenol (1:1:1:1:1, mg mL⁻¹) to achieve the same final concentration as for individual compounds. Stock solutions of the examined compounds was added to 100 mL of test medium containing *Anabaena variabilis* and *Microcystis aeruginosa* cells at the nominal concentrations of 5, 10, 15, 25, 50, 75 and 100 mg L⁻¹. Test and control samples were incubated in the presence of investigated bisphenols for 14 days and maintained under the same conditions as described above. After 0, 1, 2, 3, 7, 8, 10, 11, 14 days of exposure, cyanobacterial samples were collected for the biomass and chlorophyll *a* concentration measurements.



RESULTS

Table 1. The toxicity of bisphenol A and its analogues to cyanobacteria *Anabaena variabilis* and *Microcystis aeruginosa* (14 days growth inhibition). Experimental EC₅₀ values (mg L⁻¹) are shown with 95% confidence intervals (x ± SD) representing effective concentrations resulting in 50% reduction in the biomass content as compared to control treatment.

BPs	<i>Anabaena variabilis</i>		<i>Microcystis aeruginosa</i>	
	Dose-response equation (R ²)	EC ₅₀ ± SD (14 d) [mg L ⁻¹]	Dose-response equation (R ²)	EC ₅₀ ± SD (14 d) [mg L ⁻¹]
BPA	y = -0.0086x + 1.1807 (0.8049)	78.96 ± 3.95	y = -0.0064x + 0.8559 (0.7365)	55.27 ± 2.76
BPAF	y = -0.0081x + 0.6041 (0.3738)	12.88 ± 0.64	y = -0.0036x + 0.6637 (0.4967)	45.51 ± 2.28
BPB	y = -0.0116x + 0.9235 (0.7793)	36.53 ± 1.83	y = -0.0082x + 0.8628 (0.8117)	44.20 ± 2.21
BPBP	y = -0.0018x + 1.0616 (0.4611)	320.23 ± 16.01	y = -0.0012x + 1.0828 (0.3939)	488.61 ± 24.43
BPC	y = -0.0102x + 0.8210 (0.8059)	31.51 ± 1.58	y = -0.0114x + 1.1228 (0.8120)	54.87 ± 2.74
BPE	y = -0.0059x + 0.9806 (0.8792)	81.54 ± 4.08	y = -0.0094x + 1.1886 (0.8437)	73.54 ± 3.68
MIX	y = -0.0111x + 0.8582 (0.6027)	32.32 ± 1.62	y = -0.0055x + 0.8378 (0.7594)	60.88 ± 3.04

CONCLUSION

- BPAF, BPB and BPC were found to be more toxic to *Anabaena variabilis* and *Microcystis aeruginosa* than BPA.
- Mixture of bisphenol analogues exhibit toxic effect similar to or even stronger than that of bisphenol A.
- The use of bisphenol analogues as a replacement of BPA in various consumer products is questionable and may be hazardous to aquatic organisms, such as cyanobacteria.



EXTRACTION OF PET MICROPLASTICS FROM SOIL AND DIFFERENT SOIL AND COMPOST MIXTURES

Pia Leban^{1*}, Franja Prosenc², Mojca Bavcon Kralj¹, Tjaša Griessler Bulc¹

¹University of Ljubljana, Faculty of Health Sciences, Department for Sanitary Engineering, Ljubljana, Slovenia. ²University of Ljubljana, Faculty of Health Sciences, Research Institute, Ljubljana, Slovenia.

Contact*: cepic.p@gmail.com

OUTLINE

Polymer polyethylene terephthalate (PET) is a commonly and widely used polymer, usually intended for packaging as well as clothing. It can be found as microplastics (MP) in water, soil, compost and sewage sludge. The method for extraction and quantification of MP from soil has not yet been standardised. We compare oil extraction, which takes advantage of the lipophilic surface properties of most plastics, and a commonly used density separation method, which separates MP from soil based on the density difference of MP and the saline solution used.

METHODS

Oil extraction:

- 10 g of soil or soil and compost mixture, a defined number of PET MP particles, 50 mL of distilled water and 3 mL of olive oil were put in a PTFE cylinder.
- Firstly, the closed cylinder was shaken, then left settling for 2h and finally put into the freezer overnight.
- The sample was pushed out of a cylinder with a piston and the oil layer with MP was left to thaw on a filter and then filtered through a glass fibre filter and rinsed with water and subsequently with hexane.
- For samples rich in organic matter (soil and compost mixtures), an oxidation step was added. The filter was put in a beaker with Fenton reagent until the reaction was complete.
- Protocol adapted with changes from Scopetani *et al.*, (2020).

Density separation:

- 10 g of soil or soil and compost mixture, a defined number of PET MP particles and 50 mL of ZnCl₂ solution were put into a beaker.
- The sample was stirred 3x for 2 min and left for 2 h to sediment and to get MP floating on the surface.
- The supernatant was filtered through a glass fibre filter.
- The filter was put in a beaker with Fenton reagent until the oxidation reaction was complete.
- Protocol adapted with changes from Konechnaya *et al.*, (2020).

RESULTS

Oil extraction:

Pros and cons:

- ➔ Safe and cheap method
- ➔ Without the use of any hazardous saline solutions
- ➔ Applicable to different polymer types (with different density, it has a small role in the MP recovery)
- ➔ Applicable also to many different soil types and compost mixtures
- ➔ Not time efficient (overnight freezing process)
- ➔ Custom made equipment (PTFE cylinder and piston)
- ➔ Oil affinity to different polymer types
- ➔ Require an additional step to remove organic substances from a sample
- ➔ Using food sources (olive oil)
- ➔ Oil needs to be removed before further analysis (hexane)

Recovery:

From 90-100 % (Crichton *et al.*, 2017; Mani *et al.*, 2019), **our recovery 93 %**. The recovery was on average lower in compost than in soil (90.5 % < 96.5 %) and on average lower for the low-density polymers (89.1 %) than for the medium-density and high-density (95.5 %) polymers (Scopetani *et al.*, 2020).

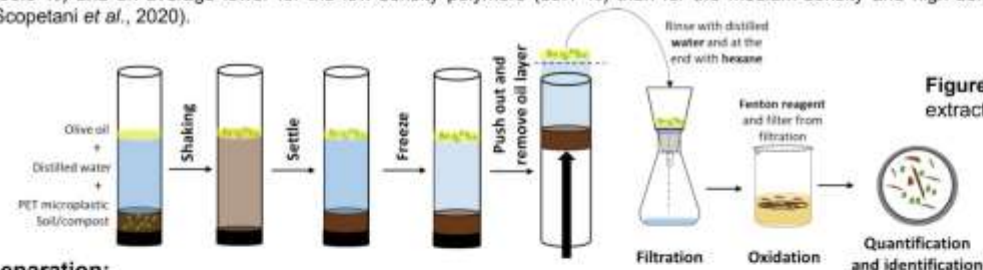


Figure 1: Oil extraction method.

Density separation:

Pros and cons:

- ➔ Simple method, without special equipment and with easy application in laboratory
- ➔ Saline solutions with sufficiently high density available for extraction of PET MP
- ➔ Applicable to many different soil types and compost mixtures
- ➔ Expensive method (saturated saline solutions)
- ➔ Hazardous solutions (toxic to the environment – NaI, react with organic matter – CaCl₂)
- ➔ ZnCl₂ solution can react with natural components of sediment, especially carbonates (resulting in bubbling and foam), which can hamper the procedure (Möller *et al.*, 2020)
- ➔ Require an additional step (or more) to remove organic matter

Recovery:

On average higher than 90 % (Li *et al.*, 2020; Vermeiren *et al.*, 2020), but mostly range from 94 % to 97 % (with SD between 0.3% and 3.3% with decreasing particle sizes) (Konechnaya *et al.*, 2020). **Yet to be tested and optimised by us.**

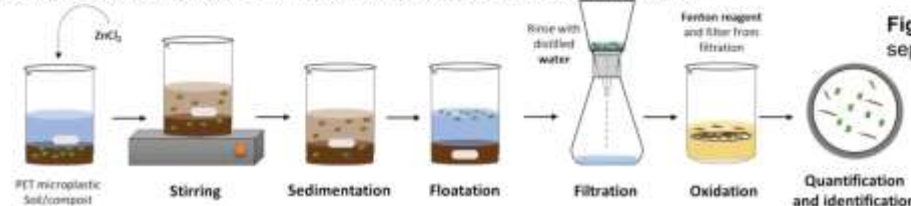


Figure 2: Density separation method.

CONCLUSIONS

By optimising and testing both on a wide range of PET concentrations and sizes and different matrices with varying organic matter content, we will be able to depict, which method is more suitable and yields better recoveries.

Further work will focus on quantification and identification of MP in environmental samples.

REFERENCES

- Crichton E M, Noll M, Gee E A, Ross P S. A novel, density-independent and FTIR-compatible approach for the rapid extraction of microplastics from aquatic sediments. *Anal Methods* 2017, 9(9): 1419-1428. DOI: 10.1039/C6AY02733D
- Konechnaya O, Lichmatz S, Dskowitzky L, Schwentbauer J. Optimized microplastic analysis based on size fractionation, density separation and μ -FTIR. *Water Sci Technol* 2020, 81(4): 834-844. DOI: 10.2166/wst.2020.173
- Li J, Song Y, Cai Y. Focus topics on microplastics in soil: analytical methods, occurrence, transport, and ecological risks. *Environ Pollut* 2020, 257: 113570. DOI: 10.1016/j.envpol.2019.113570
- Mari T, Frelund S, Kueberer A, Burkhardt-Holm P. Using castor oil to separate microplastics from four different environmental matrices. *Anal Methods* 2019, 11(13): 1785-1794. DOI: 10.1039/C8AY02559B
- Möller J N, Lüder M G, Laforsch C. Finding microplastics in soils: A review of analytical methods. *Environ Sci Technol* 2020, 54(4): 2076-2090. DOI: 10.1021/acs.est.9b04618
- Scopetani C, Chelazzi O, Mikola J, et al. Olive oil-based method for the extraction, quantification and identification of microplastics in soil and compost samples. *Soil Total Environ* 2020, 733: 139338. DOI: 10.1016/j.scitotenv.2020.139338
- Vermeiren P, Muñoz C, Nejlina K. Microplastic identification and quantification from organic rich sediments: A validated laboratory protocol. *Environ Pollut* 2020, 262: 114298. DOI: 10.1016/j.envpol.2020.114298

ACKNOWLEDGEMENTS

This work was supported by the Slovenian Research Agency, research core funding No. P3-0368 (Mechanisms of Health Maintenance), and research project No. Z2-2643 (Agri-IMPact: Microplastic Prevalence and Impact in Agricultural Fields).



Removal process optimisation for emerging pollutants onto two biochars synthesised with classic and microwave induced pyrolysis

Olivera Paunovic¹, Sabolc Pap^{1,2}, Helena Prosen³, Ida Krasevec³, Polonca Trebse⁴, Maja Turk Sekulic¹

¹Faculty of Technical Sciences, University of Novi Sad, Novi Sad, Serbia; ²Environmental Research Institute, North Highland College, University of the Highlands and Islands, Thurso, Scotland; ³ Faculty of Chemistry and Chemical Technology, University of Ljubljana, Ljubljana, Slovenia; ⁴ Faculty of Health Sciences, University of Ljubljana, Ljubljana, Slovenia
Contact: [Olivera Paunovic: o.paunovic88@gmail.com](mailto:Olivera.Paunovic: o.paunovic88@gmail.com)

OUTLINE

We investigated the removal efficiencies of emerging pollutants benzotriazole and its derivatives (OHBZ, 4MBZ, 5MBZ, CIBZ and DMBZ) with the variation of different process parameters (e.g., pH, contact time, initial concentration) onto two functionalised biochars. Microwave induced and classic pyrolysis were used to synthesise the biochars from wild plum (WpOH) and apricot kernels (AsPhA), respectively.

EXPERIMENTAL METHODS

It was started with the examination of four low-cost lignocellulosic biochars, and after initial screening, AsPhA and WpOH were selected for further experiment. It was performed in batch experiments. The specified mass of biochar was mixed with 50 ml solution of mixed pollutants in a colonial flask and mixed on a mechanical shaker. The effect of initial pH (2-9), contact time (5-420 min) and initial compounds concentration (1-50 mg/L) were studied. Biochar dosage was 0.4 mg/L.

CONCLUSION

Removal efficiency was optimal at pH 4 for WpOH and at pH 6 for AsPhA and equilibrium was reached for both adsorbents after 240 minutes. Maximum adsorption capacity showed CIBZ (98.1 mg/g) for WpOH and DMBZ (120.41 mg/g) for AsPhA. It was shown that both adsorbents were efficient for benzotriazole and its derivatives removal. AsPhA was more efficient and suitable under neutral environment.

RESULTS

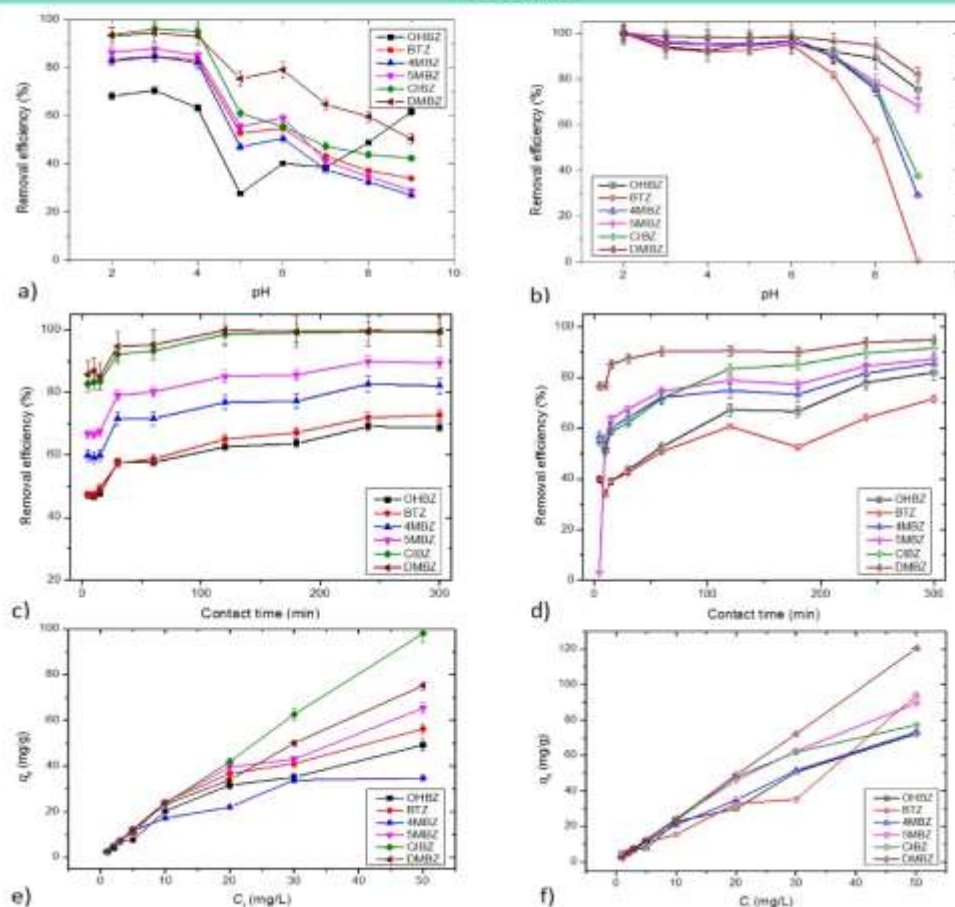


Figure 1: Influence of the pH value on removal efficiency on (a) WpOH; (b) AsPhA

Influence of contact time on removal efficiency on (c) WpOH and (d) AsPhA

Influence of initial concentration on adsorption capacity on (e) WpOH and (f) AsPhA



University of Ljubljana



CHALLENGES IN REMOVAL OF EMERGING CONTAMINANTS FROM THE WASTEWATER THROUGH HYBRID TREATMENT SYSTEM: AN ECO-FRIENDLY APPROACH

Sanja Radovic¹, Sabolc Pap^{1,2}, Jelena Prodanovic³, Barbara Bremner², Maja Turk Sekulic¹

¹ University of Novi Sad, Faculty of Technical Sciences, Department of Environmental Engineering and Occupational Safety and Health, Trg Dositeja Obradovića 6, 21 000 Novi Sad, Serbia, ² Environmental Research Institute, North Highland College, University of the Highlands and Islands, Thurso, Scotland, KW14 7JD, UK, ³ University of Novi Sad, Faculty of Technology Novi Sad, Bulevar Cara Lazara 1, 21000 Novi Sad, Serbia; Contact: Sanja Radovic, sanjaradovic@uns.ac.rs

OUTLINE

This work proposes an eco-friendly hybrid technology for the removal of two target emerging water pollutants - diclofenac (DCF) and naproxen (NPX) from wastewater. Hybrid technology consists of coagulation and adsorption processes. Eco-friendly coagulant was obtained from common bean (*Phaseolus vulgaris*), whereas low-cost adsorbent was obtained from apricot kernels magnetised with FeSO_4 .

EXPERIMENTAL METHODS

Coagulation and adsorption processes were successively applied in the mentioned order. Model water (200NTU, pH 6, spiked with 1 mg/L of DCF and NPX) was used. Coagulation was done in Jar tester after which treated water underwent adsorption process (120 min, room temperature, adsorbent dose: 1.25, 2.5, 5 and 12.5 g/L). HPLC-MS/MS was used for determination of residual DCF and NPX concentrations.

CONCLUSION

Tested hybrid technology proved its high efficiency for the removal of DCF and NPX within determined optimal conditions. There is space for further improvement and optimisation of the utilised technology. Important justifications for the application of hybrid systems in wastewater treatment are both economical and ecological aspects.

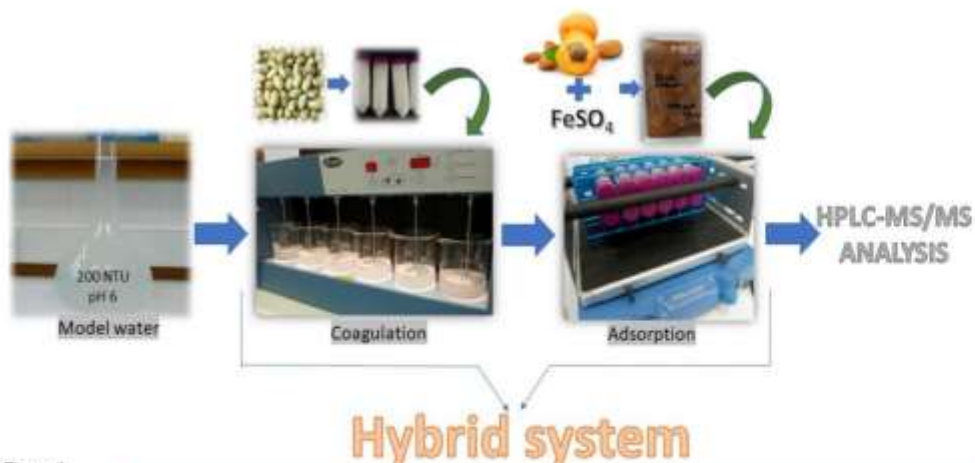


Figure 1

Figure 1: Simplified schematic view of hybrid process

Figure 2: Removal efficiency of (a) diclofenac and (b) naproxen

by hybrid system which used coagulant obtained with ultrasound extraction and magnetised low-cost adsorbent (UVO& FeSO_4) or coagulant obtained with conventional solid/liquid extraction and magnetised low-cost adsorbent (KVO& FeSO_4)

RESULTS

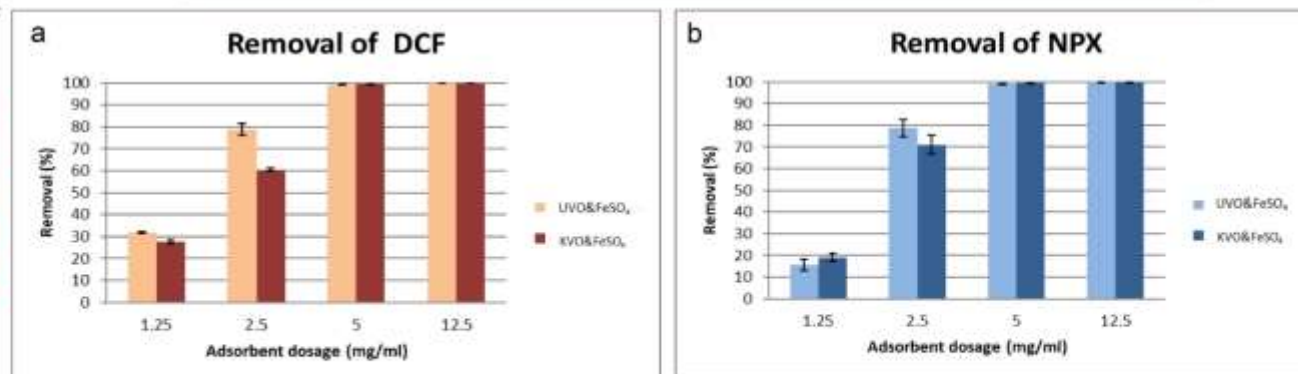


Figure 2



Anodised Microflowers On The Surface of Titanium

Niharika Rawat¹, Metka Benčina², Ita Junkar², Aleš Igljč^{*1,3}

¹Laboratory of Physics, Faculty of Electrical Engineering, University of Ljubljana, Tržaska cesta 25, 1000 Ljubljana, Slovenia, ²Department for Surface Engineering and Optoelectronics, Jožef Stefan Institute, Jamova cesta 39, 1000 Ljubljana, Slovenia, ³Laboratory of Clinical Biophysics, Chair, Faculty of Medicine, University of Ljubljana, 1000 Ljubljana, Slovenia

Contact*: ales.iglic@fe.uni-lj.si

OUTLINE

Electrochemical anodization using plasma¹ has garnered attention in various applications ranging from biomedical to photocatalytic applications. Titanium (Ti) and its alloys have the most promising biomaterial properties² due to their high tensile strength, corrosion resistance and flexibility. In the present work, we modified surface of Ti without using fluorine based electrolyte.

METHODS

Cleaned titanium foil of 0.1 mm thickness, 99.9% purity are used to modify surface of titanium (Ti). A biocompatible sodium chloride (NaCl) based electrolyte is used as a medium for surface structuring of Ti foil. For this purpose, a conventional electrochemical anodization technique is used where Ti is used as anode and NaCl along with distilled water (d.H₂O) was used as an electrolyte solution. We used gaseous plasma jet as a cathode for electrolysis and to set-up a two electrode system.

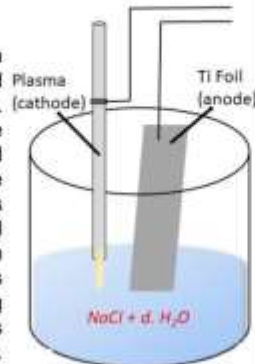


Figure 1. Schematic of anodisation setup.

Anodization was carried out for different time intervals i.e. 30 minutes, 1 Hour and 2 Hour to understand the effect of anodization time on the surface of Ti. Surface analysis of Ti for different time was done through SEM.

CONCLUSIONS

We have demonstrated the fabrication of TiO₂ layer on the surface with a flower like morphology significantly different from those obtained in conventional anodization processes. This was achieved using chloride based electrolyte indicating towards the utilization of Cl⁻ ions³ as a catalyst for surface modification of Ti. This synthesis provides a biocompatible alternate for fabricating TiO₂ structure free from fluorine ions which impact the biocompatibility of TiO₂ nanotubes⁴ synthesised using conventional anodization setup.

RESULTS

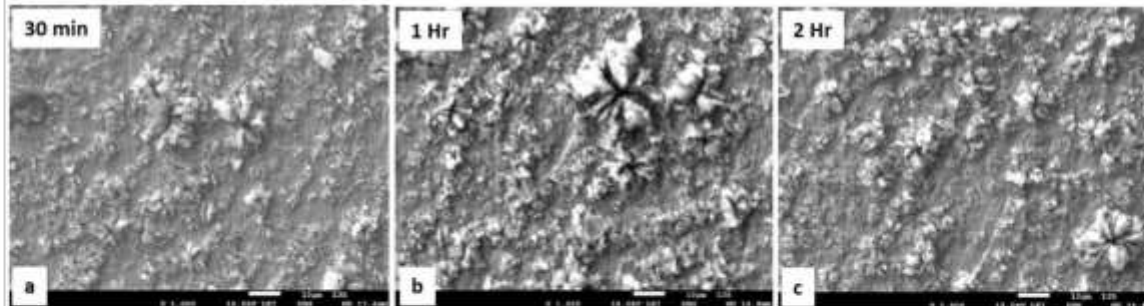


Figure 2. SEM images of anodized Ti foils for (a) 30 minutes (b) 1 Hour and (c) 2 Hours.

The results of SEM analysis show that the anodization with plasma leads to formation of Ti microstructures as shown in Fig. 2. Longer exposure time enable formation of microflower titanium oxide structures on the surface as presented in Fig. 2(b) and Fig. 2(c). As the exposure time increased more microflowers protrude from the Ti surface indicating a more homogeneous morphology.

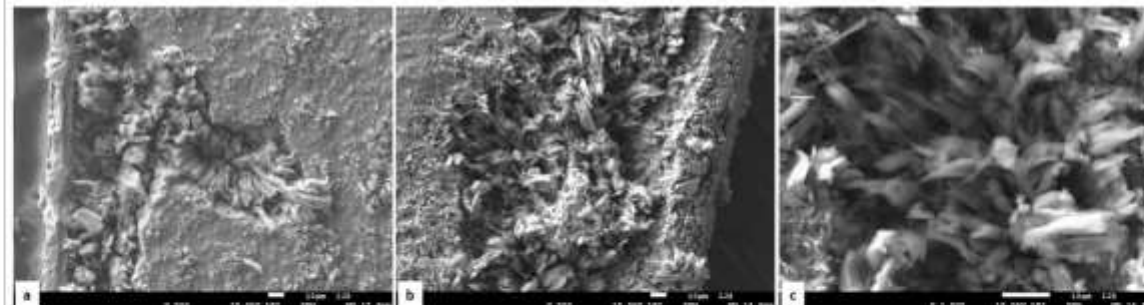


Figure 3. Cross-section SEM images of microstructures formed on Ti surface after 2 Hours of treatment.

From the cross-sectional images presented in Figure 3 we can see that the morphology of the surface is just like clusters protruding from the surface. It could be established from SEM images that these clusters aggregate to form the petals of flower like microstructures seen in Figure 2. More study on the role and parameters of plasma affecting electrolysis need to be studied in details. These structures can be used for different biological applications especially for biomedical implants.

REFERENCES

1. Fang, J., Levchenko, I., & Ostrikov, K. K. (2014). Atmospheric plasma jet-enhanced anodization and nanoparticle synthesis. *IEEE Transactions on Plasma Science*, 43(3), 765-769.
2. TROMBOCITI, I. S. (2019). Performance of annealed TiO₂ nanotubes in interactions with blood platelets. *Materiali in tehnologije*, 53(6), 791-795.
3. Hahn, R., Macak, J. M., & Schmuki, P. (2007). Rapid anodic growth of TiO₂ and WO₃ nanotubes in fluoride free electrolytes. *Electrochemistry communications*, 9(5), 947-952.
4. Junkar, I., Kulkarni, M., Drašler, B., Rugelj, N., Mazare, A., Flašker, A., ... & Mozetič, M. (2016). Influence of various sterilization procedures on TiO₂ nanotubes used for biomedical devices. *Bioelectrochemistry*, 109, 79-86.

ACKNOWLEDGEMENTS

This research work was supported by the Slovenian Research Agency (ARRS) grants P2-0232

DISRUPTION OF PHOSPHOLIPID MEMBRANES WITH MAGNETO-MECHANICAL ACTUATION USING BARIUM-HEXAFERRITE NANOPLATELETS

Tanja Goršak^{1,2}, Mitja Drab³, Dejan Križaj⁴, Marko Jeran^{3,5}, Julia Genova⁶, Slavko Kralj¹, Darja Lisjak^{1,2}, Veronika Kralj-Iglič⁵, Aleš Iglič³, Darko Makovec¹

¹Department for Materials Synthesis, Jožef Stefan Institute, Jamova 39, SI-1000 Ljubljana, Slovenia; ²Jožef Stefan International Postgraduate School, Jamova 39, SI-1000 Ljubljana, Slovenia; ³Laboratory of Physics, Faculty of Electrical Engineering, University of Ljubljana, Tržaška 25, SI-1000 Ljubljana, Slovenia; ⁴Laboratory of Bioelectromagnetics, Faculty of Electrical Engineering, University of Ljubljana, Tržaška 25, SI-1000 Ljubljana, Slovenia; ⁵Laboratory of Clinical Biophysics, Faculty of Health Sciences, University of Ljubljana, Zdravstvena pot 5, SI-1000 Ljubljana, Slovenia; ⁶Institute of Solid State Physics, Bulgarian Academy of Sciences, Tzarigradsko 72, 784 Sofia, Bulgaria

Contact*: marko.jeran@fe.uni-lj.si & ales.iglic@fe.uni-lj.si

OUTLINE

Recently, various approaches were proposed for the destruction of different cancer cells using magnetic nanoparticles (MNPs) in combination with low-frequency AMF, *in vitro* and *in vivo*. Generally, the authors reported a significant decrease in the cell viability and cell apoptosis. This ascribes a lot of importance to the possible agglomeration of the MNPs during treatment.

METHODS

Preparation of nanoplatelet (NPL) suspensions

The substituted barium-hexaferrite NPLs were synthesized hydrothermally. The NPLs were coated with dextran in stable aqueous suspensions in several steps. The final suspensions were colorlessly stable, even in complex biological media. The dextran-grafted NPLs are referred to as HF-DEX. To modify the surface charge of the NPLs, a mixture of 90% dextran and 10% (3-maleopropyl)triethoxysilane (APS) was also grafted onto the NPLs surfaces (the NPLs HF-DEX+). The APS contains amino groups, which provide a positive surface charge on the NPLs.

Formation of giant unilamellar vesicles (GUVs)

The GUVs were prepared using a modified electroformation method from 1-glycyl-2-oleoyl-sn-glycero-3-phosphocholine (POPC) on two Pt electrodes in 0.3 mol/L sucrose solution at pH 7.0.

Characterization

The NPLs were characterized using a transmission electron microscope (TEM, Jeol 2010F) and a probe spherical-aberration corrected (CS) scanning transmission electron microscope (STEM, Jeol ARM 200CF). The magnetic properties of the NPLs were measured with a vibrating-sample magnetometer (VSM, LakeShore 7407) after they were aligned in the magnetic field. The zeta-potential was measured in suspensions diluted with distilled water to <0.1 mg/mL as a function of the pH using a ZetaPALS instrument (Brookhaven Instruments Corporation). The hydrodynamic size of the NPLs in suspension (at a concentration of 0.1 mg/mL) was measured with dynamic light scattering (DLS, Fritsch, Analysette 12 DynaStar).

Magneto-mechanical actuation (MMA)

The GUVs were exposed to magnetic nanoplatelets (HF-DEX or HF-DEX+) with the final concentration of the NPLs ranging from 1 μ g/mL to 1 mg/mL, and the pH was adjusted to an exact value with diluted HCl (pH 4.2, 5.2, or 7.0). The suspension of GUVs with NPLs was then exposed to a uniaxial, isotropic AMF at various frequencies and amplitudes. The solutions of the GUVs with added NPLs were monitored with a phase-contrast optical microscope (Nikon Eclipse N2000-e) while exposed to the AMF. To quantify the effect of MMA, the GUV/NPL suspensions were exposed to the AMF for fast periods of time and subsequently analyzed with the microscope.

Magnetic actuation of GUVs in an external alternate magnetic field (AMF)

Theoretical description of the mechanism of force transfer between the nanoplatelet and the membrane and derived a term for determining the efficiency of local torque transfer of adsorbed magnetic nanoparticles to biological membranes.

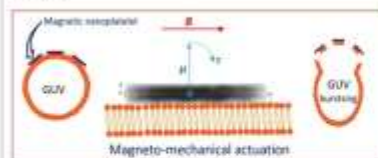


Figure 1: The main idea of the research work.

EXPERIMENT

The GUVs were exposed to barium-hexaferrite nanoplatelets (NPLs, ~50 nm wide and 3 nm thick) with unique magnetic properties dominated by a permanent magnetic moment that is perpendicular to the platelet, at different concentrations (1–50 mg/mL) and pH values (4.2–7.4) of the aqueous suspension. The GUVs were observed with an optical microscope while being exposed to a uniaxial AMF (3–100 Hz, 2.2–10.6 mT).

RESULTS

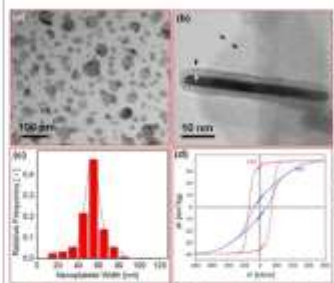


Figure 2: BF STEM (bright field STEM) image of dextran-grafted HF-DEX NPLs lying flat on the specimen support (a) and TEM image of a NPL oriented edge-on (b). The silica coating is marked with arrows. (c) Distribution of NPL widths expressed as an equivalent effective diameter. (d) Magnetic hysteresis loops for hexaferrite NPLs measured perpendicular (PER) and parallel (PAR) to their magnetic easy axes.

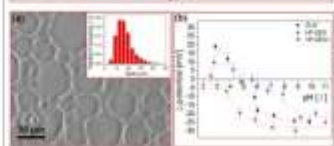


Figure 3: (a) Optical micrograph of GUVs (inset: distribution of GUV size) and (b) zeta-potential as a function of pH for suspensions of GUVs and NPLs. HF-DEX and HF-DEX+ nanoplatelets were suspended in a 0.3 mol/L aqueous glucose solution.

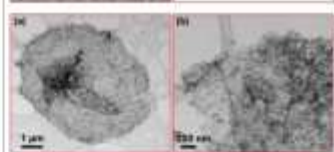


Figure 4: TEM images of a dried suspension of GUVs with HF-DEX nanoplatelets prepared at pH 4.2.

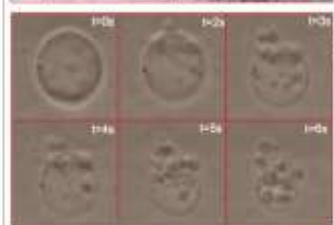


Figure 5: Time lapse image of a GUV with HF-DEX+ NPLs exposed to AMF ($B = 7$ mT, $f = 3$ Hz).

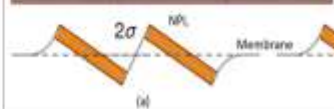


Figure 6: Two neighboring NPLs increase the lateral tension by a factor of 2, whether their magnetic dipole moments μ point in the same (a), or different directions (b).

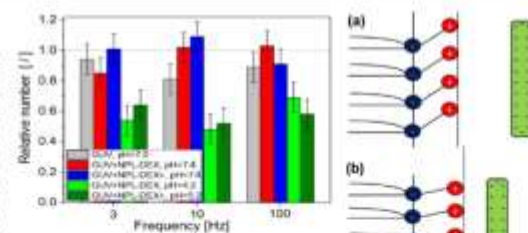


Figure 7: Relative number of GUVs after they were exposed to different NPLs (NPL-DEX or NPL-DEX, 0.01 mg/mL) for different pH values of the suspension (pH = 7.0, 5.2, 4.2) and treated with the AMF (10 minutes, $B = 7.0$ mT) at different frequencies (3, 10 and 100 Hz).

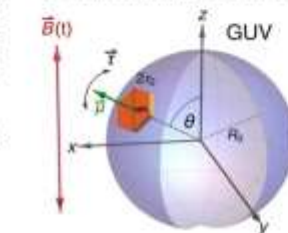


Figure 8: Schematic of a NPL at a polar angle θ attached to the outer membrane of a GUV with exaggerated proportions. The radius of the GUV is R_G , while the effective radius of the NPL is r_N . The AMF, shown with the red arrow, pulls and pushes the NPL into and from the GUV membrane, locally increasing its lateral tension τ . A symmetric situation applies to NPLs that adsorb with the magnetic moment pointing inwards.

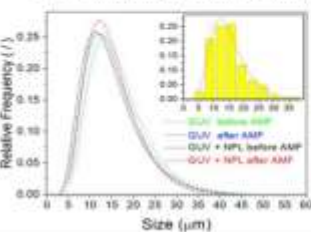


Figure 9: Size distribution of GUVs with and without NPLs (NPL-DEX+, pH = 5.2), before and after exposure to AMF ($f = 10$ Hz, $B = 7$ mT, $t = 10$ min). The empirical size distributions measured from optical micrographs were fitted with lognormal curves (see inset). No significant changes in the size distribution suggests a local, rather than a global effect of increased surface tension.

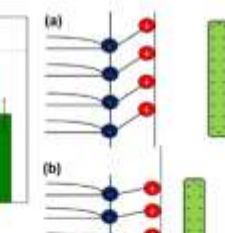


Figure 10: Schematic presentation of the average lipid dipolar (zwitterionic) headgroup orientation as a function of the distance from the negatively charged, plate like NPL, as predicted by molecular dynamics simulations and statistical thermodynamics modeling. At smaller distances the average orientation of the lipid headgroups changes from inclined (panel (a)) to more perpendicular (panel (b)).

CONCLUSIONS

When the NPLs were electrostatically attached to the GUV membranes, the MMA induced cyclic fluctuations of the GUVs' shape corresponding to the AMF frequency at the low NPL concentration (1 μ g/mL), whereas the GUVs were bursting at the higher concentration (10 μ g/mL). Theoretical considerations suggested that the bursting of the GUVs is a consequence of the local action of an assembly of several NPLs, rather than a collective effect of all the adsorbed NPLs.

The GUVs proved to be an efficient and relatively flexible model system (when compared to cell models) to study the MMA.

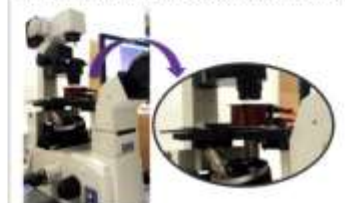


Figure 11: Optical microscope with a magnetic coil.

REFERENCE

Goršak T, Drab M, Križaj D, Jeran M, Genova J, Kralj S, Lisjak D, Kralj-Iglič V, Iglič A, Makovec D. Magneto-mechanical actuation of barium-hexaferrite nanoplatelets for the disruption of phospholipid membranes. *J. Coll. Interface Sci.* 579, 508-519, 2020.

ACKNOWLEDGEMENTS

The support of the Slovenian Research Agency (ARRS) within the Project L2-8166, P2-0232 and P3-0388 is acknowledged. We also acknowledge the CENN Nanocenter for the use of VSM equipment. We would like to acknowledge the fruitful discussions with Dr. S. Čopar and Dr. A. Kregar.



A novel approach to predicting hip dislocation in children with cerebral palsy: a case report

Petra Schara^{1*}, Karin Schara¹

¹University medical centre Ljubljana, Ljubljana, Slovenia

Contact*: petra.schara@gmail.com

OUTLINE

The prevalence of hip displacement in patients with cerebral palsy (CP) is reported between 1% and 75% (1). Early detection and prediction of hip dislocation is beneficial to the treatment of these patients. The purpose of this report was to demonstrate the use of Hipstress method in such patients.

METHODS

Male patient, 12 years of age with spastic CP, GMFCS IV, treated at the Orthopaedic Surgery Department University medical centre Ljubljana was chosen. Anteroposterior radiograph of the hips before surgery was obtained. The geometrical parameters were measured (Figure 1b). The biomechanical parameters of the left hip were calculated using the Hipstress method that consists of mathematical models for resultant hip force (2) in one legged stance and for determination of contact hip stress distribution (3).

CONCLUSIONS

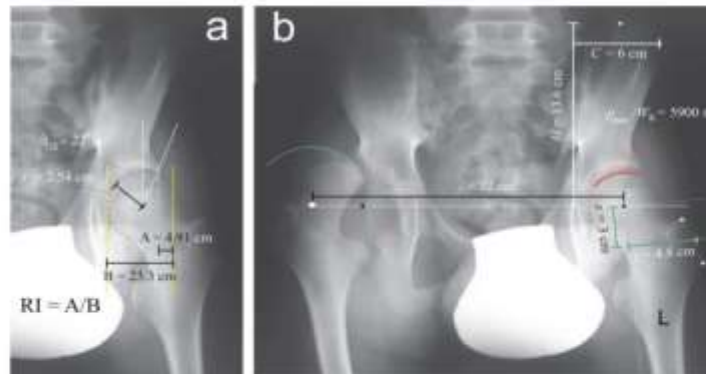
Recognizing hip displacement in children with CP depends on clinical signs and regular radiographs of the hips however initial stages can be difficult to detect. We have shown that assesment of the hips using the Hipstress method aids in earlier recognition of hips at risk for dislocation.

Further analysis is needed to assess the use of this method in planning the surgical treatment, assessing its success and odds of relaxation/reoperation.

RESULTS

The most common methods used to detect hip displacement in children with CP is migration index (MI). MI is defined as percentage of the bony width of the femoral capital epiphysis which falls lateral to a line drawn vertically from the bony lateral margin of the acetabulum (Perkins' line), on an anteroposterior pelvic radiograph. Surgical intervention is indicated if MI is greater than 0.3 (4). Some authors advocate for use of acetabular index (AI) as well. While MI reflects the consequences, a biomechanical parameter (contact hip stress) may also elucidate the mechanism of hip dislocation. According to the mathematical model within the Hipstress method, unfavourable stress distribution in the one-legged stance is characterized by a monotonous decrease of contact hip stress in the medial direction and by small functional angle of the weight bearing area. This is expressed by a positive hip stress gradient index (Gp).

An anteroposterior radiograph of a patient with CP shows dislocation of the right hip. The left hip appears not to be dislocated (Figure 1a). The MI of the left hip is 0.21. The calculation of hip stress distribution with the Hipstress method shows positive hip stress gradient index (Gp) in the left hip. MI did not show excessive migration of the femoral head but the unfavourable distribution of contact hip stress indicated a risk for dislocation. As the hip geometry before dislocation of the right hip was considered symmetric, the fact that the right hip underwent dislocation supports the indication that the geometry of these hips presents a risk for dislocation when standing on the leg.



The geometrical parameters used for calculation of the hip stress distribution according to the HIPSTRESS method were: interhip distance (I), pelvic height (H), pelvic width (C), position of the effective muscle attachment point on the greater trochanter (x and z) (Figure 1b), radius of the femoral head (r) and centre-edge angle (β CE) (Figure 1a), and the biomechanical parameters of the patient's left hip were: peak hip stress normalized to body weight $p_{max}/Wb = 5907 \text{ m}^{-2}$, position of the stress pole ($\theta = 38$ degrees) and normalized index of stress gradient $Gp/Wb = 39400 \text{ m}^{-3}$.

REFERENCES

- (1) Soo, B.; Howard, J.J.; Boyd, R.N.; Reid, S.M.; Lanigan, A.; Wolfe, R.; Reddiough, D.; Graham, H.K. Hip displacement in cerebral palsy. *J. Bone Jt. Surg. Am.* 2006, 88, 121–129.
- (2) Igljic A, Srakar F, Antolic V, Kraš Igljic V, Batagelj V. Mathematical analysis of Chiari osteotomy. *Acta Orthop Iugosl.* 1990; 20:35-39.
- (3) Kralj-Igljic V, Dolinar D, Ivanovski M, List I, Daniel M. Role of biomechanical parameters in hip osteoarthritis and avascular necrosis of femoral head. *Applied Biological Engineering - Principles and Practice*, Naik GR (Ed.), InTech, DOI: 10.5772/30159; 2012.
- (4) Robb JE, Hägglund G. Hip surveillance and management of the displaced hip in cerebral palsy. *J Child Orthop.* 2013; 7: 407-413.

ACKNOWLEDGEMENTS

The authors wish to thank the authors of Hipstress method and Prof. Veronika Kralj-Igljic.

EXTRACELLULAR VESICLES AND THEIR USE IN INNER EAR

Nejc Steiner^{1*}, Saba Battelino¹

¹ Clinic for otorhinolaryngology and cervicofacial surgery
University Medical Centre Ljubljana
Contact*: steiner.nejc@gmail.com

INTRODUCTION

Extracellular vesicles (EVs) are a heterogeneous group of **nanometrically sized cell-derived membranous structures** which can originate from any cell, including plant cell or bacteria. They were found in many body fluids including platelet-rich plasma (PRP) which is a blood-derived product with immune, hemostatic and regenerative effects. PRP is expected to contain important concentrations of EVs which could be important contributors to PRPs effects. (1)

CLASSIFICATION

Is done based on **physical characteristics, biochemical composition** and by descriptions of **conditions or cell of origin**. But mostly they are classified as:

- o **MICROVESICLES:** 50–500 nm
 - formed by budding.
- o **EXOSOMES:** 50–150 nm
 - formed by exocytosis of intracellular compartments. (1)

MODE OF ACTION OF EXTRACELLULAR VESICLES

EVs exert a physiological or pathological response when reaching a target cell. Target cell can be adjacent, distant or an origin cell. The latter implies an important role of EVs in autoregulation. There are three modes of action of EVs:

1. binding with plasma cell membranous receptors (cellular signalling).
2. the fusion of EV and plasma membrane which causes a cytosolic release of EV cargo.
3. Uptake of EV by plasma membrane with endocytosis. (1)

EV IN INNER EAR

Only a few studies regarding EVs in inner have been published. In theory EVs could serve as a potential carriers for inner ear delivery of different effectors.

Gene therapy for hearing disorders is **not yet as advanced**, mostly because gene **delivery** to sensory hair cells of the inner ear is **inefficient**.

- In order to achieve better delivery Bence György et. all. demonstrated that a vector, exosome-associated AAV, is a **potent carrier** of transgenes **to all inner ear hair cells** and **may be useful for gene therapy for deafness**. (2)

Drug- and noise-related hearing loss are associated with inflammatory responses in the inner ear.

- **Intracochlear delivery** of a combination of pro-resolving mediators, specialized proteins and lipids might have a profound effect on the **prevention of sensorineural hearing loss**. They **accelerate the return to homeostasis** by modifying the immune response rather than by inhibiting inflammation. Gilda M. Kalinec et. all. provided evidence that auditory hair cells generated abundant **EVs** that can be **loaded** with cocktail of **molecules** aimed at **accelerating inflammation resolution** and **improving** the organ response to **inflammation damage**. (3)

Hair cell death and consequent hearing loss are common results of treatment with **ototoxic drugs**, including the widely used aminoglycoside antibiotics.

- Andrew M. Breglio et. all. studied how to decrease the negative effect of ototoxic drugs. They showed that in response to **heat stress**, inner ear tissue **releases exosomes** that **improved the survival of hair cells** exposed to the aminoglycoside antibiotic neomycin, whereas **inhibition** or depletion of exosomes from the extracellular environment **abolished the protective effect of heat shock**. (4)

Described studies indicate that extracellular vesicles have a **role in intercellular communication of the inner ear** and can **mediate nonautonomous hair cell survival**. In **future** extracellular vesicles may serve as nanocarriers for the **delivery of therapeutics against hearing loss**.

REFERENCES

1. Vozel, D. *et al.* 'Treatment with platelet- and extracellular vesicle-rich plasma in otorhinolaryngology- a review and future perspectives', in *Advances in Biomembranes and Lipid Self-Assembly*. Academic Press. 2020
2. György B, Sage C, Indzhukulian AA, Scheffer DI, Brisson AR, Tan S, Wu X, Volak A, Mu D, Tamvakologos PI, Li Y, Fitzpatrick Z, Ericsson M, Breakefield XO, Corey DP, Maguire CA. Rescue of Hearing by Gene Delivery to Inner-Ear Hair Cells Using Exosome-Associated AAV. *Mol Ther*. 2017
3. Kalinec GM, Gao L, Cohn W, Whitelegge JP, Faulk KF, Kalinec F. Extracellular Vesicles From Auditory Cells as Nanocarriers for Anti-inflammatory Drugs and Pro-resolving Mediators. *Front Cell Neurosci*. 2019
4. Breglio AM, May LA, Barzik M, Welsh NC, Francis SP, Costain TQ, Wang L, Anderson DE, Petralia RS, Wang YX, Friedman TB, Wood MJ, Cunningham LL. Exosomes mediate sensory hair cell protection in the inner ear. *J Clin Invest*. 2020



DETERMINATION OF RESULTANT HIP FORCE AND CONTACT HIP STRESS FROM MAGNETIC RESONANCE IMAGES

Jovana Mitić^{1*}, Matej Daniel², Slavica Ponorac³, Raja Gošnak Dahmane¹, Veronika Kralj-Iglič^{1*}

¹Faculty of Health Sciences, University of Ljubljana, Ljubljana, Slovenia, ²Czech Technical University in Prague, Prague, Czech Republic, ³University Medical Centre Ljubljana, Ljubljana, Slovenia

Contact*: jovana.mitic@ir-rs.si, veronika.kralj-iglic@fe.uni-lj.si

OUTLINE

Biomechanical parameters of the hip joint such as forces and stresses are associated with hip development^{1,2} and are useful in the study of the mechanisms underlying diseases as well as in preventing and planning surgical and therapeutic procedures of individual subjects^{2,3}. To determine biomechanical parameters of the hip we have used HIPSTRESS mathematical models within HIPSTRESS method, in which the human body is considered as composed of segments subjected to muscle forces, weight and resultant intersegment forces⁴.

METHODS

Magnetic resonance imaging⁵ (Fig. 2) was used retrospectively to measure origins, insertions and cross-sectional areas of the hip joint muscles^{4,6}. The image data was taken for the purpose of examining the proximal femora of a 17-year-old boy with Ewing's sarcoma, and data from the healthy side was used. The input data on positions of muscle attachment points were assessed directly from magnetic resonance images, and by re-scaling the data of the acknowledged HIPSTRESS model⁴ according to the shape of pelvis and proximal femora. The resultant hip force and the distribution of contact stress were calculated using three different mathematical models within the HIPSTRESS method (validated HIPSTRESS model with reduction method⁴, HIPSTRESS model using the magnetic resonance images and optimization method and two-dimensional one-muscle model⁷).



Fig. 1: Scheme of the hip articular sphere with stress pole and geometrical and biomechanical parameters of the one-muscle model in the frontal plane of the body¹. I: interhip distance, H: pelvic height, C: pelvic width, CE: center edge angle of Wiberg, Wb: body weight, WL: weight of a leg, F: effective muscle force, IF: inclination of the muscle force, pmax: peak contact stress, IF: functional angle of weight bearing, R: resultant hip force

The HIPSTRESS model for resultant hip force R is based on equilibria of forces and torques while the HIPSTRESS model for stress considers Hooke's law for cartilage between acetabulum and femoral head and connection between contact stress p and resultant hip force $R = \int p \, dA$, where dA is an area element. Integration is performed over the load bearing area.

CONCLUSIONS

All three models yielded the magnitude of the resultant hip force and peak stress on the load bearing area within 20 % difference. As assessment of muscle attachment points is time consuming, use of two dimensional images is justified in population studies. In clinical practice, the use of magnetic resonance images to evaluate geometrical and biomechanical data is optional, since it provides more information of the individual subject.

RESULTS

We established that the validated HIPSTRESS model overestimates the value of hip force by 16 % and peak hip stress by 20 % (Table 1), while one-muscle model overestimates force by 9 % and peak hip stress by 1 % in comparison to HIPSTRESS model with magnetic resonance. The biomechanical parameters calculated by using the magnetic resonance images were taken as a reference. The validated HIPSTRESS model and one-muscle model underestimated the inclination of the resultant hip force and the position of the stress pole with respect to reference (Table 1), while the validated HIPSTRESS model and the one-muscle model overestimated resultant hip force and peak stress for less than 20 % with respect to the reference. We found that the added muscles in the HIPSTRESS model with magnetic resonance did not significantly contribute to the value of the hip joint load.

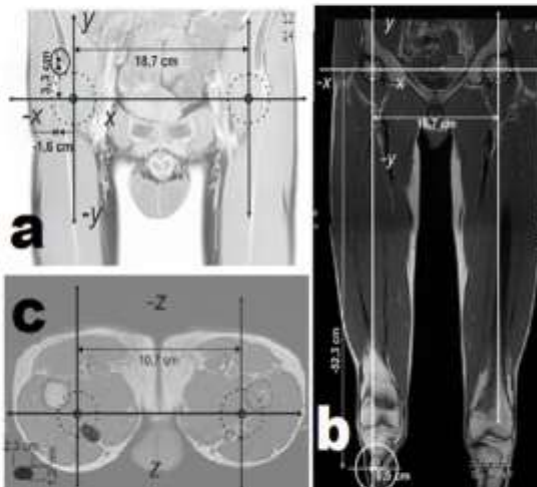


Fig. 2: The attachment points of rectus femoris muscle at the upper body segment (a) and lower body segment (b), and assessment of the cross-section of the muscle (c). The attachment point at panel (a) is marked by a black dot and at panel (b) by a white dot. The cross-section of the muscle in panel (c) is fitted by an ellipse which is also shown in the lower-left corner of the panel (c)

Table 1: Biomechanical parameters of the hip joint calculated by three models within the HIPSTRESS method

	Model		
	Validated HIPSTRESS model	HIPSTRESS model with magnetic resonance	One-muscle model
	9 muscles reduction method	15 muscles optimization method	1 muscle
Biomechanical parameters			
R/W_b	2,87	2,44	2,67
β_R [°]	7,0	9,9	6,1
θ [°]	10	4,5	11
p_{max}/W_b [m ⁻²]	2972	2414	2420

R/W_b : resultant hip force normalized by body weight in the one-legged stance, β_R : inclination of resultant hip force, θ : position of stress pole, p_{max}/W_b : contact peak stress

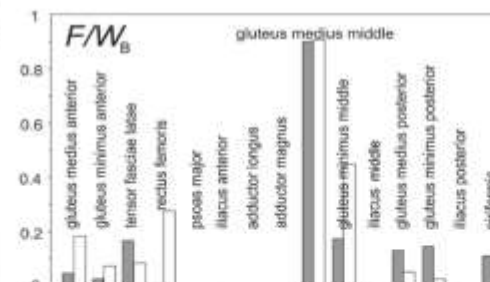


Fig. 3: The distribution of load between the muscles in the HIPSTRESS models. Load distribution obtained by an optimization method involving 15 muscles (white columns) compared to a reduction method involving nine muscles (gray columns)

REFERENCES

- Daniel M, Iglič A, Kralj-Iglič V, Konvicková S (2005). Computer system for definition of the quantitative geometry of musculature from CT images. *Comput Methods Biomech Biomed Engin* 8(1): 25–9.
- Hosrieh FS, Zuidewijk ME, Versteeg M et al (2017). Cam deformity and acetabular dysplasia as risk factors for Hip osteoarthritis. *Arthritis Rheumatol* 69(1): 86–93.
- Genda E, Iwasaki N, Li G, MacWilliams BA, Barrance PJ, Chao EY (2001). Normal hip joint contact pressure distribution in single-leg standing—effect of gender and anatomic parameters. *J Biomech* 34(7): 895–905.
- Kralj-Iglič V (2015). Validation of mechanical hypothesis of hip arthritis development by HIPSTRESS method. In: Chen Q, ed. *Osteoarthritis: progress in basic research and treatment*. Rijeka: InTech, 131–56.
- Sokletos T, Ahlawat S, Montgomery E, Chellan M, Jacobs MA, Fayad LM (2016). Multiparametric assessment of treatment response in high-grade soft-tissue sarcomas with anatomic and functional MR imaging sequences. *Radiology* 278(3): 831–40.
- Iglič A, Srakar F, Antolčić V, Kralj-Iglič V, Batagelj V (1990). Mathematical analysis of Chan osteotomy. *Acta Orthop Jugosl* (2012–3): 35–9.
- Uršič B, Kocjančič B, Rommolo A, Iglič A, Kralj-Iglič V, Zupanc O (2020). Assessment of coxarthrosis risk with dimensionless parameters. *Acta Bioeng Biomech*, in print.

ACKNOWLEDGEMENTS

The authors acknowledge prof. Aleš Iglič, PhD, and Urška Puh, PhD, for professional support and guidance. The authors also thank Slovenian Research Agency for grants P3-0388 and P2-0323.

QUALITY MANAGEMENT TOOLS AND RESEARCH ACTIVITIES: AN INNOVATIVE CROSS-CONTAMINATION

Annamaria Kisslinger (1), Darja Božič (2), Giorgia Adamo (3), Meiyu Gai (4), Sabrina Picciotto (3), Marko Jeran (2), Christopher Stanly (5), Pamela Santonicola (5),

Samuele Raccosta (6), Carolina Paganini (7), Umberto Capasso (7), Antonella Cusimano (3), Daniele Romancino (3), Rita Carrotta (6), Vincenzo Martorana (6), Rosina Noto (6), Nicolas Touzet (8), Paolo Arosio (7), Elia Di Schiavi (5), Mauro Manno (6),

Gabriella Pocsfalvi (5), Svenja Morsbach (4), Katharina Landfester (4), Ales Iglic (2), Veronika Iglic (2), Antonella Bongiovanni (3) and Giovanna L. Liguori (9)

(1) National Research Council of Italy (CNR), Institute of Experimental Endocrinology and Oncology (IEOS), Napoli, Italy, (2) Faculty of Health Sciences, University of Ljubljana, Ljubljana, Slovenia (3) CNR, Institute for Biomedical Research and Innovation (IRIB), Palermo, Italy, (4) Max-Planck Institute for Polymer Research, Mainz, Germany, (5) CNR, Institute of Biosciences and BioResources (IBBR), Napoli, Italy, (6) CNR, Institute of Biophysics, Palermo, Italy, (7) ETH Zurich Institute for Chemical and Bioengineering, Zurich, Switzerland, (8) Institute of Technology Sligo (ITSligo), Sligo, Ireland (9) CNR, Institute of Genetics and Biophysics (IGB), Napoli, Italy

OUTLINE

Quality Management in scientific R&D is emerging as an essential tool to ensure valuable and robust outcomes, within a framework of best practice (1-4). In line with the need of integrating Quality standards within biological research, recent EU calls for research projects either require or strongly suggest a transversal Quality Management work package (WP) to ensure the training, control, and application of Quality methods. Recent examples of the application of International Organization for Standardization—ISO 9001:2008 standards in research structures have indicated many advantages in terms of governance, control, efficiency, and results. The EV field is very sensible to standardization and reproducibility issues and can take great advantages from the implementation of one or more Quality Management (QM) tools to support research activities as well as to set-up and validate common scientific procedures (5).

METHODS

According to our previous experience in realizing a Total Quality Management (TQM) model for biomedical research laboratories (quality4lab.cnr.it/en) we developed a **Quality Management Plan (QMP)**, compatible to **UNI EN ISO 9001:2015 standards** and customized for the needs of EV research. The **VES4US QMS** has been created by the Quality Managers of the Project with the contribution and support of all the Partners, discussed and validated by Coordinator and SC. This document defines the **Quality Management System (QMS)** developed and implemented by the **VES4US Consortium** to ensure the quality, consistency and reliability of the project results and deliverables (5).

RESULTS

Quality Management can be divided into three process groups, shown with the relative outcomes in **Figure 1**. In the **planning phase (Fig. 2)**, **VES4US QMS** was developed to be very light, focused and flexible as well as customized for the needs of a multicentre and multidisciplinary research project. Special care has been devoted to the development of a **Laboratory Notebook**, in both electronic and paper version, and of **Standard Operating Procedures**. In the **executing phase (Fig. 3)**, different SOPs were developed, validated and distributed among partners to guarantee homogeneity and reproducibility of the procedures. The **VES4US QMS** is being continuously updated and improved and feedbacks are usually collected by means of Audits and CheckLists as shown in **Figure 4**.

Figure 2. PLANNING



Figure 1. QMS_PROCESSES



Figure 3. EXECUTING

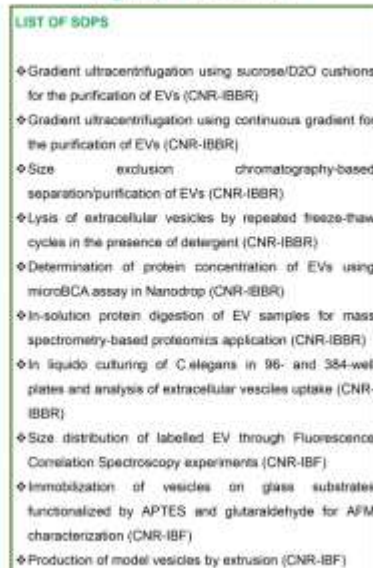


Figure 4. MONITORING



CONCLUSIONS

The **VES4US QMS** represents an innovative approach with cross application in research environments. Research activities and Quality Management should meet, mix and contaminate to produce new tools and methodologies that are really tailored on research and researcher identity and can really support and not cage knowledge. The **VES4US QMS** could be an operating model for EV research project networks and more generally for research projects, characterised by high risks, strong interdisciplinary and multicentre character, and focusing on the development and standardization of new potentially breakthrough technologies.

REFERENCES

1. A. Bongiovanni et al, Applying Quality and Project Management methodologies in biomedical research laboratories: a public research network's case study. *Accredit. Qual. Assur.* 20 (2015) 203–213.
2. F.A. Diglio et al, Quality-based model for Life Sciences research guidelines. *Accredit. Qual. Assur.* 21 (2016) 3. S.
3. Manciniet al, Applying Design of Experiments Methodology to PEI Toxicity Assay on Neural Progenitor Cells. in: *Math. Model. Biol.*, 2015.
4. A. Mascia et al, An original approach to quality in a life science research laboratory: the Failure Mode and Effect Analysis (FMEA) Accreditation and Quality Assurance, 2020.
5. G. L. Liguori and A. Kisslinger, Standardization and reproducibility in EV research: the support of a Quality management system ABLSA: Biological Membrane Vesicles: Scientific, Biotechnological and Clinical Considerations Volume 32, 2020. doi.org/10.1016/bs.abl.2020.05.005



ANKLE DORSIFLEXION RANGE OF MOTION MEASUREMENT TOOLS

Helena Žunko^{1*}, Renata Vauhnik²

¹University of Ljubljana, Biotechnical Faculty, Ljubljana, Slovenia ²University of Ljubljana, Faculty of Health Sciences, Ljubljana, Slovenia
Contact*: helena.zunko@gmail.com

OUTLINE

Increasing the range of ankle dorsiflexion (ADROM) is a common physiotherapeutic goal. Valid, reliable, and accurate goniometric measurements are required in order to assess the effectiveness of therapeutic procedures and further treatment planning. Weight-bearing measurement is gaining popularity, since the procedure is reliable and more suitable for functional assessment than non weight-bearing ADROM measurement procedures (1,2). Numerous different measurement procedures have been developed. The aim of this poster is to present various measurement tools for weight-bearing ADROM measurements.

METHODS

Literature review was conducted using databases PubMed, Cochrane, Medline, PEDro and Cobiss.

CONCLUSIONS

There is a wide variety of measurement tools available. Standardisation of measurement procedures is necessary.

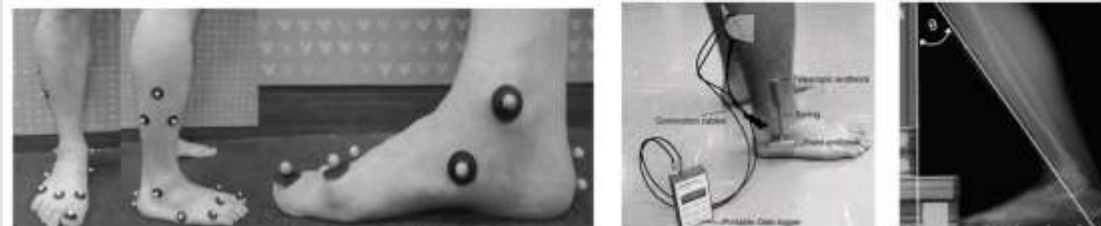
RESULTS



Universal standard goniometer, Digital gravity goniometer, Liquid gravity goniometer (1), Mobile goniometer application (1)



Centimeter tape measure (1), Special device (3), Leg motion system (4)



Motion capture system (5), Electric goniometer (6), Radiological measurement (7)

REFERENCES

- Žunko H, Puh U (2016). Zanesljivost merjenja obsega gibljivosti skočnega sklepa v stoječem položaju – pregled literature. *Fizioterapija* 24(1): 25–33.
- Powden CJ, Hoch JM, Hoch MC (2015). Reliability and minimal detectable change of the weight-bearing lunge test: A systematic review. *Manual Therapy* 20: 524–32.
- Watson CP, Boland RA, Refshauge KM (2008). Measurement reliability of swelling in the acute ankle sprain. *Foot Ankle Int* 1(12): 4.
- Romero Morales C, Calvo Lobo C, Rodriguez Sanz D, Sanz Corbalán I, Ruiz Ruiz B, López López D (2017). The concurrent validity and reliability of the Leg Motion system for measuring ankle dorsiflexion range of motion in older adults. *PeerJ*. Jan 3;5:e2820
- Kim EJ, Shin HS, Lee JH, Kyung MG, Yoo HJ, Yoo WJ, Lee DY (2018). Repeatability of a multi-segment foot model with a 15-marker set in normal children. *Clin Orthop Surg*. Dec;10(4):484-490.
- Tarnita D., Oncescu A.T. (2020) Sensors used for human gait monitoring. In: Dumitru I., Covaciu D., Racila L., Rosca A. (eds) *The 30th SIAR International Congress of Automotive and Transport Engineering. SMAT 2019*. Springer, Cham.
- MacDonald D, Vicenzino B (2019). How Much Does the Talocrural Joint Contribute to Ankle Dorsiflexion Range of Motion During the Weight-Bearing Lunge Test? A Cross-sectional Radiographic Validity Study. *J Orthop Sports Phys Ther*. Dec;49(12):934-941.

ACKNOWLEDGEMENTS

The authors acknowledge the financial support from the Slovenian Research Agency (research core funding no. P3-0388).



COAGULATION PROFILE OF BRACHYCEPHALIC DOGS WITH BRACHYCEPHALIC OBSTRUCTIVE AIRWAY SYNDROME

Alenka Nemec Svete, Vladimira Erjavec*

University of Ljubljana, Veterinary Faculty, Small Animal Clinic,
Gerbičeva 60, 1000 Ljubljana, Slovenia
Contact*: vladimira.erjavec@vf.uni-lj.si

OUTLINE

Brachycephalic Obstructive Airway Syndrome (BOAS) is characterised by numerous airways anomalies, which are associated with a variety of clinical signs. In addition, BOAS is also associated with dysfunction of other systems (e.g., pulmonary, digestive, cardiovascular, coagulation and immune) and should be considered a systemic disorder. The presence of a hypercoagulable state was detected in clinically healthy Bulldogs and severely affected BOAS patients using thromboelastography. However, the results of routine coagulation tests have not yet been reported in BOAS patients.

The aim of the present study was to determine coagulation profile, including prothrombin time (PT), activated partial thromboplastin time (APTT) and D-dimer concentration in dogs with various grades of BOAS and healthy non-brachycephalic dogs.

METHODS

Dogs: Seventy-four client-owned dogs with BOAS and 8 healthy age-matched non-brachycephalic dogs. All BOAS patients were admitted to the Small Animal Clinic for surgical treatment of BOAS. The diagnosis of BOAS was based on clinical signs of upper airway obstruction and anatomical anomalies.

Inclusion criteria: history, clinical examination, complete blood count and white blood cell differential count, blood gas analysis, biochemistry and owner questionnaire.

Exclusion criteria: concurrent diseases.

Coagulation analyses: coagulation parameters were measured with an automated coagulation analyser STA Satellite (Diagnostica STAGO, France) and commercially available reagents (all Diagnostica Stago, France): Neoptimal® (PT), Cephascreen® (APTT) and LIATEST® D-Di (D-dimer).

Statistical analysis: IBM® SPSS 24.0 (USA); Kruskal-Wallis test followed by multiple comparisons with Bonferroni correction.

The significance level: 5%.

CONCLUSIONS

We may conclude that the routine coagulation parameters in BOAS patients are not altered.

However, further studies that include larger groups of BOAS patients and control dogs, as well as other haemostasis parameters are warranted.

RESULTS

The BOAS patients were classified into grade 1, grade 2 and grade 3 (Table 1), according to the severity of the disease. Patients in grade 3 were significantly older ($p = 0.028$) than grade 1 patients (Table 1), which could be due to the progressive nature of the disease.

Table 1: Demographic data of brachycephalic dogs with various grades of BOAS and healthy non-brachycephalic dogs (Control)

	Grade 1	Grade 2	Grade 3	Control
Number	13	28	33	8
Sex (F/M)	6/7	12/16	11/22	5/3
Age (months)				
Median (IQR)	13 (8.5 – 28.5)	33.5 (16.5 – 52.8)	36.0 (19.5 – 67.0)*	45.0 (27.0 – 55.5)
Weight (kg)				
Median (IQR)	8.5 (6.5 – 12.1)	10.0 (8.5 – 12.6)	12.2 (9.5 – 15.3)	12.2 (9.5 – 15.3)

*Significant difference ($p = 0.028$) in comparison to Grade 1 patients. IQR, interquartile range

Median values of most of the routine coagulation parameters remained within reference ranges in all grades of BOAS patients and control dogs (Table 2). Median values of PT in grade 1 patients and control dogs were slightly above the upper value of the reference range; however, the dogs were clinically healthy.

In addition, we did not find a significant difference between BOAS patients and control dogs in any of the measured coagulation parameters.

Table 2: Coagulation parameters (median (IQR)) of brachycephalic dogs with various grades of BOAS and healthy non-brachycephalic dogs (Control)

	Grade 1	Grade 2	Grade 3	Control	Reference ranges
PT (s)	9.35 (8.93 – 9.85)	8.90 (8.50 – 9.25)	8.70 (8.35 – 9.05)	9.25 (8.63 – 9.60)	6.9 – 9.0
APTT (s)	15.5 (14.3 – 17.3)	14.3 (13.5 – 17.5)	13.6 (12.9 – 15.5)	14.3 (13.5 – 15.5)	13.1 – 17.7
D-dimer (µg/L)	120 (97.5 – 165.0)	175 (120.0 – 210.0)	190 (120.0 – 240.0)	150 (140.0 – 180.0)	23.0 – 654.0



CT image of a brachycephalic dog (French Bulldog)



CT image of a mesocephalic dog (poodle)



Automated coagulation analyser STA Satellite (Diagnostica Stago, France)

REFERENCES

1. Bauer N, Erlep O, Moritz A. Reference intervals and method optimization for variables reflecting hypocoagulatory and hypercoagulatory states in dogs using the STA Compact automated analyzer. *J Vet Diagn Invest* 2009; 21: 803–14.
2. Crane C, Rozanski EA, Abelson AL, deLaforcade A. Severe brachycephalic obstructive airway syndrome is associated with hypercoagulability in dogs. *J Vet Diagn Invest* 2017; 29 (4): 570–3.
3. Geffre A, Grollier S, Hanot C et al. Canine Reference Intervals for Coagulation Markers Using the STA Satellite® and the STA-R Evolution® Analyzers. *J Vet Diagn Invest* 2010; 22: 690–5.
4. Hoareau GL, Mellema M. Pro-coagulant thromboelastographic features in the bulldog. *J Small Anim Pract* 2015; 56 (2): 103–7.
5. Meola SD. Brachycephalic airway syndrome. *Top Companion Anim Med* 2013; 28: 91–6.



French Bulldog

ACKNOWLEDGEMENTS

The authors acknowledge the financial support of the Slovenian Research Agency (Research program P4-0053).

The authors thank Rebeka Turk and Luka Šparš, undergraduate students of Veterinary medicine, for the help with collection and preparation of blood samples, and Estera Pogorevc for providing CT images.

Towards the Development of a novel continuous Extracellular Vesicle production system in plants

Maneea Moubarak¹; Pasquale Chiaiese² and Gabriella Pocsfalvi^{1,*}

1-EVs-MS Research Group, Institute of Biosciences and BioResources (IBBR), National Research Council, (CNR), 80131 Napoli, Italy

2-Department of Agricultural Sciences, University of Federico II, Italy

Contact*: gabriella.pocsfalvi@ibbr.cnr.it.com

OUTLINE

Extracellular vesicles (EVs) are small nanostructures surrounded by a lipid bilayer-based biomembrane. They are secreted by all types of cells. They are widely studied in mammalian cells when compared to plant cells. EV-like vesicles have been isolated from different parts of edible plants, like ginger and carrot roots or grapes, grapefruit¹, clementine² and tomato fruits. Plant-derived nanovesicles are being exploited as delivery vectors for nutraceuticals and cosmeceuticals. There is a longstanding debate on the capability of plants to secrete EVs outside their semi-rigid cell wall³.

GreenEV is a H2020-MSCA-IF-2019 European project started on 1st December, 2020. Its main objective is to develop a novel continuous EV production system. In greenEV project we will study two model plants: tomato (*S. lycopersicum* L) and ginkgo. Here, we present our preliminary results in the establishment of cell tissue culture of tomato for the production of EVs using two varieties of tomato, M82 and Microtom.

METHODS

Cell tissue culture:

The tomato seeds were sterilized according to established protocols. Seeds were cultured on Murashige and Skoog (MS) medium under aseptic conditions. The cultures were incubated under controlled conditions at 25°C for germination. Segments of leaves, stems and roots taken from the in vitro grown seed plants and were used for callus induction in MS medium containing 2,4-Dichlorophenoxy acetic acid (2,4-D) at 2mg/L (w/v). After two sub-culturing, calli were placed on the cell suspension culture medium, i.e. MS liquid media with 2,4-D (2 mg/L) without any agar and was maintained under suitable conditions. Cell suspension cultures were initiated by culturing cells in liquid media. 4 successive subcultures were collected for counting the cells and to isolate EVs.

Isolation of EVs:

The EVs were isolated from cell suspension culture from the three different parts (stems, leaves and roots) by using differential ultracentrifugation (dUC) method. Isolated EVs were characterized by protein content using the micro BCA assay with nanodrop detection. Density of the EV containing fractions were determined by iodixanol gradient ultracentrifugation. SDS PAGE analysis was performed under standard conditions.

The various steps used in this work is shown in Fig 1.



Figure 1 Simplified workflow used in this work

RESULTS

The seeds started to grow after 1-2 weeks. All segments from leaves, stem and root on the MS medium with 2,4-D (2 mg/L) were characterized as being fast callus induction (Fig 2A,B). For initiation of the suspension cell culture and for subculturing liquid media containing 2,4-D at 2mg/L were found to be effective. Within 4 subculturing these media gave rise loose, friable cells from cultured callus (Fig 3A,B).

High yields of EVs were obtained from the different suspension cultures using dUC isolation method (Table 1). M82 leaf suspension culture produced the highest EV protein amount (92 µg/mL culture medium) followed by Microtom leaf and root. The highest EV yield per cell was associated to Microtom root (233 pg protein per cell) followed by M82 leaf. Based on this data the best EV producing batch culture system were M82 leaf and Microtom root (Fig 4).

Protein profiles of the EVs isolated from the different batch suspension culture by SDS are shown in Fig 5.

The density of EVs was measured for the M82 stem samples using iodixanol continuous gradient ultracentrifugation. Two visible bands were observed at 1.098 and 1.117 g/mL densities (Fig 6A,B).

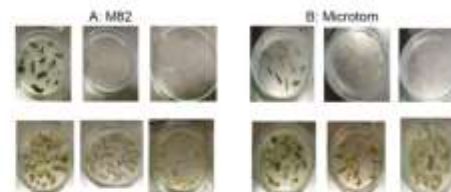


Figure 2. Explants and callus from *S. Lycopersicum* L. A) M82 and B) Microtom varieties.



Fig 4. Isolation of EVs by differential and density gradient ultracentrifugation



Fig 3: Maintenance for cell suspension culture from *S. Lycopersicum* L. A) M82 and B) Microtom varieties.

Table 1 Yield of EVs obtained in *S. Lycopersicum* L (M82 and Microtom) batch suspension cultures expressed in protein amounts (µg/cell)

Plant part	Variety	Total volume of suspension culture (mL)	Total quantity of protein (mg)	EV yield µg/mL culture	Number of cells x 10 ⁶	EV yield (pg/cell)
leaf	M82	110	10.08	92	69	146
seed	M82	86	2.75	32	29	94
root	M82	82	4.803	59	47	102
leaf	Microtom	30	2.38	79	17	129
seed	Microtom	132	5.4	41	42	130
root	Microtom	136	9.51	70	41	233

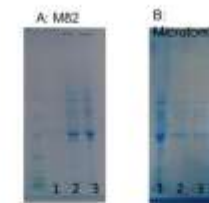


Figure 5. SDS-PAGE protein profiles of EVs isolated by dUC from the suspension cultures of root, stem and leaves A) M82 and B) Microtom varieties: 1 Root, 2 Stem and 3 Leaf.

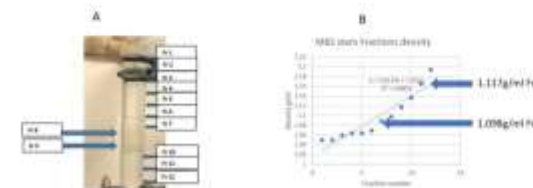
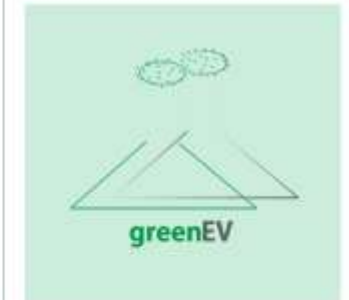


Fig 6. Iodixanol gradient ultracentrifugation separates M82 stem suspension culture derived EVs into two visible bands A) Fraction 8 and Fraction 9 and B) The graph shows the density of the different fractions showed in A.

CONCLUSIONS

We successfully set up the batch suspension cultures for M82 and Microtom tomato varieties to produce between 30-136 mL culture supernatant. These were used to isolate EVs using the established differential ultracentrifugation procedure. Protein concentrations were measured and isolates were successfully characterized for protein profiles. SDS-PAGE profiles of EVs show complex protein patterns. Iodoanal gIUC was applied to separate the EVs into two visible bands within the EV density range. Preliminary results show that cell suspension culture is a promising source of plant EVs.



REFERENCES

- Wang B et al. Targeted drug delivery to intestinal macrophages by bioactive nanovesicles released from grapefruit. *Mol Ther* . Mar;20(3):522-534 [2013]
- Stanly C et al Membrane Transporters in Citrus clementine Fruit Juice-Derived Nanovesicles. *Int. J. Mol. Sci.* 20, 6205-2-11[2019]
- Cui Y et al. Plant extracellular vesicles. *Protoplasma* 257(1) [2019]

ACKNOWLEDGEMENTS

 This project has received funding from the European Union's Horizon 2020 research and innovation programme under the Marie Skłodowska-Curie grant agreement No 885575 project acronym "greenEV".



This project has received funding from the European Union's Horizon 2020 research and innovation programme under grant agreement No 8011338

Nanoalgosomes: analyses of the cellular uptake

Sabrina Picciotto ⁽¹⁾, Giorgia Adamo ⁽¹⁾, Daniele Romancino ⁽¹⁾, Estella Rao ⁽²⁾, Angela Paterna ⁽²⁾, Samuele Raccosta ⁽²⁾, Rosina Noto ⁽²⁾, Rita Carrotta ⁽²⁾, Nicolas Touzet ⁽³⁾, Mauro Manno ⁽²⁾, Antonella Bongiovanni ⁽¹⁾

(1) Institute for Biomedical Research and Innovation (IRIB) - National Research Council of Italy (CNR), Italy; (2) Institute of Biophysics - National Research Council of Italy (CNR), Italy; (3) Institute of Technology Sligo – ITSligo

Contact*: antonella.bongiovanni@cnr.it

OUTLINE

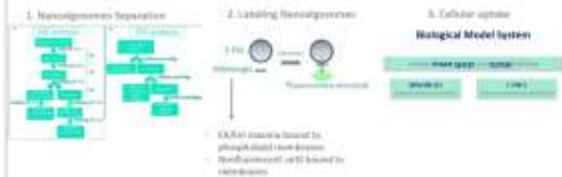
VES4US is a European project funded by the Horizon 2020 Future and Emerging Technology (ET) Open program, which aims to develop an innovative platform for the efficient production of extracellular vesicles (EVs) from a renewable biomass, enabling their exploitation as safe and effective products in the field of nanomedicine, cosmetics and nutraceuticals (<https://ves4us.eu>).

Here, we describe the newly discovered subtypes of EVs derived from microalgae, which we named **nanoalgosomes**. Specifically, we focus on the cellular uptake of the nanoalgosomes, confirming that nanoalgosomes actively bypass cell membrane and that they were uptaken through an energy-dependent mechanism.

METHODS

From the microalgae conditioned culture media we isolated two EV sub-populations: nanovesicles and nanovesicles with two different methods: 2D-Differential ultracentrifugation (2D-U) the classical method for EV enrichment and tangential flow filtration (TFF).

For labeling of EVs, we selected a specific fluorescent dye: DiI1049, whose fluorescence is activated in acidic environments, and specifically enhanced when bound to the lipid membrane of EVs, with a higher specificity and with respect to only binding to hydrophobic protein regions. This makes the [DiI1049] fluorescent signal highly EV-specific. The fluorescent nanoalgosomes were produced as follows: 5x10⁷ EV particles/ml were stained with 100 nM of DiI1049, previously filtered by 20-nm filters. After 2-hour incubation temperature, we diluted the samples for 24h with 2.5 mM AMCO against PBS without Ca and Mg. Then the fluorescent nanoalgosomes have been incubated with cells. To perform nanoalgosomes cellular uptake we have used normal and tumor cell of the same origin as a biological model system.



CONCLUSIONS

The cellular uptake of DiI1049-stained and DiI1049-stained nanoalgosomes is a specific and active process that occurs in a time- and dose-dependent mode.

Figures

Figure 1

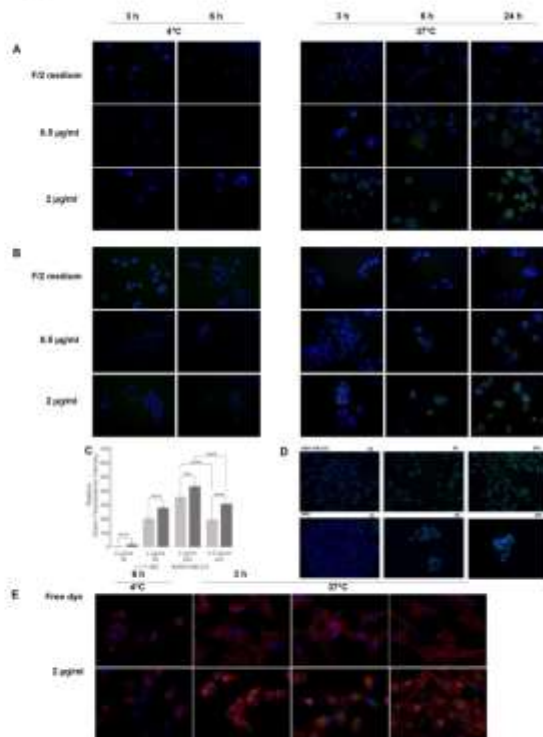


Figure 1. Representative fluorescence microscopy images showing the cellular uptake of DiI1049-labeled EVs (green) in MCF-7 (A) and H460 (B) cell lines (scale in 5µm), incubated with different concentrations of EVs at 37°C for 1, 6 and 24 hours. EV uptake using non-conditional EV media and stained with DiI1049 and 4°C incubation are shown as negative controls. Mean fluorescence intensity (MFI) of MCF-7 (A) and H460 (B) cells and H460 (B) cells incubated with 1 µg/ml EVs at 37°C for 1, 6 and 24 hours, or with 0.1 µg/ml EVs at 37°C for 24 hours are reported as relative values against the green fluorescence intensity of cells treated with the red-conditional EV media at 37°C for 24 hours. The data are presented as means ± SD (***) p < 0.001, **** p < 0.0001. (C) Similar results are obtained with H460-stained DiI1049-labeled EVs. (D) Similarly, representative fluorescence microscopy images showing the cellular uptake of DiI1049-labeled EVs in MCF-7 (A) and H460 (B) cell lines are shown.

Figure 2

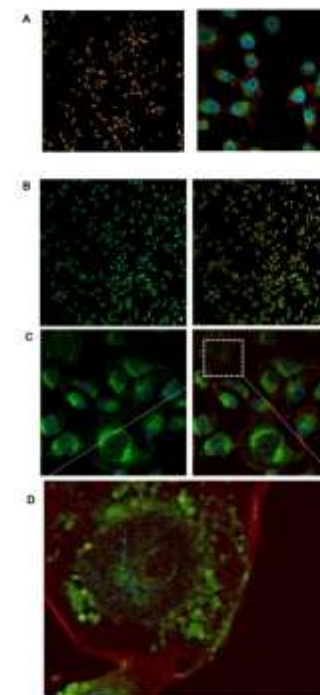


Figure 2. Representative confocal images of MCF-7 cells (scale in 5µm) incubated with 100 µg/ml of fluorescent nanoalgosomes (green) at 37°C for 24h, followed from a section at focal depth of 7 µm towards surface (z-axis) at -15, 0, 15 and 30 µm of magnification respectively. The independent technical replicates (n=2) were performed.

RESULTS

Once established that DiI1049-stained EVs are not cytotoxic, modifications in geometry of different concentrations and timing, we have determined the cross-linking communication among the microalgae cells and the human cells, by testing the cellular uptake.

Cells were incubated with different concentrations of DiI1049-stained EVs (10, 100, 1000 µg/ml) for different incubation times, namely 1, 6 and 24 hours. To confirm that nanoalgosomes actively bypass cell membrane and that they were uptaken through an energy-dependent mechanism, we incubated cells at 4°C as negative control. As shown in Figure 1A, the H460 cells rapidly bypass the cellular membrane in MCF-7 cells, to accumulate in specific cellular compartments after 1 hour, especially in the perinuclear region, only at the temperature of 37°C. Their distribution in the cytoplasm compartment was mainly visible after 24 hours (Fig. 1A-C), respect to samples incubated at 4°C in which there were no detectable fluorescence (Fig. 1A-D, left rows). Similarly, the control H460 cells have bypassed the MCF-7 cells, although slowly (4 hours) and to a significant lower amount (Fig. 3B-C). In addition, we used also specific green fluorescence by replacing the same dyes using as a further negative control the DiI1049-labeled using non-conditional EV media and stained with DiI1049. No fluorescence signal was detected from negative control images, for all the conditions analyzed (Fig. 1A-D). Similar results were obtained with H460-stained DiI1049-labeled EVs and DiI1049-labeled DiI1049-stained EVs (green) (Fig. 3D and E), respectively.

To clearly discriminate between EV attachment to the cell surface and their uptake, detailed confocal imaging was performed. The intracellular localization of DiI1049-stained EVs was consistent with most cells showing an accumulation of green fluorescence signal close to the nucleus and also accumulated in the nuclear area cytoplasm; some cells showing a more dispersed signal within (Fig. 1A-E).

ACKNOWLEDGEMENTS

The authors acknowledge scientific contribution from the VES4US consortium and financial support from the VES4US project funded by the European Union's Horizon 2020 research and innovation programme under grant agreement No 8011338.

EXTRACELLULAR VESICLES PRODUCTION FROM MICROALGAE: A RENEWABLE BIOPROCESS

Angela Paterna¹, Estella Rao¹, Samuele Raccosta¹, Giorgia Adamo², Sabrina Picciotto², Rosina Noto¹, Rita Carrotta¹, Fabio Librizzi¹, Vincenzo Martorana¹, Daniele P. Romancino², Nicolas Touzet³, Antonella Bongiovanni², Mauro Manno^{1*}

¹Institute of Biophysics (IBF) - National Research Council of Italy (CNR), Palermo, Italy. ²Institute for Research and Biomedical Innovation (IRIB) - National Research Council of Italy (CNR), Palermo, Italy. ³Centre for Environmental Research Innovation and Sustainability Institute of Technology Sligo, Sligo, Ireland.

Contact*: mauro.manno@cnr.it

OUTLINE

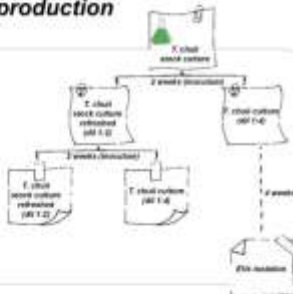
The presented work highlights the optimization of the extracellular vesicles production process. EVs are isolated using Tangential Flow Filtration (TFF) from cultures of the microalgae strain *Thalassiosira weissflogii*. Some TFF parameters have been evaluated, such as feed or permeate flow, the resulting vesicles production have been compared in terms of isolation yield, in order to establish the optimal protocol for EVs isolation. Moreover, aiming to identify *Thalassiosira weissflogii* as a renewable bioprocess for extracellular vesicles production, the feasibility of recycling microalgae cells has been investigated, starting a new cultivation from the TFF processed microalgae culture.

METHODS

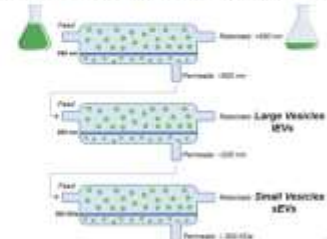
EVs production

Microalgal cultivation

- ✓ Microalgae strain *Thalassiosira weissflogii*
- ✓ Cultivation in bioreactors, in dark conditions and under continuous air flow
- ✓ Vesicles isolation after 4 weeks



Schematic representation of multiple clarification by ultrafiltration



Vesicles isolation



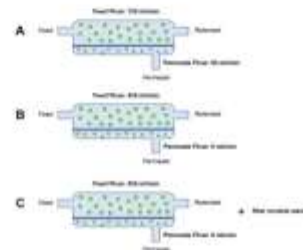
Tangential Flow Filtration (TFF)

CONCLUSIONS

The improvement of the TFF method for the isolation of EVs from *T. weissflogii* demonstrates that the yield of the process increases employing lower feed and permeate flows followed by a wash of the filter module. Interestingly, the optimization of the production process provides for the recycling of microalgae cell cultures, suggesting *T. weissflogii* as a renewable bioprocess suitable for the described renewable bioprocess.

RESULTS

Optimization of TFF parameters to maximize process yield



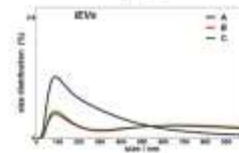
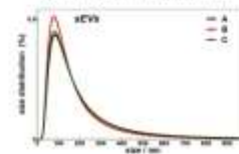
Process Control Parameters (mean ± SD)	Small Vesicles (sEVs)			Large Vesicles (lEVs)		
	A	B	C	A	B	C
Isolation yield (%)	31 ± 6	33 ± 3	41	16	7	14
Δ average hydrodynamic diameter (nm)	80 ± 5	95 ± 5	95 ± 5	128 ± 15	160 ± 15	160 ± 15
Recovery ratio (%)	100 ± 0	100 ± 0	100 ± 0	76 ± 5	100 ± 0	100 ± 0

*Process control has been determined by means of BCA assay.
 †Average hydrodynamic diameter and Recovery ratio have been determined by light scattering measurements.

Condition C, involving a feed flow of 450 ml/min, a permeate flow of 0 ml/min and also a wash of the filter module, leads to the highest yield of isolated EVs.

Different conditions have been investigated in order to increase the yield of isolation process. Moreover, large and small vesicles have been concentrated and diluted through a smaller 500 kDa membrane reaching enriched samples of EVs in PBS.

Dynamic light scattering measurement



Thalassiosira weissflogii (Image courtesy: IRIB, CNR)

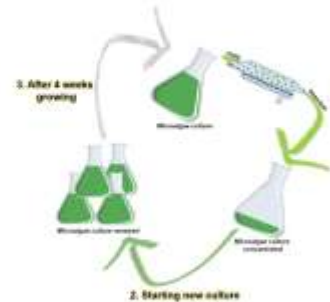
REFERENCES

Théry C, et al. Minimal information for studies of extracellular vesicles 2018 (MISEV2018): a position statement of the International Society for Extracellular Vesicles and update of the MISEV2014 guidelines. *Journal of Extracellular Vesicles*. 2018;7:1-32. DOI: 10.1080/20013079.2018.1535758

Khan M, et al. The promising future of microalgae: current status, challenges, and optimization of a sustainable and renewable industry for isotaxins, lipid, and other products. *Marine Cell Fact*. 2018;17:1-36. DOI: 10.1007/s12034-018-0879-x.

Adamo G, et al. Nanoparticles: introducing extracellular vesicles produced by microalgae. *Journal of Extracellular Vesicles*, submitted.

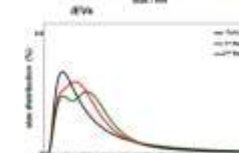
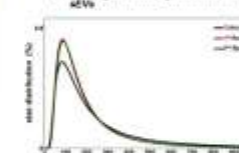
EVs production is a Renewable bioprocess



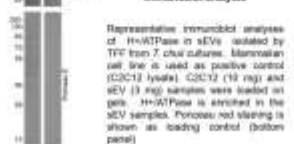
Process Control Parameters (mean ± SD)	Small Vesicles (sEVs)			Large Vesicles (lEVs)		
	A	B	C	A	B	C
Isolation yield (%)	11	25.75	32.6	11	6.02	14.77
Δ average hydrodynamic diameter (nm)	32 ± 0	32 ± 0	32 ± 0	32 ± 0	122 ± 10	122 ± 10
Recovery ratio (%)	100 ± 0	100 ± 0	100 ± 0	100 ± 0	100 ± 0	100 ± 0

*Process control has been determined by means of BCA assay.
 †Average hydrodynamic diameter and Recovery ratio have been determined by light scattering analysis.
 ‡nd, not determined.

Dynamic light scattering measurement



Innovator analysis



Representative immunoblot analysis of Hsp70 in sEVs isolated by TFF from *T. weissflogii* cultures. Mannitolin cell line is used as positive control (C2C12 lysate). C2C12 (10 ng) and sEV (3 ng) samples were loaded on gels. Hsp70 is enriched in the sEV samples. Proteins not staining is shown as loading control (bottom panel).

1. First step TFF: Cells clarification. Microalgae culture is processed through the TFF system with a membrane of 500 nm. The retentate is concentrated until a final volume of 100 ml.
2. Retentate is used to restart a new inoculum starting a renewed microalgae culture.
3. After 4 weeks of cultivation, microalgae are available to another EVs isolation process.

ACKNOWLEDGEMENTS

The authors acknowledge financial support from the VES4US project funded by the European Union's Horizon 2020 research and innovation programme under grant agreement No 8011336.





The importance of considering sample specificities in optimization of centrifugation-based vesicle harvesting

Darja Božič^{1,2*}, Matej Hočevar³, Manca Pajnič¹, Marko Jeran^{1,2}, Aleš Iglič^{2,4}, Veronika Kralj-Iglič¹

¹Laboratory of Clinical Biophysics, Faculty of Health Sciences, University of Ljubljana, Slovenia, ²Laboratory of Physics, Faculty of Electrical Engineering, University of Ljubljana, Slovenia, ³Department of Physics and Chemistry of Materials, Institute of Metals and Technology, Slovenia, ⁴Laboratory of Clinical Biophysics, Faculty of Medicine, University of Ljubljana, Slovenia

Contact*: darja.bozic@fe.uni-lj.si

OUTLINE

The isolation of cellular vesicles (CV) is generally lacking knowledge about physico-chemical properties of complex biological samples. With this example of sedimentation of haemoglobin-filled erythrocyte- and platelet-derived vesicles in buffer or plasma medium, respectively, we try to demonstrate that monitoring of processing is crucial in optimization of centrifugation-based CV isolation protocols.

METHODS

4.5 mL of blood of an author volunteer was collected into an evacuated tube with added trisodium citrate. After centrifugation of blood at 300g, sedimented erythrocytes and plasma with platelets were separated. Erythrocytes were resuspended in citrate-phosphate buffer saline (citrate-PBS). After a week of storage at 4°C, the samples of platelets in plasma (S-Pit) and erythrocytes in buffer (S-Erc), were subjected to sequential centrifugation in which the supernatant of each step was subjected to the following one. Pellets and supernatants were analysed by flow cytometry (MacQuant, Miltenyi, Germany) and scanning electron microscopy (JSM-6500F, JEOL, Japan).

Table 1: Steps of sequential centrifugation.

The volumes of samples were adjusted to the limits of the employed centrifuges, rotors and available sample containers. Both samples, S-Erc and S-Pit were subjected to the following series of steps: (step 1) vacutainer tubes, steps 2-4: culture tubes, steps 1-4: large benchtop centrifuge Centric 400R, Dornel, SLO; step 5: small benchtop centrifuge Centric 200R with swinging rotor Lilliput, Dornel, SLO (the supernatant from step 4 was divided into corresponding number of samples); steps 6-7: ultracentrifuge L8-70M, SW-50Ti, Beckman, USA). The volume of samples after supernatant transfer was adjusted with citrate-PBS.

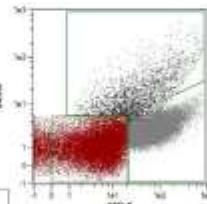


Figure 1: Gating strategy in FCM analysis. Events corresponding to small vesicles (dark red), platelets/platelet remnants and large vesicles (grey) and erythrocyte ghosts and cell debris (black). Events corresponding to erythrocytes were out of range of the presented scattering window.

Step	Sample V (mL)	Speed (g)	Time (min)
1	5 (s-trial 4 (s-Pit))	300	10
2	4	1000	10
3	4	1000	10
4	4	4000	10
5	1,2	10000	20
6	5	50000	70
7	5	100000	70

RESULTS

An echinocyte shedding haemoglobin filled CVs is shown in Fig 2A and vesicles emerging from the cell remnants can be seen in Fig 2B)&2H). Increase of concentration of small CVs in the supernatants of the sample S-Erc in the steps 2-5 (detected by

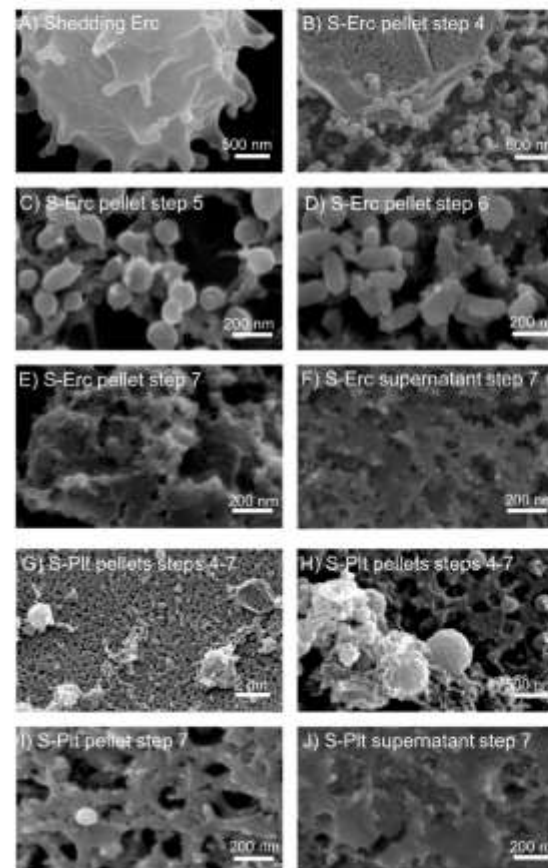


Figure 2: SEM imaging of pellets of S-Erc (A-F) and S-Pit (G-J) after different steps of sequential centrifugation.

FCM Fig 3A) indicate their formation during the processing. In case of S-Erc, majority of larger cell remnants was removed in step 4, and vesicles of different shapes were found in the pellets (round to progressively elongated CVs Fig. 2B-D); while in case of S-Pit, vesicle shapes in pellets up to the 6th step appeared similar under SEM and contained both - CVs and large cell remnants (Fig. 2G-H). In the 7th step, vesicles were hardly recognizable in pellets of both samples- S-Erc and S-Pit. Samples that underwent centrifugation pull 100.000g contained amorphous material (Fig. 2E,I); vesicles were hardly recognizable. Appearance of soluble fraction (supernatant after 7th step) after SEM preparation is presented in (Fig. 2F,J).

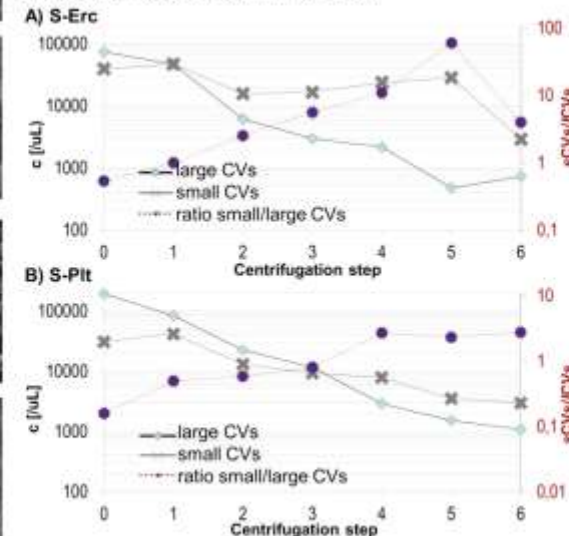


Figure 3: Concentration of CVs in the supernatants after each step of sequential centrifugation of S-Erc (A) and S-Pit (B) sample.

CONCLUSIONS

Ultracentrifugation is not prerequisite to sediment small CVs. Isolation of CVs by centrifugation requires deeper knowledge on their sedimentation behaviour in their current environment of the surrounding medium. The effectors include not only the solutes in the medium, but also larger and smaller species around the particles in focus. Concentration, size, density and shape of each species should be considered along with its sedimentation path in a specific centrifugation container.

Centrifugation at 100.000 g was found unnecessary and potentially result in loss of CV integrity. We suppose that disrupted membranes of cells and CVs may form vesicles that have similar topology and certain portion of same molecules as CVs that were present in the initial sample. However, the post-disruption-assembled vesicles most probably differ from genuine CVs in the amounts and ratios of components. The identity of the material which is being harvested in the isolate can be controlled by adjusting centrifugation parameters according to the specificities of a particular sample.

ACKNOWLEDGEMENTS

 This project has received funding from the European Union's Horizon 2020 research and innovation programme under grant agreement No 801338

Slovenian Research Agency (ARRS, research core fundings No.P2-0132, P2-0232, P3-0388 and projects No. Z2-9215, J2-8166, J1-9162, L3-2621)